“Development and Evaluation of cRGD-Modified Lipopolymeric Nanoplexes for Delivering CRISPR/Cas9 Ribonucleoproteins for Therapeutic Genome Editing”

THESIS

Submitted in partial fulfillment of the requirements for the degree of

DOCTOR OF PHILOSOPHY

by

Deepak Kumar Sahel

2018PHXF0037P

Under the Supervision of

Dr. Deepak Chitkara

and co-supervision of

Dr. Anupama Mittal

BIRLA INSTITUTE OF TECHNOLOGY AND SCIENCE PILANI

(RAJASTHAN)

2023

CERTIFICATE

This is to certify that the thesis entitled **"Development and Evaluation of cRGD-Modified Lipopolymeric Nanoplexes for Delivering CRISPR/Cas9 Ribonucleoproteins for Therapeutic Genome Editing"** submitted by **Mr. Deepak Kumar Sahel** ID No. **2018PHXF0415P** for the award of Ph. D. Degree of the Institute embodies the original work done by him under our supervision.

SUPERVISOR

Dr. DEEPAK CHITKARA

Associate Professor,

Department of Pharmacy,

BITS Pilani, Pilani Campus,

Rajasthan, India-333031

CO-SUPERVISOR

Dr. ANUPAMA MITTAL

Associate Professor,

Department of Pharmacy,

BITS-Pilani, Pilani Campus,

Rajasthan, India-333031

Date:

Place: Pilani, Rajasthan

DECLARATION

I hereby declare that the work carried out in this thesis entitled **"Development and Evaluation of cRGD-Modified Lipopolymeric Nanoplexes for Delivering CRISPR/Cas9 Ribonucleoproteins for Therapeutic Genome Editing"** is an original piece of research work carried out by me under the guidance of Dr. Deepak Chitkara (Supervisor) and Dr. Anupama Mittal (Co-Supervisor) at BITS Pilani, Pilani Campus, Pilani, India. This thesis has not been submitted by me for the award of any other degree from any other university/institute.

Deepak Kumar Sahel

Date:

Place: Pilani, Rajasthan

Dedicated To

My Father

I would be honored to dedicate this thesis to my father, **Mr. Dharam Pal**, whose unwavering commitment to my upbringing has been underscored by the profound sacrifices he made, setting aside his own aspirations.

My Mother

I humbly wish to dedicate this thesis to my beloved mother, **Mrs. Sumitra Devi**, whose unwavering prayers and boundless support have been instrumental in enabling me to accomplish this work.

My Tau Ji

I would like to wholeheartedly dedicate this thesis to my Tau Ji, **Maj. Hariom Sharma**, whose unwavering commitment to my primary education has been a beacon of guidance throughout my life. His tireless dedication and constant efforts have consistently steered me towards the path of righteousness, for which I am forever grateful.

Deepak Kumar Sahel

Table of Contents

Acknowledgments

At the very beginning, I would like to bow down to the creator of everything, ***"The Almighty God,"*** for bequeathed with blessing, knowledge, and strength to make substantial contributions in the Pharmacy field. Without the blessings of the almighty, it would not have been possible for me to achieve my dreams.

First and foremost, I would like to express my heartfelt gratitude to my supervisor, **Prof. Deepak Chitkara**, for his invaluable contributions to my journey. His unwavering faith in me, constant inspiration, encouragement, constructive feedback, and unwavering support have played a pivotal role in my accomplishments. I am committed to following the path he has illuminated for me, and I will forever cherish the kind words he shared. Without a doubt, I can confidently say that he is the epitome of an exceptional supervisor.

I am immensely thankful to **Prof. Anupama Mittal** for her guidance and mentorship as my co-supervisor. Her expertise in various biological techniques, instruments, and assays has been instrumental in shaping my research abilities.

My sincere appreciation goes to my DAC members, **Prof. Anil Jindal** and **Dr. Richa Srivastava**, for their valuable insights and suggestions that have enhanced the quality of my Ph.D. thesis.

I would also like to extend my gratitude to my collaborators, **Dr. Debojyoti Chakraborty**, **Dr. Sivaprakash Ramalingam**, **Dr. Anupama Kumari**, **Dr. Vivek Singh**, and **Dr. Sujata Mohanty**. Their thoughtful discussions and teachings have expanded my knowledge and enriched my research endeavors. Special thanks are due to **Dr. Sushil Yadav** for his continuous support in

facilitating animal experimentation in my Ph.D work. I am deeply thankful to all the faculty members for their direct and indirect support throughout my academic journey.

I would like to extend my heartfelt regards to my late grandfather, **Shri Tiku Ram**, and my late grandmother, **Shrimati Suraj Kaur**. Their presence and love have left an indelible mark on my life, and I cherish their memory.

I would like to thank my father, **Mr. Dharam Pal**, my mother, **Mrs. Sumitra Devi**, my elder sisters **Preeti** and **Priya**, and my brothers-in-law, **Mr. Naveen Sharma** and **Mr. Sumesh Kaushik**, I offer my sincere gratitude for their unwavering love and support. Throughout the years, their presence and encouragement have played a vital role in my Ph.D. journey.

I am deeply grateful to my Tau Ji, **Mr. Hariom Sharma**, and Tai Ji, **Mrs. Sushila Devi**, for their unconditional love and unwavering faith in me. Their constant support has been a source of strength and inspiration.

I am blessed to have brothers who have directly or indirectly supported me throughout my life. I would like to express my gratitude to **Mr. Kundan Lal**, **Mr. Kapil Sharma**, **Mr. Sagar**, **Mr. Shashikant**, **Mr. Manish Sharma**, **Mr. Khemu**, **Mr. Anil Sharma**, and **Mr. Sunil Sharma**. Their presence has been a pillar of support, and I am thankful for their contributions.

A special mention of gratitude goes to my elder brother, **Mr. Yashwant Vats**. His presence has brought immense happiness and joy to my life. I treasure his unconditional love, and I am truly fortunate to have a brother like him by my side.

I would like to express my special gratitude to my brother-in-law, **Adv. Rajender Kaushik**, for his unwavering support. His constant belief in me has been a tremendous source of

motivation, inspiring me to continually strive for personal growth and excellence. It is with deep appreciation that I dedicate this thesis to him, acknowledging his significant impact on my journey.

The one person who inspired me to do my Ph.D. and it all started because of him, **Dr. Kushal Kumar** (Drug Controller Officer); I extend my heartfelt thanks to him for everything he has done for me. I want to acknowledge the profound professional relationship that has evolved into a genuine connection with **Dr. Manu Dalela**. I am sincerely grateful for his unwavering presence and continuous support. His positive mindset, extensive knowledge, and invaluable suggestions have been a delight to receive and have greatly contributed to my academic pursuits.

I would like to raise a toast to my friend, **N. Sai Bhargav**, for providing unwavering moral support throughout the highs and lows of my Ph.D. journey. Despite his ridiculously silly conversations, his presence brought cheerfulness and helped alleviate stress in my life. I extend my heartfelt gratitude to him. A special mention of appreciation goes to my best friend, the epitome of a wonderful person, **Ms. Reena Jatyan**. Her support has been unconditional and invaluable, and I am truly grateful for her presence in my life. I also want to express my sincere thanks to another special friend, **Mr. Prabhjeet Singh**, for his unwavering support. His presence has been a source of strength and encouragement. Furthermore, I extend my special thanks to my dear juniors, **Mr. Abhay Tharmatt** and **Mr. Gangadhari Giriprasad**, for their kind and unwavering support throughout my journey. Their presence has been invaluable, and I am thankful for their contributions.

A professional collaboration provided me with an elder brother, **Dr. Mohd Azhar**, who always encouraged and motivated me to improve. I would like to thank him for all his efforts to make my Ph.D. life easy; without him, it would have been a different story that I can't even imagine.

My special thanks to **Dr. Saurabh Sharma** and **Dr. Santosh Khadagale** for their moral and professional support throughout my Ph.D. to till date. I want to thank my colleague cum brother **Mr. Sangam Giri Goswami,** for his unconditional support. His valuable input made it easy for me to finish my work on time.

I would like to express my heartfelt gratitude to a dear and special friend, **Dr. Meenakshi Kaira**, for her unwavering support throughout the years. Together, we shared dreams and aspirations, and I am proud to say that I have accomplished them with great pride. Thank you, dear friend, for standing by my side. Your presence has been invaluable, and I am truly grateful for our friendship..

I appreciate my colleagues, **Mr. Imran Ansari, Mr. Arihant K Singh**. **Ms. Moumita Basak**, **Mr. Shubham Salunkhe**, **Mr. Sai Pradyuth**, **Ms. Sonia Guha**, and **Dr. Yogeshwaran** for their incredible support in the lab. I want to thank my seniors, **Dr. Sudeep Sudesh Pukale**, **Dr. Kishan Italiya**, and **Dr. Samrat Mazumdar**, for their help in the primary stages of my Ph.D. Also, thanks to **Mr. Mohd Salman** for his experimental support during my Ph.D.

I thank Indian Council for Medical Research (ICMR), India, for their financial support through the **Senior Research Fellowship** (File No: 45/66/2019-Nano-BMS). I appreciate **Sun Pharma Foundation** for giving me Best Research Scholar Award 2022. Also, I sincerely acknowledge BITS-Pilani, Pilani campus, for all the research facilities and positive environment.

(Deepak Kumar Sahel)

List of Abbreviations

~	Approximately equal to
<	Less than
>	More than
±	Plus or minus
µg	Micro gram
µL	Microliter
AAV	Adeno Associated Virus
ADAR	Adenosine Deaminase Acting On RNA
adRP	Autosomal Dominant Retinitis Pigmentosa
ADVIRC	Autosomal Dominant Vitreo Retino Choroidopathy
API	Active Pharmaceutical Ingredient
ARPE	Adult Retinal Pigment Epithelial Cells
ARPE	Adult Retinal Pigment Epithelial Cells
ARPE	Adult Retinal Pigment Epithelial Cells
ATRA	All *Trans* Retinoic Acid
BHMP	2, 2- Bis (Hydroxymethyl) Propionic Acid (BHMP)
BSA	Bovine Serum Albumin
CASFISH	Cas9 Mediated Fluorescence *In Situ* Hybridization
CHM	Choroideremia
CIRTS	CRISPR/Cas Inspired RNA Targeting System
CjCas9	*Campylobacter Jejuni* Originated Cas9
CNV	Choroidal Neovascularization

CO_2	Carbon Dioxide
COD	Cone Cell Degeneration
CORD	Cone and Rod Degeneration
CPCSEA	Committee for the Purpose of Control and Supervision of Experiments on Animals
CPPs	Cell Penetrating Peptides
CRISPR	Clustered Randomly Interspaced Short Palindromic Repeats
CRISPRa	Activating CRISPR
CRISPRi	Interfering CRISPR
crRNA	CRISPR RNA
CSNB	Congenital Stationary Night Blindness
DAPI	4',6-Diamidino-2-Phenylindole
dCas9-KRAB	dCas9 Protein Fused with Transcriptional Repressor KRAB
DCM	Dichloromethane
DEE	Diethyl Ether
DIPEA	N, N-Diisopropylethylamine
DLS	Dynamic Light Scattering
DMD	Duchenne Muscular Dystrophy
DMEM	Dulbecco's Modified Eagle Medium
DMSO	Dimethyl Sulfoxide
DNP	Dendrimer-Based Nanoparticles
DOTAP	1,2-Dioleoyl-3- Trimethylammonium propane
DSB	Double Strand Break
DTT	Dithiothreitol

EDC.Hcl	1-Ethyl-3-(3-Dimethylaminopropyl) Carbodiimide Hydrochloride
eGFP	Enhanced Green Fluorescent Protein
EIAV	Equine Infectious Anemia Virus
EMA	European Medicines Agency
FDA	Food and Drug Administration
GFP	Green Fluorescence Protein
gRNA	Guide RNA
HDR	Homology-Directed Repair
HEPES	4(2-Hydroxyethyl)-1- Piperazineethanesulfonic Acid
HIF1	Hypoxia Inducible Factor 1
HoBt	Hydroxybenzotriazole
IAEC	Institutional Animal Ethics Committee
Indel	Insertion/Deletion
IPA	Isopropanol
IRD	Inherited Retinal Dystrophies
IVIS	*In Vivo* Imaging System
IVT	*In Vitro* Transcription
KCl	Potassium Chloride
LB	Luria Bertani Broth
LCA	Leber's Congenital Amaurosis
LNPs	Lipid Nanoparticles
LNPs	Lipid Nanoparticles
LVs	Lentiviral Vectors

MERTK	Mer Tyrosine Kinase
$MgCl_2$	Magnesium chloride
miRNA	micro-RNA
MTT	(3-(4,5-Dimethylthiazol-2-yl)-2,5-Diphenyltetrazolium Bromide)
mV	Milli Volt
NCs	Nanocapsules
NFW	Nuclease-Free Water
ng	Nano gram
NHEJ	Non-Homologous End Joining
nm	Nano meter
NmCas9	*Neisseria Meningitidis* Originated Cas9
º C	Degree Centigrade
PAM	Protospacer Adjacent Motif
PAMAM	Polyamidoamine
PBS	Phosphate Buffer Saline
PDI	Polydispersity Index
PDMAEMA	Poly[2-(Dimethylamino)Ethyl Methacrylate]
PEG-PLGA	Poly(Ethylene Glycol)-b- Poly(Lactic Acid)-co- Glycolic Acid)
PEI	Polyethyleneimine
PLL	Poly(L-lysine)
PM	Polymeric Micelles
PNPs	Polymeric Nanoparticles
RDs	Retinal Dystrophies

REPAIR	RNA Editing for Programmable A to I Replacement
RES	Reticuloendothelial System
RNPs	Ribonucleoproteins
ROP	Ring-Opening Polymerization
RP	Retinitis Pigmentosa
RPE	Retinal Pigment Epithelium
RT	Retention Time
SCID	Severe Combined Immunodeficiency
sgRNA	Single Guide RNA
siRNA	Short Interfering RNA
spCas9	*Streptococcus Pyogenes* Originated Cas9
ssODN	Single Stranded Oligo deoxyribonucleotide
stCas9	*Streptococcus Thermophilus* Originated Cas9
T7E	T7 Endonuclease
TALEN	Transcription Activator Like Effector Nuclease
TEM	Transmission Electron Microscopy
tracrRNA	Transactivating CRISPR RNA
USH1	Usher Syndrome Type 1
USH2	Usher Syndrome Type 2
USH3	Usher Syndrome Type 3
VEGF A	Vascular Endothelial Growth Factor A
w.r.t	With Respect To
w/w	Weight by Weight

wAMD	Wet Age-Related Macular Degeneration
XLRP	X linked Retinitis Pigmentosa
XLRS	X linked Juvenile Retinoschisis
ZFN	Zinc Finger Nuclease

List of Tables

List of Figures

concentrations after 7 days. Green arrows suggest blood vessels on the surface of the retina, and star marks indicate minimal mononuclear cell infiltration in the eye; however, retinal pigment epithelium (RPE) shows a normal appearance.

ABSTRACT

Retinal dystrophic conditions (RDIs), specifically wet-age-related macular degeneration, are characterized by choroidal neovascularization due to the overexpression of vascular endothelium growth factor A (VEGFA). Anti-VEGF antibodies are used as first-line treatment but have ample limitations, such as high cost and risk of retinal damage and resistance, and therefore, necessitating the development of a novel strategy. CRISPR/Cas9 is a molecular scissor that could provide precise and site-specific gene editing *via* double-strand break (DSB) mediated non-homologous end joining (NHEJ) or homology-directed repair (HDR) repair pathways. Despite outstanding specificity and precision, CRISPR components (plasmids, mRNA, and ribonucleoprotein) have several limitations owing to their high molecular weight, hydrophilicity, degradation in the presence of nuclease/proteases, poor cellular uptake, and supranegative charge, etc. Viral vectors are the gold standard for CRISPR delivery but possess ample limitations related to immunogenicity, limited payload capacity, and inability to deliver Cas9 ribonucleoprotein. Interestingly, nanotechnology has been reported for its immense potential to improve nucleic acid delivery *in vitro* and *in vivo*. This thesis focuses on developing and evaluating non-viral lipopolymeric nanoplexes that efficiently deliver the CRISPR plasmids and CRISPR/Cas ribonucleoproteins *in vitro* and *in vivo*.

In chapter 1, we discussed all the possibilities and challenges in the utility of CRISPR/Cas9 gene editing in the treatment of RDs. We also have insight into the role of non-viral nanocarriers and their applications in gene delivery.

In Chapter 2, we have synthesized a cholesterol and morpholine grafted cationic lipopolymer, i.e, mPEG b-(CB-{g-cationic chain; g-Chol; g-Morph}), using a series of chemical reactions and explored it for *in vitro* and *in vivo* delivery of CRISPR/Cas9 plasmid. Briefly, the

lipopolymer was utilized to prepare blank lipopolymeric nanoplexes using the w/o/w double emulsion solvent evaporation method, which showed a particle size and zeta potential of 93 ± 12 nm, and +15.8 ± 0.7 mV, respectively. The plasmid-loaded lipopolymeric nanoplexes showed a particle size and zeta potential of 141±16 nm and 5.9±0.5, respectively. *In vitro* transfection assay showed ~60 % of transfection efficiency in ARPE-19 cells with a gene-editing of ~22%. The *in vivo* tissue distribution was performed in *swiss albino* mice, where the plasmid-loaded lipopolymeric nanoplexes were found to accumulate in the liver and lung tissues.

In Chapter 3, the Cas9 proteins (SpCas9-EGFP and DspCas9-EGFP) were purified from the E.Coli using the HPLC system assisted with the HisTrap column. Briefly, the SpCas9-EGFP and SpDCas9-EGFP plasmids were expressed in the E.Coli to produce green fluorescent (EGFP) tagged SpCas9 and SpDCas9 proteins followed by cell lysis, protein extraction and purification using HisTrap column assisted HPLC system. The proteins were further evaluated for their purity using SDS-PAGE, RNP complex formation, zeta potential, endonuclease activity/DNA binding activity, and fluorescence property etc. The yield of purified protein was 4-5 mg/liter of LB media.

In Chapter 4, the blank lipopolymeric nanoplexes were used to prepare Cas9 RNPs loaded lipopolymeric nanoplexes. The RNPs lipopolymeric nanoplexes showed a particle size of 117.3±7.6 nm and zeta potential of 6.17±1.04 mV. The RNPs lipopolymeric nanoplexes transfected the HEK293T cells in a time-dependent manner with the highest efficiency i.e ~80% after 6 h of incubation. As per the CASFISH experiment, the RNPs were found localized within the nucleus after 48 h. Further, the gene editing assays, i.e., T7E and TIDE, showed 55% Indel efficiency. Further, the RNPs lipopolymeric nanoplexes were found stable in an *in vivo* environment and could transfect the muscle cell after 6 h of the intramuscular injection in *swiss albino* mice.

In Chapter 5, a cRGD conjugated lipopolymer (cRGD-Mal-PEG-b-p(MTC-Chol)) was synthesized and used with cationic lipopolymer (mPEG b-(CB-{g-cationic chain; g-Chol; g-Morph}) in a ratio of 1:9 to form cRGD modified hybrid lipopolymeric nanoplexes. The RNPs loaded, cRGD modified lipopolymeric nanoplexes (cRGD-RNPs-HyNPXs) exhibited a particle size and zeta potential of 175±20 nm and 2.15±0.9 mV, respectively. The cRGD-RNPs-HyNPXs possess ample advantages, such as rapid complex formation with RNPs, good complexation efficiency for RNPs, stability up to 194 h, efficient transfection (~70%), and VEGF-A gene editing (~40%). Further, the cRGD-RNPs-HyNPXs had good vitreous diffusibility and were able to transfect retinal cells *in vivo* in the rat after 48h of the intravitreal injection. The initial retinal toxicity data indicated the non-toxic nature of the cRGD-RNPs-HyNPXs up to a dose of 250 µg/animal. Moreover, the cRGD-RNPs-HyNPXs have shown transfection of retinal cells *in vivo* in Wistar rats after intravitreal injection followed by VEGFA gene editing with an Indel frequency of ~10%.

Conclusively, we have developed and explored cRGD modified lipopolymeric nanoplexes for *in vitro* and *in vivo* delivery of CRISPR/Cas9 components for therapeutic gene editing.

Chapter 1

Introduction

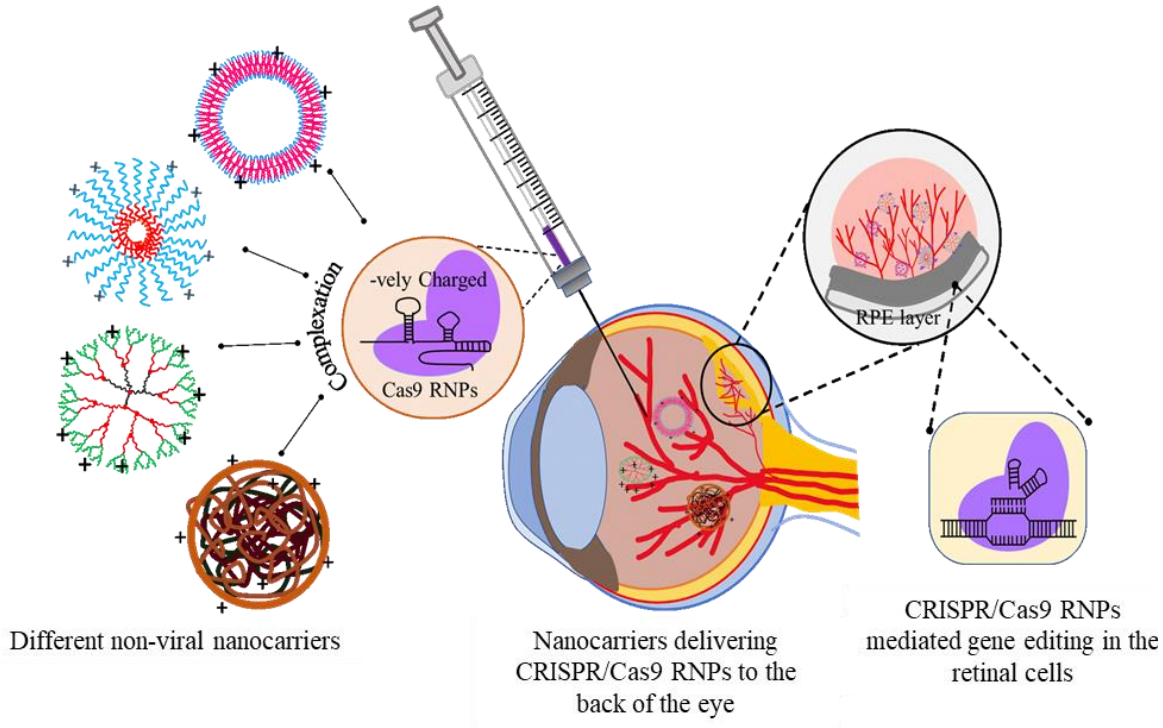

- Retinal dystrophies seeking gene editing
- CRISPR/Cas9 system
- Challenges in CRISPR/Cas9 delivery to retina
- Role of non-viral nanocarriers in CRISPR/Cas9 delivery

1.1. Introduction

Prokaryotes, especially bacteria, dwell in various environments, including unfavorable conditions. This means they have many methods by which they adapt to survive in harsh habitats. The defense systems acting undefined naturally include restriction-modification, abortive infection, and surface exclusion systems [2]. Recent studies have also shown an acquired immune system, such as the Clustered Regularly Interspaced Short Palindromic Repeats (CRISPR), in prokaryotic organisms, both in bacteria and archaea. These are repeat sequence elements with 21-37 bp in length, separated by spacers of similar size but varying composition. It forms a part of the adaptive immune system developed for protection against the attacking phage. The bacterium cleaves the genome of the invading virus and assimilates short viral genetic segments amongst its CRISPR sequences, which constitute the pathogen-specific spacer elements. Thus, when the same virus attacks the bacterium subsequently, the CRISPR RNA (crRNA) and *trans*-activating CRISPR RNA (tracrRNA) guide the organism's CRISPR-associated (Cas) endonuclease to the foreign DNA complementary to its sequence, thereby degrading the invading viral genome [3]**.** A protospacer adjacent motif (PAM) present only in the viral genome and not in the bacterium helps it differentiate itself from non-self, thus cleaving and inactivating the virus [4]**.**

CRISPR/Cas was discovered in 1987 and was first demonstrated as a therapeutic gene editing tool in mammalian cells in 2013 by Zhang and Church [5]. Since then, it has been identified as a potential therapeutic tool for genome editing and has been extensively studied for its application in many genetic and non-genetic diseases, including retinal dystrophies, cancer, hematological disorders, muscular dystrophies, neurodegenerative diseases, etc. The updated classification of CRISPR-Cas systems is based on the sequences of the Cas genes, the order of the repeats within the CRISPR arrays, and the organization of the Cas operons [6]. According to this system, there are three classes of CRISPR-Cas, i.e., types I–III. Each type is

further divided into subtypes, ranging from I-A to I-F, II-A to II-C, III-A, and III-B. The Cas1 and Cas2 genes are present in all CRISPR-Cas types, and the presence or absence of specific Cas proteins is the primary basis of classification. For example, the Cas3, Cas9, and Cas10 proteins are hallmarks of CRISPR/Cas types I, II, and III, respectively. Some systems do not have the distinct Cas proteins of types I-III and are termed unclassified (type U) [7]**.** As per the latest classification by Makarova et al. in 2020, the CRISPR/Cas system has two classes, six types, and 33 subtypes (Figure 1.1).

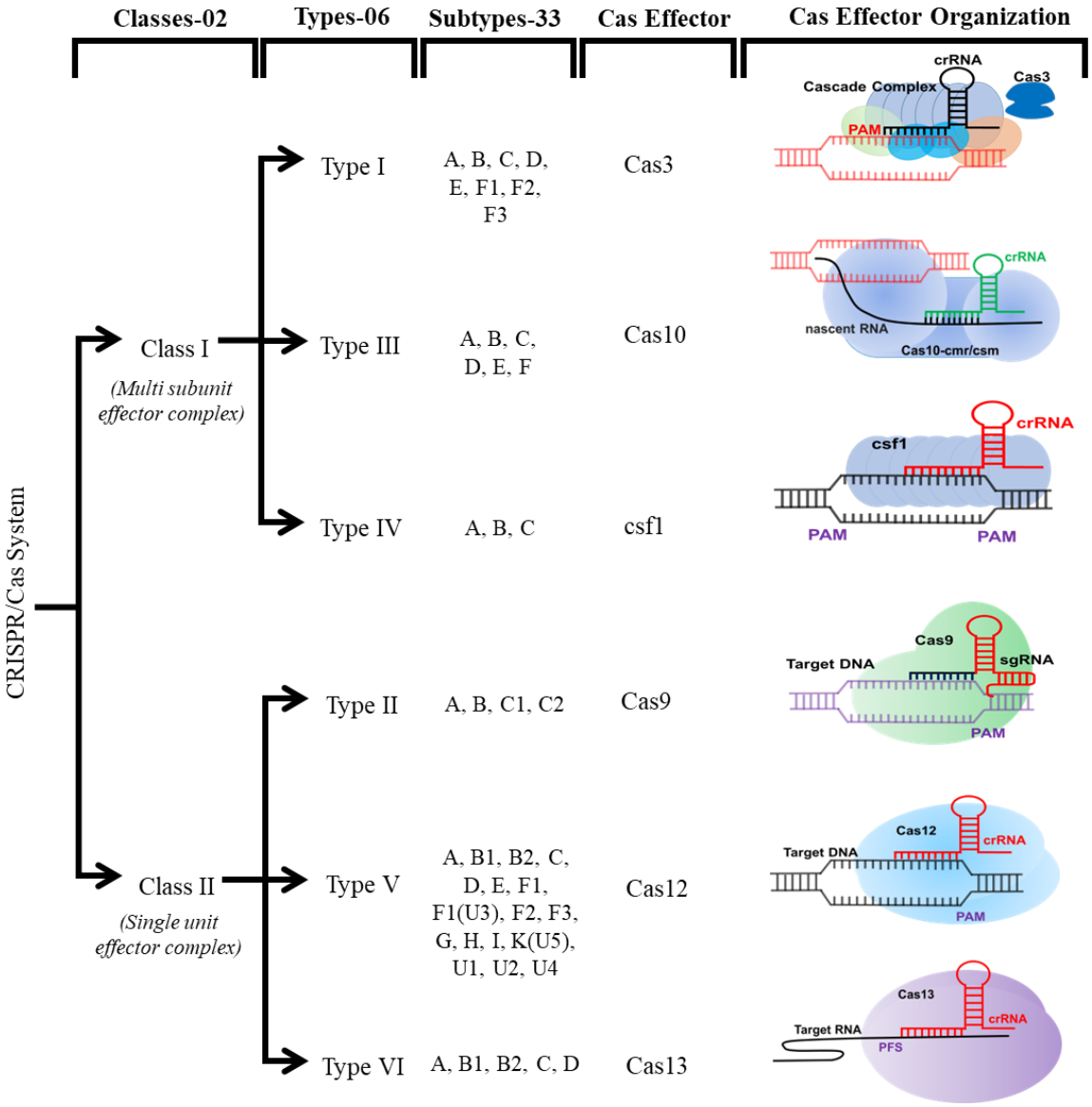

Figure 1.1. Latest classification of CRISPR/Cas system

The mechanism of action involves the formation of a ribonucleoprotein complex (RNP) that consists of the Cas9 protein and a guide RNA (gRNA) that can bind to the location directed by the gRNA on the genomic DNA. Upon attaching, Cas9 cleaves the viral DNA, creating a double-stranded break that allows additional DNA modifications on the site [8]. The Cas9 nucleases are designed to lead to a DNA double-strand break (DSB) at the target site. Repair of the strands occurs through error-prone non-homologous end joining (NHEJ) or homology-directed repair (HDR). When a template is absent, NHEJ is activated, resulting in insertions and/or deletions (indels) that damage the target genome loci. The HDR pathway follows when a donor template is present with homology to the targeted locus, enabling precise edits [9].

Recently, the CRISPR-Cas system has progressed as a remarkable engineering tool for carrying out precise and regulated genetic modifications in many microorganisms such as *Escherichia coli, Staphylococcus aureus, Lactobacillus reuteri, Clostridium beijerinckii, Streptococcus pneumonia, and Saccharomyces cerevisiae* [10]. Many steps are involved in applying CRISPR/Cas for bacterial genome editing. The first one is selecting the target space in the genome that will also decide the guide RNA to be developed. Until now, various parameters such as sequence setting, gRNA binding stability, chromatin accessibility, and PAM sequence have been discussed as important factors. Many software tools have been developed to forecast the on-site and off-site cleavage efficiency of sgRNAs, including CRISPOR, JATAYU, and CHOPCHOP, amongst many others. The tool generates a series of sgRNA at different PAM sites within the targeted gene, which are then aligned based on their efficiency in terms of the expected on-target and off-target binding potential and the other variables discussed above [11]. Many other parameters, such as specificity and mismatch concerns, must be investigated while creating a therapeutic tool. Moving forward, CRISPR/Cas9 system was adopted in three significant forms, i.e. plasmid, mRNA, and purified

active ribonucleoprotein complex. All these forms have their inherent advantages and limitations (Figure 1.2) and are therefore utilized accordingly for therapeutic purposes.

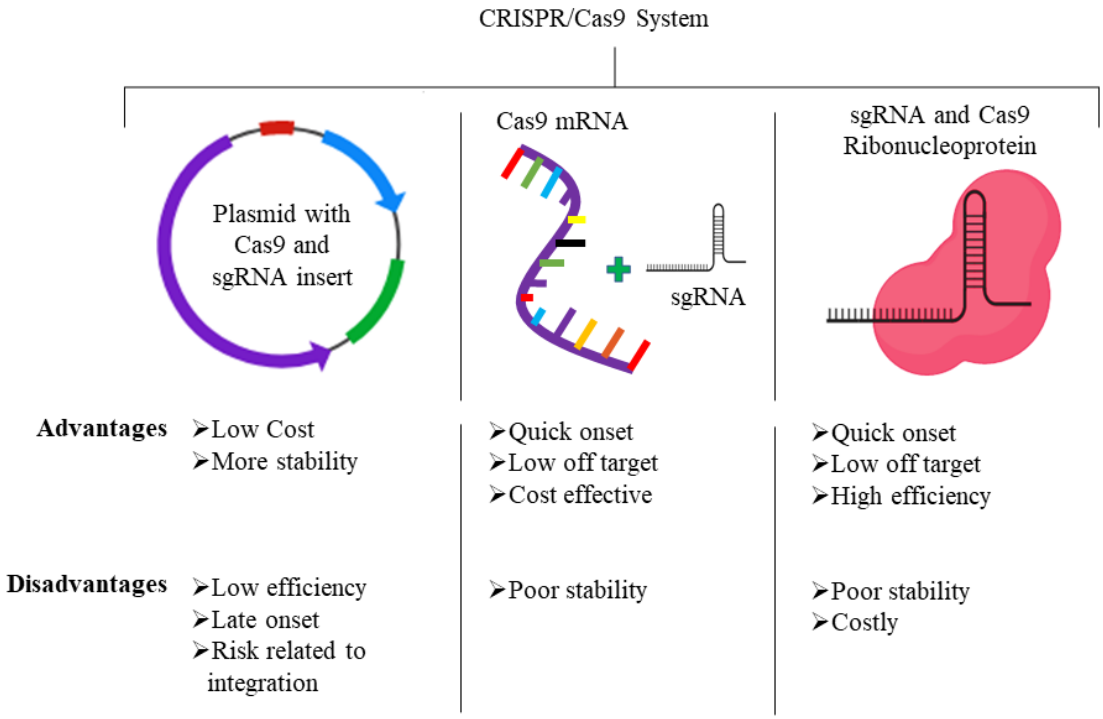

Figure 1.2. Various forms of CRISPR/Cas9 including plasmid, mRNA and ribonucleoproteins (RNPs) that could be delivered to achieve significant gene editing to treat retinal dystrophies

However, CRISPR/Cas9 expressing plasmid is the ancient form of deliverable CRISR and offers several advantages discussed below.

(i) Versatility: CRISPR/Cas9 plasmid delivery allows targeted gene editing in various cell types and organisms, making it applicable to various research areas and potential therapeutic interventions.

(ii) Customizability: Plasmids can be easily designed and modified to incorporate Cas9 variants, gRNA sequences, or other functional elements. This flexibility enables researchers to customize the CRISPR/Cas9 system for experimental or therapeutic purposes.

(iii) Cost-effectiveness: Plasmids are relatively inexpensive to produce than other delivery methods like viral vectors. They can be generated in large quantities and easily scaled up, making CRISPR/Cas9 plasmid delivery a cost-effective option for many laboratories.

CRISPR/Cas9 plasmid delivery also presents some challenges discussed below.

(i) Efficiency: One of the challenges of CRISPR/Cas9 plasmid delivery is achieving high editing efficiency in target cells. Efficient delivery and expression of Cas9 and gRNA are crucial for successful gene editing. However, not all cell types are equally amenable to plasmid delivery, and some may exhibit low transfection efficiency.

(ii) Off-target effects: Although CRISPR/Cas9 technology is highly specific, there is still a risk of off-target effects, where unintended DNA sequences may be edited. Careful design, validation of gRNA sequences, and thorough assessment of potential off-target effects are necessary to minimize this risk.

(iii) Delivery barriers: High molecular weight and sensitivity towards degradation by nucleases make their *in vivo* delivery challenging.

(iv) Immunogenicity: Plasmid delivery can sometimes activate immune responses, leading to inflammation or rejection. This immune response may limit the effectiveness of CRISPR/Cas9 plasmid delivery, particularly for *in vivo* applications.

As the field of gene editing continues to advance, scientists are actively working to overcome these challenges and improve the efficacy and safety of CRISPR/Cas9 plasmid delivery.

Eye-related diseases, especially retinal dystrophies, are degenerative conditions marked with clinical and genetic heterogeneity and affect 1 out of every 4000 people all over the globe. More than 238 mutant genes that decide the phenotype are explored till now. The complexity of the neuronal pathways, the physiological barrier due to the anatomy of the eyes, the structure of each cell, and the diversity of functions of each retinal layer create many challenges in developing therapeutic strategies for these diseases. The most common site where the therapeutic agents need to work is the posterior part of the eyes, which is quite accessible through conventional routes. The intravitreal route is beneficial in such cases with some risk of eye damage and requires expertise. There are treatments for dystrophic conditions, such as

wAMD, wherein anti-VEGF antibodies are injected through the intravitreal and were found to be beneficial. But the treatment needs multiple dosing over time and can cause eye damage due to multiple intravitreal injections. Therefore, a more relevant system must be developed to overcome such hurdles. Gene editing in recent times has grown to treat diseases characterized by a gene mutation. CRISPR/Cas9 system could be directed towards a specific gene sequence to edit a mutation. This technique has been explored for retinal diseases since the unique anatomical position, immune-privileged nature, blood-retinal barrier, and identified underlying mutation make the eye, specifically the retina, amenable for therapeutic gene editing [12, 13].

Table 1.1. Pros and cons of the viral and non-viral delivery carriers used for CRISPR/Cas9 delivery to the eye

Delivery vehicle	Pros	Cons
Viral vectors (Lentivirus, Adenovirus, baculovirus)	• High transfection ex vivo • High efficiency	• Risk of insertion mutagenesis [14] • Immune response [14] • Low loading efficiency • Low *in vivo* efficiency • Difficult to handle • High cost • Cannot deliver RNPs
Non-Viral vectors (Polymeric nanoparticles, dendrimers, exosomes, Liposomes, Lipid nanoparticles, polymeric micelles)	• Low cost • Ease of handling • Ease of preparation • High loading • Can be prepared for target delivery • Low immunogenicity [15] • Can deliver RNPs • *In vivo* stability • Less risk of mutagenesis [15] • Flexibility	• Comparative low efficiency and transfection • Toxicity [15] • Scalability

Wherein it provides immense potential because of its one-time treatment possibilities *via* gene editing. CRISPR/Cas9 tool, however, is facing several delivery difficulties due to its considerable molecular weight. Although some viral vectors are available with limitations

(Table 1.1), developing an efficient delivery vehicle for CRISPR/Cas is the need of the hour. Nanotechnology-based non-viral carriers such as polymeric nanoparticles, liposomes, micelles, dendrimers, etc. are currently being explored positively for the delivery of CRISPR/Cas9. This review highlights the current scenario of retinal dystrophic conditions and potential CRISPR/Cas-based nanomedicines used in treatment.

1.2. Applications of CRISPR/Cas system: Beyond double-strand break

After the success of the spCas9 as a gene-editing tool, it has been explored more for several other applications. Despite the specificity, the large size (1368 amino acids) of spCas9 makes it challenging to deliver using viral vectors. Therefore, ample variants or orthologs have been discovered till now. *Campylobacter jejuni* (CjCas9) (984 amino acid) is the smallest Cas9 nuclease discovered in 2017 [16]**.** Later in 2017, the Zhang group discovered Cas13 as a new orthologue having RNA targeting potential [17]. In 2013, Qi et al. used a dead version of Cas9 (i.e. dCas9) RNPs to suppress the gene expression by interfering with the RNA polymerase binding mechanism [18]. Additionally, the same group reported the application of dCas9 protein fused with transcriptional repressor KRAB (dCas9-KRAB) in gene silencing (CRISPRi) [19]. Later in 2013, dCas9 protein fused with transcriptional activators VP64 was explored as a gene activator, i.e. CRISPRa, making CRISPR a suitable tool for transcriptional programming [20]. In 2017, the Liu group reported CRISPR as a base editor without introducing DSB [21]. dCas9 fused with epigenome modifier, or the fluorescent tag was also used for the epigenome editing [22] and imaging [23], respectively. Recently, CRISPR/Cas system was also utilized as a diagnostic tool for detecting Covid-19 infection [24]. Collectively, CRISPR/Cas has ample application beyond DSB-mediated gene editing. CRISPR has been potentially recognized as a tool for diagnostics, epigenome editing, gene regulation (CRISPRi/CRISPRa), imaging, etc (Figure 1.3).

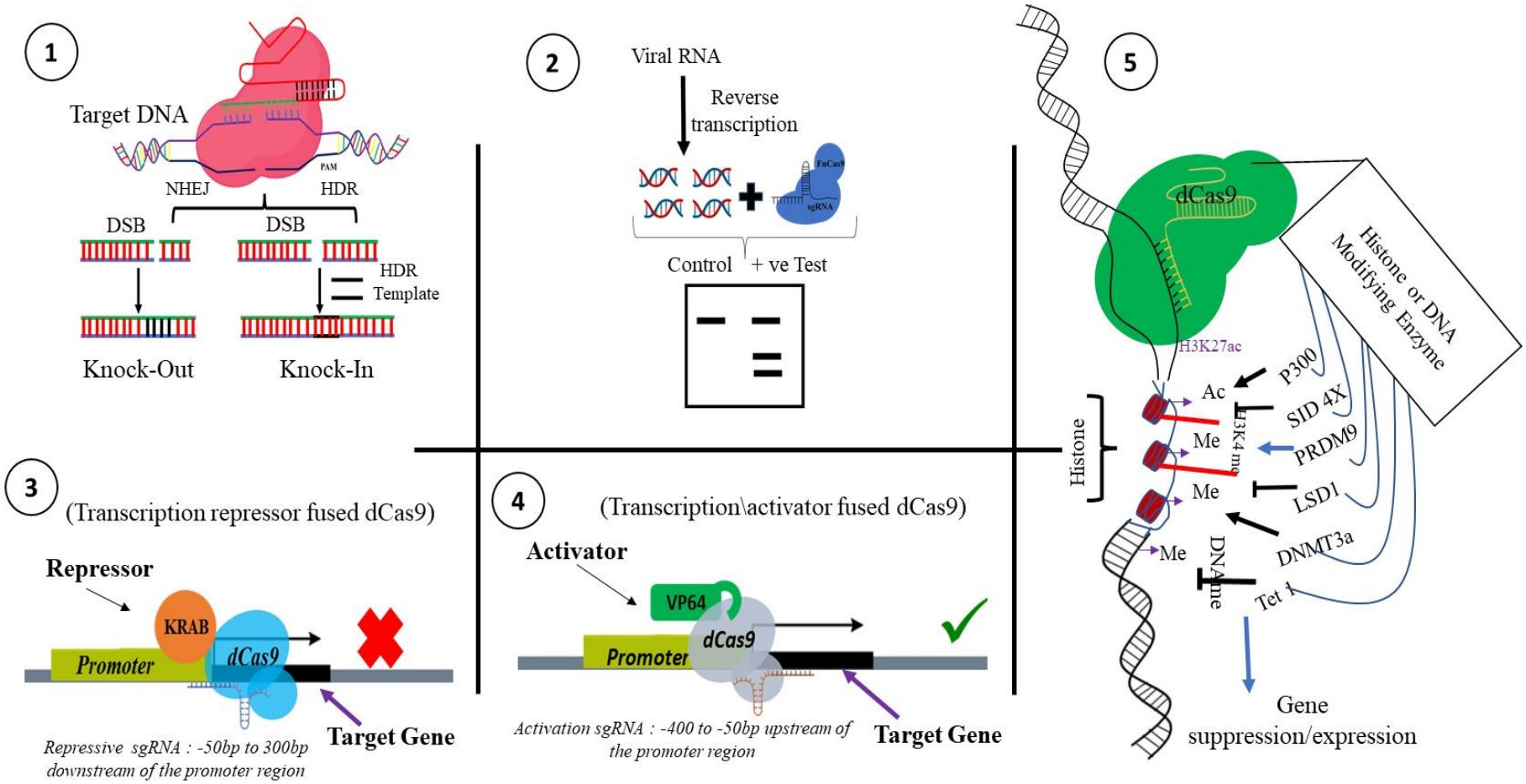

Figure 1.3. Applications of CRISPR/Cas technology, 1: Double strand break mediated *knock out* or *knock in*, 2: Diagnostic application, 3: dCas9 mediated transcription repression, 4: dCas9 mediated transcription activation, and 5: Epigenome editing.

1.3. Retinal dystrophies

The mammalian retina is being widely studied for genetic disorders for the following reasons. Multiple phenotypes of the retina can be directly observed, and photographs can be recorded. The effects of psychophysical parameters (acuity, field, color contrast) can be documented, and retinal electrophysiology can be used to assess retinal functions [25]. Lastly, the ease of visualization of the retina has led to the development of many animal models that have led to a better understanding of pathways leading to photoreceptor death [26]. Worldwide, 1 in every 2000 people suffers from inherited retinal dystrophies (IRD). Individuals with IRD typically present with progressive vision loss that ultimately results in blindness. Since these diseases are genetic and clinically heterogeneous, hardly any effective treatments are available. Multiple cells, gene, and drug-based therapies are in different phases of clinical trials for IRD [27]. Inherited retinal diseases (IRD) are distinguished by continuous degeneration of retinal pigment epithelium (RPE) and the neural retina. These dystrophies are of various types, such as cone-dominant dystrophy (cone-rod/cone dystrophy), rod-dominant dystrophy (retinitis pigmentosa/RP/ rod-cone dystrophy), pattern dystrophy, macular dystrophy (Best macular dystrophy, Stargardt disease, Sors by fundus dystrophy), photoreceptors and bipolar cells abnormality (congenital stationary night blindness [CSNB], X-linked retinoschisis, hereditary choroidal diseases, and vitreoretinopathies (Stickler syndrome, Wagner syndrome) [28, 29]**.**

1.3.1. CRISPR/Cas for correcting retinal dystrophies

Genome therapy using CRISPR-Cas in ophthalmic diseases may be promising, considering the scale of impact on society and the various monogenic disorders of the eye [30]. Hopes are high to attenuate inherited retinal disorders due to the multiple clinical trials initiated for specific retinal conditions with advancing gene therapy technology [31]. Table 1.2 shows various pre-clinical studies related to using the CRISPR/Cas system to treat retinal dystrophies. Over the last two decades, eye tissue has become a frontline organ for gene therapy. It is

achieved either by using viral vectors to transfer correct cDNA copies or through RNA intrusion to knockdown proteins with dominant-negative traits or toxic inclusion of functionalities via gene silencing [32]. Before the arrival of gene therapy, retinal dystrophies were incurable [33]. Indeed, IRDs have been demonstrated as ideal candidates for gene therapy because: (i) they are inherited diseases linked to multiple genes, and a subset of them show monogenic inheritance [34], (ii) the cells which are affected (PRs and RPE) can be accessed by various clinical and surgical procedures [35], (iii) the non-invasive diagnosis methods used in the clinics for IR patients could be translated to animal models and (iv) availability of animals models to study the eye conditions. The Phase III data for Spark Therapeutics' gene therapy product (i.e., SPK-RPE65) for treating patients with visual impairment caused by RPE65 gene defects provides hope for clinical translation opportunities. SPK-RPE65 is an AAV2 gene therapy that delivers the RPE65 gene via subretinal injection to patients with a defective RPE65 gene. Clinical trial outcomes were found beneficial, and the therapy, SPK-RPE65, was approved by the FDA in 2019 with the trade name of LUXTURNA for treating vision loss in the patient [36]. The therapy is based on recombinant adeno-associated virus (AAV) vectors expressing the human *RPE65* cDNA using a viral promoter as a control [36]. Although gene therapy provides immense potential for treating various genetic diseases, it poses some disadvantages, like off-target effects and DNA mutation risk. These disadvantages limit their application in several cases.

Therefore, gene editing tools such as ZFN and TALEN have been developed to treat genetic diseases. Moreover, in recent times CRISPR/Cas9-based gene editing tool is being explored for the treatment of genetic disease through its unique site-specific gene editing efficiency. Here, multiple guide RNAs are being used simultaneously to target various sites in the genome, a striking feature of the CRISPR/Cas system [37]. A significant advantage of deploying CRISPR-Cas is that it is an RNA-based system; thus, custom guide RNAs can be

efficiently designed to target within the genome. At the same time, ZFN and TALEN systems are protein-DNA interfaces, which are protein-dependent, making it difficult to engineer for a given target [38]. The potential for multiplexed genome surgery is another interesting feature of the CRISPR-Cas system using several gRNAs for the concomitant editing of multiple sites within the genome [37].

The CRISPR system in Streptococcus pyogenes is being reconstituted in mammalian cells such that the RNA-guided genome targeting has shown high effectiveness in human cells [39]. Some of the significant mutation-based retinal dystrophic conditions are discussed below.

1.3.1.1. Leber's Congenital Amaurosis (LCA)

LCA has been known to be the most severe retinal dystrophy as it potentially leads to congenital blindness in less than one year of age. Fourteen mutated genes have been identified by homozygosity mapping, linkage analysis and genome analysis in LCA patients and children with retinal degeneration constituting approximately 70% of the cases [40]. LCA is mainly associated with severe defects, including roving eye movements called nystagmus. Also, slow reactions of the pupil and lack of electroretinographic reactions are some of the symptoms in children [41, 42]. Genes involved in LCA encode proteins which are responsible for retinal functions, such as photoreceptor morphogenesis (CRB1, CRX), vitamin A cycling (LRAT, RPE65, RDH12), phototransduction (AIPL1, GUCY2D), guanine synthesis (IMPDH1), and outer segment phagocytosis (MERTK) and also intra-photoreceptor ciliary transport processes (CEP290, RPGRIP1, LCA5, TULP1) [40]. The most prominently studied gene for LCA is mutations in the RPE (*RPE65*) gene, which is responsible for encoding retinoid isomerase [30], whereas the most frequently occurring mutations are associated with the *CEP290* (15%), *GUCY2D* (12%), and *CRB1* (10%). Around 20% of patients in north-western Europe have an intronic *CEP290* mutation (p.Cys998X). An AVV-CRISPR system has been developed for *in*

vivo treatment of autosomal dominant retinitis pigmentosa (adRP) and LCA10 in mice. In this study, the AAV-SpCas9 vector was delivered via subretinal injections that target the RHO or CEP290 and Nrl (neural retina leucine zipper transcription factor) gene in mouse models for adRP. The outcomes of the study showed the expression of spCas9 protein in the retinal cells of the mice for 9.5 months. While the authors have deployed different AAV serotypes and different vector doses, the results proved effective restoration of RP or LCA10 phenotype without off-target effects and adverse toxic reactions [43, 44]. Later, the strategy was adopted to successfully resolve the RHO gene mutation in human cells. CRISPR/Cas9 technology has proved effective at targeting genes/alleles in an efficient and specific manner in this study, demonstrating that it could be used in the treatment of RP and other genetic disorders, including dominant human conditions.

1.3.1.2. Age-related macular degeneration

Age-related macular degeneration (AMD) is a multi-genetic disorder influenced by multiple genes [30]. Wet AMD, the neovascular form of AMD, is marked by abnormal growth of the choroidal vessels in the macula region of the retina, resulting in loss of central vision. The macula is enriched with cone photoreceptors and is responsible for bright light activities and color vision [45]. Neovascularization in wet D occurs due to the overproduction of vascular endothelial growth factor (VEGF); hence anti-VEGF agents become the therapy of choice [46]. Currently, wet AMD patients are treated with intravitreal injection of anti-VEGF agents such as ranibizumab, aflibercept and bevacizumab [47]. For the treatment of AMD, AAV-CRISPR systems have also been developed based on CjCas9 (*Campylobacter jejuni*) [48] and LbCpcf1 nucleases (nucleases which are a member of the type-V CRISPR-Cas systems). In the study, authors packaged the CjCas9 gene, its corresponding sgRNA sequence, along with a marker gene into an adeno-associated virus (AAV) vector. Being highly specific,

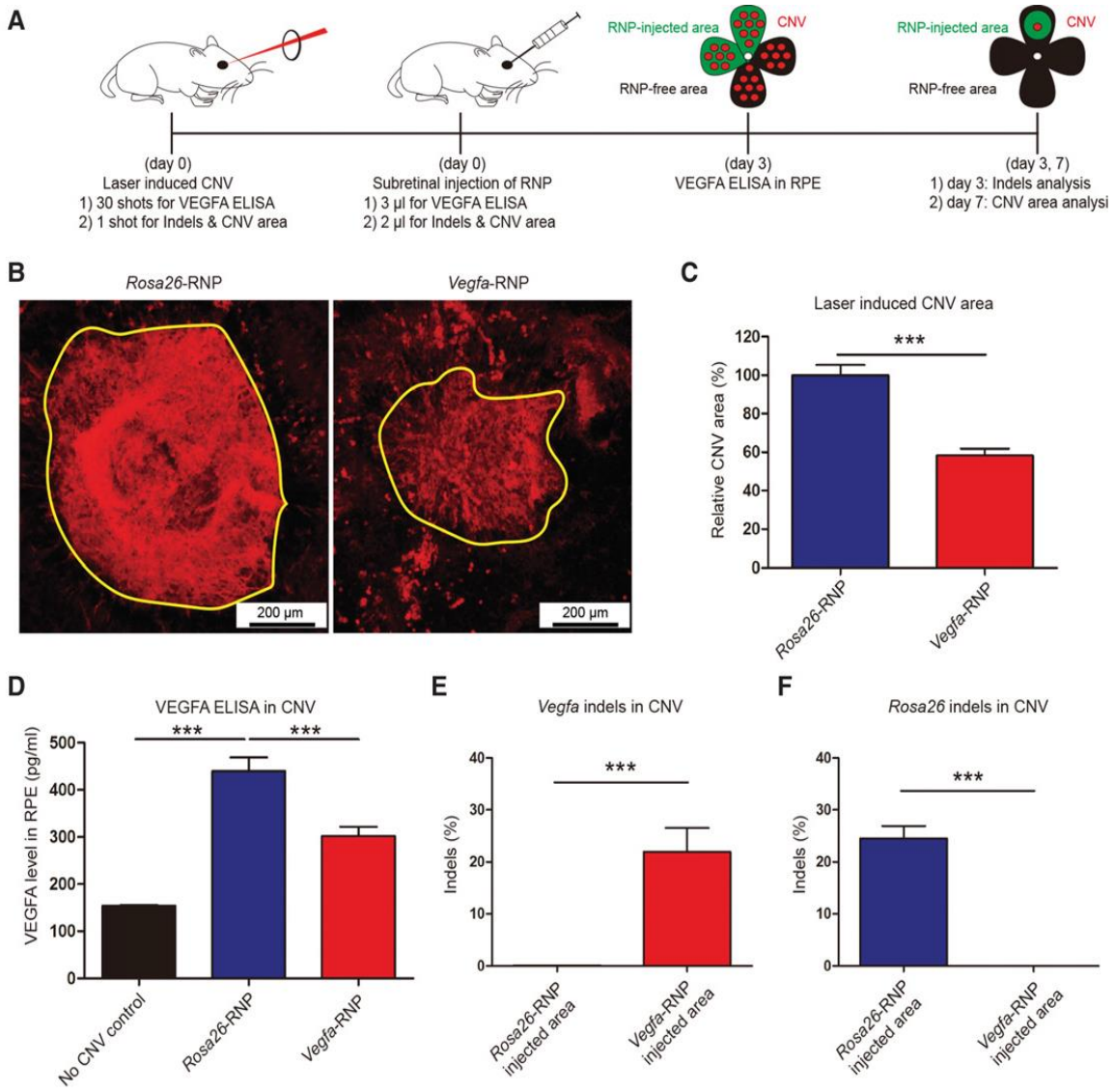

Figure 1.4. VEGF A gene editing efficiency of Cas9 RNPs in retinal dystrophy in mice. A) The overall study outline, herein, CNV model was developed in mice using laser followed by subretinal injection of VEGF A targeting Cas9 RNP. After 7 days of injection RPE complexes were analyzed for CNV area and deep sequencing was performed to evaluate gene editing in the targeted cells/tissues. Meanwhile, after 3 days of injection VEGFA ELISA was also performed. (B) Representative laser-induced CNV stained with isolectin B4 (IB4) in C57BL/6J mice injected with the Rosa26-specific Cas9 RNP (as a control) or the Vegfa-RNP. The area of CNV is demonstrated as yellow line. C) CNV area. D) level of VEGF A in the CNV area. E) Gene editing in terms of indel in RPE cells at VEGFA targeted site. Reprinted from Kim et al 2017, licensed under CC BY 4.0 (https://creativecommons.org/licenses/by/4.0/legalcode). Copyright © 2017 Kim, K., Park, S.W., Kim, J.H., Lee, S.H., Kim, D., Koo, T., Kim, K.E., Kim, J.H and Kim, J.S. Published by Cold Spring Harbor Laboratory Press.

CjCas9 can cleave only a restricted number of sites in the human or mouse genome. Hence, when delivered using AAV, CjCas9 lead to targeted mutations in the retinal pigment epithelium (RPE) cells. CjCas9 can be specifically targeted to the *Vegfa* or *Hif1a* gene in RPE cells thereby, decreasing the size of laser-induced choroidal neovascularization, making *in vivo* genome editing with CjCas9 a new advancement in the therapy of AMD. Further, the results indicated an Indel efficiency of 22±3 and 31±2 percentage for VEGFA and Hifla genes, respectively, at 6 weeks post-injection of AAV-CjCas9 intravitreally. Moreover, the effect of Indel was also seen at the protein level, where a significant decrease in VEGF-A protein was observed in RPE cells with respect to the control group. In 2017, Kim et al. targeted the VEGFA gene to treat wAMD using mouse and human cell lines, i.e. NIH3T3 and ARPE19. In this study, sgRNA/Cas9 expressing plasmid and Cas9 RNPs were delivered using lipofectamine 2000, wherein Cas9 RNPs showed 82 ± 5% and 57 ± 3% indel in NIH3T3 and ARPE-19 cells, respectively. A comparative study indicated that the Cas9 RNPs were more effective with respect to plasmid on 2nd day of transfection. Further, it was observed that level of VEGF A mRNA and protein reduced to 40 ± 8% and 52 ± 9%, respectively, in ARPE cells after Cas9 RNPs treatment. For *in vivo* efficacy evaluation, Cy3-labeled RNPs were delivered via intravitreal injection. The results indicated the accumulation of Cy3 dye into RPE cells after 3 days post injection, and 25 ± 3% of indel was also detected in RPE cells at the delivery site. Moreover, the CNV model was also developed in mice using a laser (to mimic wAMD) followed by subretinal injection of Cas9 RNPs. After 3 days, 22 ± 5% indel was observed in RPE cells for the VEGFA gene. Additionally, Cas9 RNPs treatment significantly reduced CNV area by 8 ± 4% and VEGF A protein level (Figure 1.4) [49].

1.3.1.3. Retinitis Pigmentosa

Retinitis pigmentosa (RP), affecting 1 in 4000 people, has become the leading cause of progressive blindness [50]. Classical RP, also known as rod-cone dystrophy, is identified by

"tunnel vision", which is a progressive loss of peripheral vision. The first signs include nyctalopia, the development of night blindness and difficulties in adapting to the dark that occurred through the loss of rod function in the early years of life [51]. The RPE, or retinal pigment epithelium, starts losing its pigment due to the loss of a photoreceptor that ultimately leads to the accumulation of intraretinal melanin deposits, which look like a "bone spicule" conformation. However, the central vision remains intact until the last stages. It can be inherited through different transmission modes, such as autosomal dominant, autosomal recessive, or X-linked, and is heterogeneously related to mutations in at least 79 genes [50]. RP is mainly of two types, MERTK-associated and RPGR X-linked. The RPE apical membrane contains light-sensitive photoreceptors, and its turnover is enabled by MERTK (Mer tyrosine kinase), the receptor involved in the phagocytosis of the rods and cones [52]. These photoreceptors must be continuously recycled for efficient working, disrupted by mutations in *MERTK*, leading to degradation and loss of photoreceptors [53]**.** Meta analyses have revealed that only 3% of MERTK type RP are due to autosomal recessive transmission [54, 55] and cause macular atrophy and early-age photoreceptor abnormality [56, 57]. Mutations in RP GTPase regulator (RPGR), an X-linked RP, is seen in 1 in 3,500 people. RPGR, along with the Δ subunit of rod cGMP phosphodiesterase, regulates the proteins, and its dysfunction leads to progressive loss of central vision and night blindness [58-61]**.** Some *in vitro* and *in vivo* studies have been reported where retinitis pigmentosa has been treated using CRISPR/Cas9 technology. For example, CRISPR/Cas9 tool in a rat model of autosomal dominant retinitis pigmentosa (adRP) by Bakondi et al. in 2016 to ablate mutation in the rhodopsin gene (RhoS334). In this study, sgRNA/Cas9 plasmid (targeting exon 1 immediately upstream of a PAM unique to the RhoS334 locus) was administered intravitreally in S334ter-3 rats. Genome analysis of transfected retinal cells confirmed a cleavage efficiency of 33% and 36% in two rats. Also, improved visual acuity and extensive preservation of the retina were observed *via*

immunohistology following sgRNA/Cas9 plasmid injection [62]. In addition, a CRISPR/Cas-based strategy was developed by Latella et al. for editing RHO gene mutations. In this study, a plasmid was designed that contained an insert for two sgRNAs, targeting the RHO gene to cause DSB followed by NHEJ. The study's outcome dictated the successful editing of the RHO gene, which further downregulated the expression of the RHO protein.

Further, Bassuk et al. treated X-linked retinitis pigmentosa (XLRP) by correcting RPGR point mutation using CRISPR/Cas9 in iPSCs. In this report where CRISPR was used to treat the pathogenic mutation in iPSCs obtained from a patient with photoreceptor degeneration. The authors screened 21 different sgRNAs for editing, where g58 was the most compelling. Therefore, g58/Cas9 expressing plasmid was designed and transfected into iPSCs along with an RPGR single-stranded oligodeoxyribonucleotide (ssODN), which acts as a donor during the HDR pathway. Further, deep sequencing was performed, and the data revealed the successful mutation correction in 13% of transfected cells [63].

Moreover, the results showed that TAG (premature stop codon) gets replaced by GAG (wild-type codon), which encodes glutamate at residue 1024. On the other hand, no changes in the mutation were seen in the untransfected iPSCs. Further, it was concluded that the correction rate of 13% was significantly fruitful and can be improved by minimizing error-prone NHEJ by inhibiting DNA ligase IV at the DNA cleavage site.

In addition, a CRISPR/Cas-based strategy was developed by Latella et al. for editing RHO gene mutations in a mouse model of ADRP. In this study, a plasmid contained an insert for two sgRNAs, targeting the RHO gene (exon 1) having a P23H dominant mutation. Firstly, the gene editing was performed *in vitro* in HeLa cells, where 70%, 76%, and 82% of Indel frequency was observed with sgRNA1, sgRNA3, and 2sgRNA, respectively. Additionally, the RHO expression was also observed using Real-time Taqman PCR wherein 35%, 25% and 20% of reduction in expression was seen with cells treated with sgRNA1, sgRNA3, and 2sgRNA,

respectively. Later, the electroporation of CRISPR/Cas plasmid containing 2sgRNA and GFP expression was performed subretinally in P23 RHO transgenic mice. The GFP-expressing section of the retina was isolated and evaluated for the Cas9 expression, wherein the Cas9 expression was limited to the cells expressing GFP along with 84 edited sequences [64].

1.3.1.4. Choroideremia

Choroideremia is named from the complete loss of the choroid, retina, and retinal pigment epithelium, exposing the underlying white sclera, which is unique to the disease [65]. Choroideremia (CHM) is an X-linked recessive degenerative retinal dystrophy affecting 1 in 50,000 individuals and is only associated with males. Due to mutations in *the CHM* gene, which encodes for Rab escort protein 1 (REP1) and its dysfunction leads to progressive loss of vision and choroid atrophy. It starts with night blindness in the early years of life, with a gradual decline in peripheral vision and legal blindness by 50-70 years of age [66]**.** The CHM disease is characterized by retinal thickening, resulting from Müller cell activation and photoreceptor layer hypertrophy. This further causes RPE depigmentation, degeneration of photoreceptors and retinal remodelling. Hence, retinal remodelling is considered a possible strategy for in-vivo studies [67]**.**

1.3.1.5. Stargardt Disease

Stargardt disease is an autosomal recessive genetic disorder majorly caused by mutations in the ABCA4 (ATP-binding cassette, subfamily A, member 4) gene and is the most common form of juvenile-onset macular degeneration. It is characterized by the loss of central vision due to the gradual accumulation of cytotoxic lipofuscin within the RPE [68]. This disease affects at least 1 in 10,000 people, with approximately 31,000 cases in the United States. The disorder consists of a fast macula degeneration resulting from the deposition of lipid-enriched deposits called lipofuscin (comprised mainly of A2E, a vitamin A derivative) in

the retinal pigment epithelium (RPE) cell layer. Due to this, the interaction between photoreceptors and RPE is affected, causing the death of photoreceptors by hampering their ability to uptake nutrients and perform the visual cycle [69].

1.3.1.6. Usher Syndrome

With a prevalence of 1 in 20,000, Usher Syndrome is one of the common forms of syndromic IRD. Its unique features include RP and hearing loss [70]**.** The heterogenous syndrome is classified into three subtypes depending on the progression and severity of the hearing loss and the age of onset of the RP. Usher syndrome type 1 (USH1) is the most critical; Usher syndrome type 2 (USH2) presents moderate to severe symptoms and is most frequently observed. Lastly, Usher syndrome type 3 (USH3) is characterized by a moderate phenotype, and the onset of the disease and its progression could vary on a case-by-case basis [71]**.** Usher syndrome type 1 (USH1) is the most common cause of deaf-blindness in humans, characterized by vestibular dysfunction, profound congenital deafness and retinitis pigmentosa and is inherited in an autosomal recessive manner. USH1 is caused due to mutations in myosin VIIA, which encodes for an organelle transport protein within the RPE [46]. In 2017, Fuster-Garca et al. proposed using CRISPR/Cas9 gene editing to restore the c.2299delG mutation in the USH2A gene. Human dermal fibroblast (HDFs) cells were isolated from a USH2 patient with c.2299delG mutation and used for gene editing. Briefly, using nucleofection, a Cas9 RNPs (comprising Cas9 (15 µg) and sgRNA (20 µg)) was transfected into HDFs of the regular patient, yielding 18% indel frequency. Subsequently, RNPs were co-delivered with ssODN-2299, which yielded HDR efficiency of 5%. Similarly, HDFs of the patient with c.2299delG mutation were transfected with ssODN with a WT sequence and the PAM sequence ablated. The results revealed 6% indel frequency and a 2.5% HDR [72].

1.3.1.7. Best disease

Bestrophin, encoded by the BEST1 (VMD2) gene, is a transmembrane protein expressed on the basolateral aspect of the RPE cells and is responsible for the conduction of chlorine across the RPE. Mutations in the BEST1 (VMD2) gene, and hence bestrophin, hampered the fluid transport across the RPE, thereby causing debris to build up between the RPE and photoreceptors. Consequently, atrophic macula scar and central visual loss occur quickly, leading to Best disease or Vitelliform macular dystrophy. It affects between 1 and 9/100,000 people and is inherited in an autosomal dominant manner. Many other retinal dystrophies can also occur due to BEST1 mutations, including retinitis pigmentosa and ADVIRC (Autosomal Dominant Vitreo Retino Choroidopathy). Biallelic mutations lead to multifocal small egg yolk deposits leading to Recessive Best Disease. Neovascularization in the choroid, along with haemorrhage and leak into the retina, further aggravates the disease condition, and intravitreal anti-VEGF agents can be used for successful therapy [73]. In the year 2020, Sinha et al. demonstrated gene augmentation's effectiveness in treating the best disease. Induced pluripotent stem cell-derived retinal pigment epithelium (iPSC-RPE) was used as an *in vitro* Best disease model for this objective. Gene augmentation restored BEST1 gene activity and improved rhodopsin degradation. Meanwhile, some of the mutations did not respond to the gene augmentation; therefore, CRISPR/Cas9 was used to investigate the efficiency of site-specific gene editing in iPSCs RPE models. The findings revealed that CRISPR/Cas9 edits the mutant BEST1 gene while leaving the wild-type BEST1 gene intact. Off-target indels were also tested; however, no evidence of off-target gene editing was reported. The study overall revealed the application of CRISPR/Cas-based precise and specific gene editing for the management of retinal dystrophies [74].

1.3.1.8. X-linked juvenile retinoschisis

RS1 is a retinoschisis gene that encodes a protein responsible for cell adhesion. Mainly observed in males, RS1 mutations cause the development of cystic cavities in the retina's centre that enlarge gradually with age, along with decreased visual acuity. As the dystrophy progresses in the retinal periphery, the condition of the split retina worsens with large atrophic holes; hence, the residual retinal blood vessels are left hanging in the vitreous cavity above the retina, which may result in vitreous haemorrhage. It has been observed that people with this disease usually have a refractive error of long-sightedness. Worldwide, about 1 in every 5000 to 25000 suffer from the condition. Children who suffer slowly lose out on central vision; however, most children can complete a fully sighted education with the help of magnified texts and teachers for visual support. The primary therapy for retinal cysts is the topical or oral administration of carbonic anhydrase inhibitors, although a significant improvement in symptoms is rare [73]. Huang et al. developed a base editing strategy to cure XLRS in 2019. Using patients' induced pluripotent stem cells (hiPSCs), a 3D retinal organoid model with XLRS characteristics was created *in vitro*. CRISPR/Cas9 targeting the C625T mutation in the RS1 gene was introduced as a plasmid using a viral vector to evaluate the model. According to the findings, CRISPR effectively repairs gene mutations while correcting the phenotypes by up to 50%. The findings also revealed the existence of off-target indel, a CRISPR constraint [75].

1.3.1.9. Congenital stationary night blindness (CSNB)

CSNB, also called nyctalopia, is a non-progressive type of night blindness. Patients suffering from this condition have difficulty observing in low light. The symptoms start early in children, along with low amplitude nystagmus, strabismus and reduced visual acuity [76]. Associated with 17 genes, CSNB is a polygenic disease, and diagnosis involves

electroretinography to measure photoreceptor function. The ERG results may show a lack of rod functioning or incomplete functioning of both cone and rod, as well as abnormal fundus upon examination. The state of complete CSNB is caused when bipolar cell signalling is disrupted, leaving a single intact alternate pathway [77]. CSNB is of four subtypes - Schubert Bornstein (branched into complete and incomplete), Riggs, Fundus Albipunctatus and Oguchi Disease, of which the last two types show abnormal fundus. Myopia and photophobia are two of the prominent features observed in patients. Children with 'incomplete' CSNB may not be aware of the condition as the symptoms are mild and central vision is reduced from average [73].

1.3.1.10. Achromatopsia

Achromatopsia is a rare autosomal recessive disease affecting only 1 in 30,000 to 40,000 people. Mutations in six genes have been identified as responsible for this disease. 75% cases are due to CNGB3 and CNGA3, while the rest are accounted by GNAT2, PDE6C, PDE6H and ATF6. There is complete colour blindness, and central vision is diminished. Patients have to deal with profound photophobia and nystagmus in the early months. However, the nystagmus in achromatopsia patients is pendular or horizontal, unlike the roving nystagmus of LCA. The diagnosis involves electrophysiology, where it is observed that the function of cone photoreceptors is absent, and rods function normally. Usually, the complete form is seen, and the incomplete form with a milder phenotype tends to be much rare. The symptoms of the disease are mostly constant, and the glare and photophobia can be managed by incorporating red/brown shade glasses [73].

Table 1.2. Retinal dystrophies treated *via* genome engineering approach using different delivery strategies

Retinal Dystrophy	Mutant Gene	Therapeutic approach	Host	Mode of delivery	Result	Year	Ref
Leber's Congenital Amaurosis (LCA10)	RPE65	Gene therapy	Homo sapiens	AAV Vector	Slight visual function improvement	2015	[78]
	RPE65	CRISPR/Cas9	Rd12 mice	AAV Vector	RPE65 mutation correction	2019	[79]
	CEP290	CRISPR/Cas9	iPSCs	Plasmid vector	Successful repairment of mutations	2017	[80]
Age-related macular degeneration (wAMD)	VEGFA gene	CRISPR/Cas9	Mouse	Subretinal injection of Cas9 RNPs	Reduction in CNV area after Cas9 RNPs injection in mice bearing laser-induced AMD	2017	[49]
	VEGFA gene	CRISPR/Cas9	Mice	Lentiviral vector	*In vivo* disruption of VEGFA gene *in vivo* with 84% indel efficiency	2017	[81]
	VEGFA/HIF1 a gene	CRISPR-LbCpf1	Mouse	AAV vector	A long-term effect was seen when LbCpf1 targeted to Vegfa, or Hif1a was introduced as a therapeutic in CNV to avoid the hurdles during multiple injection strategies. CNV, potentially avoiding repetitive injections.	2018	[82]
	RP1L1	CRISPR/Cas9	Zebrafish	Direction injection of gRNA and Cas9 into the embryo	Generated model of RP1L1-associated photoreceptor disease and the first zebrafish model of photoreceptor degeneration with reported subretinal drusenoid deposits, a feature of age-related macular degeneration.	2020	[83]

Retinitis Pigmentosa (RP)	RPGR gene (exon 8)	CRISPR/Cas9	Mice	AAV vector	Successful development of Rpgr knock-out mouse model	2020	[84]
	RHO gene (P23H mutation)	CRISPR/Cas9	Mice	Plasmid vector	Successful editing in mutant P23H allele with a rate of approx 45%.	2018	[85]
	PDE6B gene	CRISPR/Cas9	Mice	Plasmid Vector	Repaired mutation efficiently	2016	[86]
	RHO gene	CRISPR/Cas9	Xenopus laevis	Co-injection of Cas9, eGFP mRNAs, and sgRNAs into fertilized eggs.	Introduced and characterized in-frame and out-of-frame Indel in three genes encoding rhodopsin.	2017	[87]
	RHO gene	CRISPR/Cas9	Rat	Plasmid vector	Improvement in visual function by preventing retinal degeneration	2016	[62]
	NRL gene	CRISPR/Cas9	Mouse	AAV vector	Successfully preserved cone cell function and improved survival of rod cells	2017	[88]
	RPGR	CRISPR/Cas9	Patient-derived iPSCs	Plasmid vector	Approx 13% of RPGR gene copies showed mutation correction and conversion to the wild-type allele.	2016	[63]
Usher Syndrome	USH2A gene	CRISPR/Cas9	HEK293 cells	pX330 vector	Repaired mutations efficiently	2017	[89]

	USH2A gene	CRISPR/Cas9	iPSCs,HEK 293T Cells	Plasmid vector	Repaired mutations efficiently with minimal off-target effects.	2020	[90]
Best disease	BEST1 gene mutations	CRISPR/Cas9	Ipsc	Lentiviral vector	Successfully reversal of the mutation with minimal off-target effects	2020	[74]
X-linked Juvenile retinoschisis (XLRS)	*RS1* gene mutations (C625T)	CRISPR/Cas9	hiPSCs	Plasmid vector	Showed a high efficiency of mutation repair	2019	[75]
	RS1gene mutation (*p.Y65X)*	TALEN	Mice	TALEN mRNA was co-injected into fertilized eggs	RS1-KI mice were viable, fertile and did not show significant physical abnormalities.	2018	[91]
Achromatopsia	CNG B3	Gene therapy	Mouse and Dog	AAV-hCNGB3 vectors via injection	Successfully rescued the function of cone photoreceptors.	2016	[92]
Progressive cone and cone-rod dystrophies	*RPGIP1*	Gene therapy	Dog	rAAV mediated *Rpgrip1* gene transfer via injection	Successfully rescued both cone and rod functions.	2014	[93]

1.3.1.11. Progressive cone and cone-rod dystrophies

As the name suggests, cone cell degeneration (COD) or cone followed by rod degeneration (CORD) are progressive retinal dystrophies seen from a young age. The significant difference between them is that rod involvement increases the severity of the disease, and by age 40, these people reach the stage of legal blindness [94]**.** Examination of the fundus and macula reveals an atrophic appearance or deposits of retinal pigments seen variably in different patients. Mutations in over 30 genes and molecular causes have been identified in around 20% and 74% of autosomal dominant and X-linked COD/CORD, respectively, while 23-25% of autosomal recessive types have been worked out [95].

Several ongoing clinical trials prove that gene therapy has made retinal dystrophies curable [30]. Furthermore, constraints such as multiple intravitreal injections resulting in physical retinal damage and resistance render the current therapy ineffective. Fortunately, the eye, and specifically the retina, is accessible to therapeutic gene editing due to its unique anatomical position, immune-privileged nature, presence of the blood-retinal barrier, and known underlying mutations [13]. As a result, the eye has been extensively studied for gene editing. However, just a few RDs in preclinical evidence related to effective gene editing utilizing CRISPR/Cas have been published, and more research in this field is needed.

Interestingly, some preclinical studies have been published wherein wAMD was treated by employing a CRISPR/Cas-based tool to knock out the VEGF A gene in RPE cells. Off-target effects and the deletion of some uncleared functions of the concerned gene are two key pitfalls that could be encountered with CRISPR. On the other hand, several groups are working to integrate data and screen for off-target effects [96-98]. It will be intriguing to observe if a CRISPR/Cas-based gene editing method can prevent angiogenesis

Table 1.3. Factor affecting the use of CRISPR/Cas system for gene editing in RDs

S. No	Factor	Description
1.	Ethical Issue [99]	While using CRISPR/Cas9, ethical issues will be there since CRISPR/Cas-based gene editing could result in serious off-target gene manipulations.
2.	Selection of gene [100]	For example, in LCA, 14 genes have mutations. Therefore, one should be clear about the gene that needs to be edited to improve the complications associated with the specific RD.
3.	*Knockout* [101]	*Knockout* is not always beneficial until and unless the role of the gene has been vastly understood. For instance, the *knockout* of the VEGF A gene is shown in wAMD to stop angiogenesis. But it cannot apply to every gene because one gene can be involved in various cellular functions, and *knockout* could cause the loss of some essential cellular functions.
4.	*Knockin* [102]	Some of the RDs require HDR. Since NHEJ is more prominent than *with respect to* HDR, one should consider this factor while utilizing the CRISPR/Cas technique.
5.	Vitreal barrier [103]	The presence of vitreous fluid may retard the diffusion of the CRISPR/Cas component toward the posterior segment of the eye. Additionally, the nucleases/proteases present in the vitreous could degrade the CRISPR components.
6.	Targeted Delivery	RD requires editing of the gene in retinal cells only; therefore, delivering the CRISPR/Cas component to retinal cells could be challenging.
7.	Off-target effect	While designing sgRNA for a specific gene, one should ensure the specificity of the sgRNA toward the gene of interest. Else, it could lead to undesired gene editing.
8.	PAM sequence [101]	As it is known that the CRISPR/Cas perform DSB near the PAM sequences (NGG, GGG); however, it is not always possible to have a PAM sequence at the desired gene editing site.
9.	Limited delivery route	Blood retinal barrier limits the distribution of therapeutic agents to the eye tissue, therefore, localized injection is the only potential alternative. Localized injection such as intravitreal (IVT) injection has the risk of eye damage and requires trained healthcare personnel.

in wAMD in clinical trials as it directly eliminates the fundamental cause of RDs. Further, the CRISPR/Cas-based therapy could also treat RDs with a single dose injection. We have discussed various factors that could be considered while adopting CRISPR/Cas9 to treat RDs (Table 1.3).

1.3.2. Use of CRISPR/Cas system for genome editing in RDs

The three main approaches for CRISPR-based genome editing include the use of (a) plasmid DNA (pDNA) that expresses the Cas9 protein and sgRNA, (b) mRNA that encodes the Cas protein, and (c) ribonucleoproteins (RNP) which is a complex of Cas9 protein and sgRNA. Among reported approaches, the plasmid-based approach is the simplest, while the RNP-based approach showed minimal off-target effects. Nevertheless, these CRISPR components should be delivered to the target cells, followed by their translocation to the nucleus. Due to the cargo's nature, different challenges, including packaging, immunogenicity, mutagenesis, extra- and intra-cellular barrier, etc., must be overcome to achieve efficient genome editing (Figure 1.5).

1.3.2.1. Vector packaging

The major challenge in delivering CRISPR components for therapy is their packaging into a single vector system. This problem is prevalent in all the approaches for CRISPR-based genome editing, be it a plasmid, RNA, or nucleoprotein. The maximum possible size for the cargo gene through the AAV route is ~4.7 kb, whereas that of the SpCas9 gene alone is ~4.3 kb. Hence, for the adeno-associated virus method, inserting additional CRISPR components like sgRNAs or extra genes becomes a hurdle. To solve this issue, various techniques, such as using a smaller-sized Cas9 (SaCas9) or splitting Cas9 into two vectors, have been propagated, but their feasibility for therapeutic applications has to be evaluated [104]. For the packaging of RNPs, viral vectors cannot be used. The use of non-viral vectors possesses many problems, be

it the high molecular weight of the protein, the highly negative charge, and/or the stability of the RNPs.

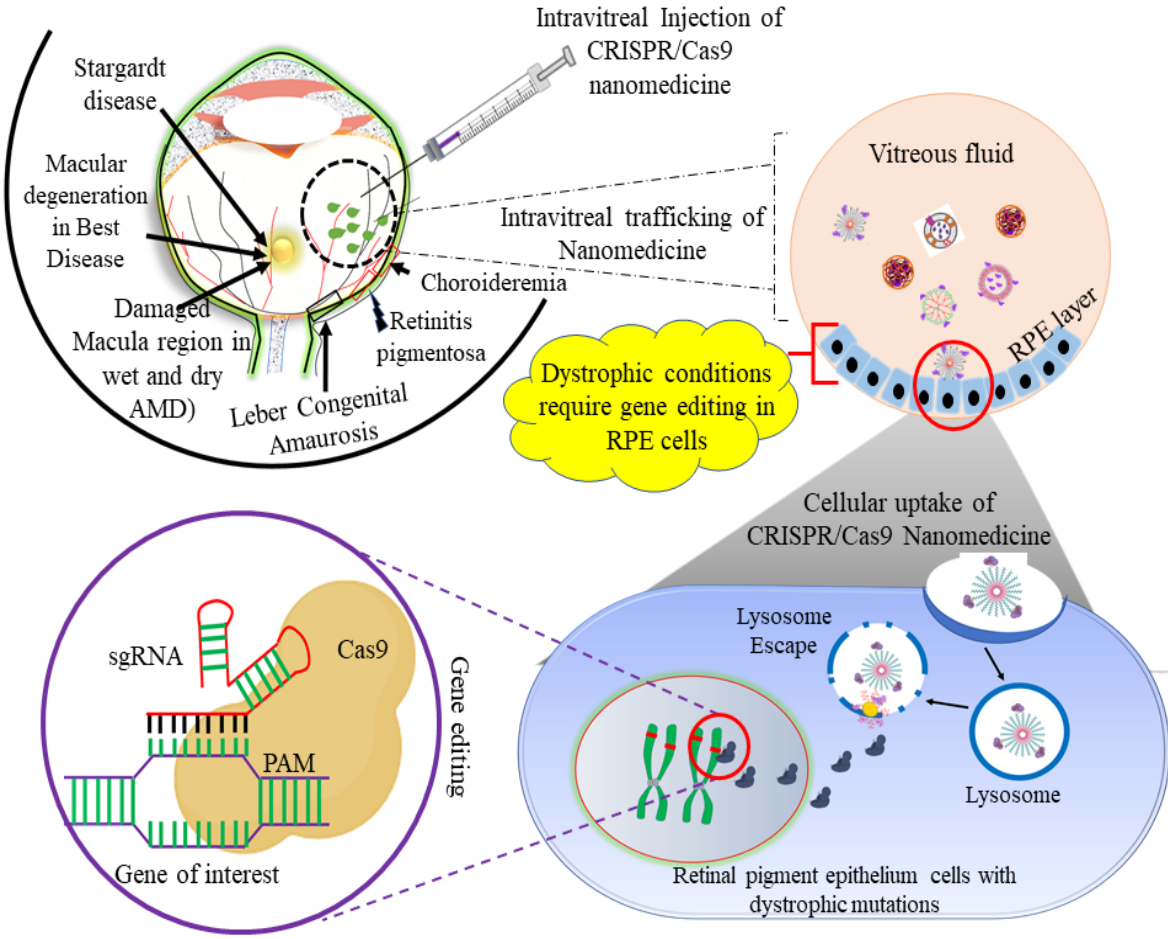

Figure 1.5. Schematic representation of nanomedicine trafficking in the treatment of retinal dystrophic conditions starting from 1) intravitreal injection, 2) diffusion through vitreous fluid, 3) cellular uptake, 4) endosomal escape and 5) interest specific gene editing.

1.3.2.1.1. Immunogenicity

CRISPR/Cas9 is a bacterial immune system; therefore, being bacteria-derived, they could lead to the immune response in the host. Specifically, if the gene-based approach is used, it could lead to the integration of Cas9 protein into the cells of the host. The expression of ectopic Cas9 protein in the individual could cause an MHC class I mediated immune response thereby, eliminating Cas9-expressing cells [105]. A study by Chew et al. showed that the *in*

vivo delivery of AAV vector delivery prompted immunogenicity not against the viral antigens but against the Cas9 protein. According to this result, the immunogenicity of AAV-CRISPR-Cas9 has been considered a critical property that destabilizes the host system and will negatively impact its application *in vivo* [106]**.** The best results have been found with a protein-based delivery of the CRISPR-Cas system, which has shown the least potential immunogenicity, as the ectopicCas9 protein is present only transiently in the host cells [104].

1.3.2.1.2. Insertional mutagenesis

Often, the vectors may get inserted in random sites within the genome, thereby causing mutagenesis of essential genes. When trials were conducted using a retroviral vector-based gene-therapy approach to treat SCID (Severe combined immunodeficiency), it caused the leukemic transformation, as the virus integrated into the host DNA [107] and triggered abnormal expression of the targeted gene**.** Tumorigenesis can result from vector insertions when the integration occurs near a protooncogene, thus posing a greater risk for integrating viral vector-based CRISPR delivery systems. This issue has been circumvented using non-integrating viral vectors such as AAV-based and protein/RNA-based CRISPR delivery systems [104].

1.3.2.1.3. Systemic delivery

CRISPR/Cas system must be delivered in cells or tissue of interest without risking any off-target effects. Therefore, transdermal or localized delivery routes are more advantageous than systemic delivery of CRISPR/Cas, significantly reducing immunogenicity, avoiding off-target effects, and improving the target cell edit efficiencies. In the case of retinal dystrophies**,** localized injections are given via intravitreal or subretinal administrations.

1.3.2.1.4. Targeted delivery

Targeting may be defined as a preferential accumulation of the active agent at a predetermined site which could be a tissue or organ (first-order targeting), a specific cell type (second-order targeting), or an intracellular site of targeted cells (third-order targeting). Targeting is important because the therapeutic product can cause many adverse effects and damage the non-target cells. It also decreases the drug concentration required to produce the desired effect at the site of action. One of the advantages that viral vectors provide is tissue tropism, which will be beneficial for targeted CRISPR/Cas9 delivery [108]. But, if non-viral vectors are employed, specific moieties such as peptides and antibodies will be required for targeting [109]. However, such targeting is quite difficult to achieve due to complications in packaging that may arise due to the insertion of extra biomolecules into a delivery vector along with the CRISPR components.

1.3.2.1.5. Transfection and editing efficiency

CRISPR/Cas9 components must be successfully delivered in sufficient quantity into the target cells by transfection, a prerequisite for efficient genome editing. Transfection methods are of three types, viral, chemical, and physical. Among these, the most used non-viral method is electroporation. But, due to the high electric field strength and accompanying electrochemical reactions, electroporation often causes high post-transfection mortality [110]. The editing efficiency for CRISPR/Cas9 obtained *in vivo* is much lower than that achieved *in vitro* in cell lines. In another study, when Cas9-RNP was delivered locally into the mouse's inner ear, it caused 20% GFP fluorescence loss. This small percentage may work in some diseases, such as liver tyrosinemia and muscular dystrophy. The editing efficiency is also linked to delivery efficiency. Recently Cas9-RNP delivery efficiency up to ~95% in cultured cells has been attained, although the *in vivo* delivery efficiency remains unexplored [111].

1.3.2.1.6. Off-target effects

One of the most significant setbacks for genome editing technology is the off-target effects. Off-target effects occur when the specially engineered sgRNA, apart from targeting the gene of interest, targets the non-specific genes [112, 113]. TALENs usually have lesser toxicity and greater specificity than ZFNs. Also, with CRISPRs, different cells may carry different edits even if they get edited by a single gRNA. It has been shown that even a single mismatch between base pairs can decrease binding to a great extent. A mismatch occurring at the 5′ end of the target is much more destructive than the 3′ end. In the case of CRISPR therapy, off-target effects have also been a significant problem. Secondary targets of the sgRNA, which have multiple mismatches concerning the sgRNA, undergo mutations at a rate similar to the desired target [114]. The CRISPR/Cas off-target effects are further amplified when the viral gene delivery method is employed, possibly due to the long-term constitutive expression of Cas9/sgRNA that leads to continued exposure of Cas9/sgRNA to non-specific genes. Various techniques are being developed to eliminate off-target effects, such as designing sgRNA of high specificity [115, 116]. *In vivo* effects for these systems have not been fully developed for the off-target effects. The best technique in this regard remains the protein-based delivery of CRISPR since there is only a transient exposure of the host genome to the Cas9/sgRNA, thus decreasing off-target events [117].

1.4. Ocular delivery: Challenges and Opportunities for nanomedicine

Anatomically, anterior and posterior segments of the eye are affected by vision-threatening disorders. Most currently available ophthalmic preparations are eye drops possessing poor bioavailability through the conjunctival route [118]. Significant physiological and anatomical barriers impede the delivery of active pharmaceutical ingredients (API) to affected eye areas. Tear film, eye blinking, efflux pump, and nasolacrimal drainage are some

barriers to drug absorption [119]. Further, the static barrier chamber of the eye (stroma, cornea and blood-retinal barrier) and dynamic barrier (lachrymation, lymph flow and conjunctival blood) of the anterior chamber limits the bioavailability of drug given via the ophthalmic route [118]. Most dystrophic conditions require delivery of the therapeutic agent to the posterior portion of the eye and are limited by static barriers including the blood-retinal barrier, Bruch's membrane, and sclera. choroid, and the dynamic barriers, i.e. lymph and choroidal blood flow [120]. The intravitreal route is the most common mode of administering drugs to the eye's posterior chamber [121]. On the same note, there are some limitations, such as patient compliance, the need for expert handling, the risk of retinal detachment, risk of cataracts and haemorrhage [122]. Attempts have been made to overcome existing problems related to the delivery of molecules towards the posterior portion of the eye using nanotechnology-based delivery carriers. Nano size and surface charge of nanoparticle help target specific retention and conjugation *in vivo*. Also, nanoparticles with higher zeta potential are supposed to have higher stability.

Additionally, cationic nanoparticles are more applicable for topical ophthalmic delivery, as conjunctiva and cornea have a negative charge on the surface [123]. Therefore, electrostatic interaction helps in the internalization of nanoparticles into the eye. For intravitreal injection, anionic nanoparticle diffuses more effectively through the vitreous as it is composed of anionic hyaluronic acid, which helps anionic particles to reach the posterior chamber of the eye without any interaction [124]. On the other hand, cationic nanoparticle interacts with anionic hyaluronic species and remain undiffused and entrapped in the vitreous. Therefore, an anionic nanoparticle charge eases the intravitreal delivery of cargo to the posterior part of an eye [125]. Several nanocarrier systems have been explored for ocular delivery, including polymeric micelles, liposomes, polymeric nanoparticles, nano-emulsion/suspension, solid lipid nanoparticles,

microparticles, etc. These nanocarrier systems provide advantages such as targeted delivery, enhanced bioavailability, sustained release, improved residence time in ocular space etc. [126].

Additionally, the intraocular route significantly benefits ocular retinal delivery over the systemic route. The systemic route poses hurdles such as the blood-retinal barrier, systemic toxicity of the drug administered, poor target specificity, rapid clearance, off-target effects, and only 1-2 % of drug reaches the eye *via* the systemic route. Hence intravitreal route can provide distinct advantages, and nanomedicines could serve as potential therapeutics for the treatment of retinal dystrophic conditions. On the same note, there are some clinical complications with intravitreal injection, such as patient compliance, infectious endophthalmitis, intraocular inflammation, rhegmatogenous retinal detachment, intraocular pressure elevation, ocular haemorrhage, glaucoma, cataract, non-infectious uveitis, rare ocular side effects, etc. Although, these complications can be minimized by reviewing patient medical history, appropriate ocular examination, ancillary diagnostic testing, individualized medical decision-making, and proper follow-up by a clinician.

1.5. Delivery Strategies used for CRISPR/Cas9 components

Many genome engineering applications have been developed for CRISPR/Cas systems for *in vitro* studies in cell lines; however, achieving an efficient *in vivo* delivery of the CRISPR/Cas system is a significant challenge as multiple components need to be delivered to the target cell to produce the desired effect. Nucleofection, electroporation, and lipid-based deliveries have been tried for plasmid DNA (that encodes for the Cas9-sgRNA) through the cell membrane [127]. Electroporation is a technique in which high voltage is applied to create pores in the cell membrane so that direct transfection can occur in the cells both *in vitro* and *in vivo* [128]. Electroporation can be highly toxic as it disturbs the cell membrane and may even lead to cell death [129]. Microinjection of rapidly dividing single cells has been used in the

case of more giant cells, such as fertilized embryos, wherein the CRISPR components are directly injected into the single cell to create varieties of *knockout* and transgenic animals. However, this is a technically demanding procedure [130]. These mechanical methods are preferred for *in vitro* editing as they are reproducible, simple, and have high gene expression levels.

Further, delivery through these direct methods has been used *ex vivo* in cells harvested from patients and then reintroduced into their bodies. Existing literature revealed direct methods' accuracy and efficiency, but these methods are limited to *in vitro* or *ex vivo* applications. However, efficient *in vivo* delivery systems need further research and technical advancements.

Delivering payload specifically to any organ in the body should have some common factors that need to be considered, such as immune response, hematological toxicity, targeted delivery, distribution, etc. However, additional factors must be considered for the retinal delivery of the therapeutic agent. The blood-retinal barrier limits the amount of payload that reaches the eye after intravenous injection; thus, localized injections (such as subretinal, intravitreal, corneal permeation, etc.) are mostly preferred for a retinal delivery route. Fortunately, the anatomical location also makes the eye more feasible to localized injection. Vitreous fluid is one of the significant barriers to retinal delivery. The viscosity and anionic charge of the vitreous fluid must be considered while developing a nano-carrier-based delivery system [131]. As reported earlier, the high positive charge nanoparticle accumulates within the vitreous due to electrostatic interaction with anionic hyaluronic acid in the vitreous [132].

Similarly, particle size also considerably impacts vitreous diffusibility [133]; reports say that the particle size below 50 nm showed rapid clearance from the vitreous. Since the vitreous volume is significantly less, the injection volume is limited to a certain amount (25-

100 ul). Therefore, the nanocarrier should have sufficient payload capacity to deliver the desired payload concentration in that limited injection volume. Being a sense organ, the eye is more sensitive to toxicity, and therefore while selecting a nano-carrier, the toxicity issue should be considered. Although the immune-privileged nature of the eye provides opportunities to use different biomaterial used in delivery, despite that, toxicity may lead to the loss of eye integrity and could cause vision loss. Chitosan is the best example, which is known to cause retinal toxicity by inducing an immune response in the eye [134]. Increased intraocular pressure is also a significant challenge in intravitreal delivery, and specific measures must be taken to resolve this issue. A trained professional must give the intravitreal injection dose because any mistake could lead to a serious eye injury. Additionally, multiple frequent injections need to be avoided in case of retinal delivery.

1.5.1. *Viral* vectors

CRISPR therapy has been developed for the primary purpose of treating inherited genetic diseases. Thus, the carrier package needs to be structured with high specificity, with no toxicity and rapid elimination after gene delivery [135]. The viral vectors are the most widely used method for the efficient delivery of nucleic acid that encodes for the required protein. But, as we have seen in the earlier section, even the viral delivery of CRISPR/Cas components causes undesirable effects such as immunogenicity and insertional mutations, hence restricting their clinical application [136].

Broadly, three types of viral vectors, i.e., adenoviral, lentiviral, and adeno-associated viral (AAV), have been used to deliver genes that encode Cas9 into cells of interest. While the adenoviral vectors can elicit severe immunogenic reactions against the complex capsid proteins, the lenti and retroviral vectors have the risk of host gene integration and insertional mutations. Adeno-associated viruses (AAVs) are known for their low immunogenicity and target specificity based on their serotypes and are preferred gene delivery vectors. Without

genome integration, they also show good transduction efficiencies and long-term transgene expression [137]. Various changes, such as removing the endogenous Rep protein and encoding double self-complementary replicase of the viral genome (scAAVs), have reduced the integration of the vector and improved their transduction efficiency by about 140 times [137, 138]. However, the AAV-based viral vectors have limited packaging capacity due to their small genome size and this limits the packaging of large gene cargos such as Cas9 and makes it difficult to accommodate other regulatory elements such as promoters, polyadenylation signals, and selection markers. Splitting the spCas9 into two parts will make the genes fit into the vector, but it reduces the delivery and edit efficiencies [139].

AAVs have been successfully used for *in vivo* gene delivery and have shown long-term therapeutic effects for up to six years in LCA patients administered with an AAV2 vector encoding RPE65 [78, 140]. AAV and adenovirus delivered RPE65 in the *rd12* mouse model of LCA2 (which showed a nonsense mutation in *RPE65*) have been shown to restore vision significantly [141, 142]. The efficacy of AAV gene therapy was convincingly demonstrated in 2008 to treat Leber congenital amaurosis. Many phases I and IIa trials for the subretinal delivery of AAV2-*RPE65* cDNA have shown no serious adverse effects, along with improved pupillary reflexes, visual acuity and mobility in a few of the treated patients [78, 143, 144]. The first AAV-based gene therapy drug, Glybera, was approved by the European Medicines Agency (EMA) in 2012 for the delivery of the LPLD gene, with Luxturna becoming the first AAV gene therapy product to receive US Food and Drug Administration (FDA) approval five years later, for the delivery of RPE65 gene.

Since AAVs pose a significant problem of packaging, many smaller Cas9 orthologs have been isolated from *Streptococcus thermophilus* (StCas9) [145], *Staphylococcus aureus* (SaCas9) [146], *Campylobacter jejuni* (CjCas9 and *Neisseria meningitidis* (NmCas9) [147]. Kim et al. used a combination of SaCas9 and CjCas9 together, and gRNAs incorporated into a

single AAV. Their results showed that the cleaving action was as efficient as SpCas9 for *in vitro* applications. In a recent study, *Lachnospiraceae bacterium* (LbCpf1) was used to prepare Cpf1 nuclease, which was put together with the CRISPR RNA (crRNA) into a single AAV vector [82] showcasing excellent prospects for its use as an *in vivo* genome editing tool in the therapy of angiogenesis-related disorders.

Adenoviral vectors (AVs) are not the most used delivery vectors due to immunological concerns; however, their more giant genomes, episomal nature of intracellular maintenance and efficient transduction are advantages for *in vivo* delivery systems. The have a high packaging capacity (~30–40 kb pairs), which can fit all the required elements**.** Thus, a single virus vector can express the Cas protein and one or many sgRNAs. To facilitate homology-directed repair, large donor DNA sequences can also be co-delivered. Hence, the Cas proteins and sgRNA are expressed proportionately within cells, and the episomes may get lost in dividing cells, thereby allowing only transient Cas9 expressions and reduced off-target risks. AVs have been successfully used for *in vivo* genome editing in mice, although immune-related toxicities were observed [148]. However, immunogenicity is not a concern for *in vitro* editing of cell lines and stem cells. One of the first studies on AV was conducted in 1996 by Bennett et al. to study retinal disease in an animal model. They delivered the cDNA encoding phosphodiesterase β subunit into the rd1 mouse model photoreceptors and showed a successful delay of photoreceptor degeneration by six weeks. The disadvantage of AV therapy is its relatively high immunogenicity and the existence of neutralizing antibodies in humans against specific serotypes such as Ad5, which renders the vector ineffective in most patients [149]. Studies have shown that subretinal delivery causes a lower T cell-mediated immune response than intravitreal injections [150, 151]. AVs are now used to inhibit retinoblastoma growth in a mouse model and reduce retinal and choroidal neovascularization in rat and rabbit models [152-154].

Lentiviral vectors (LVs) are currently one of the most used vectors in clinical applications where long-term effects are desired. Lentiviruses belong to the family of viruses known as *Retroviridae*; they are RNA viruses which integrate into the host DNA using reverse transcriptase and integrase enzymes. The nonpathogenic equine infectious anaemia virus (EIAV) was the pioneer to start a human clinical trial with the lentivirus. Studies have shown that lentiviral vectors are safe and effective for gene delivery into the photoreceptor cells of humans [155-158]. LV packaging capacity is higher than AAVs in the range of approximately 8 to 9 kb. LVs can transduce both non-dividing and dividing cells with very high efficiency and integrate into the host cell genomes to enable long-term transgene expression. However, long-lasting expression of Cas proteins may increase the risk of unwanted off-target edits [159]. To address this concern, self-inactivating constructs were engineered with two sgRNAs: one against the Cas9 gene and one against the target sequence of interest, thus allowing only transient expression of Cas9 to achieve the desired target site edits.

Among the viral delivery methods, adeno-associated virus vectors are most preferred because of their mild immune response and absence of pathogenicity. AAVs can target non-dividing but have a limited packaging size. The development of the shorter dCas9 of 1 kb size has overcome this limitation to some extent [15]. Newer approaches are now being explored to decrease cytotoxicity and escape neutralising antibodies to improve *in vivo* transduction efficiencies. As a result, some of the AAV-based gene therapy products are already in clinical trials for the treatment of RDs (Table 1.4)

Table 1.4. List of therapeutic molecules in clinical trials for the treatment of RDs

Retinal dystrophy	Targeted gene	Phase	Therapeutic approach	Year	NCT ID
Leber Congenital Amaurosis	CEP290 Intron 26(IVS26)	I/II	subretinal EDIT-101 (CRISPR/Cas9)	2019-24	NCT03872479
	CEP290 p.Cys998X	I/II	Intravitreal QR-110(Antisense oligonucleotides)	2017-19	NCT03140969
		I/II		2019-21	NCT03913130
		II/III		2019-21	NCT03913143
	RPE65	I	Subretinal rAAV2-CBSB-hRPE65	2007-26	NCT00481546
		I/II	Subretinal tgAAG76(rAAV2/2.hRPE65p.hRPE65)	2007-14	NCT00643747
		I/II	rAAV2-CBSB-hRPE65	2009-17	NCT00749957
		I	Subretinal AAV2-hRPE65v2	2007-18	NCT00516477
		III		2012-29	NCT01208389
		I/II		2010-26	NCT00999609
		I	Subretinal rAAV2-hRPE65	2009-17	NCT00821340
		I/II	Subretinal rAAV2-CBSB-hRPE65 Applied	2009-17	NCT00749957
		I/II	Subretinal rAAV-2/4.hRPE65	2011-14	NCT01496040
		I/II	Subretinal AAV2/5-OPTIRPE65	2016-18	NCT02781480
		I/II		2016-23	NCT02946879
Choroideremia	REP1	I/II	Subretinal rAAV2.REP1	2015-25	NCT02077361
		I/II	Subretinal rAAV2.REP1	2011-17	NCT01461213
		II	Subretinal AAV2.REP1	2016-21	NCT02407678
		II	Subretinal rAAV2.REP1	2016-18	NCT02671539
		II	Subretinal rAAV2.REP1	2015-18	NCT02553135
		II	Subretinal BIIB111(AAV2-REP1)	2018-22	NCT03507686
		III	Subretinal AAV2-REP1	2017-20	NCT03496012
	CHM	I	Intravitreal 4D-100	2020-23	NCT04483440
		I/II	Subretinal AAV2-hCHM	2015-22	NCT02341807

Retinitis Pigmentosa	PDE6B	I/II	Subretinal AAV2/5-hPDE6B	2017-24	NCT03328130
	RLBP1	I/II	Subretinal CPK850	2018-26	NCT03374657
	PDE6A	I/II	Subretinal rAAV.hPDE6A	2019-25	NCT04611503
	USH2A	I/II	Intravitreal QR-421a	2019-22	NCT03780257
Advanced Retinitis Pigmentosa	ChR2	I/II	Intravitreal RST-001	2015-35	NCT02556736
Autosomal Dominant Retinitis Pigmentosa	RHO	I/II	unilateral IVT injection QR-1123	2019-21	NCT04123626
X-linked juvenile retinoschisis	RS1	I/II	Intravitreal rAAV2tYF-CB-hRS1	2015-23	NCT02416622
		I/II	Intravitreal AAV8-scRS/IRBPhRS	2015-23	NCT02317887
X-linked Retinitis Pigmentosa	RPGR	I/II	sub-retinal BIIB112	2017-20	NCT03116113
		I/II	Intravitrea 4D-125	2020-23	NCT04517149
		I/II	Subretinal AAV2/5-RPGR	2017-20	NCT03252847
		I/II	Subretinal AGTC-501 (rAAV2tYF-GRK1-RPGR)	2018-26	NCT03316560
		III	sub-retinal AAV5-RPRG	2021-22	NCT04671433
Achromatopsia	CNGB3	I/II	Subretinal rAAV2tYF-PR1.7-hCNGB3	2016-25	NCT02599922
		I/II	Subretinal rAAV.hCNGA3	2015-27	NCT02610582
Leber Hereditary Optic Neuropathy	ND4	III	GS010; Sham intravitreal injection	2016-19	NCT02652767
		III		2016-18	NCT02652780
		I	Intravitreal scAAV2-P1ND4v2	2014-23	NCT02161380
		---	Intravitreal rAAV2-ND4	2011-15	NCT01267422

Usher syndrome Type 1B	---	I/II	Subretinal SAR422459	2012-19	NCT01505062
	---	I/II	Blood draw for the laboratory assessment	2013-32	NCT02065011
Stargardt's Macular Degeneration	---	I/II	Long term follows up in all patients who received SAR422459 in previous study TDU13583	2012-34	NCT01736592
	---	I/II	SAR422459	2011-19	NCT01367444
Neovascular Age-Related Macular Degeneration	---	I	Subretinal RetinoStat	2011-15	NCT01301443
	---	I		2012-29	NCT01678872
	---	I	Intravitreal AAV2-sFLT01	2010-18	NCT01024998
	---	I/II	Subretinal rAAV.sFlt-1; Control (ranibizumab alone)	2011-17	NCT01494805

Abbreviations: RPE65: Retinal pigmented epithelium-specific protein with molecular mass 65 kDa; CEP290: Centrosomal Protein 290; ChR2: Channelrhodopsin-2; PDE6B: Phosphodiesterase 6B; RLBP1: Retinaldehyde-binding protein 1; USH2A: Usherin; PDE6A: Phosphodiesterase 6A; RHO: Rhodopsin; RPGR: Retinitis pigmentosa GTPase regulator; REP1: Rab escort protein 1; CHM: Choroideremia; RS1: Retinoschisin.

1.5.2. *Non-viral* vectors

The problems associated with viral vectors, such as immunogenicity and packaging issues, have paved the way for developing non-viral systems that are usually better characterized and can be modified chemically to meet the delivery requirements [160]. However, non-viral vectors have concerns related to toxicity, biocompatibility, adverse immunological reactions, and the risk of release of therapeutic material into non-targeted sites. They also suffer from low *in vivo* delivery efficiency, although this problem is being solved with advancements in material sciences. Nanotechnology-based formulations are expected to provide ample benefits over existing approaches [161]. These include (i) sustained release of medicament, (ii) improved uptake in retinal cells, (iii) better vitreous penetrability, (iv) could be tailored to achieve cell-specific delivery, and (v) reduced vitreal clearance leading to the improved exposure time. Improved success has been achieved with newer polymer- and lipid-based complexes that have the required properties to effectively transport their genetic cargo across multiple physiological barriers. As a result, ample nano-based products are approved by the FDA or under investigation (Table 1.5).

For the delivery of CRISPR/Cas components *via* non-viral vectors, mechanisms of direct conjugation of the active molecule to the excipient have been adopted, such as gRNA or Cas protein conjugation with cell-penetrating peptides (CPPs). Studies by Ramakrishna et al. in HEK293T cells have demonstrated that the conjugation has led to 72% and 62% editing efficiencies with plasmids and RNPs, respectively. But, these CPP systems have not proven efficient in crossing all delivery barriers [117]. The following are the current non-viral delivery systems used for CRISPR/Cas9 delivery (Figure 1.6).

Table 1.5. List of nanomedicines approved or under clinical investigation for treating RDs

Retinal dystrophy	Status	Nanomedicine	Molecule	NCT ID	Reference
Age related macular degeneration	Approved by FDA	Liposome (Product name; Visudyne®)	Verteporfin	NCT00121407	[162]
	Approved by FDA		Pegaptanib sodium	NCT00549055	[162]
Wet Age-related macular degeneration		Aptamer–polymer nanoparticle (Product name: Macugen®)			
Diabetic macular edema	Approved by FDA	Nonbiodegradable implant (Product name: ILUVIEN®)	Fluocinolone acetonide	NCT04469595	[163]
Macular edema	Approved by FDA	Suspension (Product name: Kenalog)	Triamcinolone acetonide	NCT00101764	
	Phase II	Lipid-based nanoparticle Product name: TLC399 (ProDex))	Dexamethasone sodium phosphate	NCT03093701	

1.5.2.1. Lipoplexes

In 1987, the scientific expression ‘‘lipofection’’ was first used to describe a lipidic system used for gene transfection [164]. It is one of the oldest and most widely used techniques for gene transfer. Lipids have been extensively studied for their characteristics as nanocarriers, and to electrostatically complex with a negatively charged gene, a positively charged cationic lipid is incorporated in the carrier. Commercially available cationic lipids include N-[1-(2,3-

dioleyloxy) propyl]-N,N,N-trimethyl-ammonium chloride (DOTMA), 1,2-dioleoyl-3-Trimethylammoniumpropane (DOTAP),1,2-dimyristyloxypropyl-3-dimethyl-hydroxyethylammonium bromide (DMRIE). and 2,3-dioleyloxy-N-[2(sperminecarboxamido) ethyl]-N,N-dimethyl-1-propanaminium trifluoroacetate (DOSPA) [165]. Wang et al., in their experiments, showed that CRISPR/Cas RNP could be administered into the cell using biodegradable cationic lipid nanoparticles, leading to the effective knockout of genes [166]. The delivery of supercharged Cre protein and Cas9:sgRNA complexed with bio-reducible lipids into cultured human cells (HeLa-DsRed cells) enabled gene recombination and genome editing with efficiencies greater than 70%. Further, disulfide linkages in the lipid material can

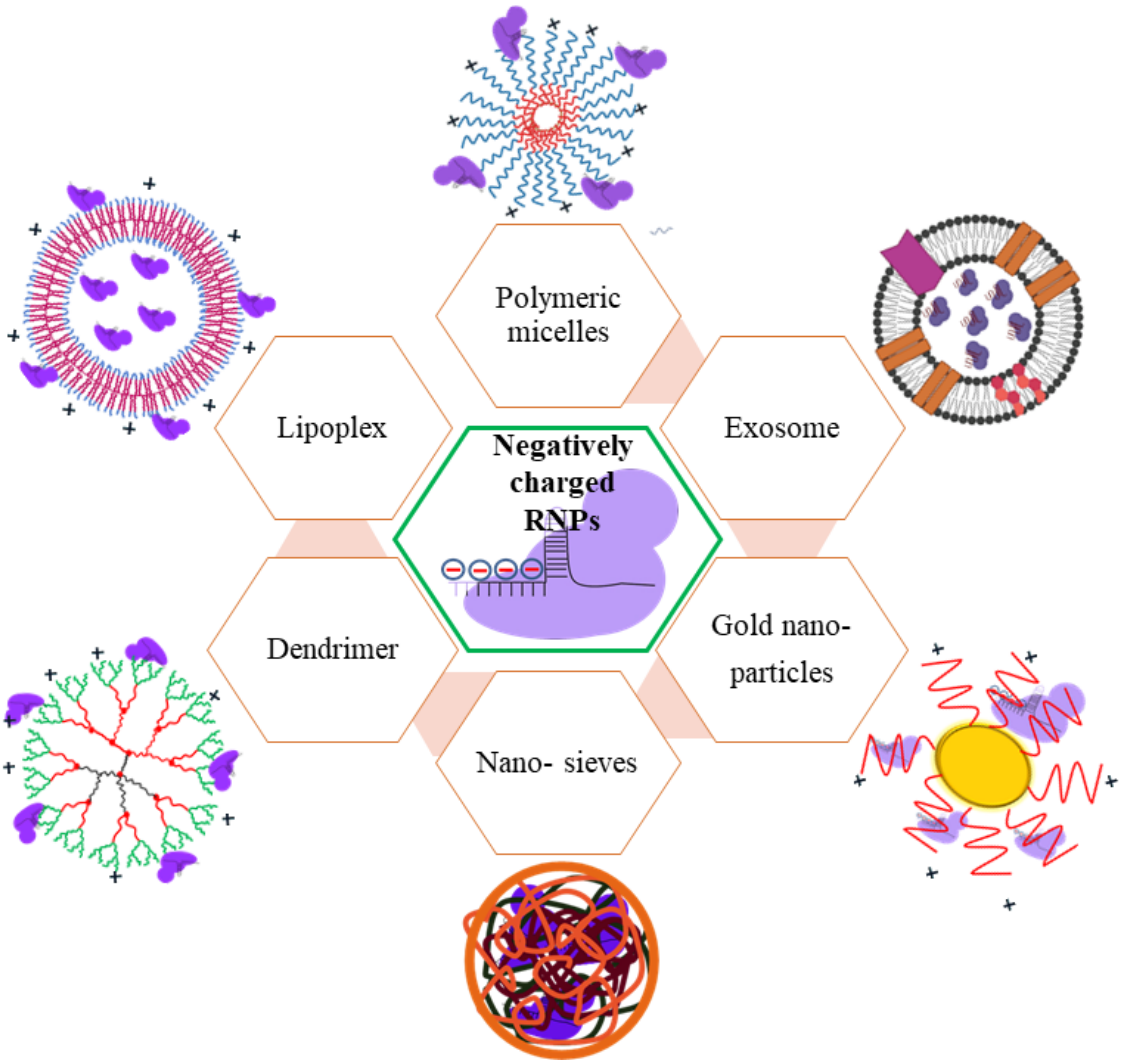

Figure 1.6. Potential non-viral vectors has been explored for delivering CRISPR/Cas RNPs *in vitro* and *in vivo*.

trigger release by the degradation of endosomal particles leading to endosomal release. In addition, the author demonstrated that these lipids are effective for functional protein delivery into the mouse brain for gene recombination *in vivo* [167]. In 2020, Wei et al. used a mixture of lipids (5A2-SC8, DOTAP, DMG-PEG, Chol, DOPE) to prepare a lipidic system i.e. 5A2-DOT with different concentrations of DOTAP (10 - 50 mol%). The nanoformulation showed sufficient payload for Cas9 RNPs and efficient, precise gene editing (for the TdTomato gene) in mice brains and muscles when administered locally. Further, when the formulation was given intravenously also showed significant gene editing in liver and lung tissues [168].

1.5.2.2. Polyplexes

Various types of polymer complexes are being used for CRISPR/Cas delivery. Cationic polymers pose lesser immunogenicity problems and are much easier to synthesize on a large scale. Those which have gained attraction include polyethyleneimine (PEI), poly(L-lysine) (PLL), poly[2-(dimethylamino) ethyl methacrylate] (PDMAEMA), and polyamidoamine (PAMAM) dendrimers [169]. Among polymeric vectors, polyethyleneimine (PEI) has been extensively researched. Scientists in 1995 carried out the first successful transfection using PEI, after which it is regarded as a gold standard in the study of polymeric non-viral carriers due to their high transfection efficiency. The characteristics of PEI which make it suitable for gene transfer are its “proton sponge” nature and high charge density [170]. Like cationic lipids, PEI can be complexed with nucleic acids, induce endosomal uptake, and release in the cytoplasm of the cell. A study by Zhang et al. shows a formulation made up of PEI-β-cyclodextrin to deliver plasmids coding for sgRNA and Cas9 in HeLa cells, achieving gene knockout [171]. PEI has also been used in a formulation by Sun et al., in which they have used DNA as a nanomaterial for the coating of CRISPR/Cas. These particles were encapsulated by

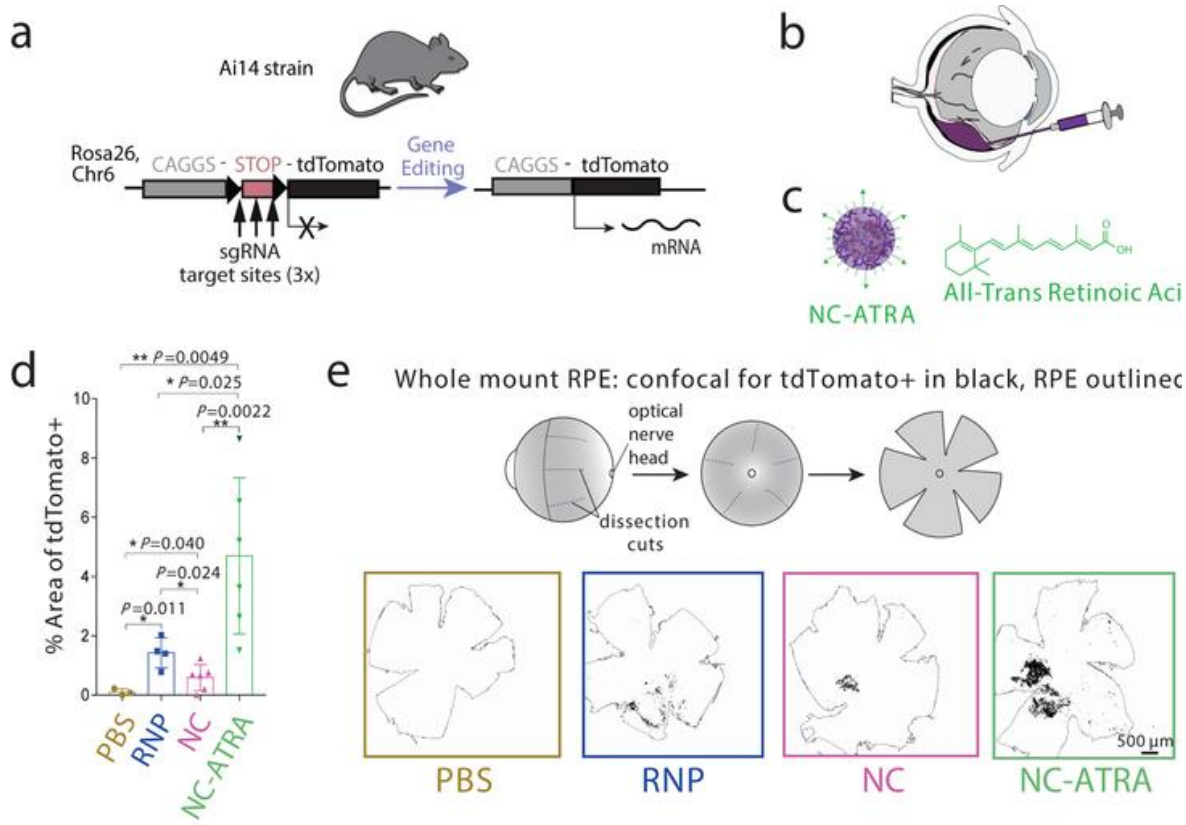

Figure 1.7. *In vivo* gene editing efficiency of RNP loaded nanocapsule in mice.Graphicalillustration of the a) TdTomato gene, b) site of intravitreal injection in mice eye, c) ATRA targeted nanocapsule. d) post injection in vivo gene editing in RPE layer quantified in terms of tdTomato positive area (%) in different treatment groups, e) mounted RPE layer of the mouse treated with PBS, RNP, NCs and NC-ATRA, herein black area represents TdTomato signals after 12 days of treatment. Reprinted by permission from Guojun Chen et al, Springer Nature, Nature Nanotechnology, A biodegradable nanocapsule delivers a Cas9 ribonucleoprotein complex for in vivo genome editing, Guojun C, Amr AA, Yuyuan W, Pawan KS, Samantha R, Ruosen X, Masatoshi S, Bikash RP, Krishanu S, and Shaoqin G, Copyright ©2019

PEI to enhance endosomal release. These particles were directly injected in mice with EGFP tumours, and the resulting phenotypes showed knockout of EGFP [172]. Apart for PEI, the High charge density Poly(L-lysine) (PLL**),** a synthetic polypeptide**,** which is a prerequisite for efficient plasmid DNA complexation and condensation, makes its good choice for gene delivery. However, due to the absence of buffering capacity (required for endosomal escape), PLL displays lower transfection efficiency than other polyplex systems [173]. Further, the

high-molecular-weight PLL leads to a high level of cytotoxicity as it interacts with serum proteins, causing rapid elimination of the complexes from the system. Studies have shown that a PLL-PEG copolymer can help solve these issues and facilitates its duration in the system [174]. The success of PLL-PEG copolymer in gene delivery has been proved in both *in vitro* and *in vivo* studies. In a study conducted in 2004 on treating cystic fibrosis (CF), PLL-PEG was explored as a gene delivery construct carrying the cystic fibrosis transmembrane regulator encoding gene [175]. Poly[2-(dimethylamino) ethyl methacrylate], PDMAEMA is another non-viral delivery method. A water-soluble cationic polymer, in current applications polysaccharide-modified PDMAEMAs, is gaining significance in CRISPR/Cas delivery [136]. In 2020, Carlos et al. synthesized magnetite/silver-pDMAEMA conjugate and evaluated it for the delivery of CRISPR plasmid. It showed 16.4% loading efficiency with minimum toxicity. Further, colocalization studies were performed in SH-Y5Y cells with lysotracker, and data indicated that Pearson's correlation coefficient approached 0.240 ± 0.024 after 0.5 h and decreased to 0.215 ± 0.029 in a statistically significant manner after 4 h. Collectively, the magnetite/silver-pDMAEMA showed endosomal escape after 4 h of internalization and showed effective delivery potential *in vitro* [176]**.** In 2019, Chen et al developed Cas9 RNPs loaded nanocapsule (NCs) composed of cationic polymer and liposome components along with a glutathione cleavable linker in between. The nanocapsule carry 40% of RNPs content with a particle size of 25 nm. The research focused on *in vivo* gene editing, performed in eyes and muscles of transgenic Ai14 mice (having three sv40 polyA transcription terminators as stop cassette for TdTomato gene). NCs were decorated with all-trans-retinoic acid (NTRA, binds to inter-photoreceptor retinoid-binding protein) to form NTRA-NCs, and evaluated for gene editing in RPE cells in the eyes of Ai14 mice (Figure 1.7). Further, mice were injected with PBS, naked RNPs, NCs and ATRA-NCs subrationally and eyes tissue were excised after 12 days post injection. NCs showed considerable and ATRA-NCs showed significantly higher

gene editing in RPE cells in terms of TdTomato fluorescence. Moreover, the NCs were injected intramuscular and NCs showed gene editing and a strong TdTomato fluorescence was observed in muscle tissues. Collectively, the study explored the potential role of non-viral biodegradable nanocapsule in the delivery of high molecular weight Cas9 RNPs for *in vivo* gene editing application [177].

1.5.2.3. Dendriplexes

Polyamidoamine dendrimers (PAMAM) are commercially available for gene transfer and are one of the most frequently used systems [178]. The structure comprises a core surrounded by polymeric branches, and the surface expresses primary cationic amines that help it complex to nucleic acids. PAMAM dendrimers are known to be generation-dependent; low-generation (G0–G3) dendriplexes have poor gene transfection efficiencies and are less cytotoxic, but higher-generation (G4–G8) PAMAMs have improved gene transfection efficiencies and are more cytotoxic [179]. Yu et al., in their research, prepared a formulation made up of a lipid and dendrimer hybrid. The structure consisted of a long hydrophobic alkyl chain and a low-generation hydrophilic PAMAM dendron. In this way, the system exhibited the pros of both lipids and polymers in delivering siRNA and achieved the efficient gene-silencing effect *in vitro* and *in vivo* [180]. Another finding by Park et al., L-arginine was used to transform the surface of PAMAM, enhancing gene transfection efficiency due to ease of complexation [181]. In 2019, Liu et al., synthesized boric acid rich 5 (G5) amine-terminated polyamidoamine (PAMAM)dendrimer (P4) for CRISPR/Cas9 RNPs delivery. The P4 dendrimer nanoparticle loaded with RNPs showed a particle size of 300 nm. The functionalized dendrimer showed efficient delivery and 45% of EGFP gene *knockout* in EGFP-HEK293T cells, analyzed *via* flow cytometry. Further, another set of experiments was performed to evaluate gene editing efficiency, and CRISPRMax was taken as standard along with the P4

dendrimer. CRISPR/Cas9 RNPs were designed for targeting adeno-associated virus integration site 1 (*AAVS1*) and haemoglobin subunit beta (*HBB*), and transfection assay were performed followed by T7E assay, where results indicate Indel frequency of 23.1% and 17.5% for AAVS gene with P4 dendrimer/RNPs and CRISPRMax/RNPs respectively. Likewise, an indel frequency of 1.1 and 9.7% was observed for the HBB gene with P4 dendrimer/RNPs and CRISPRMax/RNPs, respectively. This study explored the potential role of dendrimers as a delivery vehicle for CRISPR/Cas9 [182].

1.6. CRISPR/Cas-based RNA editing approach in retinal degeneration diseases

Theoretically, G>A or T>C single-base mutations in any gene related to inherited retinal degeneration could be corrected by using base editing [183]. Nevertheless, all diseases are not equally responsive to RNA editing. AAV-mediated gene replacement provides effective treatment for small gene deliveries. On the other hand, a higher rate of mutant allele-specific editing is required for dominant diseases where the mutant alleles have to be efficiently knocked out. Interestingly, more prominent recessive genes (>4.2 kb) are difficult to correct by gene replacement using AAV and require *in-situ* editing either *in vitro* or *in vivo*. Stone et al. have listed the significant recessive genes, such as ABCA4, USH2A, CEP290, MYO7A, EYS, and CDH23, along with their relative frequency in patients with inherited retinal degeneration [184]. The most common single nucleotide mutation is G>A, amenable to currently available base editing techniques. The proportion of G>A or T>C mutation in CEP290 and ABCA4 genes was 9% and 32%, respectively [184]. Further, 6% of the mutations observed in the USH2A gene result in the creation of premature stop codon, while missense and donor/acceptor splice mutations were predominantly seen in the ABCA4 gene. Collectively, the data suggested the dominance of G>A mutation (~75 in number) in both genes, leading to premature stop codons. Humans have adenosine deaminase acting on RNA

(ADAR) enzymes, which play a crucial role in adenosine to inosine conversion (A→ I) [185]. Since inosine is read as guanosine by the splicing and translation apparatus, ADARs can also alter RNA splicing to restore regular reading frames and modify amino acid sequences.

In 2017, Cox et al. explored a new system called 'REPAIR' (RNA Editing for Programmable A to I Replacement), which aimed to cleave RNA at a specific site using a novel protein Cas13a, isolated from the *Leptotrichia wadei*. Cas13a binds to the RNA-RNA hybrid,

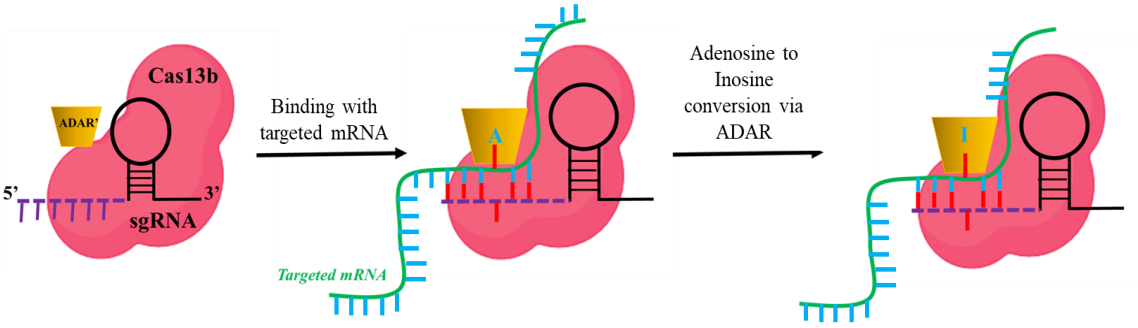

Figure 1.8. Schematic representation of mRNA editing using Cas13b in retinal dystrophic conditions (adopted from ref. [1])

unlike the DNA-RNA hybrid bound by Cas9 and is also a part of the bacterial CRISPR-mediated RNA interference system [186]. The Cas13-based RNA editing technique may be advantageous over conventional DNA editing, as DNA manipulations are permanent in cellular genomes and may have unanticipated long-term side effects. A synthetic RNA targeting system developed with a human protein, with Cas13-likessRNA recognizing properties. This system, termed CIRTS (CRISPR/Cas inspired RNA targeting system), is an engineered modular RNA-guided RNA-targeting effector system synthesized from human proteins and provides a new toolset to overcome the size and immunogenicity limitations of bacterial CRISPR-Cas systems. (Rauch et al., 2019) This system consists of an engineered gRNA that carries sequences complementary to the target RNA and also carries a sequence to recruit an engineered hairpin binding protein and a non-specific ssRNA binding protein for complex stabilization and an ADAR2-like effector protein to enable base editing (Figure 1.8). CIRTS8 system, when

delivered in the form of a plasmid construct, could achieve 47% edit efficiency in HEK293T cells without significant off-target edits [183]. RNA editing thus provides immense potential in repairing pathogenic mutations in many diseases such as Duchenne's muscular dystrophy, cystic fibrosis, hurler's syndrome, etc. RNA edits are also reversible and offer improved safety in therapeutic considerations. Inducible RNA editors with automatic switch off systems and external stimuli triggered to switch-on systems further improve the safety profiles of RNA editing [187].

1.7. Conclusions

CRISPR/Cas system has emerged as a rapidly evolving therapeutic tool in genomic engineering. Genome therapy using CRISPR/Cas in ophthalmic diseases is a boon for society, considering its impact on thousands of people's lives. It offers newer hopes of developing promising therapeutics for the treatment of inherited retinal disorders. In the past 20 years, the eye and ocular diseases have caught the limelight of gene therapy and cell therapeutic efforts, mainly for the unique anatomical location that enables accessible interventions, detailed imaging and documentation; the privileged immune status of the eye; the existence of blood-retinal barrier safety that ensures long-term ocular retention and containment of therapeutics; and finally for the huge societal impact of even marginal improvements in vision to patient beneficiaries. Gene therapeutics, either alone or when combined with gene editing strategies, can enable the delivery of regular gene copies, *in situ* mutation editing for normal protein and RNA expression; and targeted disruption of dominant mutant alleles or their transcripts for the reversal of disease phenotypes. Several pre-clinical studies have been initiated using viral and non-viral vectors to deliver CRISPR components for therapeutic applications. While watching the fast pace of developments in this field is exciting, it is prudent to move forward responsibly, considering both the ethical and societal implications. It is essential to exercise well-informed

caution and consider both the intended and unintended outcomes while designing gene editing-based therapeutic strategies.

References

[1] Cox DBT, Gootenberg JS, Abudayyeh OO, Franklin B, Kellner MJ, Joung J, et al. RNA editing with CRISPR-Cas13. Science (New York, NY) 2017;358:1019-27.

[2] Samson JE, Magadan AH, Sabri M, Moineau S. Revenge of the phages: defeating bacterial defences. Nature reviews Microbiology 2013;11:675-87.

[3] Horvath P, Barrangou R. CRISPR/Cas, the immune system of bacteria and archaea. Science (New York, NY) 2010;327:167-70.

[4] Mojica FJM, Diez-Villasenor C, Garcia-Martinez J, Almendros C. Short motif sequences determine the targets of the prokaryotic CRISPR defence system. Microbiology (Reading, England) 2009;155:733-40.

[5] Jinek M, Chylinski K, Fonfara I, Hauer M, Doudna JA, Charpentier E. A programmable dual-RNA–guided DNA endonuclease in adaptive bacterial immunity. science 2012;337:816-21.

[6] Makarova KS, Haft DH, Barrangou R, Brouns SJ, Charpentier E, Horvath P, et al. Evolution and classification of the CRISPR-Cas systems. Nature reviews Microbiology 2011;9:467-77.

[7] Burmistrz M, Pyrc K. CRISPR-Cas Systems in Prokaryotes. Polish journal of microbiology 2015;64:193-202.

[8] Alkan F, Wenzel A, Anthon C, Havgaard JH, Gorodkin J. CRISPR-Cas9 off-targeting assessment with nucleic acid duplex energy parameters. Genome biology 2018;19:177-018-1534-x.

[9] Ma Y, Zhang L, Huang X. Genome modification by CRISPR/Cas9. The FEBS journal 2014;281:5186-93.

[10] Javed MR, Sadaf M, Ahmed T, Jamil A, Nawaz M, Abbas H, et al. CRISPR-Cas System: History and Prospects as a Genome Editing Tool in Microorganisms. Current microbiology 2018;75:1675-83.

[11] Haeussler M, Schonig K, Eckert H, Eschstruth A, Mianne J, Renaud JB, et al. Evaluation of off-target and on-target scoring algorithms and integration into the guide RNA selection tool CRISPOR. Genome biology 2016;17:148-016-1012-2.

[12] Vázquez-Domínguez I, Garanto A, Collin RWJ. Molecular Therapies for Inherited Retinal Diseases-Current Standing, Opportunities and Challenges. Genes 2019;10:654.

[13] Burnight ER, Giacalone JC, Cooke JA, Thompson JR, Bohrer LR, Chirco KR, et al. CRISPR-Cas9 genome engineering: Treating inherited retinal degeneration. Progress in retinal and eye research 2018;65:28-49.

[14] Bulcha JT, Wang Y, Ma H, Tai PWL, Gao G. Viral vector platforms within the gene therapy landscape. Signal Transduct Target Ther 2021;6:53-.

[15] Lino CA, Harper JC, Carney JP, Timlin JA. Delivering CRISPR: a review of the challenges and approaches. Drug delivery 2018;25:1234-57.

[16] Kim E, Koo T, Park SW, Kim D, Kim K, Cho HY, et al. In vivo genome editing with a small Cas9 orthologue derived from Campylobacter jejuni. Nature communications 2017;8:14500.

[17] Abudayyeh OO, Gootenberg JS, Essletzbichler P, Han S, Joung J, Belanto JJ, et al. RNA targeting with CRISPR–Cas13. Nature 2017;550:280-4.

[18] Qi LS, Larson MH, Gilbert LA, Doudna JA, Weissman JS, Arkin AP, et al. Repurposing CRISPR as an RNA-guided platform for sequence-specific control of gene expression. Cell 2013;152:1173-83.

[19] Gilbert LA, Larson MH, Morsut L, Liu Z, Brar GA, Torres SE, et al. CRISPR-mediated modular RNA-guided regulation of transcription in eukaryotes. Cell 2013;154:442-51.

[20] Chavez A, Scheiman J, Vora S, Pruitt BW, Tuttle M, Iyer EP, et al. Highly efficient Cas9-mediated transcriptional programming. Nature methods 2015;12:326-8.

[21] Gaudelli NM, Komor AC, Rees HA, Packer MS, Badran AH, Bryson DI, et al. Programmable base editing of A• T to G• C in genomic DNA without DNA cleavage. Nature 2017;551:464-71.

[22] Lei Y, Zhang X, Su J, Jeong M, Gundry MC, Huang Y-H, et al. Targeted DNA methylation in vivo using an engineered dCas9-MQ1 fusion protein. Nature communications 2017;8:1-10.

[23] Deng W, Shi X, Tjian R, Lionnet T, Singer RH. CASFISH: CRISPR/Cas9-mediated in situ labeling of genomic loci in fixed cells. Proceedings of the National Academy of Sciences 2015;112:11870-5.

[24] Acharya S, Mishra A, Paul D, Ansari AH, Azhar M, Kumar M, et al. Francisella novicida Cas9 interrogates genomic DNA with very high specificity and can be used for mammalian genome editing. Proceedings of the National Academy of Sciences 2019;116:20959-68.

[25] Francis PJ. Genetics of inherited retinal disease. Journal of the Royal Society of Medicine 2006;99:189-91.

[26] Pacione LR, Szego MJ, Ikeda S, Nishina PM, McInnes RR. Progress toward understanding the genetic and biochemical mechanisms of inherited photoreceptor degenerations. Annual Review of Neuroscience 2003;26:657-700.

[27] Sundaramurthi H, Moran A, Perpetuini AC, Reynolds A, Kennedy B. Emerging Drug Therapies for Inherited Retinal Dystrophies. Advances in Experimental Medicine and Biology 2019;1185:263-7.

[28] Berger W, Kloeckener-Gruissem B, Neidhardt J. The molecular basis of human retinal and vitreoretinal diseases. Progress in retinal and eye research 2010;29:335-75.

[29] Dias MF, Joo K, Kemp JA, Fialho SL, da Silva Cunha A, Jr., Woo SJ, et al. Molecular genetics and emerging therapies for retinitis pigmentosa: Basic research and clinical perspectives. Progress in retinal and eye research 2018;63:107-31.

[30] DiCarlo JE, Mahajan VB, Tsang SH. Gene therapy and genome surgery in the retina. The Journal of clinical investigation 2018;128:2177-88.

[31] Sengillo JD, Justus S, Cabral T, Tsang SH. Correction of Monogenic and Common Retinal Disorders with Gene Therapy. Genes 2017;8:10.3390/genes8020053.

[32] Yanik M, Muller B, Song F, Gall J, Wagner F, Wende W, et al. In vivo genome editing as a potential treatment strategy for inherited retinal dystrophies. Progress in retinal and eye research 2017;56:1-18.

[33] Colella P, Auricchio A. Gene therapy of inherited retinopathies: a long and successful road from viral vectors to patients. Human Gene Therapy 2012;23:796-807.

[34] Daiger SP, Sullivan LS, Bowne SJ, Koboldt DC, Blanton SH, Wheaton DK, et al. Identification of a Novel Gene on 10q22.1 Causing Autosomal Dominant Retinitis Pigmentosa (adRP). Advances in Experimental Medicine and Biology 2016;854:193-200.

[35] Liang FQ, Anand V, Maguire AM, Bennett J. Intraocular delivery of recombinant virus. Methods in Molecular Medicine 2001;47:125-39.

[36] Schimmer J, Breazzano S. Investor Outlook: Focus on Upcoming LCA2 Gene Therapy Phase III Results. Human gene therapyClinical development 2015;26:144-9.

[37] Cong L, Ran FA, Cox D, Lin S, Barretto R, Habib N, et al. Multiplex genome engineering using CRISPR/Cas systems. Science (New York, NY) 2013;339:819-23.

[38] Barrangou R, Doudna JA. Applications of CRISPR technologies in research and beyond. Nature biotechnology 2016;34:933-41.

[39] Mali P, Yang L, Esvelt KM, Aach J, Guell M, DiCarlo JE, et al. RNA-guided human genome engineering via Cas9. Science (New York, NY) 2013;339:823-6.

[40] den Hollander AI, Roepman R, Koenekoop RK, Cremers FP. Leber congenital amaurosis: genes, proteins and disease mechanisms. Progress in retinal and eye research 2008;27:391-419.

[41] Aleman TS, Jacobson SG, Chico JD, Scott ML, Cheung AY, Windsor EA, et al. Impairment of the transient pupillary light reflex in Rpe65(-/-) mice and humans with leber congenital amaurosis. Investigative ophthalmology & visual science 2004;45:1259-71.

[42] Simonelli F, Ziviello C, Testa F, Rossi S, Fazzi E, Bianchi PE, et al. Clinical and molecular genetics of Leber's congenital amaurosis: a multicenter study of Italian patients. Investigative ophthalmology & visual science 2007;48:4284-90.

[43] Giannelli SG, Luoni M, Castoldi V, Massimino L, Cabassi T, Angeloni D, et al. Cas9/sgRNA selective targeting of the P23H Rhodopsin mutant allele for treating retinitis pigmentosa by intravitreal AAV9.PHP.B-based delivery. Human molecular genetics 2018;27:761-79.

[44] Tsai YT, Wu WH, Lee TT, Wu WP, Xu CL, Park KS, et al. Clustered Regularly Interspaced Short Palindromic Repeats-Based Genome Surgery for the Treatment of Autosomal Dominant Retinitis Pigmentosa. Ophthalmology 2018;125:1421-30.

[45] Friedman DS, O'Colmain BJ, Munoz B, Tomany SC, McCarty C, de Jong PT, et al. Prevalence of age-related macular degeneration in the United States. Archives of ophthalmology (Chicago, Ill: 1960) 2004;122:564-72.

[46] Chan L, Mahajan VB, Tsang SH. Genome Surgery and Gene Therapy in Retinal Disorders. The Yale journal of biology and medicine 2017;90:523-32.

[47] Fogli S, Del Re M, Rofi E, Posarelli C, Figus M, Danesi R. Clinical pharmacology of intravitreal anti-VEGF drugs. Eye (London, England) 2018;32:1010-20.

[48] Jo DH, Koo T, Cho CS, Kim JH, Kim JS, Kim JH. Long-Term Effects of In Vivo Genome Editing in the Mouse Retina Using Campylobacter jejuni Cas9 Expressed via Adeno-

Associated Virus. Molecular therapy : the journal of the American Society of Gene Therapy 2019;27:130-6.

[49] Kim K, Park SW, Kim JH, Lee SH, Kim D, Koo T, et al. Genome surgery using Cas9 ribonucleoproteins for the treatment of age-related macular degeneration. Genome research 2017;27:419-26.

[50] Zhang Q. Retinitis Pigmentosa: Progress and Perspective. Asia-Pacific journal of ophthalmology (Philadelphia, Pa) 2016;5:265-71.

[51] Hartong DT, Berson EL, Dryja TP. Retinitis pigmentosa. Lancet (London, England) 2006;368:1795-809.

[52] Nandrot EF, Kim Y, Brodie SE, Huang X, Sheppard D, Finnemann SC. Loss of synchronized retinal phagocytosis and age-related blindness in mice lacking alphavbeta5 integrin. The Journal of experimental medicine 2004;200:1539-45.

[53] Nandrot EF, Anand M, Almeida D, Atabai K, Sheppard D, Finnemann SC. Essential role for MFG-E8 as ligand for alphavbeta5 integrin in diurnal retinal phagocytosis. Proceedings of the National Academy of Sciences of the United States of America 2007;104:12005-10.

[54] Abu-Safieh L, Alrashed M, Anazi S, Alkuraya H, Khan AO, Al-Owain M, et al. Autozygome-guided exome sequencing in retinal dystrophy patients reveals pathogenetic mutations and novel candidate disease genes. Genome research 2013;23:236-47.

[55] Patel N, Aldahmesh MA, Alkuraya H, Anazi S, Alsharif H, Khan AO, et al. Expanding the clinical, allelic, and locus heterogeneity of retinal dystrophies. Genetics in medicine : official journal of the American College of Medical Genetics 2016;18:554-62.

[56] Mackay DS, Henderson RH, Sergouniotis PI, Li Z, Moradi P, Holder GE, et al. Novel mutations in MERTK associated with childhood onset rod-cone dystrophy. Molecular vision 2010;16:369-77.

[57] Ksantini M, Lafont E, Bocquet B, Meunier I, Hamel CP. Homozygous mutation in MERTK causes severe autosomal recessive retinitis pigmentosa. European journal of ophthalmology 2012;22:647-53.

[58] Churchill JD, Bowne SJ, Sullivan LS, Lewis RA, Wheaton DK, Birch DG, et al. Mutations in the X-linked retinitis pigmentosa genes RPGR and RP2 found in 8.5% of families with a provisional diagnosis of autosomal dominant retinitis pigmentosa. Investigative ophthalmology & visual science 2013;54:1411-6.

[59] Meindl A, Dry K, Herrmann K, Manson F, Ciccodicola A, Edgar A, et al. A gene (RPGR) with homology to the RCC1 guanine nucleotide exchange factor is mutated in X-linked retinitis pigmentosa (RP3). Nature genetics 1996;13:35-42.

[60] Hong DH, Li T. Complex expression pattern of RPGR reveals a role for purine-rich exonic splicing enhancers. Investigative ophthalmology & visual science 2002;43:3373-82.

[61] Linari M, Ueffing M, Manson F, Wright A, Meitinger T, Becker J. The retinitis pigmentosa GTPase regulator, RPGR, interacts with the delta subunit of rod cyclic GMP phosphodiesterase. Proceedings of the National Academy of Sciences of the United States of America 1999;96:1315-20.

[62] Bakondi B, Lv W, Lu B, Jones MK, Tsai Y, Kim KJ, et al. In Vivo CRISPR/Cas9 Gene Editing Corrects Retinal Dystrophy in the S334ter-3 Rat Model of Autosomal Dominant Retinitis Pigmentosa. Molecular therapy : the journal of the American Society of Gene Therapy 2016;24:556-63.

[63] Bassuk AG, Zheng A, Li Y, Tsang SH, Mahajan VB. Precision Medicine: Genetic Repair of Retinitis Pigmentosa in Patient-Derived Stem Cells. Scientific reports 2016;6:19969.

[64] Latella MC, Di Salvo MT, Cocchiarella F, Benati D, Grisendi G, Comitato A, et al. In vivo Editing of the Human Mutant Rhodopsin Gene by Electroporation of Plasmid-based CRISPR/Cas9 in the Mouse Retina. Mol Ther Nucleic Acids 2016;5:e389-e.

[65] MacLaren RE, Groppe M, Barnard AR, Cottriall CL, Tolmachova T, Seymour L, et al. Retinal gene therapy in patients with choroideremia: initial findings from a phase 1/2 clinical trial. Lancet (London, England) 2014;383:1129-37.

[66] Zinkernagel MS, MacLaren RE. Recent advances and future prospects in choroideremia. Clinical ophthalmology (Auckland, NZ) 2015;9:2195-200.

[67] Noshiro M, Nishimoto M, Okuda K. Rat liver cholesterol 7 alpha-hydroxylase. Pretranslational regulation for circadian rhythm. The Journal of biological chemistry 1990;265:10036-41.

[68] Charbel Issa P, Barnard AR, Herrmann P, Washington I, MacLaren RE. Rescue of the Stargardt phenotype in Abca4 knockout mice through inhibition of vitamin A dimerization. Proceedings of the National Academy of Sciences of the United States of America 2015;112:8415-20.

[69] Zaneveld J, Wang F, Wang X, Chen R. Dawn of ocular gene therapy: implications for molecular diagnosis in retinal disease. Science ChinaLife sciences 2013;56:125-33.

[70] Kremer H, van Wijk E, Marker T, Wolfrum U, Roepman R. Usher syndrome: molecular links of pathogenesis, proteins and pathways. Human molecular genetics 2006;15 Spec No 2:R262-70.

[71] Sanjurjo-Soriano C, Kalatzis V. Guiding Lights in Genome Editing for Inherited Retinal Disorders: Implications for Gene and Cell Therapy. Neural plasticity 2018;2018:5056279.

[72] Fuster-García C, García-García G, González-Romero E, Jaijo T, Sequedo MD, Ayuso C, et al. USH2A Gene Editing Using the CRISPR System. Mol Ther Nucleic Acids 2017;8:529-41.

[73] Keil S, Fielder A, Sargent J. Management of children and young people with vision impairment: diagnosis, developmental challenges and outcomes. Archives of Disease in Childhood 2017;102:566-71.

[74] Sinha D, Steyer B, Shahi PK, Mueller KP, Valiauga R, Edwards KL, et al. Human iPSC Modeling Reveals Mutation-Specific Responses to Gene Therapy in a Genotypically Diverse Dominant Maculopathy. American Journal of Human Genetics 2020;107:278-92.

[75] Huang KC, Wang ML, Chen SJ, Kuo JC, Wang WJ, Nhi Nguyen PN, et al. Morphological and Molecular Defects in Human Three-Dimensional Retinal Organoid Model of X-Linked Juvenile Retinoschisis. Stem cell reports 2019;13:906-23.

[76] Boycott KM, Maybaum TA, Naylor MJ, Weleber RG, Robitaille J, Miyake Y, et al. A summary of 20 CACNA1F mutations identified in 36 families with incomplete X-linked congenital stationary night blindness, and characterization of splice variants. Human genetics 2001;108:91-7.

[77] van Genderen MM, Bijveld MM, Claassen YB, Florijn RJ, Pearring JN, Meire FM, et al. Mutations in TRPM1 are a common cause of complete congenital stationary night blindness. American Journal of Human Genetics 2009;85:730-6.

[78] Bainbridge JW, Smith AJ, Barker SS, Robbie S, Henderson R, Balaggan K, et al. Effect of gene therapy on visual function in Leber's congenital amaurosis. The New England journal of medicine 2008;358:2231-9.

[79] Jo DH, Song DW, Cho CS, Kim UG, Lee KJ, Lee K, et al. CRISPR-Cas9-mediated therapeutic editing of Rpe65 ameliorates the disease phenotypes in a mouse model of Leber congenital amaurosis. Science advances 2019;5:eaax1210.

[80] Burnight ER, Gupta M, Wiley LA, Anfinson KR, Tran A, Triboulet R, et al. Using CRISPR-Cas9 to Generate Gene-Corrected Autologous iPSCs for the Treatment of Inherited Retinal Degeneration. Molecular therapy : the journal of the American Society of Gene Therapy 2017;25:1999-2013.

[81] Holmgaard A, Askou AL, Benckendorff JNE, Thomsen EA, Cai Y, Bek T, et al. In Vivo Knockout of the Vegfa Gene by Lentiviral Delivery of CRISPR/Cas9 in Mouse Retinal Pigment Epithelium Cells. Molecular therapyNucleic acids 2017;9:89-99.

[82] Koo T, Park SW, Jo DH, Kim D, Kim JH, Cho HY, et al. CRISPR-LbCpf1 prevents choroidal neovascularization in a mouse model of age-related macular degeneration. Nature communications 2018;9:1855-018-04175-y.

[83] Noel NCL, Nadolski NJ, Hocking JC, MacDonald IM, Allison WT. Progressive Photoreceptor Dysfunction and Age-Related Macular Degeneration-Like Features in rp1l1 Mutant Zebrafish. Cells 2020;9:10.3390/cells9102214.

[84] Hu S, Du J, Chen N, Jia R, Zhang J, Liu X, et al. In Vivo CRISPR/Cas9-Mediated Genome Editing Mitigates Photoreceptor Degeneration in a Mouse Model of X-Linked Retinitis Pigmentosa. Investigative ophthalmology & visual science 2020;61:31.

[85] Li P, Kleinstiver BP, Leon MY, Prew MS, Navarro-Gomez D, Greenwald SH, et al. Allele-Specific CRISPR-Cas9 Genome Editing of the Single-Base P23H Mutation for Rhodopsin-Associated Dominant Retinitis Pigmentosa. The CRISPR journal 2018;1:55-64.

[86] Wu WH, Tsai YT, Justus S, Lee TT, Zhang L, Lin CS, et al. CRISPR Repair Reveals Causative Mutation in a Preclinical Model of Retinitis Pigmentosa. Molecular therapy : the journal of the American Society of Gene Therapy 2016;24:1388-94.

[87] Feehan JM, Chiu CN, Stanar P, Tam BM, Ahmed SN, Moritz OL. Modeling Dominant and Recessive Forms of Retinitis Pigmentosa by Editing Three Rhodopsin-Encoding Genes in Xenopus Laevis Using Crispr/Cas9. Scientific reports 2017;7:6920-017-07153-4.

[88] Yu W, Mookherjee S, Chaitankar V, Hiriyanna S, Kim JW, Brooks M, et al. Nrl knockdown by AAV-delivered CRISPR/Cas9 prevents retinal degeneration in mice. Nature communications 2017;8:14716.

[89] Fuster-Garcia C, Garcia-Garcia G, Gonzalez-Romero E, Jaijo T, Sequedo MD, Ayuso C, et al. USH2A Gene Editing Using the CRISPR System. Molecular therapyNucleic acids 2017;8:529-41.

[90] Sanjurjo-Soriano C, Erkilic N, Baux D, Mamaeva D, Hamel CP, Meunier I, et al. Genome Editing in Patient iPSCs Corrects the Most Prevalent USH2A Mutations and Reveals Intriguing Mutant mRNA Expression Profiles. Molecular therapyMethods & clinical development 2019;17:156-73.

[91] Chen D, Xu T, Tu M, Xu J, Zhou C, Cheng L, et al. Recapitulating X-Linked Juvenile Retinoschisis in Mouse Model by Knock-In Patient-Specific Novel Mutation. Frontiers in molecular neuroscience 2018;10:453.

[92] Ye GJ, Budzynski E, Sonnentag P, Nork TM, Sheibani N, Gurel Z, et al. Cone-Specific Promoters for Gene Therapy of Achromatopsia and Other Retinal Diseases. Human Gene Therapy 2016;27:72-82.

[93] Lheriteau E, Petit L, Weber M, Le Meur G, Deschamps JY, Libeau L, et al. Successful gene therapy in the RPGRIP1-deficient dog: a large model of cone-rod dystrophy. Molecular therapy : the journal of the American Society of Gene Therapy 2014;22:265-77.

[94] Thiadens AA, Phan TM, Zekveld-Vroon RC, Leroy BP, van den Born LI, Hoyng CB, et al. Clinical course, genetic etiology, and visual outcome in cone and cone-rod dystrophy. Ophthalmology 2012;119:819-26.

[95] Roosing S, Thiadens AA, Hoyng CB, Klaver CC, den Hollander AI, Cremers FP. Causes and consequences of inherited cone disorders. Progress in retinal and eye research 2014;42:1-26.

[96] Naeem M, Majeed S, Hoque MZ, Ahmad I. Latest Developed Strategies to Minimize the Off-Target Effects in CRISPR-Cas-Mediated Genome Editing. Cells 2020;9:1608.

[97] Garrood WT, Kranjc N, Petri K, Kim DY, Guo JA, Hammond AM, et al. Analysis of off-target effects in CRISPR-based gene drives in the human malaria mosquito. Proceedings of the National Academy of Sciences of the United States of America 2021;118:e2004838117.

[98] Modrzejewski D, Hartung F, Lehnert H, Sprink T, Kohl C, Keilwagen J, et al. Which Factors Affect the Occurrence of Off-Target Effects Caused by the Use of CRISPR/Cas: A Systematic Review in Plants. Front Plant Sci 2020;11:574959-.

[99] Gonzalez-Avila LU, Vega-López JM, Pelcastre-Rodríguez LI, Cabrero-Martínez OA, Hernández-Cortez C, Castro-Escarpulli G. The Challenge of CRISPR-Cas Toward Bioethics. Front Microbiol2021. p. 657981.

[100] Hejtmancik JF, Daiger SP. Understanding the genetic architecture of human retinal degenerations. Proceedings of the National Academy of Sciences of the United States of America 2020;117:3904-6.

[101] Uddin F, Rudin CM, Sen T. CRISPR Gene Therapy: Applications, Limitations, and Implications for the Future. Front Oncol 2020;10:1387-.

[102] Liu M, Rehman S, Tang X, Gu K, Fan Q, Chen D, et al. Methodologies for Improving HDR Efficiency. Frontiers in genetics 2019;9:691-.

[103] Smith DW, Lee C-J, Gardiner BS. No flow through the vitreous humor: How strong is the evidence? Progress in retinal and eye research 2020;78:100845.

[104] Mout R, Ray M, Lee YW, Scaletti F, Rotello VM. In Vivo Delivery of CRISPR/Cas9 for Therapeutic Gene Editing: Progress and Challenges. Bioconjugate chemistry 2017;28:880-4.

[105] Neefjes J, Jongsma ML, Paul P, Bakke O. Towards a systems understanding of MHC class I and MHC class II antigen presentation. Nature reviewsImmunology 2011;11:823-36.

[106] Chew WL, Tabebordbar M, Cheng JK, Mali P, Wu EY, Ng AH, et al. A multifunctional AAV-CRISPR-Cas9 and its host response. Nature methods 2016;13:868-74.

[107] Hacein-Bey-Abina S, Garrigue A, Wang GP, Soulier J, Lim A, Morillon E, et al. Insertional oncogenesis in 4 patients after retrovirus-mediated gene therapy of SCID-X1. The Journal of clinical investigation 2008;118:3132-42.

[108] Zincarelli C, Soltys S, Rengo G, Rabinowitz JE. Analysis of AAV serotypes 1-9 mediated gene expression and tropism in mice after systemic injection. Molecular therapy : the journal of the American Society of Gene Therapy 2008;16:1073-80.

[109] Peer D, Karp JM, Hong S, Farokhzad OC, Margalit R, Langer R. Nanocarriers as an emerging platform for cancer therapy. Nature nanotechnology 2007;2:751-60.

[110] Xu X, Gao D, Wang P, Chen J, Ruan J, Xu J, et al. Efficient homology-directed gene editing by CRISPR/Cas9 in human stem and primary cells using tube electroporation. Scientific reports 2018;8:11649-018-30227-w.

[111] Mout R, Ray M, Yesilbag Tonga G, Lee YW, Tay T, Sasaki K, et al. Direct Cytosolic Delivery of CRISPR/Cas9-Ribonucleoprotein for Efficient Gene Editing. ACS nano 2017;11:2452-8.

[112] Cho SW, Kim S, Kim Y, Kweon J, Kim HS, Bae S, et al. Analysis of off-target effects of CRISPR/Cas-derived RNA-guided endonucleases and nickases. Genome research 2014;24:132-41.

[113] Fu Y, Foden JA, Khayter C, Maeder ML, Reyon D, Joung JK, et al. High-frequency off-target mutagenesis induced by CRISPR-Cas nucleases in human cells. Nature biotechnology 2013;31:822-6.

[114] Carroll D. Genome engineering with targetable nucleases. Annual Review of Biochemistry 2014;83:409-39.

[115] Kleinstiver BP, Pattanayak V, Prew MS, Tsai SQ, Nguyen NT, Zheng Z, et al. High-fidelity CRISPR-Cas9 nucleases with no detectable genome-wide off-target effects. Nature 2016;529:490-5.

[116] Slaymaker IM, Gao L, Zetsche B, Scott DA, Yan WX, Zhang F. Rationally engineered Cas9 nucleases with improved specificity. Science (New York, NY) 2016;351:84-8.

[117] Ramakrishna S, Kwaku Dad AB, Beloor J, Gopalappa R, Lee SK, Kim H. Gene disruption by cell-penetrating peptide-mediated delivery of Cas9 protein and guide RNA. Genome research 2014;24:1020-7.

[118] Agrahari V, Mandal A, Agrahari V, Trinh HM, Joseph M, Ray A, et al. A comprehensive insight on ocular pharmacokinetics. Drug delivery and translational research 2016;6:735-54.

[119] Cholkar K, Patel SP, Vadlapudi AD, Mitra AK. Novel strategies for anterior segment ocular drug delivery. Journal of ocular pharmacology and therapeutics : the official journal of the Association for Ocular Pharmacology and Therapeutics 2013;29:106-23.

[120] Nickla DL, Wallman J. The multifunctional choroid. Progress in retinal and eye research 2010;29:144-68.

[121] Edelhauser HF, Rowe-Rendleman CL, Robinson MR, Dawson DG, Chader GJ, Grossniklaus HE, et al. Ophthalmic drug delivery systems for the treatment of retinal diseases: basic research to clinical applications. Investigative ophthalmology & visual science 2010;51:5403-20.

[122] Shikari H, Silva PS, Sun JK. Complications of intravitreal injections in patients with diabetes. Seminars in ophthalmology 2014;29:276-89.

[123] Tsai CH, Wang PY, Lin IC, Huang H, Liu GS, Tseng CL. Ocular Drug Delivery: Role of Degradable Polymeric Nanocarriers for Ophthalmic Application. International journal of molecular sciences 2018;19:10.3390/ijms19092830.

[124] Varela-Fernandez R, Diaz-Tome V, Luaces-Rodriguez A, Conde-Penedo A, Garcia-Otero X, Luzardo-Alvarez A, et al. Drug Delivery to the Posterior Segment of the Eye: Biopharmaceutic and Pharmacokinetic Considerations. Pharmaceutics 2020;12:10.3390/pharmaceutics12030269.

[125] Patel A, Cholkar K, Agrahari V, Mitra AK. Ocular drug delivery systems: An overview. World journal of pharmacology 2013;2:47-64.

[126] Souto EB, Dias-Ferreira J, Lopez-Machado A, Ettcheto M, Cano A, Camins Espuny A, et al. Advanced Formulation Approaches for Ocular Drug Delivery: State-Of-The-Art and Recent Patents. Pharmaceutics 2019;11:10.3390/pharmaceutics11090460.

[127] Ding Q, Regan SN, Xia Y, Oostrom LA, Cowan CA, Musunuru K. Enhanced efficiency of human pluripotent stem cell genome editing through replacing TALENs with CRISPRs. Cell stem cell 2013;12:393-4.

[128] Hung KL, Meitlis I, Hale M, Chen CY, Singh S, Jackson SW, et al. Engineering Protein-Secreting Plasma Cells by Homology-Directed Repair in Primary Human B Cells. Molecular therapy : the journal of the American Society of Gene Therapy 2018;26:456-67.

[129] Hui SW. Overview of drug delivery and alternative methods to electroporation. Methods in molecular biology (Clifton, NJ) 2008;423:91-107.

[130] Xu W. Microinjection and Micromanipulation: A Historical Perspective. Methods in molecular biology (Clifton, NJ) 2019;1874:1-16.

[131] Subrizi A, del Amo EM, Korzhikov-Vlakh V, Tennikova T, Ruponen M, Urtti A. Design principles of ocular drug delivery systems: importance of drug payload, release rate, and material properties. Drug Discovery Today 2019;24:1446-57.

[132] Käsdorf BT, Arends F, Lieleg O. Diffusion Regulation in the Vitreous Humor. Biophys J 2015;109:2171-81.

[133] Tavakoli S, Kari OK, Turunen T, Lajunen T, Schmitt M, Lehtinen J, et al. Diffusion and Protein Corona Formation of Lipid-Based Nanoparticles in the Vitreous Humor: Profiling and Pharmacokinetic Considerations. Molecular pharmaceutics 2020;18:699-713.

[134] Yu H, Wu W, Lin X, Feng Y. Polysaccharide-Based Nanomaterials for Ocular Drug Delivery: A Perspective. Frontiers in bioengineering and biotechnology 2020;8:601246-.

[135] Wilbie D, Walther J, Mastrobattista E. Delivery Aspects of CRISPR/Cas for in Vivo Genome Editing. Accounts of Chemical Research 2019;52:1555-64.

[136] Li L, He ZY, Wei XW, Gao GP, Wei YQ. Challenges in CRISPR/CAS9 Delivery: Potential Roles of Nonviral Vectors. Human Gene Therapy 2015;26:452-62.

[137] Nakai H, Yant SR, Storm TA, Fuess S, Meuse L, Kay MA. Extrachromosomal recombinant adeno-associated virus vector genomes are primarily responsible for stable liver transduction in vivo. Journal of virology 2001;75:6969-76.

[138] McCarty DM, Monahan PE, Samulski RJ. Self-complementary recombinant adeno-associated virus (scAAV) vectors promote efficient transduction independently of DNA synthesis. Gene therapy 2001;8:1248-54.

[139] Zetsche B, Volz SE, Zhang F. A split-Cas9 architecture for inducible genome editing and transcription modulation. Nature biotechnology 2015;33:139-42.

[140] Bainbridge JW, Mehat MS, Sundaram V, Robbie SJ, Barker SE, Ripamonti C, et al. Long-term effect of gene therapy on Leber's congenital amaurosis. The New England journal of medicine 2015;372:1887-97.

[141] Chen Y, Moiseyev G, Takahashi Y, Ma JX. RPE65 gene delivery restores isomerohydrolase activity and prevents early cone loss in Rpe65-/- mice. Investigative ophthalmology & visual science 2006;47:1177-84.

[142] Pang JJ, Chang B, Kumar A, Nusinowitz S, Noorwez SM, Li J, et al. Gene therapy restores vision-dependent behavior as well as retinal structure and function in a mouse model of RPE65 Leber congenital amaurosis. Molecular therapy : the journal of the American Society of Gene Therapy 2006;13:565-72.

[143] Hauswirth WW, Aleman TS, Kaushal S, Cideciyan AV, Schwartz SB, Wang L, et al. Treatment of leber congenital amaurosis due to RPE65 mutations by ocular subretinal injection

of adeno-associated virus gene vector: short-term results of a phase I trial. Human Gene Therapy 2008;19:979-90.

[144] Maguire AM, Simonelli F, Pierce EA, Pugh EN, Jr., Mingozzi F, Bennicelli J, et al. Safety and efficacy of gene transfer for Leber's congenital amaurosis. The New England journal of medicine 2008;358:2240-8.

[145] Kleinstiver BP, Prew MS, Tsai SQ, Topkar VV, Nguyen NT, Zheng Z, et al. Engineered CRISPR-Cas9 nucleases with altered PAM specificities. Nature 2015;523:481-5.

[146] Ran FA, Cong L, Yan WX, Scott DA, Gootenberg JS, Kriz AJ, et al. In vivo genome editing using Staphylococcus aureus Cas9. Nature 2015;520:186-91.

[147] Esvelt KM, Mali P, Braff JL, Moosburner M, Yaung SJ, Church GM. Orthogonal Cas9 proteins for RNA-guided gene regulation and editing. Nature methods 2013;10:1116-21.

[148] Wang D, Mou H, Li S, Li Y, Hough S, Tran K, et al. Adenovirus-Mediated Somatic Genome Editing of Pten by CRISPR/Cas9 in Mouse Liver in Spite of Cas9-Specific Immune Responses. Human Gene Therapy 2015;26:432-42.

[149] Yang Y, Jooss KU, Su Q, Ertl HC, Wilson JM. Immune responses to viral antigens versus transgene product in the elimination of recombinant adenovirus-infected hepatocytes in vivo. Gene therapy 1996;3:137-44.

[150] Hoffman LM, Maguire AM, Bennett J. Cell-mediated immune response and stability of intraocular transgene expression after adenovirus-mediated delivery. Investigative ophthalmology & visual science 1997;38:2224-33.

[151] Ueyama K, Mori K, Shoji T, Omata H, Gehlbach PL, Brough DE, et al. Ocular localization and transduction by adenoviral vectors are serotype-dependent and can be modified by inclusion of RGD fiber modifications. PloS one 2014;9:e108071.

[152] Bainbridge JW, Mistry A, De Alwis M, Paleolog E, Baker A, Thrasher AJ, et al. Inhibition of retinal neovascularisation by gene transfer of soluble VEGF receptor sFlt-1. Gene therapy 2002;9:320-6.

[153] Julien S, Kreppel F, Beck S, Heiduschka P, Brito V, Schnichels S, et al. A reproducible and quantifiable model of choroidal neovascularization induced by VEGF A165 after subretinal adenoviral gene transfer in the rabbit. Molecular vision 2008;14:1358-72.

[154] Wang H, Wei F, Li H, Ji X, Li S, Chen X. Combination of oncolytic adenovirus and endostatin inhibits human retinoblastoma in an in vivo mouse model. International journal of molecular medicine 2013;31:377-85.

[155] Sellon DC, Perry ST, Coggins L, Fuller FJ. Wild-type equine infectious anemia virus replicates in vivo predominantly in tissue macrophages, not in peripheral blood monocytes. Journal of virology 1992;66:5906-13.

[156] Palfi S, Gurruchaga JM, Ralph GS, Lepetit H, Lavisse S, Buttery PC, et al. Long-term safety and tolerability of ProSavin, a lentiviral vector-based gene therapy for Parkinson's disease: a dose escalation, open-label, phase 1/2 trial. Lancet (London, England) 2014;383:1138-46.

[157] Hashimoto T, Gibbs D, Lillo C, Azarian SM, Legacki E, Zhang XM, et al. Lentiviral gene replacement therapy of retinas in a mouse model for Usher syndrome type 1B. Gene therapy 2007;14:584-94.

[158] Balaggan KS, Binley K, Esapa M, Iqball S, Askham Z, Kan O, et al. Stable and efficient intraocular gene transfer using pseudotyped EIAV lentiviral vectors. The journal of gene medicine 2006;8:275-85.

[159] Shin J, Lee N, Cho S, Cho BK. Targeted Genome Editing Using DNA-Free RNA-Guided Cas9 Ribonucleoprotein for CHO Cell Engineering. Methods in molecular biology (Clifton, NJ) 2018;1772:151-69.

[160] Lee M, Kim SW. Polyethylene glycol-conjugated copolymers for plasmid DNA delivery. Pharmaceutical research 2005;22:1-10.

[161] Patra JK, Das G, Fraceto LF, Campos EVR, Rodriguez-Torres MDP, Acosta-Torres LS, et al. Nano based drug delivery systems: recent developments and future prospects. J Nanobiotechnology 2018;16:71-.

[162] Pooja D, Kadari A, Kulhari H, Sistla R. Chapter 13 - Lipid-based nanomedicines: Current clinical status and future perspectives. In: Grumezescu AM, editor. Lipid Nanocarriers for Drug Targeting: William Andrew Publishing; 2018. p. 509-28.

[163] Khiev D, Mohamed ZA, Vichare R, Paulson R, Bhatia S, Mohapatra S, et al. Emerging Nano-Formulations and Nanomedicines Applications for Ocular Drug Delivery. Nanomaterials 2021;11:173.

[164] Felgner PL, Gadek TR, Holm M, Roman R, Chan HW, Wenz M, et al. Lipofection: a highly efficient, lipid-mediated DNA-transfection procedure. Proceedings of the National Academy of Sciences of the United States of America 1987;84:7413-7.

[165] Kariko K, Muramatsu H, Welsh FA, Ludwig J, Kato H, Akira S, et al. Incorporation of pseudouridine into mRNA yields superior nonimmunogenic vector with increased translational capacity and biological stability. Molecular therapy : the journal of the American Society of Gene Therapy 2008;16:1833-40.

[166] Wang M, Zuris JA, Meng F, Rees H, Sun S, Deng P, et al. Efficient delivery of genome-editing proteins using bioreducible lipid nanoparticles. Proceedings of the National Academy of Sciences of the United States of America 2016;113:2868-73.

[167] Chang J, Chen X, Glass Z, Gao F, Mao L, Wang M, et al. Integrating Combinatorial Lipid Nanoparticle and Chemically Modified Protein for Intracellular Delivery and Genome Editing. Accounts of Chemical Research 2019;52:665-75.

[168] Wei T, Cheng Q, Min YL, Olson EN, Siegwart DJ. Systemic nanoparticle delivery of CRISPR-Cas9 ribonucleoproteins for effective tissue specific genome editing. Nature communications 2020;11:3232-020-17029-3.

[169] Li L, Hu S, Chen X. Non-viral delivery systems for CRISPR/Cas9-based genome editing: Challenges and opportunities. Biomaterials 2018;171:207-18.

[170] Akinc A, Thomas M, Klibanov AM, Langer R. Exploring polyethylenimine-mediated DNA transfection and the proton sponge hypothesis. The journal of gene medicine 2005;7:657-63.

[171] Zhang Z, Wan T, Chen Y, Chen Y, Sun H, Cao T, et al. Cationic Polymer-Mediated CRISPR/Cas9 Plasmid Delivery for Genome Editing. Macromolecular rapid communications 2019;40:e1800068.

[172] Sun W, Ji W, Hall JM, Hu Q, Wang C, Beisel CL, et al. Self-assembled DNA nanoclews for the efficient delivery of CRISPR-Cas9 for genome editing. Angewandte Chemie (International edin English) 2015;54:12029-33.

[173] Li L, Wei Y, Gong C. Polymeric Nanocarriers for Non-Viral Gene Delivery. Journal of biomedical nanotechnology 2015;11:739-70.

[174] Maruyama A, Watanabe H, Ferdous A, Katoh M, Ishihara T, Akaike T. Characterization of interpolyelectrolyte complexes between double-stranded DNA and polylysine comb-type copolymers having hydrophilic side chains. Bioconjugate chemistry 1998;9:292-9.

[175] Yin H, Kanasty RL, Eltoukhy AA, Vegas AJ, Dorkin JR, Anderson DG. Non-viral vectors for gene-based therapy. Nature reviewsGenetics 2014;15:541-55.

[176] Ramirez-Acosta CM, Cifuentes J, Castellanos MC, Moreno RJ, Munoz-Camargo C, Cruz JC, et al. PH-Responsive, Cell-Penetrating, Core/Shell Magnetite/Silver Nanoparticles for the Delivery of Plasmids: Preparation, Characterization, and Preliminary In Vitro Evaluation. Pharmaceutics 2020;12:10.3390/pharmaceutics12060561.

[177] Chen G, Abdeen AA, Wang Y, Shahi PK, Robertson S, Xie R, et al. A biodegradable nanocapsule delivers a Cas9 ribonucleoprotein complex for in vivo genome editing. Nature nanotechnology 2019;14:974-80.

[178] Madaan K, Kumar S, Poonia N, Lather V, Pandita D. Dendrimers in drug delivery and targeting: Drug-dendrimer interactions and toxicity issues. Journal of pharmacy & bioallied sciences 2014;6:139-50.

[179] Shah N, Steptoe RJ, Parekh HS. Low-generation asymmetric dendrimers exhibit minimal toxicity and effectively complex DNA. Journal of peptide science : an official publication of the European Peptide Society 2011;17:470-8.

[180] Yu T, Liu X, Bolcato-Bellemin AL, Wang Y, Liu C, Erbacher P, et al. An amphiphilic dendrimer for effective delivery of small interfering RNA and gene silencing in vitro and in vivo. Angewandte Chemie (International edin English) 2012;51:8478-84.

[181] Choi JS, Nam K, Park JY, Kim JB, Lee JK, Park JS. Enhanced transfection efficiency of PAMAM dendrimer by surface modification with L-arginine. Journal of controlled release : official journal of the Controlled Release Society 2004;99:445-56.

[182] Liu C, Wan T, Wang H, Zhang S, Ping Y, Cheng Y. A boronic acid-rich dendrimer with robust and unprecedented efficiency for cytosolic protein delivery and CRISPR-Cas9 gene editing. Science advances 2019;5:eaaw8922.

[183] Fry LE, Peddle CF, Barnard AR, McClements ME, MacLaren RE. RNA editing as a therapeutic approach for retinal gene therapy requiring long coding sequences. International journal of molecular sciences 2020;21:10.3390/ijms21030777.

[184] Stone EM, Andorf JL, Whitmore SS, DeLuca AP, Giacalone JC, Streb LM, et al. Clinically Focused Molecular Investigation of 1000 Consecutive Families with Inherited Retinal Disease. Ophthalmology 2017;124:1314-31.

[185] Zinshteyn B, Nishikura K. Adenosine-to-inosine RNA editing. Wiley interdisciplinary reviewsSystems biology and medicine 2009;1:202-9.

[186] Matsoukas IG. Commentary: RNA editing with CRISPR-Cas13. Frontiers in genetics 2018;9:134.

[187] Walters BJ, Azam AB, Gillon CJ, Josselyn SA, Zovkic IB. Advanced In vivo Use of CRISPR/Cas9 and Anti-sense DNA Inhibition for Gene Manipulation in the Brain. Frontiers in genetics 2016;6:362.

Chapter 2

Development and characterization of cationic, amphiphilic lipopolymeric nanoplexes for delivering CRISPR/Cas9 expressing plasmid

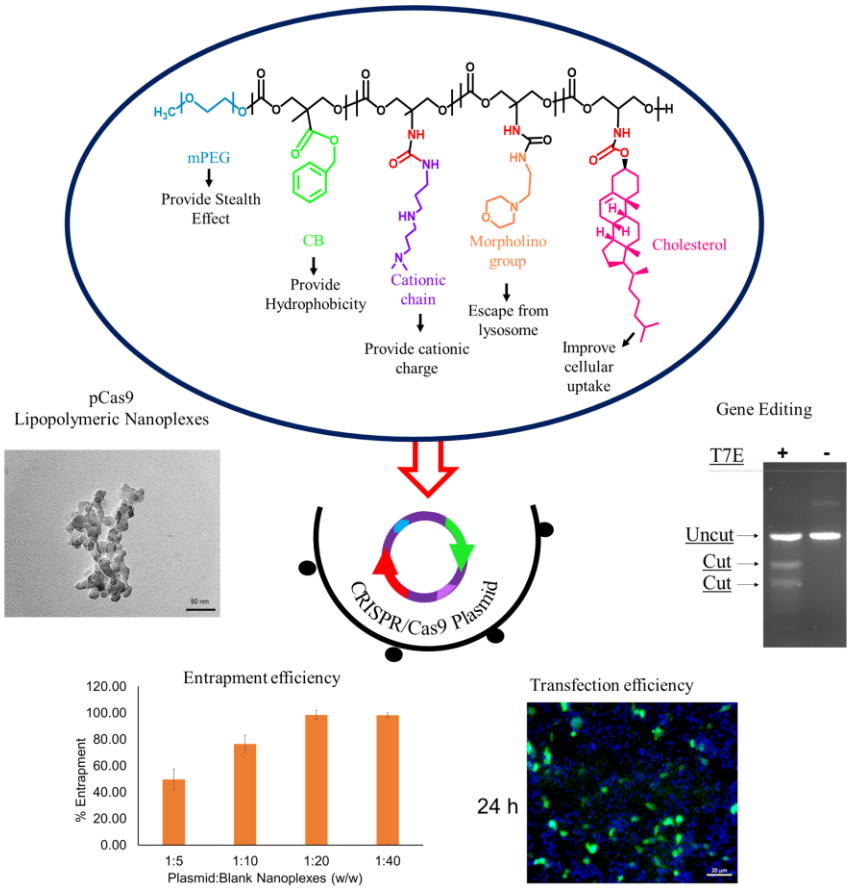

- Synthesis and characterization of cationic amphiphilic lipopolymer
- Preparation and evaluation of CRISPR/Cas9 plasmid loaded lipopolymeric nanoplexes
- *In vitro* evaluation
- *In vivo* tissue distribution

2.1. Introduction

CRISPR/Cas9 system is a mainstream molecular scissor comprising an endonuclease protein, i.e., Cas9, and a single guide RNA (sgRNA) [1, 2]. The sgRNA sequence directs the endonuclease activity of the Cas9 protein; therefore, the CRISPR/Cas9 system is sometimes also called an RNA-directed DNA cleavage system [3]. The system has proven its site-specificity and precise double-strand break (DSB) efficiency, which further leads to non-homologous end joining (NHEJ) or homology-directed repair (HDR) based insertion/deletion of the target DNA sequence [2]. Many debilitating diseases are under surveillance in a clinical trial where CRISPR therapy has been employed [4]. There are three forms of deliverable CRISPR, i.e., plasmid, mRNA, and ribonucleoprotein, each of which has its inherent pros and cons [2]. The *in vitro* and *in vivo* delivery of all three forms of CRISPR is quite challenging owing to the high molecular weight, supranegative charge, hydrophilicity, degradation in the extracellular environment by nucleases, etc. [5]. However, the viral vectors have been utilized to deliver CRISPR components, specifically the plasmid, but possess comprehensive limitations such as immunogenicity, limited payload capacity, mutagenesis, etc. [6]. For instance, the payload capacity of the adeno-associated viruses (AVVs) vector is ~4.7 kb; however, the Cas9 gene itself has a size of ~4 kb [7]. Additionally, for a functional CRISPR vector, other components, such as sgRNA, need to be incorporated [8].

Nowadays, various non-viral vectors such as lipid nanoparticles, polymeric nanoparticles, and dendrimers have been explored for their capacity to carry the CRISPR components to the cells *in vitro* and *in vivo* [2, 6]. CRISPR components, specifically the plasmid, which has an insert for Cas9 protein along with one or more sgRNAs, are easy to construct using the cloning technique and are a very stable form of deliverable CRISPR. In this way, multiplex editing could be achieved using a single constructed plasmid. Although, there are unintended drawbacks associated with the

use of plasmid, such as permanent integration of plasmid sequence in the host DNA, which could be encountered or may lead to downstream off-target concerns [6]. To the best of our knowledge, many non-viral vectors have been explored to effectively deliver CRISPR plasmids [9] through different formulation strategies. In this study, we have synthesized an amphiphilic lipopolymer (mPEG-b-(CB-{g-cationic chain; g-Chol; g-Morph}) grafted with different pendant groups, i.e., cationic chain (which provides a cationic charge which helps in condensation of negatively charged plasmid), a morpholino group (which aids in endo/lysosomal escape *via*. proton sponge effect) and a cholesterol group (which improve the cellular uptake). Overall, the polymer comprises all the necessary components for the successful delivery of the plasmid cargo to the cytosol by surpassing all the intercellular and intracellular barriers. The buffer capacity of the polymer was determined using the titration method. Further, the lipopolymer was utilized to prepare a blank nanoformulation using the double-emulsion solvent evaporation method followed by optimization of complexation at different ratios (*w/w*) of the plasmid to the polymer to form plasmid nanoplexes (pCas9 nanoplexes). The complexation efficiency of pCas9 nanoplexes was also evaluated using the zeta potential analysis and mobility shift assay. The pCas9 nanoplexes were further evaluated *in vitro* for transfection efficiency and gene editing efficiency in ARPE-19 cells. Moreover, the *in vivo* efficiency of the pCas9 nanoplexes was evaluated by a tissue distribution study using *In Vivo* Imaging System (IVIS) in *swiss albino* mice. Conclusively, this study explored insight into the role of cationic polymeric nanocarrier for the safe delivery of CRISPR plasmid *in vitro* and *in vivo*.

2.2. Materials

OptiMEM™ reduced serum media, Fetal Bovine Serum (FBS), Dulbecco's Modified Eagle Medium (DMEM), Snake skin (3.5 kD) dialysis membrane, MEGAscript™ T7 Transcription Kit,

Hoescht, CRISPRMax and DAPI (4',6-diamidino-2-phenylindole) were obtained from ThermoFischer scientific (Massachusetts, USA). T7 endonuclease I was purchased from Biolab (Delhi, India), while the Genomic DNA purification kit was purchased from Promega (Delhi, India). 3-(4,5-Dimethylthiazol-2-yl)-2,5-diphenyltetrazolium bromide (MTT) was purchased from Merck (Jaipur, India). All the primers were purchased from Imperial Life Science (ILS, Delhi, India). N,N-dimethyldipropylenetriamine (DP), Benzyl bromide, tin(II) 2-ethylhexanoate, cholesterol, methoxy poly(ethylene glycol) (mPEG, 5000 Da), hydroxybenzotriazole (HOBt), Bis(hydroxymethyl) propionic acid, 1-ethyl-3-(3-dimethylaminopropyl) carbodiimide hydrochloride (EDC.HCl) and 4-(2-aminoethyl) morpholine, HEPES buffer and Heparin sodium salt from porcine intestinal mucosa were purchased from Sigma Aldrich (St. Louis, MO). The remaining solvents and chemicals were of analytical grade and procured from local vendors.

2.3. Methodology

2.3.1. Plasmid and sgRNA sequences

Plasmid pX459-TURBO-GFP (11069 bp) was constructed by insertion of the TURBO-GFP gene sequence into the pSpCas9(BB)-2A-Puro (pX459) plasmid obtained through Addgene (www.addgene.org). Similarly, the RFP pPSM-dTOMATO (10068 bp) was also obtained through Addgene (www.addgene.org). The plasmid pX459-TURBO-GFP-5BPR2 encodes SpCas9 protein and a sgRNA targeting the 5BPR-2 gene (an intergenic region of a beta-globin gene cluster on chromosome 11) and encodes turboGFP protein. For sgRNA expression, the Plasmid pX459-TURBO-GFP-5BPR2 was constructed by inserting annealed oligo pairs 5BPR2 top: 5'-CACCgaggcacccgccactgtctc-3' and 5BPR2 bottom: 5' AAACgagacagtggcgggtgcctc-3' and ligated into the BbsI restriction sites of pX459-TURBO-GFP.

2.3.2. Synthesis of cationic lipopolymer mPEG b-(CB-{g-cationic chain; g-Chol; g-Morph})

For the synthesis of the cationic polymer, a previously reported multistep reaction scheme was adopted with slight modifications [10], as shown in Figure 2.1. Briefly, a cyclic monomer (**1**), 2-methyl-2-benzyloxycarbonylpropylene carbonate (MBC), was synthesized by mixing 2, 2- bis (hydroxymethyl) propionic acid (BHMP) with potassium hydroxide (KOH) followed by the addition of benzyl bromide in dimethylformamide at 100°C for 15 h. Obtained product, benzyl 2, 2-bis(methylol)propionate, was purified and recrystallized using toluene and further reacted with triphosgene in dichloromethane and pyridine mixture to get cyclic monomer, MBC (**1).** Furthermore, the obtained cyclic monomer was dried and used in microwave-directed ring-opening polymerization (ROP) with mPEG (molecular weight: 5000 Da) (**2**) at 135ºC for 35 minutes in the presence of tin (II) 2-ethyl hexanoate (10 mol% of mPEG) as a catalyst. A polymer, mPEG-CB (**3**), obtained was purified using ice-cold isopropanol (IPA) and diethyl ether (DEE). To obtain a polymer with free carboxyl (-COOH) groups (mPEG-b-p(CB-{g-COOH}) **(4))**, the benzylic moiety of the polymer, mPEG-CB **(3)** was reduced by palladium on carbon (Pd/C) wherein the polymer was dissolved in tetrahydrofuran and methanol (THF: MeOH, 1:1 v/v) mixture containing palladium on carbon (Pd/C) in the presence of hydrogen gas at 45 psi pressure for 6 h. The reaction mixture was centrifuged at 6500 rpm for 10 min, and the supernatant containing reduced polymer was collected and dried under vacuum to obtain a sticky and transparent mPEG-b-p(CB-{g-COOH}) **(4)** polymer. Different pendant groups *viz.*, cholesterol **(7)**, 4-(2-aminoethyl)morpholine **(6),** and N, N-dimethyldipropylenetriamine **(5)** were grafted to the free carboxyl groups of the mPEG-b-p(CB-{g-COOH}) **(4)** using EDC/HOBt coupling chemistry. Briefly, mPEG-b-p(CB-{g-COOH}) polymer **(4)** was dissolved in DMF

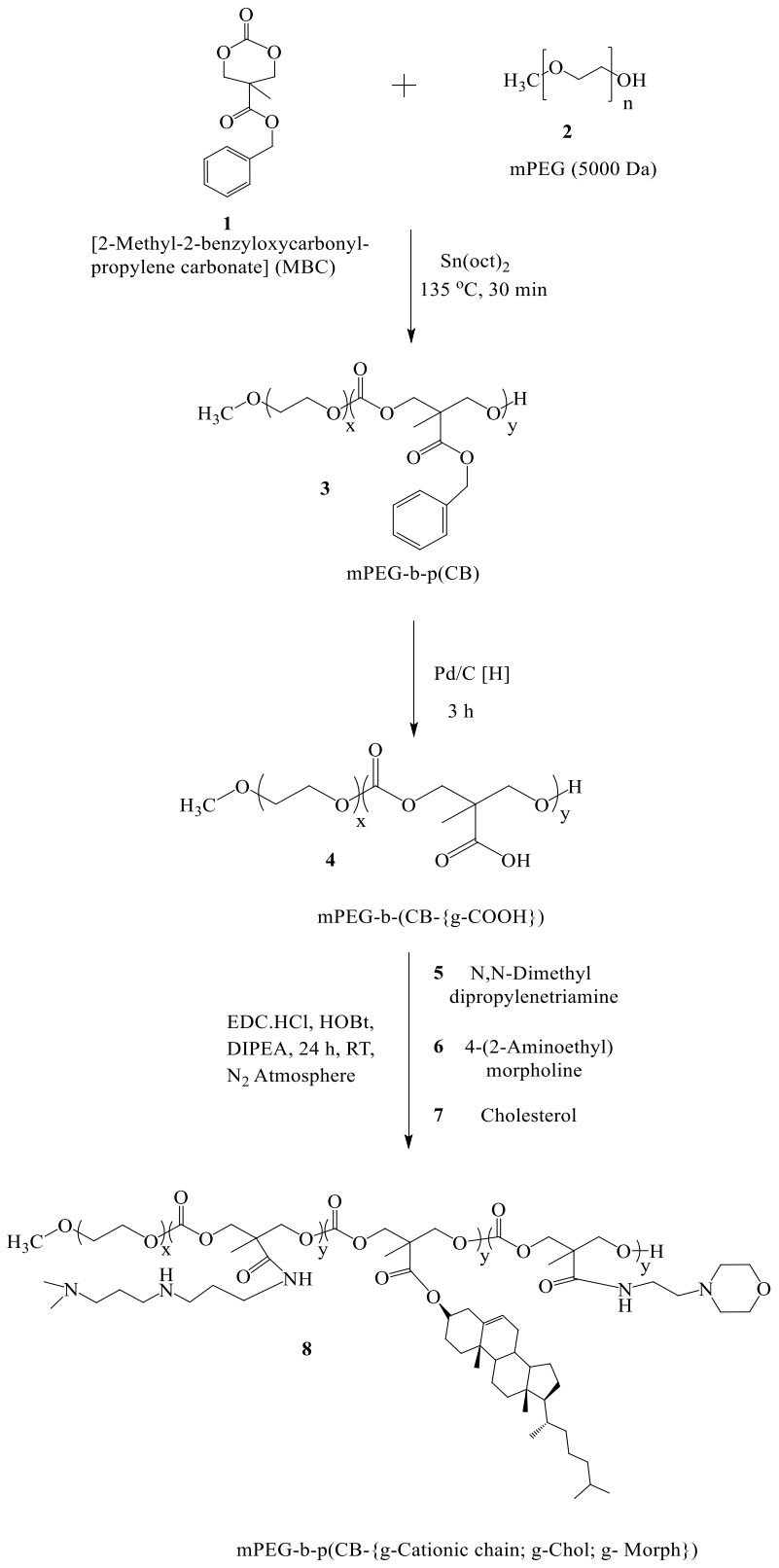

Figure 2.1. Synthesis scheme of amphiphilic lipopolymer, mPEG-b-p(CB-{g-Cationic chain; g-Chol; g- Morph}) **(8)**

for 1 h in the presence of N, N-diisopropylethylamine (DIPEA) followed by the addition of 1-ethyl-3-(3-dimethylaminopropyl)carbodiimide hydrochloride (EDC.HCl) and hydroxybenzotriazole (HOBt) at 0º C. Further, the reaction was kept under a nitrogen environment followed by the addition of N, N-dimethyldipropylenetriamine **(5)**, 4-(2-aminoethyl)morpholine **(6),** and cholesterol **(7),** and the reaction was kept for 48 hours under a nitrogen environment followed by dialysis (molecular weight cut-off of 3.5 kDa) against purified water for 6 h wherein the media was replaced after every 2 h. The contents of the dialysis bag were freeze-dried to obtain the mPEG b-(CB-{g-cationic chain; g-Chol; g- Morph}) **(8)** polymer.

All the intermediates, monomer/polymers (**1**, **3**, and **4**), as well as the final polymer **(8)**, were characterized by ^{1}H NMR acquired using Bruker (400 MHz) NMR spectrometer. The nitrogen content of (**8**) was analyzed using Elementar (Vario EL cube by Elementar Analyser system), wherein the sample was weighed accurately and burned in the presence of oxygen. The combustion product of different elements, i.e., water, nitric oxide, and carbon dioxide, were collected by different traps. The % of elements (C, H, and N) in the polymer **(8)** was calculated from the masses of combustion products.

2.3.3. Evaluation of buffer capacity of mPEG-b-(CB-{g-cationic chain; g-Chol; g-Morph})

The buffer capacity of the cationic polymer mPEG-b-(CB-{g-cationic chain; g-Chol; g-Morph}) was determined using the titration-based method as reported earlier [11]**.** Briefly, 100 µg of the polymer was dissolved in 100 µL dimethyl sulfoxide (DMSO, AR Grade, SRL, India) and diluted in deionized water to make a 2 mg/ml solution. The pH of the resulting solution was adjusted to 10.0 using 0.1 M NaOH. The buffer capacity of lipopolymer was evaluated by titration, wherein a 20 µL of 0.1 M HCl was added dropwise, followed by a measurement of change in pH every time. The HCl was added continuously till the pH reached 3.0. The 100 mM NaCl solution

was taken as a negative control with minimal buffer capacity. The change in pH was plotted against every 20 µL of 0.1 M HCl added.

2.3.4. Preparation and characterization of blank lipopolymeric nanoplexes

A previously reported method was adopted for the preparation of pCas9-loaded lipopolymeric nanoplexes [10]. Briefly, 10 mg of mPEG-b-(CB-g-cationic chain; g-Chol; g-Morph) polymer was accurately weighed and dissolved in 600 µL of dichloromethane (DCM). Further, 100 µL of nuclease-free water (NFW) was added to the polymer solution and pipetted to get a primary emulsion (w/o). The primary emulsion was further added to a secondary water phase (3 ml NFW) followed by probe sonication (20% amplitude; 3 min) to get a secondary emulsion (w/o/w). The resulting solution was kept under a vacuum using a rotary evaporator to remove DCM to get a clear formulation containing blank lipopolymeric nanoplexes. The blank lipopolymeric nanoplexes were characterized for particle size, zeta potential, and polydispersity index (PDI) using Malvern Zetasizer (Malvern Instrument Ltd., Nano ZS, USA). The blank nanoplexes were further utilized for the complex formation with the pCas9 plasmid.

2.3.5. Screening of complexation efficiency

The complexation efficiency of the cationic blank lipopolymeric nanoplexes with anionic pCas9 plasmid was evaluated using zeta potential analysis, agarose gel-based mobility shift assay, and UV-Visible spectroscopy.

Briefly, a fixed amount of pCas9 plasmid (i.e. 100 ng) was incubated with a predetermined amount of blank lipopolymeric nanoplexes (in ng) in a ratio (pCas9:blank lipopolymeric nanoplexes) of 1:0, 1:0.5, 1:1, 1:2.5, 1:5, 1:10, 1:20 and 0:20 followed by incubation for 30 min at room temperature. Further, the resulting pCas9-loaded lipopolymeric nanoplexes were evaluated

for zeta potential (Malvern Zetasizer, Malvern Instrument Ltd., Nano ZS, USA) to determine the complexation efficiency. Herein, the decrease in zeta potential was considered as an indication of complexation. The naked pCas9 plasmid alone and blank lipopolymeric nanoplexes were taken as controls.

Further, the complexation was evaluated using mobility shift assay. Briefly, the predetermined ratios (in w/w), i.e., 1:0, 1:0.5, 1:1, 1:2.5, 1:5, 1:10, 1:20, and 0:20 of pCas9:blank lipopolymeric nanoplexes were prepared and incubated for 30 min at room temperature followed by resolution on 2% agarose gel at 110 V for 30 min. The gel was visualized under the Gel Doc system (Gel Doc XR+ Gel Documentation system), and the retardation in the mobility of the pCas9 was considered as a function of complexation. The naked pCas9 plasmid and blank lipopolymeric nanoplexes were taken as controls.

The quantitative measurement of the complexation efficiency of lipopolymeric nanoplexes for pCas9 plasmid was further evaluated using a spectroscopy-based analysis. Briefly, the pCas9-loaded lipopolymeric nanoplexes were prepared at four different ratios (in w/w) i.e., 1:5, 1:10, 1:20, and 1:40 of pCas9:blank lipopolymeric nanoplexes. The pCas9-loaded lipopolymeric nanoplexes were centrifuged at 21,000 rpm for 30 min, and the supernatant was analyzed using Nanodrop (Simplinano™ spectrophotometer, Biochrom, Harvard Bioscience. Inc.) at 260/280 nm reading. Herein, the naked pCas9 and blank lipopolymeric nanoplexes were taken as controls. The following formula was used to calculate the complexation efficiency.

$$\text{Complexation efficiency (\%)} = \frac{(\text{Initial concentration} - \text{Concentration in supernatant})}{\text{Initial concentration}} \text{x } 100$$

2.3.6. Transmission electron microscopy (TEM)

The morphological evaluation of the pCas9-loaded lipopolymeric nanoplexes was carried out using TEM analysis (HR-TEM; TEC-NAI 200 Kv TEM, FEI Electron Optics, Eindhoven, Netherlands). Briefly, 1 mg/ml of solution of pCas9-loaded lipopolymeric nanoplexes was diluted 20 time and a small aliquot was placed on a small 400 mesh carbon-coated copper grids. The excess amount of fluid was decarded and the samples were observed under TEM (HR-TEM; TEC-NAI 200 Kv TEM, FEI Electron Optics, Eindhoven, Netherlands).

2.3.7. Cell culture-based assays

The ARPE-19 cells were obtained from Dr. Vivek Singh, Senior Scientist, LVPEI, Hyderabad, India, and cultured overnight in DMEM (Dulbecco's modified Eagle's Medium, ThermoFisher, MA, USA) containing 10% of FBS (Fetal Bovine Serum, ThermoFisher, MA, USA) and 100 µg/ml of antibiotic (Penicillin-streptomycin, 100X, ThermoFisher, MA, USA) at 37°C with 5% CO_2 under humidified environment. During transfection, the DMEM media was replaced by OptiMEM reduced serum media (ThermoFisher, MA, USA).

2.3.7.1. Transfection assay in mammalian cells

The previously reported method with slight modification was adopted for the transfection experiment [10]. Briefly, ARPE-19 cells were seeded in a 24-well cell culture plate with a density of 2 X 10^4 cells/well and allowed to grow overnight at 37°C with 5% CO_2. Next day, the media was replaced by 250 µL OptiMEM media (ThermoFisher, MA, USA) containing pCas9-TURBO-GFP-loaded lipopolymeric nanoplexes (pCas9: blank lipopolymeric nanoplexes; 1:20) with a net 1 ug of the pCas9-TURBO-GFP plasmid. The cells were incubated at 37°C with 5% CO_2 for different time points (6 h, 12 h, 24h and 48 h) and were washed thrice with PBS, stained with

Hoechst, and observed under fluorescence microscope (Vert A1, Zeiss). Later, the cells were washed, trypsinized, centrifuged at 1200 rpm for 3 min, and redispersed in PBS followed by analysis using a flow cytometer (Beckman Coulter, USA). The data were interpreted quantitatively by using CytExpert software (version 2.3). Herein, the Lipofectamine-3000 (ThermoFisher, MA, USA) was taken as a standard transfecting agent.

2.3.7.2. T7 endonuclease-based indel analysis

For indel analysis, a previously reported T7E assay method was adopted [5]. Briefly, the ARPE-19 cells were treated with different ratios of pCas9 (pX459-TURBO-GFP-5BPR2) loaded lipopolymeric nanoplexes followed by incubation for 72 h). Further, the genomic DNA was isolated from the cells using DNeasy Blood & Tissue Kit (Qiagen, Germany). The target DNA sequence was amplified using predesigned PCR primers; the purified PCR product was hybridized and treated with T7E enzyme, followed by incubation for 15 min at 37°C. The sample was immediately loaded on 2% agarose gel and resolved at 110 V for 30 min. The gel was visualized under the Gel Doc system (Gel Doc XR + Gel Documentation system), and the indel (%) was calculated using the following formula.

$$\%\, Indel \;=\; 100\, x\, (1 - \; (1 \;\; fraction\, cleaved) 1/2)$$

2.3.8. *In vivo* tissue distribution study

The *in vivo* tissue distribution study of pCas9-TURBO-GFP loaded lipopolymeric nanoplexes was carried out in *Swiss albino* mice as per the guidelines of the Committee for the Purpose of Control and Supervision of Experiments on Animals (CPCSEA) after the approval of the protocol from the Institutional Animal Ethics Committee (IAEC; Protocol No-IAEC/RES/30/02). Briefly, the *Swiss albino* mice (Male, 20-25 g) were randomly divided into two

groups (n=03), and 1st group was injected with 1 mg/kg pCas9-TURBO-GFP plasmid containing lipopolymeric nanoplexes intravenously *via* tail vein and 2nd group was injected with 1 mg/kg naked pCas9-TURBO-GFP plasmid *via* the same route. The mice were kept under observation for 72 h and then sacrificed, followed by isolation of all the vital organs, including the heart, liver, lungs, kidney, and spleen. The organs were placed under *In Vivo* Imaging System (IVIS, Lumina XR, Perkin Elmer, UK) to evaluate GFP expression. The background auto-fluorescence was normalized during the data acquisition using negative control tissues.

2.4. Results

2.4.1. Synthesis and characterization of mPEG-b(CB-{g-cationic chain; g-Chol; g-Morph}) polymer

Cationic amphiphilic copolymer, mPEG-b-p(CB-{g-cation chain; g-Chol; g- Morph}) (**8**), was synthesized using a multistep reaction scheme as shown in Figure 2.1, wherein ring-opening polymerization of cyclic monomer [MBC, **(1)**] was done with mPEG **(2)** as chain initiator to obtain mPEG-b-p(CB) **(3)** amphiphilic copolymer. The structure, composition, and molecular weight of mPEG-b-p(CB) was determined using ^{1}H NMR (400 MHz, CDCl3) (shown in Figure 2.2) that showed a molecular weight of 21,240 Da with 70 units of MBC (Table 2.1). The benzylic groups in the polycarbonate block of mPEG-b-p(CB) **(3)** were reduced using Pd/C catalyzed hydrogenation to obtain mPEG-b-p(CB-{g-COOH}) **(4)** amphiphilic copolymer with free –COOH group as confirmed using ^{1}H NMR (400 MHz, DMSO-d6) with the disappearance of benzylic protons at δ7.3 (e) (C6H5, m, 5H) (Figure 2.2). mPEG-b-(CB-{g-COOH}) **(4)** amphiphilic copolymer was found to have a molecular weight of 16,650 Da with 65 free –COOH groups (Table 2.1) in the polycarbonate block. In the next step, N, N-dimethyl dipropylenetriamine **(5)**, 4-(2-

aminoethyl morpholine) **(6),** and cholesterol **(7)** were grafted on the free carboxyl groups of mPEG-b-(CB-{g-

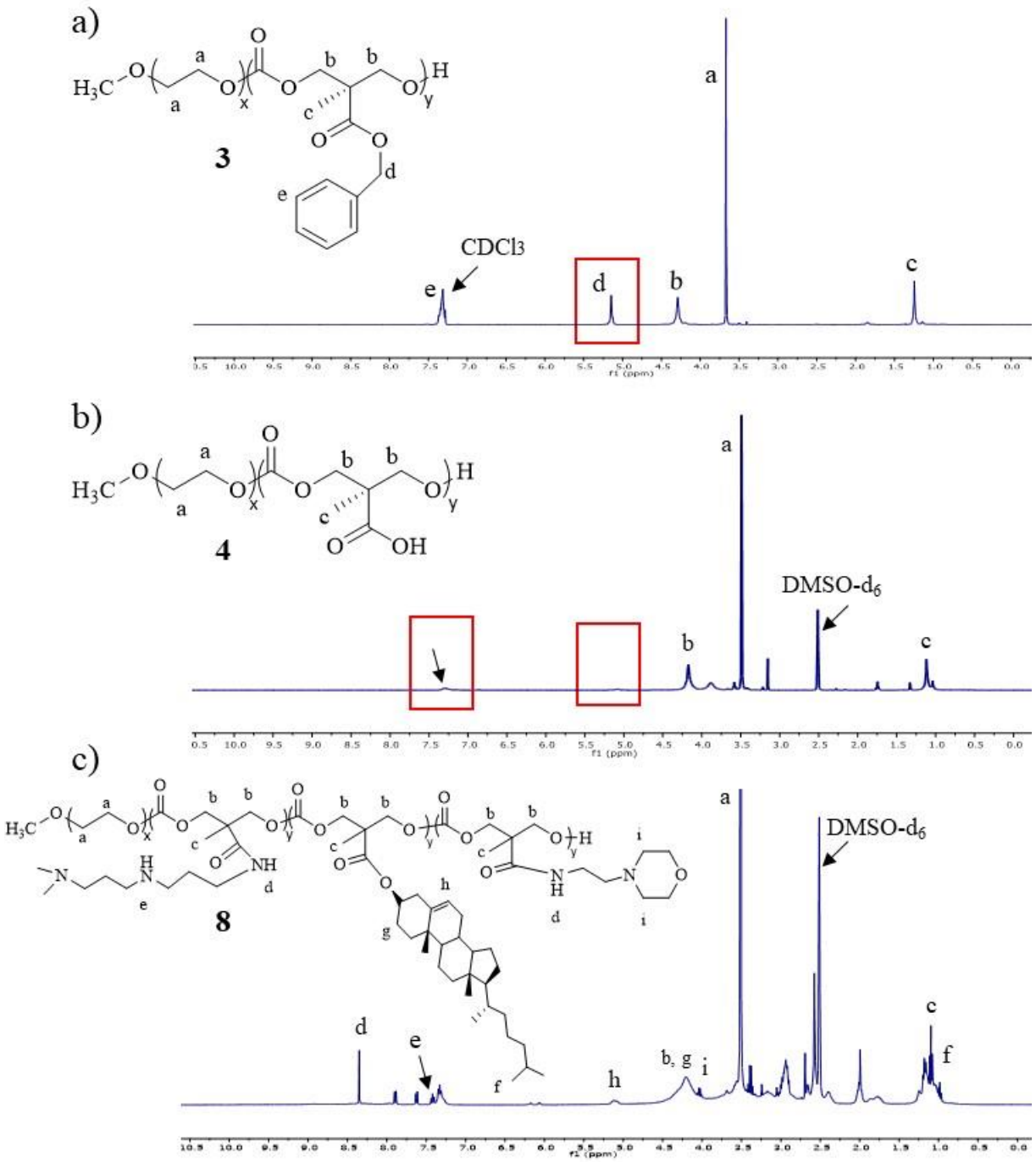

Figure 2.2. ^{1}H NMR of a) mPEG-b-p(CB) (**3**), b) mPEG-b-(CB-{g-COOH}) (**4**) and c) mPEG-b-p(CB-{g-Cationic chain; g-Chol; g- Morph}) (**8**)

COOH}) **(4)** using EDC/HOBt coupling chemistry to yield cationic amphiphilic copolymer, mPEG-b-(CB-{g-cation chain; g-Chol; g- Morph}) **(8)**. ^{1}H NMR (400 MHz, DMSO-d6) (Figure 2.2c) shows the protons corresponding to N, N-dimethyl dipropylenetriamine at δ 2.1 (e) (NH, s, 1H), δ 8.4 (d) (Amidic NH, s, 1H), 4-(2-aminoethyl) morpholine) at δ 3.7 (i) (CH2, m, 4H), δ 8.4 (d) (Amidic NH, s, 1H), and cholesterol at δ 0.8-1.0 (f) (CH3, s, 6H), δ 4.25 (g) (CH, q, 1H), δ 5.14 (h) (CH, d, 1H). Moreover, the final polymer has 5 units remaining from benzyl group showing protons at δ7.3 (e) (C6H5, m, 5H) (Figure 2.2c). The molecular weight of mPEG-b-(CB-{g-cation chain; g-Chol; g- Morph}) **(8)** amphiphilic copolymer was found to be 24,553 Da with 18 cationic chains units, 22 cholesterol units and 25 morpholine units (Table 2.1). The elemental analysis showed a 7.07 %, 6.72 % and 44.19 % of nitrogen, hydrogen and carbon content, respectively, in mPEG-b-(CB-{g-cation chain; g-Chol; g- Morph}) **(8)** amphiphilic copolymer (Table 2.1).

Table 2.1. Characterization of intermediate polymers **(3)**, (**4**) and final polymer **(8**)

Sr. No	Polymer	Monomer Units	Molecular Weight (Da)[a]	Elemental composition (%)[b]
1.	mPEG-b-p(CB) **(3)**	MBC units-70	21,240	
2.	mPEG-b-(CB-{g-COOH}) **(4)**	MCC units-65 MBC -5	16,650	
3.	mPEG-b-(CB-{g-Cationic chain; g-Chol; g- Morph}) **(8)**	Cationic chain units-18 Chol units-22 Morph units-25 MBC- 5	24,553	Carbon - 44.19 Hydrogen - 6.72 Nitrogen - 7.07

[a]Average molecular weight determined by ^{1}H NMR

[b]Elemental composition determined by Elemental Analyzer

2.4.2. Buffer capacity of mPEG b-(CB-{g-cationic chain; g-Chol; g-Morph}) polymer

The polymer mPEG-b-(CB-{g-cationic chain; g-Chol; g-Morph}) was designed in such a way that it could overcome delivery hurdles such as cellular uptake and could undergo

endo/lysosomal escape. The morpholine group in the polymer has been reported for its endo/lysosomal escape property by the proton sponge effect. The same property of the polymer was evaluated by means of its buffer capacity analysis. As shown in Figure 2.3a, the polymer solution resists change in pH and the pH reaches 3.0 by adding approximately 400 µL of 0.1 M HCl. On the other hand, the negative control solution, i.e., 100 mM NaCl solution, showed a rapid deviation in pH. This was an indication of the buffering capacity of the ionizable morpholine group in the lipopolymer.

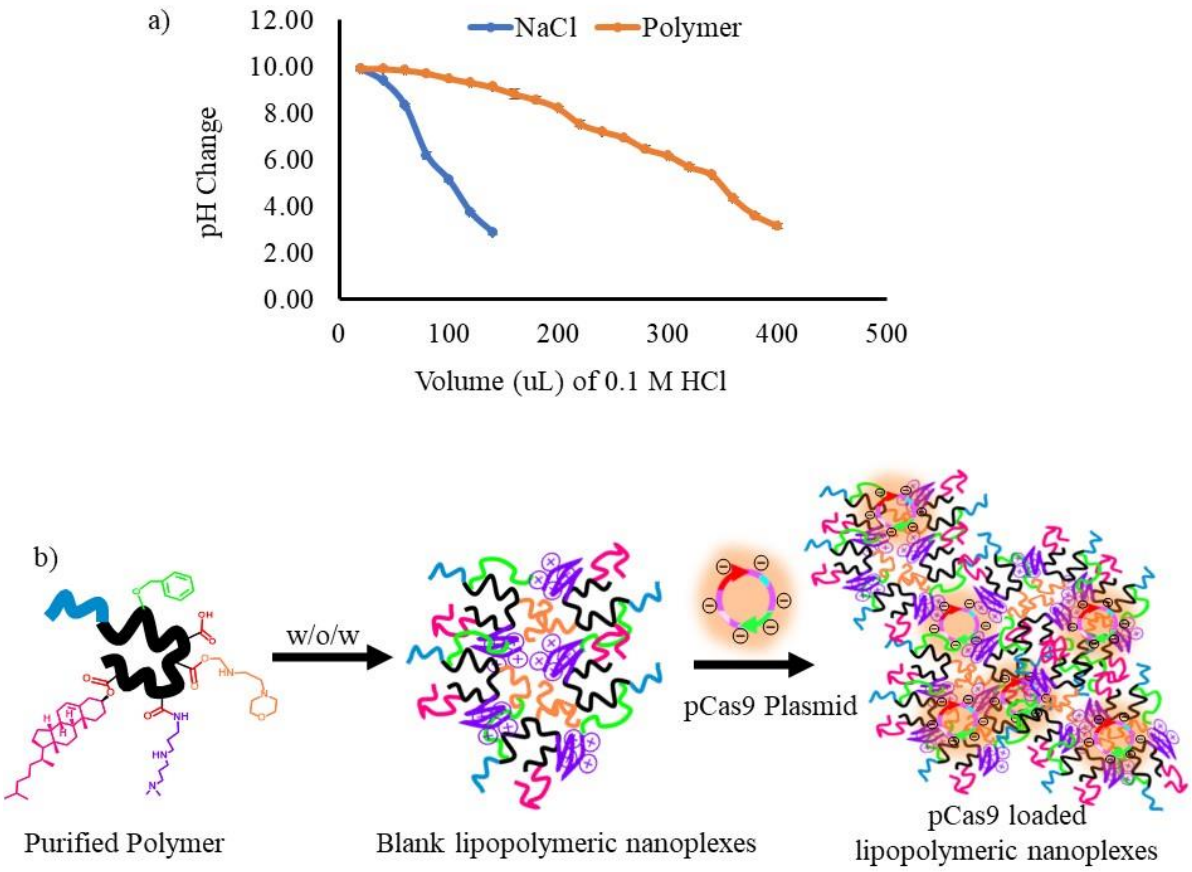

Figure 2.3. Characterization of synthesized mPEG b-(CB-{g-cationic chain; g-Chol; g-Morph}) polymer for a) buffer capacity *via* titration method using 0.1 M HCl as a titrant and b) formulation development employing w/o/w double emulsion solvent evaporation method to prepare blank lipopolymeric nanoplexes followed by incubation with pCas9 plasmid to prepare pCas9 loaded lipopolymeric nanoplexes by the means of electrostatic complexation.

2.4.3. Formulation development and characterization

The mPEG-b-(CB-{g-cationic chain; g-Chol; g-Morph}) polymer was used to prepare blank lipopolymeric nanoplexes employing a w/o/w double emulsion solvent evaporation method (Figure 2.3b). The blank lipopolymeric nanoplexes were evaluated for zeta potential, wherein we observed a value of +15.8 ± 0.7 mV. These cationic blank lipopolymeric nanoplexes were used for further studies, wherein a pCas9 plasmid (in ng) was mixed with blank lipopolymeric nanoplexes (Figure 2.3b) in a w/w ratio of 1:0, 1:0.5, 1:1, 1:2.5, 1:5, 1:10, 1:20 and 0:20. The resulting pCas9 loaded lipopolymeric nanoplexes were analyzed for the zeta potential. As shown in Figure 2.4a, the naked pCas9 plasmid showed a zeta potential of -19.8 ± 2.7 mV, and when the ratio of blank lipopolymeric nanoplexes was increased, the zeta potential shifted towards a positive value. This kind of charge shifting indicated electrostatic interaction and pCas9-loaded lipopolymeric nanoplexes formation. Desirable complexation was observed at 1:5, 1:10, and 1:20 ratio of plasmid to lipopolymeric nanoplexes. Further, similar ratios i.e. 1:0, 1:0.5, 1:1, 1:2.5, 1:5, 1:10, 1:20, and 0:20 were examined via agarose gel mobility shift assay. As shown in Figure 2.4b, the maximum complexation was seen at 1:10 and 1:20 ratios.

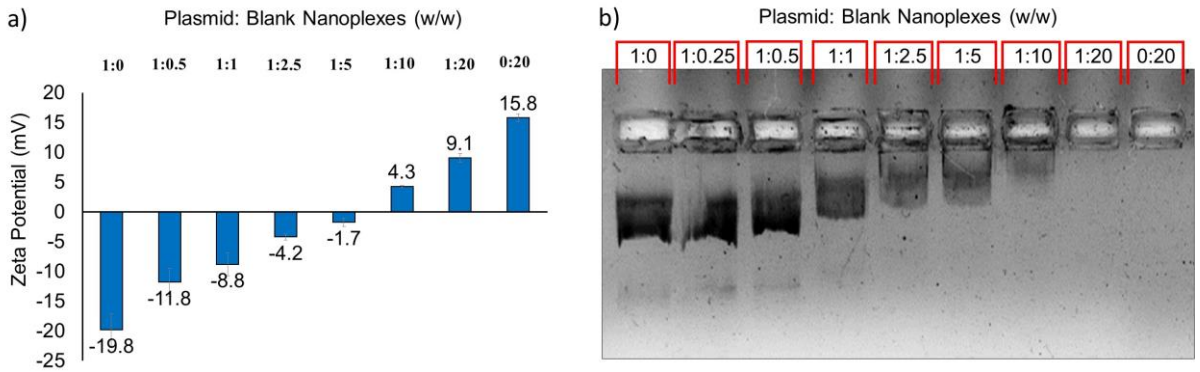

Figure 2.4. The complexation behavior of polymer with pCas plasmid evaluated using a) zeta potential analysis and b) mobility shift assay.

Further, the quantitative complexation efficiency was evaluated at four different ratios, i.e., 1:5, 1:10, 1:20, and 1:40, wherein we observed ~98% complexations at the 1:20 ratio (Figure 2.5a). There was no significant difference in complexation efficiency when the ratio was increased to 1:40. Therefore, the pCas9-loaded lipopolymeric nanoplexes at a ratio of 1:20 were further evaluated for particle size and zeta potential analysis. As shown in Figure 2.5b, the blank lipopolymeric nanoplexes and the pCas9-loaded lipopolymeric nanoplexes showed a particle size of ~93 ± 12 nm and ~141 ± 16 nm, respectively. The morphological structure of the pCas9-loaded lipopolymeric nanoplexes is shown in Figure 2.5c. However, the blank lipopolymeric nanoplexes and the pCas9-loaded lipopolymeric nanoplexes showed a zeta potential of 16.6±1.6 mV and 5.9±0.5, respectively (Figure 2.5d).

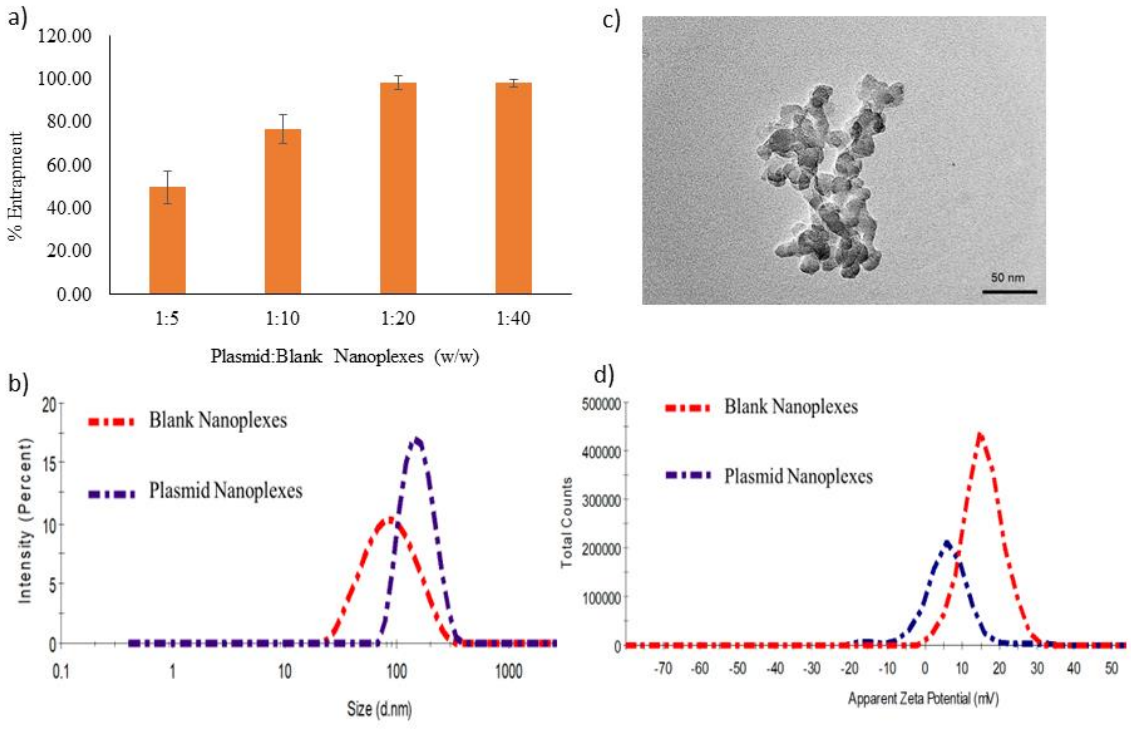

Figure 2.5. Evaluation of pCas9 loaded lipopolymeric nanoplexes for a) quantitative complexation efficiency using Nanodrop, b) particle size and c) morphology using TEM analysis and d) zeta potential.

2.4.4. *In vitro* transfection assay

Transfection efficiency is one of the most critical parameters to justify the efficiency of a non-viral nanocarrier and to examine the same, and we have used ARPE-19 cells. The plasmid (pCas-TURBO-GFP) used in this study was GFP expressing, and the % of cells transfected by pCas9-loaded lipopolymeric nanoplexes was determined by analyzing the GFP +ve cells. As per the existing reports, the plasmid expression takes 6-12 h after the successful transfection by physical methods [12]. In our case, as shown in Figure 2.6a, the transfection of pCas9-loaded lipopolymeric nanoplexes was time-dependent and maximum transfection was seen after 48 h of incubation. The possible reason could be the intracellular trafficking of the pCas9-loaded lipopolymeric nanoplexes since the nanocarriers have to surpass the intracellular barriers before

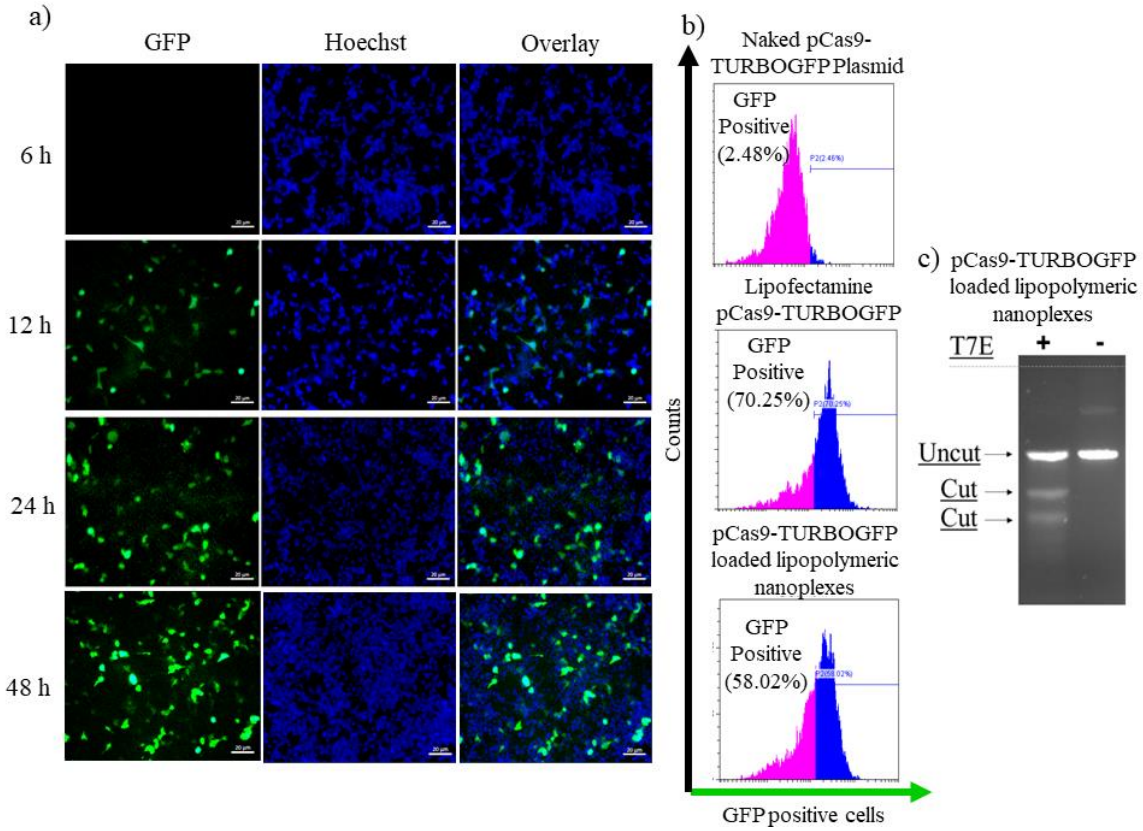

Figure 2.6. *In vitro* evaluation of pCas9-TURBOGFP plasmid loaded lipopolymeric nanoplexes in ARPE-19 cells for a) time-dependent transfection efficiency using fluorescence microscopy, b) quantitative measurement of transfection efficiency using flowcytometry and c) T7E based determination of gene editing efficiency.

the cytosolic delivery of the payload. When evaluated quantitatively, ~69% of transfection was observed (Figure 2.6b) with respect to the lipofectamine, which showed ~75% transfection. Such a finding consolidated the potential of lipopolymeric nanocarriers in gene delivery applications.

2.4.5. T7 endonuclease-based indel analysis

Although the GFP expression analysis gave an idea about the translation of pCas plasmid in the cellular environment. However, gene editing analysis is required to confirm the downstream trafficking because forming the ribonucleoprotein (RNP) complex in the cytosol, followed by its nuclear localization, is a time-consuming and complex process. T7 endonuclease 1 is the enzyme that detects the indel caused by the Cas9 RNPs via double-strand break after successful nuclear localization [13]. As shown in Figure 2.6c, ~ 22 % of indel frequency was observed in ARPE-19 cells, indicating the post-transfection expression of plasmid in the cytosol followed by gene editing by Cas9 RNPs targeting the 5BPR-2 gene.

2.4.6. *In vivo* tissue distribution

In the current study, we have used a GFP-expressing pCas-TURBO-GFP plasmid to explore the *in vivo* applicability of the polymeric nanocarrier. A total of 1 mg/kg of pCas9-loaded lipopolymeric nanoplexes were injected intravenously in *Swiss albino* mice, followed by observation for 3 days. Figure 2.7 showed IVIS images of the tissues from the mice injected with the naked pCas9-TURBO-GFP plasmid, wherein no considerable GFP fluorescence was observed. The reason could be the degradation of plasmid by nucleases present in the *in vivo* environment and the lack of cellular/tissue uptake due to its high molecular weight (~ 11000 bp). On the other

hand, in pCas9-loaded lipopolymeric nanoplexes injected mice, the GFP fluorescence can be seen in the liver and lungs tissue even after 3 days (Figure 2.7).

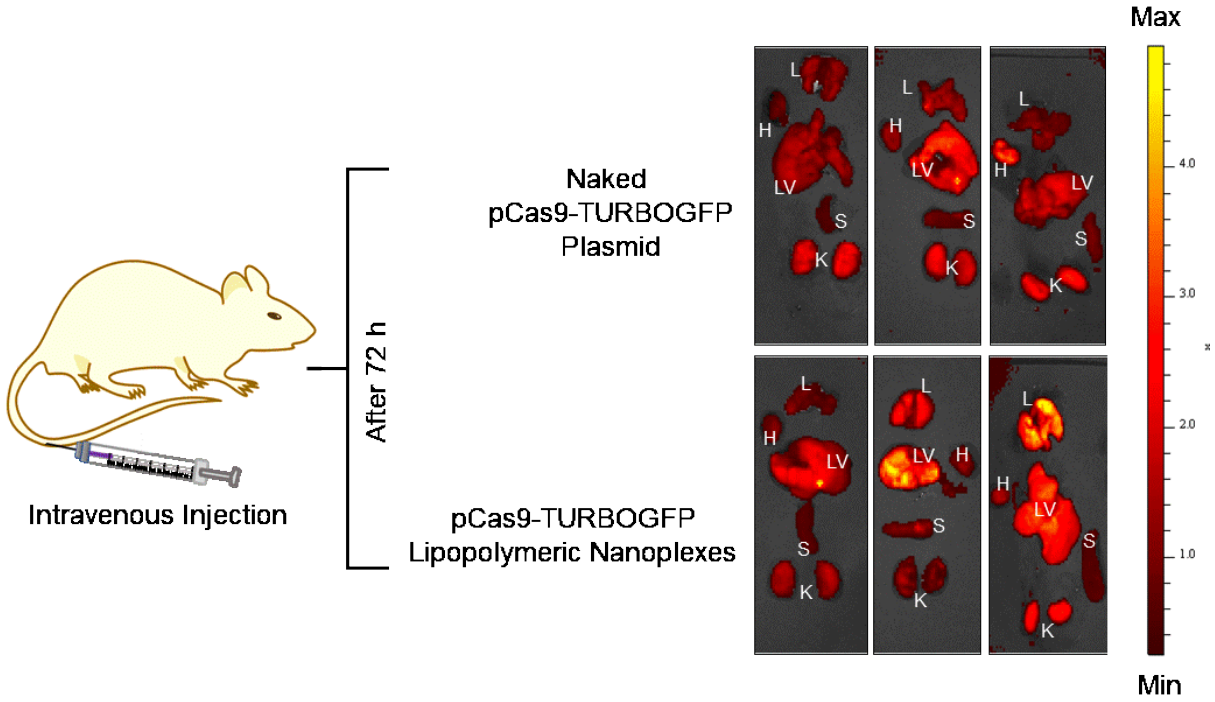

Figure 2.7. *In vivo* tissue distribution of 1 mg/kg naked pCas9-TURBO-GFP plasmid and pCas9-TURBO-GFP plasmid loaded lipopolymeric nanoplexes in *Swiss albino* mice after 72 h following intravenous injection. L=lungs, H=heart, LV=liver, S=spleen, and K=kidney.

2.5. Discussion

CRISPR/Cas9 is an RNA-guided DNA cleavage system widely explored for its site-specific precise gene editing capabilities [2]. There are three distinct forms of deliverable CRISPR including plasmid DNA, Cas9-expressing mRNA, and a functional Cas9 Ribonucleoprotein (RNPs) complex [1]**.** CRISPR/Cas9 plasmid delivery has several advantages, such as being cost-effective, easy to produce, and stable [2]. However, some inherent limitations are associated with CRISPR's plasmid DNA form, such as mutagenesis and off-target effects. However, interestingly, there are novel Cas effectors, such as Cas13a or dCas9-epigenome modulators, that could provide better control of gene expression, and therefore CRISPR plasmid could provide a more sustainable

therapeutic outcome. Viral vectors have been widely explored for the delivery of CRISPR/Cas9 cargo but possess comprehensive limitations related to immunogenicity, limited payload capacity**,** unable to deliver RNPs, etc. [9]. Now a days, the non-viral nanocarrier such as polymeric micelles (PM), polymeric nanoparticles (PNPs), lipid nanoparticles (LNPs), dendrimer-based nanoparticles (DNPs), exosomes, etc., have been explored for gene delivery applications. Additionally, the nucleic acids can be efficiently delivered inside cells using commercially available cationic lipid transfection reagents such as Lipofectamine 2000^{TM}, Lipofectamine 3000^{TM}, RNAiMAX^{TM}, etc., for the control of gene expression. The high toxicity and inflammatory side effects of the currently available transfection reagents are major drawbacks associated with these reagents limiting their *in vivo* use [14]. Polymers have been extensively studied for nucleic acid delivery due to their unique properties, such as ease of synthesis, cost-effectiveness, biodegradability, and amenability to modifications [15, 16]. We have synthesized a lipopolymer (mPEG-b-p(CB-{g-cationic chain; g-Chol; g-Morph}) for the effective delivery of CRISPR/Cas9 components. The lipopolymer comprises a polycarbonate backbone, which has been reported for its biodegradability and biocompatibility [16]. Additionally, the cationic chain provides a positive charge, which aids in condensing the negatively charged plasmid. The polymer mPEG-b-p(CB-{g-cationic chain; g-Chol; g-Morph}) was also designed to overcome intracellular hurdles, such as cellular uptake and endo/lysosomal escape. The morpholine group in the polymer is earlier reported for its endo/lysosomal escape property by the proton sponge effect. The polymer's buffering property was evaluated by its buffer capacity analysis. This buffering behavior is a function of the protonation of tertiary amine groups of the mPEG-b-(CB-{g-cationic chain; g-Chol; g-Morph}) polymer. A similar observation was reported by Ahern et al., wherein the resistance in pH change was considered as buffer capacity, which was further correlated with the proton sponge effect of

the polymer [11]. The lipopolymer was used to prepare blank nanoplexes using a previously reported method with slight modification [10]. The blank lipopolymeric nanoplexes showed a zeta potential of +15.8 mV, which could be attributed to the amine groups present in the grafted cationic chain. Furthermore, the analysis of change in zeta potential and retardation in the mobility of nucleic acids on gel electrophoresis are the standard assays for the determination of complexation of a negatively charged plasmid that has a zeta potential -19.8 mV, which complexes with the cationic polymers or lipids [5, 10, 17, 18]. As observed in our studies, 1:20 ratio was appropriate for complexation and was selected for further experiments. However, the increase in particle size of pCas9-loaded lipopolymeric nanoplexes with respect to the blank lipopolymeric nanoplexes is also an indication of complex formation, as reported in the literature [19]. Further, flow cytometry showed ~69% transfection after 48 h of incubation in a time-dependent manner. However, plasmid delivery has the inherent limitation of prolonged time requirement as the plasmid requires time to express inside the cytosol. T7E assay data showed approx. 22 % of indel frequency. Since plasmid expression takes time, incubating for longer could help achieve high gene editing efficiency.

In vivo bioimaging is a primary and less complex non-invasive method for tracking fluorescent molecules such as fluorescently labeled miRNA, proteins, fluorescent protein-expressing plasmids, bacteria, etc. [20, 21]. Several nanocarrier systems have been monitored for *in vivo* tissue distribution by loading a fluorescent dye, specifically DiR, DiL or coumarin-C6, followed by IVIS live imaging or tissue imaging. Herein, we have adopted IVIS imaging to evaluate GFP-expressing loaded lipopolymeric nanoplexes. As per the IVIS data, the GFP fluorescence could be seen in the liver tissue even after 72 h, indicating the stability of the delivered plasmids *in vivo* [22]. To achieve the tissue-specific delivery, we could modify the mPEG group

of mPEG b-(CB-g-cationic chain; g-Chol; g-Morph) polymer with targeting ligands such as a peptide, antibody, etc.

2.6. Conclusions

The polymer mPEG-b-(CB-g-cationic chain; g-Chol; g-Morph) was found to be an efficient nanocarrier for the *in vitro* and *in vivo* delivery of the large molecular weight Cas9 expressing plasmid. The pCas9 loaded lipopolymeric nanoplexes showed a good complexation efficiency at low, i.e., 1:20 w/w ratio and were able to transfect ~69% of ARPE-19 cells after 48 h of incubation time *in vitro.* Further, the gene editing analysis showed ~22 % of Indel frequency for 5BPR-2 gene. The *in vivo* biodistribution data consolidated the stability of the developed pCas9 loaded lipopolymeric nanoplexes under *in vivo* conditions. However, the lipopolymeric nanoplexes were found to be accumulated in liver and lungs tissue. Interestingly, the mPEG in the mPEG-b-p(CB-g-cationic chain; g-Chol; g-Morph) lipopolymer provides ample opportunities for targeting with cell-penetrating peptide or small molecules to make this nanocarrier system efficient for tissue specific delivery of the CRISPR/Cas9 cargos.

References

[1] Sahel DK, Mittal A, Chitkara D. CRISPR/Cas system for genome editing: progress and prospects as a therapeutic tool. Journal of Pharmacology and Experimental Therapeutics 2019;370:725-35.

[2] Lohia A, Sahel DK, Salman M, Singh V, Mariappan I, Mittal A, et al. Delivery Strategies for CRISPR/Cas Genome editing tool for Retinal Dystrophies: challenges and opportunities. Asian Journal of Pharmaceutical Sciences 2022.

[3] Jinek M, Chylinski K, Fonfara I, Hauer M, Doudna JA, Charpentier E. A programmable dual-RNA–guided DNA endonuclease in adaptive bacterial immunity. science 2012;337:816-21.

[4] Rafii S, Tashkandi E, Bukhari N, Al-Shamsi HO. Current status of CRISPR/Cas9 application in clinical cancer research: opportunities and challenges. Cancers 2022;14:947.

[5] Sahel DK, Salman M, Azhar M, Goswami SG, Singh V, Dalela M, et al. Cationic lipopolymeric nanoplexes containing the CRISPR/Cas9 ribonucleoprotein for genome surgery. Journal of Materials Chemistry B 2022.

[6] Taha EA, Lee J, Hotta A. Delivery of CRISPR-Cas tools for in vivo genome editing therapy: Trends and challenges. Journal of Controlled Release 2022.

[7] Pulman J, Sahel J-A, Dalkara D. New Editing Tools for Gene Therapy in Inherited Retinal Dystrophies. The CRISPR Journal 2022.

[8] Rouatbi N, McGlynn T, Al-Jamal KT. Pre-clinical non-viral vectors exploited for in vivo CRISPR/Cas9 gene editing: an overview. Biomaterials Science 2022.

[9] Li L, Hu S, Chen X. Non-viral delivery systems for CRISPR/Cas9-based genome editing: Challenges and opportunities. Biomaterials 2018;171:207-18.

[10] Sharma S, Mazumdar S, Italiya KS, Date T, Mahato RI, Mittal A, et al. Cholesterol and Morpholine grafted cationic Amphiphilic copolymers for miRNA-34a delivery. Molecular pharmaceutics 2018;15:2391-402.

[11] O'Keeffe Ahern J, Lara-Sáez I, Zhou D, Murillas R, Bonafont J, Mencía Á, et al. Non-viral delivery of CRISPR–Cas9 complexes for targeted gene editing via a polymer delivery system. Gene therapy 2022;29:157-70.

[12] Potter H, Heller R. Transfection by electroporation. Current protocols in immunology 2017;117:10.5. 1-.5. 9.

[13] Ehrke-Schulz E, Bergmann T, Schiwon M, Doerner J, Saydaminova K, Lieber A, et al. Quantification of designer nuclease induced mutation rates: a direct comparison of different methods. Molecular Therapy-Methods & Clinical Development 2016;3:16047.

[14] Qiu M, Glass Z, Xu Q. Nonviral nanoparticles for CRISPR-based genome editing: Is it just a simple adaption of what have been developed for nucleic acid delivery? Biomacromolecules 2019;20:3333-9.

[15] Piotrowski-Daspit AS, Kauffman AC, Bracaglia LG, Saltzman WM. Polymeric vehicles for nucleic acid delivery. Advanced drug delivery reviews 2020;156:119-32.

[16] Ansari I, Singh P, Mittal A, Mahato RI, Chitkara D. 2, 2-Bis (hydroxymethyl) propionic acid based cyclic carbonate monomers and their (co) polymers as advanced materials for biomedical applications. Biomaterials 2021;275:120953.

[17] Liu Y, Zhao G, Xu C-F, Luo Y-L, Lu Z-D, Wang J. Systemic delivery of CRISPR/Cas9 with PEG-PLGA nanoparticles for chronic myeloid leukemia targeted therapy. Biomaterials science 2018;6:1592-603.

[18] Wei T, Cheng Q, Min Y-L, Olson EN, Siegwart DJ. Systemic nanoparticle delivery of CRISPR-Cas9 ribonucleoproteins for effective tissue specific genome editing. Nature communications 2020;11:1-12.

[19] Zuris JA, Thompson DB, Shu Y, Guilinger JP, Bessen JL, Hu JH, et al. Cationic lipid-mediated delivery of proteins enables efficient protein-based genome editing in vitro and in vivo. Nature biotechnology 2015;33:73-80.

[20] Koo V, Hamilton P, Williamson K. Non-invasive in vivo imaging in small animal research. Analytical Cellular Pathology 2006;28:127-39.

[21] Matsumoto S, Tanaka F, Sato K, Kimura S, Maekawa T, Hasegawa S, et al. Monitoring with a non-invasive bioluminescent in vivo imaging system of pleural metastasis of lung carcinoma. Lung Cancer 2009;66:75-9.

[22] Li S-D, Huang L. Nanoparticles evading the reticuloendothelial system: role of the supported bilayer. Biochimica et Biophysica Acta (BBA)-Biomembranes 2009;1788:2259-66.

Chapter 3

Expression, purification and characterization of Cas9 proteins

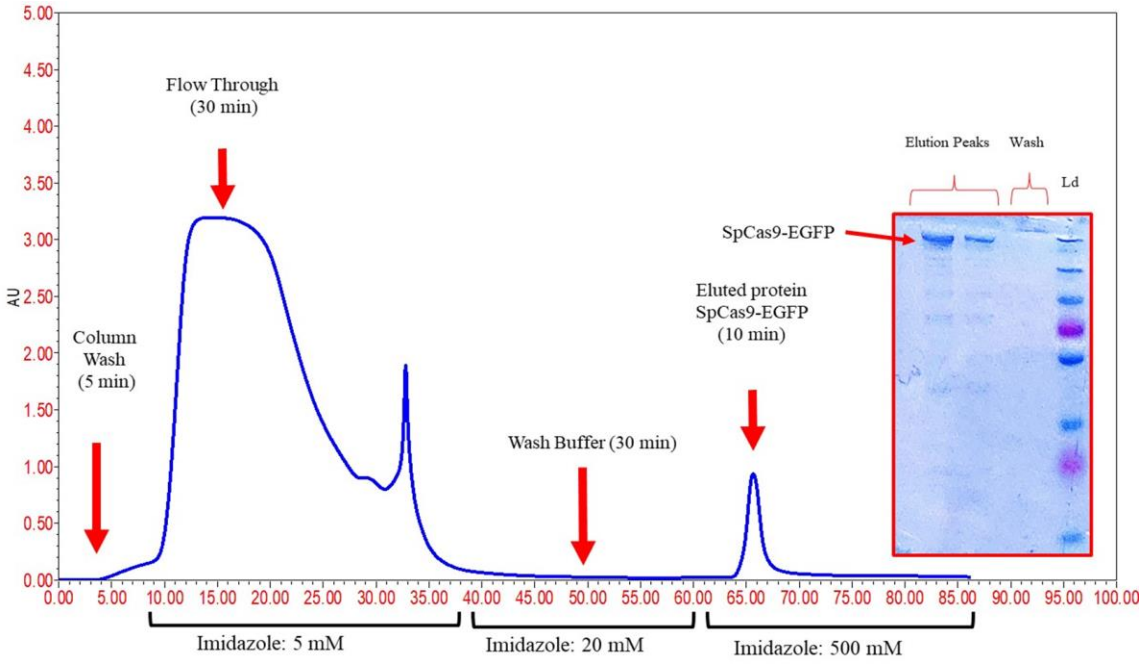

- Transformation of E.Coli with pTCas9 plasmids
- Protein expression and isolation
- Purification of Cas9 proteins using HPLC system assisted with HisTrap column
- Characterization of Cas9 proteins

3.1. Introduction

CRISPR/Cas9 system has proved its potential as a site-specific gene-editing tool [1] and is being used to correct mutations in prokaryotes and eukaryotes [2]. Higher efficiency, site-specificity, reproducibility, ease of engineering, and cost-effectiveness make CRISPR a favorite tool over other nucleases such as TALEN (Transcription activator-like effector nuclease) and ZFN (Zinc finger nuclease) [3]. Unlike other nucleases, CRISPR requires a single nuclease (Cas9 protein) for every target along with a variable single guide RNA (sgRNA) that could be easily switched depending on the target sequence [4]. Three strategies have been used for CRISPR-based gene editing, viz. plasmid-based, mRNA-based, and RNP-based. In a plasmid-based approach, CRISPR is delivered *in vitro* or *in vivo* in the form of a plasmid, which has an insert for Cas9 protein and sgRNA. However, the plasmid-based approach has disadvantages such as off-target effects, reoccurrence, time-consuming, instability, etc., [1]. Later, the strategy was modified, wherein instead of plasmid, an mRNA expressing Cas9 protein was designed and used for gene editing, but similar disadvantages were also observed with this approach [1]. Further, an intact ribonucleoprotein protein delivery strategy was developed, wherein the Cas9 protein complexed with sgRNA to form a ribonucleoprotein (RNP) complex, becomes active, and could cut the DNA on a site as directed by the sgRNA [5]. Although this strategy is quite costly [5], it was found to be more effective with reduced off-target effects, requiring less time for gene editing, better stability, and highest endonuclease activity [5].

To prepare the CRISPR/Cas9 RNP complex *in vitro*, E. coli has been used to produce Cas9 protein with the correct expression plasmid, while sgRNAs can be constructed using *in vitro* transcription (IVT). Cas9 protein was purified using the Rosetta 2 DE3 strain of bacteria by C. Anders and M. Jinek. Herein, homogenization was done to lyse the cells followed by purification

of Cas9 protein using consecutive chromatography i.e., immobilized metal affinity chromatography (IMAC), ion-exchange chromatography (IEX), and size exclusion chromatography (SEC) [6].

We have expressed and purified recombinant eGFP-tagged SpCas9 and SpDCas9 proteins from E. Coli BL21(DE3) in the present study, wherein a one-step HPLC-based method was adopted for purification. Secondary purification was done using the dialysis method. The purified proteins were evaluated for purity, RNPs complex formation, zeta potential, endonuclease activity/DNA binding properties, and fluorescent properties.

3.2. Materials

The plasmids (pET-SpCas9-EGFP/ pET-SpDCas9-EGFP) were provided by Dr. Debojyoti Chakarborty, CSIR-IGIB, New Delhi, as a kind Gift. E. Coli BL21(DE3) cells were purchased from Imperial Life Science (ILS), Gurugram, India. HisTrap column was purchased from GE Healthcare, USA, and Ni beads were procured from Bio-Red, California, USA. All other solvents and chemicals are of analytical grade and were procured from local vendors.

3.3. Methodology

3.3.1. Expression and isolation of Cas9 proteins from E.Coli

A heat shock method with slight modification was adopted for transformation. Briefly, competent E. Coli BL21(DE3) cells (ILS, Gurugram, India) were thawed on ice for 10 min, and 50 µL of cell suspension was added into a transformation tube. Further, 2.5 µL of plasmid DNA (pET-SpCas9-EGFP/ pET-SpDCas9-EGFP) with a final amount of 10 ng was added to the cells and mixed by tapping 4-5 times. The mixture was kept on ice for 30 min followed by heat shock (42°C, 10 sec) in a water bath to transform E. coli. Further, 950 µL of SOC (super optimal broth with catabolite repression) was added to the tube; pipetting was done for uniform mixing followed

by incubation for 1 h at 37°C with continuous vortexing at 150 rpm. After that 10 µL of the solution was seeded on an agar plate containing 30 mg/mL kanamycin (SRL, Mumbai, India). The plate was incubated at 37°C overnight. The next day a single colony was spiked into 25 mL of freshly prepared LB media containing 30 µg/mL of kanamycin and incubated at 37°C until the OD_{600} reached 0.5-0.6. From this primary culture, 10 mL of media was added to 1 L of freshly prepared LB media containing 30 µg/mL of kanamycin and incubated at 37°C until the OD_{600} reached 0.7-0.8. The expression of the SpCas9-EGFP/ SpDCas9-EGFP protein was induced by adding isopropyl β-d-1-thiogalactopyranoside (IPTG, 400 µM, 95.3 mg) into the bacterial suspension followed by incubation overnight at 16°C. To evaluate the protein expression, the cells with and without IPTG treatment were sonicated, centrifuged, and the 15 µL of the cell-free extract was loaded into 10% SDS-PAGE. The resolution was made for 1.5 h at 85 V, and the gel was kept in 0.2% Coomassie blue solution for 1 h to stain the resolved protein bands. The gel was destained with a destaining solution (40% methanol, 10% Glacial acetic acid in water), and the protein band near 200 KDa was visualized on the PAGE to confirm the Cas9 expression.

The protein expression was quenched by keeping the culture on the ice. The cells were harvested by centrifugation at 10000 rpm for 25 min at 4°C. The obtained cell pellet was redispersed into 15 mL of lysis buffer (500 mM NaCl, 20 mM Tris, and 10 mM imidazole, 1 L ddH2O (pH 8.0)) containing protein inhibitor cocktail (GE Healthcare, Chicago, US) and kept on ice for 30 min. The cells were sonicated (25% amplitude, 10 min, 1 sec on/1 sec off-cycle) using a probe sonicator (Vibro-cell, SONICS, Newtown, CT, USA) under cold conditions. The resulting solution was centrifuged at 15000 rpm for 45 min at 4°C to pellet down cellular debris. The supernatant containing soluble Cas9 proteins was collected, passed through a 0.2 µ syringe filter (AXIVA, New Delhi, India) to get the cell-free extract, and kept at 4 °C.

3.3.2. Chromatographic purification of His-tagged SpCas9-EGFP/SpDCas9-EGFP proteins

A HisTrap column (GE Healthcare, Chicago, US) with a 1 mL capacity was attached to an HPLC system (Waters, Massachusetts, US). The column was washed with 5 mL (5 X of the column volume) of purified water at a flow rate of 1 mL/min. Then 5 mL of lysis buffer was passed through the column for equilibration. Further, the cell-free extract containing Cas9 protein was loaded to the column with a flow rate of 2 mL/min, and UV spectra were recorded at 280 nm. The flow-through was collected as a fraction of 2 mL each. After completion of sample loading, 40-50 mL of wash buffer (500 mM NaCl, 20 mM Tris, and 20 mM imidazole, 1 liter ddH2O (pH 8.0)) was passed through the column at a flow rate of 1 mL/min until the OD_{280} attained almost zero and the peak returned to the baseline. Further, the solvent system was replaced with elution buffer (500 mM NaCl, 20 mM Tris, and 500 mM imidazole, 1 liter ddH2O (Ph 8.0)) and passed at a flow rate of 2 mL/min to elute out the Cas9 protein and 10-15 fractions (1 ml) were collected. All the collected fractions were kept on ice and characterized for purity using SDS-PAGE.

3.3.3. Characterization using SDS-PAGE

The fractions collected from the flow-through and washing step of purification by HPLC were loaded and resolved onto 10% SDS-PAGE, and a protein band near 200 KDa was visualized by staining the gel with Coomassie blue (0.2%). The fractions with minimal impurity were pooled together. For further purification, the pooled protein samples were added to the centrifugal dialysis unit (Merck, New Jersey, US) and centrifuged at 12000 rpm for 45 min to get concentrated purified protein. The purity was further determined using 10% SDS-PAGE, and concentration was analyzed using BCA Kit as per the manufacturer's protocol (Thermo Scientific, Massachusetts, US).

3.3.4 sgRNA synthesis using *in vitro* transcription

Briefly, the forward (FP) and reverse primers (RP) were designed (Table 3.1), screened, and compared for off-targets, followed by the synthesis of dsDNA using PCR. Thereupon, in vitro transcription kit (MEGAscript™ T7 Transcription Kit, Thermo Scientific) was used to synthesize sgRNA as per the manufacturer's protocol

3.3.5. Formation of RNPs complex

RNP complexes were prepared by incubating sgRNA and SpCas9-EGFP or SpDCas9-EGFP in 1:1 mole ratio at RT for 10 minutes. The RNP complex formation was evaluated by electrophoretic mobility shift assay using agarose gel electrophoresis (Bio-Rad, California, US). Herein, the naked sgRNA was taken as control. Furthermore, the zeta potential of SpCas9-EGFP or SpDCas9-EGFP protein and RNPs complexes was determined using an univette low volume cuvette in Litesizer (Anton Paar 500, Graz, Austria).

3.3.6. Transfection of spCas9-EGFP RNPs

The purified Cas9 is tagged with EGFP and, therefore also possesses fluorescent properties. To check the same, we prepared RNPs (with Cas9 concentration equal to 200 nM) by incubating spCas9-EGFP with VEGF A sgRNA followed by incubating with CRISPRMax (Thermo Scientific, Massachusetts, US) to form lipoplexes. The lipoplexes were added to HEK293T cells and incubated for 12 hours for transfection. The cells were washed thrice with PBS, stained with Hoechst (Thermo Scientific, Massachusetts, US), and observed under a confocal microscope (Zeiss, Germany).

3.3.7. *In vitro* endonuclease activity

Cas9 has an endonuclease property directed by a single guide sgRNA. To study the endonuclease activity of the purified SpCas9-EGFP, 15 pMol of SpCas9-EGFP/sgRNA-VEGFA RNPs were incubated with 500 ng of genomic DNA in 10 µL of the cut smart buffer (NEB, Massachusetts, US). The reaction mixture was kept at 37° C for 30 min, followed by visualization on 2% agarose gel to check the cleaved DNA fragment.

Table 3.1. Primers sequences for sgRNA synthesis

Primer	Genomic Region	Sequence
VEGFA_sgRNA_F.P	VEGFA, Exon 7	5'GAAATTAATACGACTCACTATAGTGTGCCCCTGATGCGATGCGGTTTTAGAGCTAGAAATAGCAAG 3'
Telomere_sgRNA_F.P	Telomere region	5'TAATACGACTCACTATAGCCAGGGCCAGGGCCAGGGCCGTTTTAGAGCTAGAA3'
Universal reverse primer	-----	5'AAAAGCACCGACTCGGTGCCACTTTTTCAAGTTGATAACGGACTAGCCTTATTTTAACTTGCTATTTCTAGCTCTAAAAC

3.3.8. DNA binding property

Since the SpDCas9-EGFP doesn't have endonuclease activity, its activity could be determined using the Cas9-mediated fluorescence *in situ* hybridization (CASFISH) assay [7]. Briefly, HEK293T cells were seeded on a sterile coverslip with a density of 5 X 10^3 cells followed by overnight incubation under a humid environment at 37° C temperature with 5% CO_2. Next day,

the cells were washed with PBS and fixed with 500 µL of chilled methanol/Acetic acid (1:1) mixture for 20 min at -20° C. The cells were washed thrice with PBS and 500 µL of blocking buffer (20 mM HEPES, 100 mM KCl, 5 mM $MgCl_2$, 1 mM DTT, 5% Glycerol, 1% BSA, 0.1% Tween 20) was added, followed by incubation at 37° C temperature for 30 min. Simultaneously, the RNPs complexes were prepared by mixing sgRNA (designed for the telomere region, given in Table 1) and SpDCas9-EGFP in a blocking buffer. Further, the RNPs were added to the HEK293T cells and incubated for 30 min, followed by washing three times with blocking buffer, stained with DAPI (Thermo Scientific, Massachusetts, US), and observed under a confocal microscope (Zeiss, Germany).

3.4. Results

3.4.1. Transformation, expression, extraction, and purification

The heat shock method was employed for the transformation of E. Coli BL21(DE3) cells resulting in the appearance of colonies over kanamycin (30 µg/mL) containing selection plates as an indication of successful transformation. The transformed E. coli were cultured again to bring them into the growing phase. Therefore, a single colony was picked and seeded into 25 mL of freshly prepared LB media containing 30 µg/mL kanamycin. The increase in turbidity in terms of OD_{600} indicates the recovery of the E. coli cells after transformation. Further, for protein production, 1 L of LB media containing 30 µg/mL kanamycin was seeded with 10 mL of primary culture of transformed E. coli and kept at 37° C. An OD_{600} of 0.75 was obtained after 5 h, following which 500 mM IPTG was added to the culture, and incubation was done at 16 ° C. Here, we have performed SDS-PAGE of the protein isolated from the cells incubated with and without IPTG. Figure 3.1 showed a dense band near 200 kDa in the protein sample of the cells treated with IPTG

only, indicating that the IPTG efficiently induced the protein expression. Further, cells were lysed using probe sonication for 10 min (1 sec on/off cycle) in cold conditions, and the cell lysis was confirmed by physical appearance wherein a decrease in viscosity and turbidity was observed.

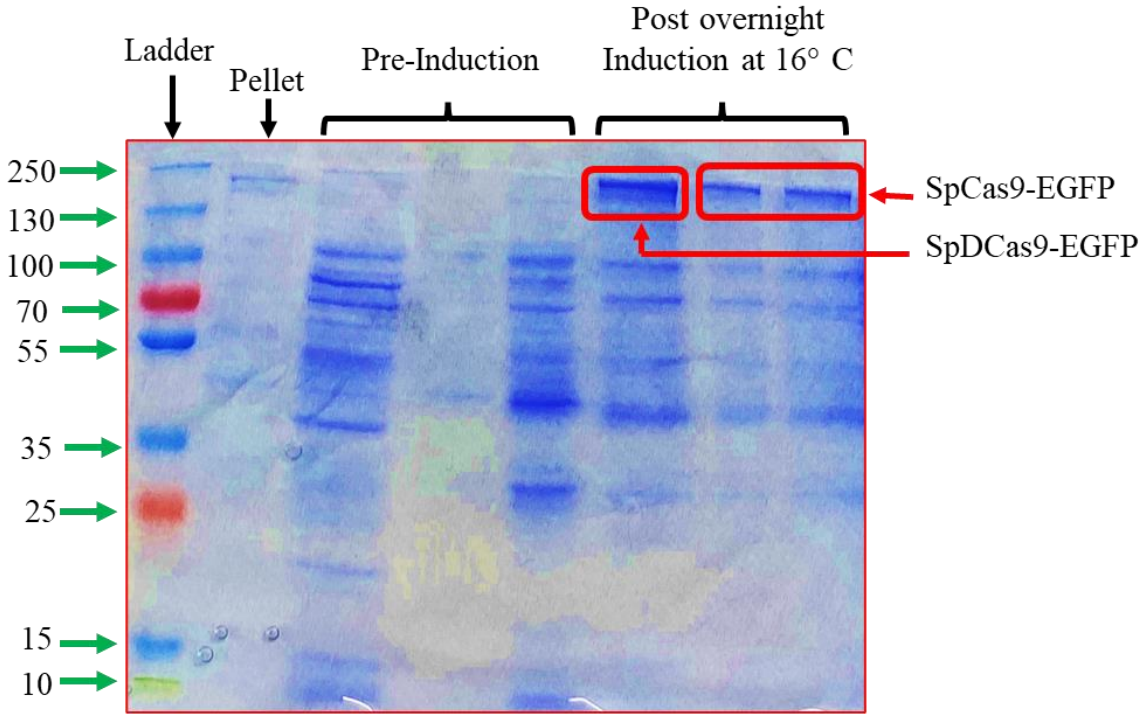

Figure 3.1. Characterization of IPTG based induction of Cas9 proteins using 10% SDS-PAGE

Cellular debris were removed by centrifugation at 15000 rpm for 45 min, which results in the clear greenish supernatant. The supernatant was syringe filtered to get a cell-free lysate which was subsequently loaded into the HisTrap column and attached to an HPLC system. The sample was loaded into a column using a pressure pump with a flow rate of 2 mL/min, and a bell-shaped peak was observed at 280 nm. Next, a wash buffer was passed through the column to remove extra proteins from the column, and this step was continued until there was a uniform baseline with OD_{280} near zero. Afterward, elution buffer was pumped through the column, and we observed a sharp peak at 280 nm in the chromatogram. Fractions of 1 mL each were collected until the peak

eluted out completely. The HPLC chromatogram of SpCas9-EGFP and SpDCas9-EGFP proteins are shown in Figure 3.2.

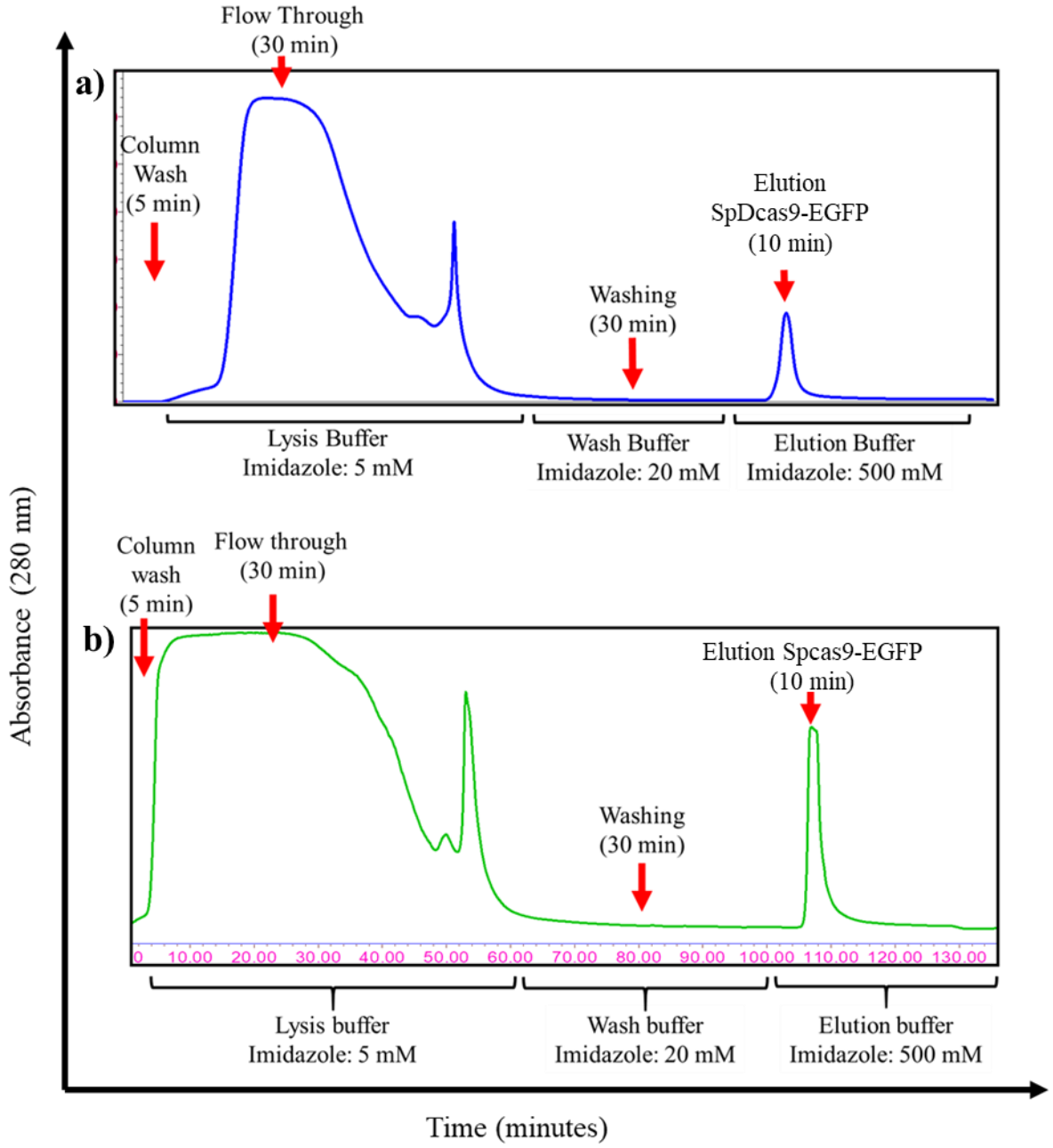

Figure 3.2. HPLC chromatogram of a) the SpCas9-EGFP and b) SpDCas9-EGFP proteins at 280 nm, showing different phases including column loading with lysis buffer (35 min, 5 mM imidazole), column washing with wash buffer (30 min, 20 mM imidazole) and Cas9 elution with elution buffer (10 min, 500 mM imidazole).

3.4.2 SDS-PAGE

SDS-PAGE is the foremost method for the identification/quality analysis of any protein *via* molecular weight-based separation. Figure 3.3 shows that there are many bands of different molecular weights in the fraction from flow through and washing steps. These bands are probably from the proteins present in the bacteria. Figure 3.3 showed a dense band near 200 kDa in the fractions from the elution step indicating the successful separation of the desired protein. Still, there were 3-4 bands as an impurity, and to further purify the protein, centrifugal dialysis was employed.

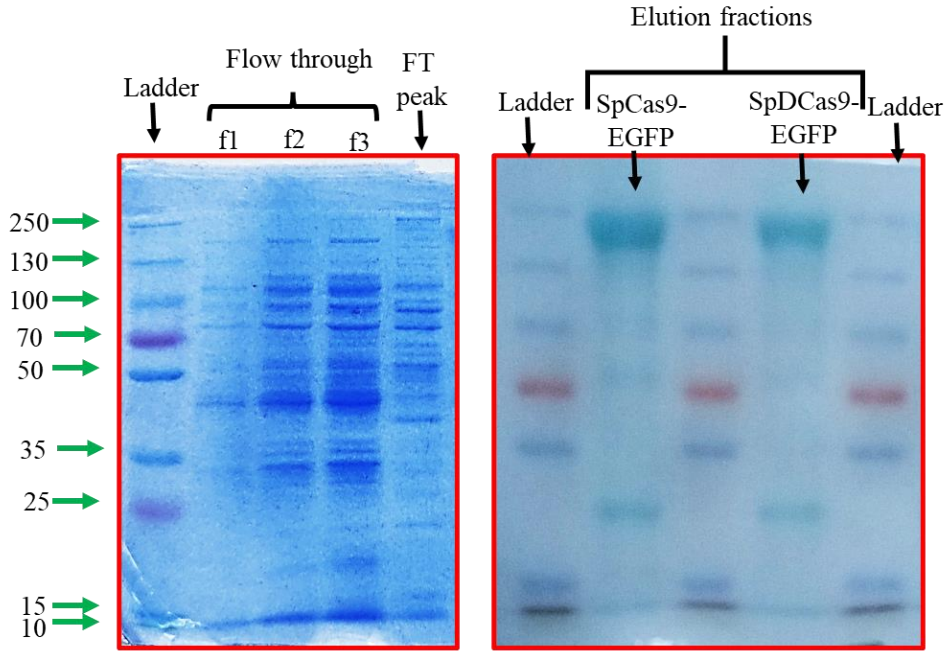

Figure 3.3. Characterization of different fractions collected from the HPLC during purification process

3.4.3. Secondary characterization of SpCas9-EGFP proteins

After dialysis, the SDS-PAGE showed a single band (Figure 3.4b) of SpCas9-EGFP, and the BCA kit was used to determine the concentration of protein, and data showed that the final concentration of 3.5 mg/mL. Further, RNPs were prepared using sgRNA synthesized via IVT.

Figure 3.4c shows the agarose gel data of RNPs complex formation; herein, the retardation of the sgRNA band confirmed that the SpCas9-EGFP formed the RNPs complex with sgRNA efficiently. Further, the SpCas9-EGFP RNPs showed a net zeta potential of -8.3 ±1.8 mV. When these RNPs were incubated with DNA substrate, they effectively cleaved the DNA utilizing their targeted endonuclease activity (Figure. 3.4d). The fluorescent property of SpCas9-EGFP was determined using confocal microscopy, wherein RNPs were transfected using CRISPRMax in HEK293T cells. Figure 3.4e showed the confocal images of the HEK293T cells after 12 h of transfection, and the

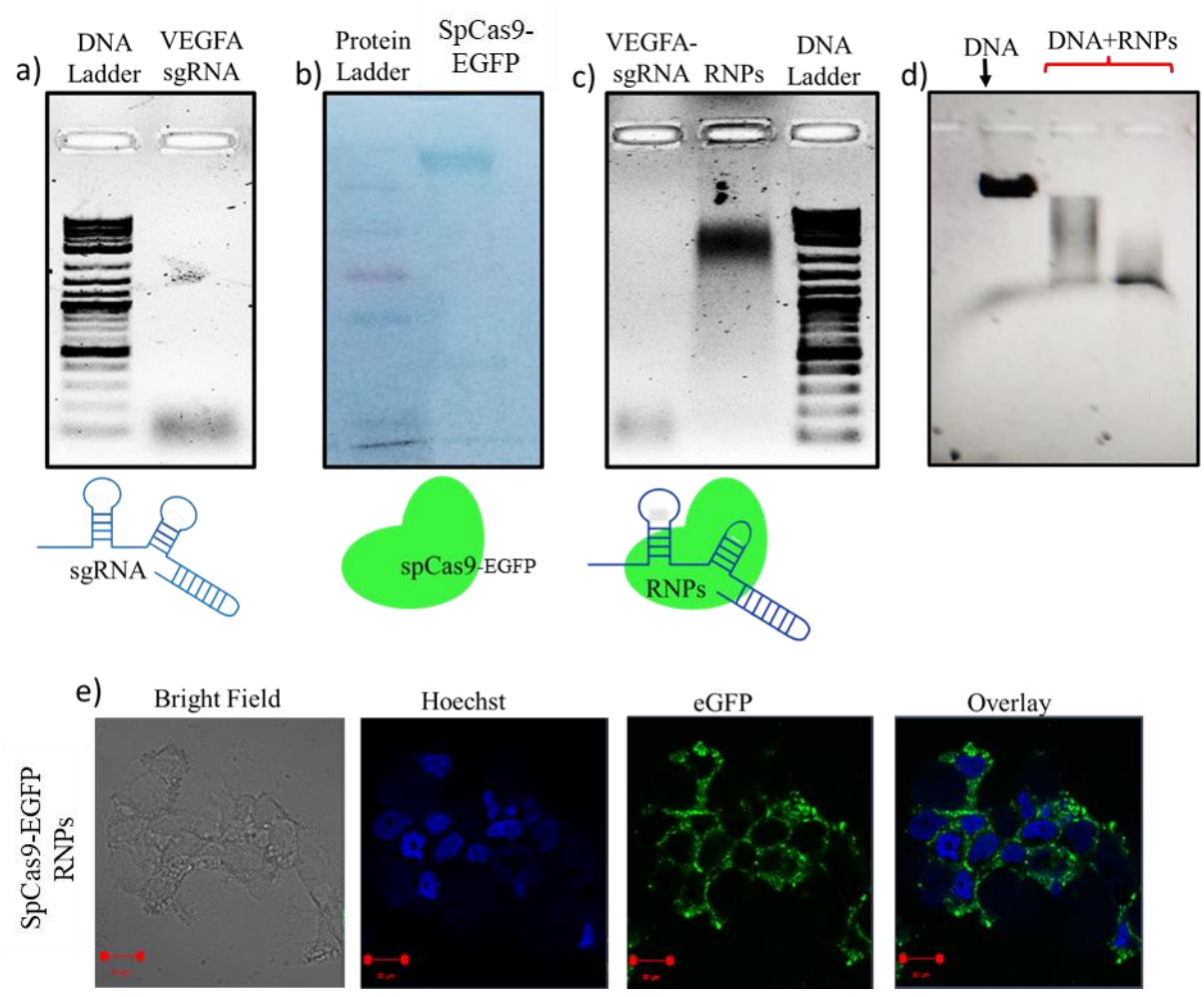

Figure 3.4. a) Agarose gel image of synthesized sgRNA using IVT, b) SDS-PAGE of SpCas9-EGFP, c) RNPs complex formation, d) *in vitro* endonuclease activity, and e) cellular uptake of RNPs (eGFP, green)

observed green color confirmed the fluorescent property of SpCas9-EGFP that has been efficiently taken up by the HEK293T cells.

3.4.4. Characterization of SpDCas9-EGFP

The SpDCas9-EGFP was found to have a good purity, as shown in Figure 3.5b. Further, the SpDCas9-EGFP was characterized for its RNPs complexes formation efficiency (Figure 3.5c) with Telo-sgRNA. Additionally, the SpDCas9-EGFP RNPs showed a net zeta potential of -7.6 ±1.3 mV. Since the SpDCas9-EGFP doesn't have endonuclease activity, its DNA binding activity could be determined using a CASFISH assay. As shown in Figure 3.5d, the nuclear localization of RNPs within the cells is the indication of the DNA binding efficiency of the SpDCas9-EGFP protein.

3.5. Discussion

CRISPR/Cas9 system has been explored for its target-specific gene editing through NHEJ and HDR repair mechanisms [1]. There are various forms in which the CRISPR system could be employed i.e, Cas9 expressing plasmid, mRNA, and ribonucleoprotein (RNPs) [2]. The foremost form of CRISPR is RNPs, composed of sgRNA and Cas9 protein complexed together [5]. For utilizing the targeting endonuclease activity of RNPs, we need to produce a purified Cas9 protein. So, the objective of this study was the effective production of Cas9 in E. coli BL21 (DE3). Due to the exogenous nature of this protein, different proteins are expressed in response. When comparing SDS gels of Cas9 proteins, there are different protein expressions even though the strain is the

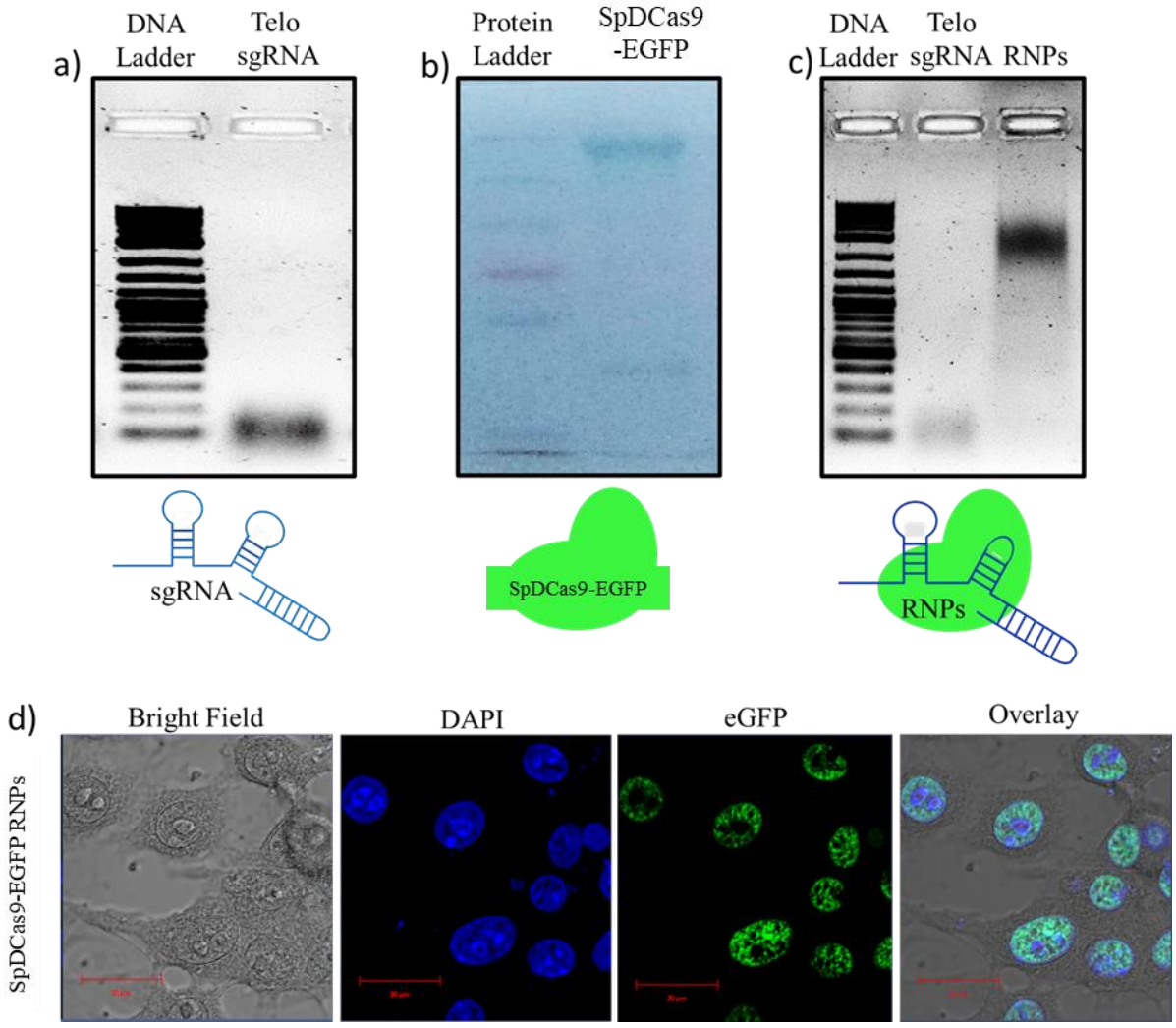

Figure 3.5. a) Agarose gel image of synthesized sgRNA using IVT, b) SDS-PAGE of SpDCas9-EGFP, c) RNPs complex formation (Telo-sgRNA/SpDCas9-EGFP), d) CASFISH based DNA binding affinity of SpDCas9-EGFP RNPs.

same and culture conditions are identical. It is reported that many proteins are expressed in response to Cas9 and are richer in histidine, making purification of Cas9 harder [8]. This is also the consequence of the nature of the proteome of E. coli BL21 (DE3). Recombinant His-tagged proteins expressed in this strain are commonly co-eluted with native E. coli proteins. This effect

is increased significantly when the expression of the recombinant protein is low, like the Cas9 protein. The native E. coli proteins have clustered histidine residues with metal-binding sites. Such a problem could be fixed with engineered E. coli BL21(DE3). The ideal conditions for Cas9 protein in this system were culture at 25 ºC with 0.2 mM of IPTG. Since Cas9 is a high molecular weight (169 kDa) and high molecular weight proteins are soluble at the lower temperature, we kept the incubation temperature at 16 ºC with an IPTG concentration of 0.4 mM. It has also been reported that the IPTG at high concentrations showed inhibition of protein expression due to increased cell [9].

HPLC system connected with the HisTrap column was used for the purification of Cas9 protein, and a 120 min run was established. The column was stabilized with lysis buffer as the sample was already in lysis buffer. For the purification of His-Tagged protein, imidazole was used as a displacement reagent that replaces His-Tagged protein and helps in the elution of desired protein [8]. The concentration of imidazole was kept at 500 mM. SDS-PAGE data confirmed the molecular weight of the eluted protein (approx. 200 kDa) and purity. Further, we evaluated the functionality of the eluted SpCas9 protein *via* different experiments. The SpCas9-EGFP protein and SpDCas9-EGFP protein form RNPs complex with VEGFA-sgRNA and Telomere-sgRNA, respectively, on incubation at RT for 10 min. The agarose gel data depicted the shift in mobility of sgRNA due to the complexation with high molecular weight Cas9 protein and confirmed RNP formation. Cas9 is a basic protein, that has a net positive charge at physiological pH 7.4 but the net charge on the RNPs is negative due to the anionic PO^{4-} groups on the sgRNA. Similar observations were seen when the RNPs were evaluated for the zeta potential. The SpCas9-EGFP RNPs and SpDCas9-EGFP RNPs showed a zeta potential of -8.3 ±1.8 mV and -7.6 ±1.3 mV, respectively. Further, the RNPs (SpCas9-EGFP) were found to retain the endonuclease activity

since they were able to cleave genomic DNA. To evaluate the fluorescent property of the SpCas9-EGFP protein, we have performed a simple fluorescent imaging-based uptake analysis. Since CRISPRMax is a standard transfecting agent used for CRISPR/Cas RNPs delivery *in vitro*, we incubated the RNPs with CRISPRMax to form lipoplexes followed by transfection in HEK293T cells. After 12 h, the cells were observed under a confocal microscope and the appearance of green color inside the cells confirmed the fluorescent property of the purified SpCas9-EGFP protein. Since the SpDCas9-EGFP doesn't have endonuclease activity, its activity could be determined using the CASFISH assay, as reported earlier [7]**.** Herein, the sgRNA was designed for the telomere region, since the telomere has multiple TTAGGG repeats, and therefore several RNPs could bind to the telomere region of the DNA and can be seen using fluorescence microscopy. A similar study has already been reported as an application of the dCas9 protein to locate a specific gene within the genome [7]. Also, this study confirms the fluorescence property of the SpDCas9-EGFP protein. Overall, we have developed a simple, robust, and HPLC-assisted method for the purification of histidine-tagged CRISPR/Cas proteins (SpCas9-EGFP/SpDCas9-EGFP) followed by their characterization.

3.6. Conclusions

Overall, the study explored an easy, time-effective, and efficient HPLC method to purify high molecular weight Cas proteins with good purity. The protein was found intact in terms of its endonuclease activity/DNA binding activity, along with a good concentration. The fluoroscence property of the wild type spCas9-EGFP and mutatnt spDCas9-EGFP protein was evaluted by confocal micorscopy. The obtained Cas9 proteins were used in the upcoming Chapters for evlauting the delivery efficency of the lipopolymeric nanocarrier.

References

[1] D.K. Sahel, A. Mittal, D. Chitkara, CRISPR/Cas system for genome editing: progress and prospects as a therapeutic tool. Journal of Pharmacology and Experimental Therapeutics 370 (2019) 725-735.

[2] A. Lohia, D.K. Sahel, M. Salman, V. Singh, I. Mariappan, A. Mittal, D. Chitkara, Delivery Strategies for CRISPR/Cas Genome editing tool for Retinal Dystrophies: challenges and opportunities. Asian Journal of Pharmaceutical Sciences (2022).

[3] T. Gaj, S.J. Sirk, S.-l. Shui, J. Liu, Genome-editing technologies: principles and applications. Cold Spring Harbor perspectives in biology 8 (2016) a023754.

[4] X. Wu, A.J. Kriz, P.A. Sharp, Target specificity of the CRISPR-Cas9 system. Quantitative biology 2 (2014) 59-70.

[5] C.A. Lino, J.C. Harper, J.P. Carney, J.A. Timlin, Delivering CRISPR: a review of the challenges and approaches. Drug delivery 25 (2018) 1234-1257.

[6] C. Anders, M. Jinek, In vitro enzymology of Cas9, Methods in enzymology, Elsevier, 2014, pp. 1-20.

[7] W. Deng, X. Shi, R. Tjian, T. Lionnet, R.H. Singer, CASFISH: CRISPR/Cas9-mediated in situ labeling of genomic loci in fixed cells. Proceedings of the National Academy of Sciences 112 (2015) 11870-11875.

[8] D.-H. Kim, J. Yu, J.C. Park, C.-B. Jeong, S. Bae, J.-S. Lee, Targeted cytochrome P450 3045C1 (CYP3045C1) gene mutation via CRISPR-Cas9 ribonucleoproteins in the marine rotifer Brachionus koreanus. Hydrobiologia 844 (2019) 117-128.

[9] F. Baneyx, Recombinant protein expression in Escherichia coli. Current opinion in biotechnology 10 (1999) 411-421.

Chapter 4

Lipopolymeric nanoplexes delivering CRISPR/Cas9 RNPs for effective genome editing

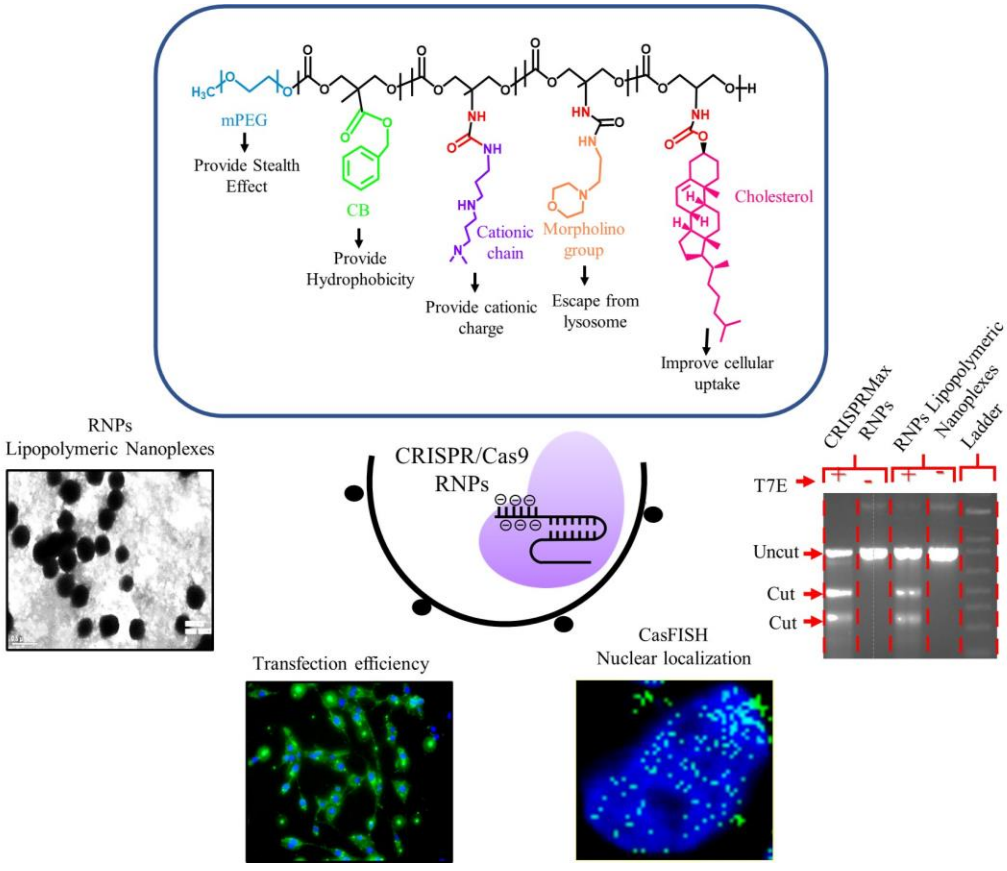

- Development and evaluation of CRISPR/Cas9 RNPs loaded lipopolymeric nanoplexes
- *In vitro* evaluation in cell line models
- Determination of nuclear localization and gene editing
- *In vivo* transfection analysis in mice

4.1. Introduction

Clustered regularly interspaced short palindromic repeat (CRISPR) is a versatile and precise genome editing tool, providing ample therapeutic opportunity in ailments with genetic and non-genetic causes [1, 2]. Till now, out of three available adaptive delivery forms of CRISPR (plasmid, mRNA, and direct Cas9 protein), protein delivery has lived up to the most effective genome editing due to advantages like lesser off-target effects, lower insertional mutagenesis, short persistent of Cas9 protein and lower immunogenic responses. CRISPR/Cas9 system consists of two main components, the first one is CRISPR-associated protein (Cas9) with endonuclease activity, and the second one is single guide RNA (sgRNA) with complementary target gene sequence. Therefore, Cas9 protein, along with sgRNA, is being delivered in the form of ribonucleoprotein (RNP) to edit genes at the desired site by causing a double-strand break (DSB) that leads to activation of cellular DNA repair using non-homologous end-joining (NHEJ) and homology-directed repair (HDR). Despite precise and effective genome editing, the large molecular weight of Cas9 protein (~165 kD), hydrophilicity, supra-negative charge (~ -20 mV), and its sensitive and fragile nature, hinder the delivery of RNPs *in vitro* as well as *in vivo*.

Previously, viral vectors were the only choice for delivering CRISPR/Cas9 tools which have a safety concern for therapeutic genome editing. Moreover, AAVs suffer from limited packaging capacity (4.7 kb) for commonly used spCas9. Hence, attempts have been made to provide *non-viral* vectors, where RNPs were delivered using cationic polymeric or lipidic nanocarriers for efficient gene editing with certain limitations such as limited payload capacity, cytotoxicity, and lack of tissue-specific targeting, instability, and limited *in vivo* application. Cationic lipid-based *non-viral* vectors also provided ample delivery opportunities; for instance, Wang et al. have recently reported a bio-reducible lipid nanocarrier complex for protein-based

Cas9 genome editing [3]. It was produced through the electrostatic interaction of cationic lipids and super-negatively charged complexes *via* protein-protein fusion. Besides, Zuris *et al*. have demonstrated that negatively charged Cas9 endonuclease proteins could be fused with anionic supercharged proteins or anionic nucleic acids, followed by complexation with the cationic lipids. They efficiently delivered Cre recombinase, TALEN- and Cas9-based transcriptional activators, and Cas9:sgRNA nuclease complexes into cultured human cells. Further, up to 80% of genome modification was observed with Cas9:sgRNA complexes compared to DNA transfection [4]. Initially, lipids were widely explored for CRISPR/delivery due to their unique properties. Zhen *et al*. delivered CRISPR/Cas9 to treat prostate cancer by using cationic liposome containing poly(ethylene glycol)-grafted 1,2-distearoyl-sn-glycero-3-phosphatidylethanolamine [5]. Further, Core-shell nanoparticles consisting of PEG phospholipid-modified cationic lipid encapsulated Cas9/sgRNA plasmid targeting Polo-like kinase 1 (PLK-1) showed an *in vitro* transfection of 47.4% in A375 cells. Further, these nanoparticles showed significant downregulation of PLK-1 protein and suppression of tumor growth in melanoma tumor-bearing mice [6]. In a recent study, cas9-sgRNA RNPs directed against the dipeptidyl peptidase-4 gene (*DPP-4*) for modulating glucagon-like peptide 1 function were delivered using nano-liposomes that disrupted DPP-4 gene expression and declined the DPP-4 enzyme activity in type 2 diabetes mellitus (T2DM) *db*/*db* mice resulting in a normalized blood glucose levels [7]. In another study, cationic lipids were used to deliver sgRNA/Cas RNPs in MCF-7 cells to knockout the MDR1 gene, responsible for the efflux of DOX. The results showed an increase in drug uptake by four-fold relative to the untreated cells by decreasing the MDR1 gene-mediated resistance [8]. Gene editing proteins need to be delivered into the nucleus for their activity; therefore, the delivery vector should possess the capability of functional delivery. In another

study, Chen et al., prepared Cas9 RNP complexed polymeric biodegradable nanocapsule having a 25 nm hydrodynamic size with robust gene editing *in vivo* in murine retinal pigment epithelium (RPE) tissue and skeletal muscle after local administration[9]. Polymeric nanocarriers also offer the freedom of chemical modification in the structure according to the requirement. For example, Lu et al. reported that micelles prepared using a polymer having an imidazole ring escape cargo from the endosome [10]. In another study, polyethylene glycol monomethyl ether (mPEG) conjugated chitosan has explored the delivery of the CRISPR/Cas system. PEGylated chitosan of low and medium molecular weight was complexed with the pSpCas9-2A-GFP plasmid, and it was observed that low molecular weight PEGylated chitosan showed optimal transfection at N/P ratio of 20. In contrast, PEGylated medium molecular weight chitosan showed optimal transfection at N/P ratio 5[11]. Liu et al. reported poly(ethylene glycol)-b-poly-(lactic acid-co-glycolic acid) (PEG-PLGA)-based cationic lipid-assisted polymeric nanoparticles (CLANs) for delivering CRISPR/Cas9 plasmid (pCas9) that efficiently disrupted CML-related BCR-ABL fusion gene and increased the survival of a CML mouse model[12]. Likewise, different hybrid polymers, as well as the lipids, have been already screened for *in vivo* delivery of CRISPR/Cas components.[2, 13, 14].

We have previously reported that cholesterol and morpholine grafted amphiphilic cationic polymeric nanocarrier efficiently deliver miRNA-34a into the cancer cell by escaping the lysosomal acidic environment [15, 16]. These cationic polymers, being positively charged, could be electrostatically complexed with the negatively charged sgRNA/cas9 RNPs to form stable nanoplexes. Herein, we report a robust gene-editing strategy based on the delivery of these anionic RNPs using cationic amphiphilic lipopolymeric nanoplexes. The double emulsion solvent evaporation method was used to prepare the cationic lipopolymeric nanoplexes, followed

by the formation of RNP lipopolymeric nanoplexes through electrostatic complexation. The characterization of RNPs lipopolymeric nanoplexes was done using particle size, zeta potential, and gel retardation assay. Further, the release behavior of RNPs was determined using a heparin competition assay, followed by the evaluation of the enzymatic activity and stability in the presence of fetal bovine serum. Fluorescent microscopy assays were performed to evaluate transfection efficiency and the uptake mechanism of sgRNA/Cas9 RNPs lipopolymeric nanoplexes in HEK293T cells. Further, confocal microscopy was done to examine intracellular trafficking and concomitant transport of RNPs to the nucleus using the CASFISH experiment. Moreover, a fluorescence quenching-based mGFP gene editing assay was performed in mGFP-HEK cells to evaluate the gene-editing efficiency of spCas9 RNPs lipopolymeric nanoplexes. T7 Endonuclease assay revealed the quantitative gene-editing efficiency of the RNPs lipopolymeric nanoplexes. An intramuscular *in vivo* transfection assay in mice was used to verify the *in vivo* durability and performance of lipopolymeric nanoplexes.

4.2. Materials

OptiMEM™ reduced serum media, Fetal Bovine Serum (FBS), Dulbecco's Modified Eagle Medium (DMEM), Snakeskin (3.5 kD), Micro BCA™ Protein Assay Kit, MEGAscript™ T7 Transcription Kit, Hoescht, CRISPRMax and DAPI (4',6-diamidino-2-phenylindole) were obtained from ThermoFischer scientific (Massachusetts, USA). T7 endonuclease I was purchased from Biolab (Delhi, India), while Genomic DNA purification kit was purchased from Promega (Delhi, India). 3-(4,5-Dimethylthiazol-2-yl)-2,5-diphenyltetrazolium bromide (MTT) was purchased from Merck (Jaipur, India). All the primers were purchased from Imperial Life Science (ILS, Delhi, India). N,N-dimethyldipropylenetriamine (DP), Benzyl bromide, tin(II) 2-ethylhexanoate, cholesterol, methoxy poly(ethylene glycol) (mPEG, 5000 Da),

hydroxybenzotriazole (HOBt), Bis(hydroxymethyl) propionic acid, 1-ethyl-3-(3-dimethylaminopropyl) carbodiimide hydrochloride (EDC.HCl) and 4-(2-aminoethyl)morpholine, HEPES buffer and Heparin sodium salt from porcine intestinal mucosa were purchased from Sigma Aldrich (St. Louis, MO). The remaining solvents and chemicals are of analytical grade and procured from local vendors.

4.3. Methodology

4.3.1. Synthesis of the cationic polymer, mPEG-b-(CB-{g-cationic chain; g-Chol; g-Morph})

The synthesis and characterization of mPEG b-(CB-g-cationic chain; g-Chol; g-Morph) polymer were identical to the data reported in Chapter 2 and can be accessed from Figure 2.1 and Figure 2.2.

4.3.2. Preparation of Ribonucleoprotein complexes (RNPs)

Single guide RNA (sgRNA) required for the RNPs preparation was synthesized by *in vitro* transcription (IVT) method using a dsDNA template. Briefly, targeted genes were screened for the protospacer adjacent motif (PAM) site and specific sgRNAs were designed using CHOPCHOP/CRISPOR software. Forward (FP) and reverse primers (RP) were designed (Table 4.1), screened, and compared for off-targets, followed by the synthesis of dsDNA using PCR. Thereupon, *in vitro* transcription kit (MEGAscript™ T7 Transcription Kit, Thermo Scientific) was used to synthesize sgRNA as per the manufacturer's protocol [9].

Further, catalytically active CRISPR-associated protein, *Streptococcus Pyogenes* Cas9 (spCas9), was expressed in *Escherichia coli* Rosetta2 (DE3) (Novagen) using a pET-based

expression vector as described in Chapter 3. The purified spCas9 protein was analyzed using BCA kit (Thermo Scientific) for its concentration [4] and was stored at - 80°C in HEPES buffer

Table 4.1. Primers sequences for sgRNA synthesis

Primer	Sequence
SgRNA_1. mGFP_FP	5'TAATACGACTCACTATAGAAGTTCGAGGGCGATACCC GTTTTAGAGCTAGAA 3'
SgRNA_2 mGFP_FP	5'TAATACGACTCACTATAGGTGAACCGCACGAGCTGAA GTTTTAGAGCTAGAA3'
SgRNA_BPR_FP	5'TAATACGACTCACTATAGCAGGAGGATGGCGTGAACC GTTTTAGAGCTAGAA3'
SgRNA_Telo_FP	5'TAATACGACTCACTATAGCCAGGGCCAGGGCCAGGGC CGTTTTAGAGCTAGAA3'
Universal_RP	5'AAAAGCACCGACTCGGTGCCACTTTTTCAAGTTGATA ACGGACTAGCCTTATTTTAACTTGCTATTTCTAGCTCTA AAAC-3'

(50 mM, pH 7.5) containing 100 µM Tris (2-carboxyethyl) phosphine hydrochloride, 10% glycerol and 300 mM NaCl.

To prepare the sgRNA/Cas9 RNPs complex, obtained sgRNA and spCas9 protein were taken in a 1:1 mol ratio. The mixture was kept for 10 min incubation at room temperature and characterized by running on 0.8 % agarose gel electrophoresis [9, 17].

4.3.3. Preparation of ribonucleoprotein lipopolymeric nanoplexes

An emulsion-based method was used for the preparation of blank lipopolymeric nanoplexes, followed by its complexation with the RNPs. Briefly, cationic lipopolymer **(8)** (3 mg) was dissolved in 600 µL of dichloromethane (DCM), followed by the addition of 100 µL of nuclease-free HEPES buffer (10 mM; pH 6.7). The mixture was sonicated at 20% amplitude for 30 seconds to obtain primary emulsion (W/O). The primary emulsion was added dropwise to 3

mL of HEPES buffer (10 mM; pH 6.7), followed by probe sonication at 20% amplitude for 3.5 min on an ice bath to get secondary emulsion (W/O/W). The organic phase was removed under vacuum (Büchi® Rotavapor®) and centrifuged at 5000 rpm for 5 min to obtain the blank nanoplexes in the supernatant. CRISPR/Cas9 RNP lipopolymeric nanoplexes were prepared by mixing the blank nanoplexes with sgRNA/Cas9 RNPs in a 1:10 ratio (w/w) and incubated at room temperature for 30 min to allow electrostatic complexation. The nanoplexes were characterized for their particle size and zeta potential (Malvern Zeta Sizer, Nano ZS) and High Resolution-Transmission Electron Microscopy (HR-TEM (TECNAI 200 Kv TEM, FEI Electron Optics, Eindhoven, Netherlands). The complexation efficiency (%) of sgRNA/Cas9 RNPs with the blank nanoplexes was determined at 2 and 5% theoretical loading (%) of the RNPs using bicinchoninic acid (BCA) assay as reported earlier [9]. Briefly, RNP nanoplexes at 2 and 5% *w/w* theoretical loadings were complexed at room temperature for 30 min to form RNPs nanoplexes followed by determination of zeta potential using Zetasizer (Malvern, Nano ZS). The nanoplexes were then centrifuged at 18000 rpm for 45 min to pelletize nanoplexes, and the sgRNA/Cas9 RNPs concentration in the supernatant was determined using the BCA kit as per manufacturers' protocol [9] (Pierce™ BCA Protein Assay Kit, Thermo Scientific™).

4.3.4. Gel retardation assay

Gel retardation assay was performed to determine the blank lipopolymeric nanoplexes to sgRNA/Cas9 RNPs ratio (µg) required to form the nanoplexes. Briefly, a fixed amount of sgRNA/Cas9 RNPs (µg) was complexed with the different amounts (in µg) of blank lipopolymeric nanoplexes in RNase-free HEPES buffer (10 mM; pH 6.7) and kept for 30 minutes at room temperature. A loading dye (5 µL) was added to the samples, which were subsequently subjected to agarose gel electrophoresis. Gel electrophoresis was performed on

0.8% agarose gel for 30 min at 110 V and visualized under the Gel Doc system (Gel Doc™XR+ Gel Documentation system) [17].

4.3.5. Heparin competition assay

A heparin competition assay was performed to understand the release behavior of sgRNA/Cas9 RNPs from the lipopolymeric nanoplexes. Heparin is a competitor anion used to release complexed DNA/RNAs from cationic polymers and lipids [18]. Herein, RNPs lipopolymeric nanoplexes were incubated with different concentrations of heparin (0.005 to 0.5 IU) at 37ºC for 30 min, followed by the addition of a loading dye (5 µL) and agarose gel electrophoresis as given above. Herein, naked RNPs and RNPs lipopolymeric nanoplexes were taken as controls.

4.3.6. RNPs lipopolymeric nanoplexes stability in fetal bovine serum (FBS)

The stability of RNPs lipopolymeric nanoplexes was determined in the presence of FBS [19]. Briefly, freshly prepared RNPs lipopolymeric nanoplexes were incubated with 20% FBS at 37ºC for predetermined time points (i.e., 0, 2, 4, 6, 8, 12, 24, and 48 h). After incubation, EDTA (10 uL) was added to inactivate the FBS. Further, heparin (0.1 IU) was added to the samples, followed by incubation at 37ºC for another 1 h to release the RNPs from the lipopolymeric nanoplexes. After that, all the samples were loaded on 0.8% agarose gel, and electrophoresis was performed at 110 V for 30 min. RNPs treated with FBS and RNPs lipopolymeric nanoplexes without FBS were kept as the positive and negative control, respectively. The gel was visualized under the Gel Doc™XR+ Gel Documentation system.

4.3.7. Endonuclease enzymatic activity of RNPs after release from lipopolymeric nanoplexes

Attrition of endonuclease activity is one of the major concerns with CRISPR/Cas9 RNPs delivery *via* nanoformulation strategy. To examine this property, developed RNPs lipopolymeric nanoplexes were treated with heparin to release RNPs and evaluated for their DNA cleavage activity [20]. Briefly, the desired amount of RNPs lipopolymeric nanoplexes containing 100 ng of Cas9 protein were treated with 0.1 IU of heparin, followed by incubation at 37°C for 30 min to release RNPs. Thereupon, 200 ng of DNA substrate (pCAGs-RFP-P2A-eGFP) having a Cas9 cleavage site was incubated with released RNPs at 37°C for 1 h. Herein, DNA substrate and DNA substrate treated with freshly prepared RNPs were kept as the negative and positive control, respectively. Samples were loaded on a 0.8% agarose gel and electrophoresis was performed at 110 V for 30 min. The gel was visualized under the Gel Doc™XR+ Gel Documentation system**.**

4.3.8. Hemocompatibility assay

Developed RNPs lipopolymeric nanoplexes were evaluated for their compatibility with the mice's blood. Briefly, 2 mL of blood *was* collected *via* retro-orbital plexus from *swiss albino* mice and centrifuged at 2000 rpm for 5 min. The supernatant was discarded, and erythrocytes were washed with PBS, followed by resuspension in normal saline. Furthermore, 1 mL of erythrocytes were taken in the microcentrifuge tube and treated with blank lipopolymeric nanoplexes, RNPs (200 nM), and RNPs lipopolymeric nanoplexes (containing 200 nM RNPs) followed by incubation for 1 h at room temperature. The untreated and Triton-X-treated erythrocytes were taken as a negative and positive control, respectively. After treatment, the samples were centrifuged at 2000 rpm for 5 min, followed by visual inspection and microscopic

evaluation for hemolysis and measurement of absorbance of the supernatant at 415 nm using a plate reader (BioTeK Epoch). Hemolysis (%) was calculated with respect to triton X, which showed 100 % hemolysis.

4.3.9. Cell culture-based assay

HEK293T and mGFP-HEK293T cells were provided by Dr. Debojyoti Chakraborty, CSIR-Institute of Genomics and Integrated Biology (CSIR-IGIB), New Delhi, as a kind gift. Cells were maintained in Dulbecco's Modified Eagle's Medium (DMEM) supplemented with 10% fetal bovine serum (FBS) and 1% antibiotics (100X penicillin/streptomycin) and kept at 37°C in a humidified atmosphere containing 5% CO2.

4.3.9.1. Transfection efficiency

To evaluate the uptake of the RNPs in HEK293T cells, sgRNA/eGFP-dCas9 RNPs were used in the study. Briefly, HEK293T cells were seeded in 24-well cell culture plates (20,000 cells/well) in DMEM media (with 10 % FBS), followed by incubation at 37°C and 5% CO_2 overnight to allow the cells to adhere. The next day, cells were washed with PBS, and media was replaced with optiMEM media containing naked sgRNA/eGFP-dCas9 RNPs (200 nM eGFP-dCas9), and sgRNA/eGFP-dCas9 RNPs lipopolymeric nanoplexes (containing 200 nM eGFP-dCas9). In this study, CRISPRMax was used as a standard transfecting agent. After predetermined time points (i.e., 1, 3, 6, and 9 h), cells were washed with PBS and counterstained with Hoechst dye (100 µg/mL, for nucleus staining) followed by observation under a fluorescence microscope (Vert A1, Zeiss) [9]. For quantitative measurement of transfection efficiency, the cells were analyzed using Flow cytometry (Beckman Coulter, USA), and the data was processed using CytExpert software (version 2.3).

4.3.9.2. CASFISH based nuclear localization

The essential requirement for the nanocarrier delivering CRISPR/Cas9 RNPs is related to its efficiency in delivering RNPs to the nucleus in its native form. Therefore, to evaluate such efficiency of developed lipopolymeric nanoplexes, a CASFISH experiment was performed [21]. Briefly, RNPs (composed of sgRNA targeting telomere region and an eGFP-dCas9) were complexed with blank lipopolymeric nanoplexes, and transfection was done in HEK293T cells followed by incubation for different predetermined time points (6h, 12h, 24h, and 48h). Further, the cells were washed thrice with PBS and counterstained with Hoechst for nucleus staining and analyzed using CLSM (Carl Zeiss, Germany). Note: The sequence of sgRNA designed for the telomere region is given in table 4.1.

4.3.9.3. Endocytosis uptake pathway

Briefly, HEK293T cells were seeded in 6-well cell culture plates (25000 cells/well) and incubated at 37ºC/ 5% CO_2 overnight. After incubation, the cells were washed with PBS and media containing different endocytic inhibitors, including nystatin (27 μM), chlorpromazine (10 μM), methyl β-cyclodextrin (3 mM) and amiloride (1 mM), was added to the cells followed by incubation for 30 min at 37ºC/ 5% CO_2. Further, the cells were washed with PBS and fresh optiMEM media containing RNPs lipopolymeric nanoplexes (200 nM eGFP-Cas9) was added and the cells were incubated for 6 h followed by analysis using fluorescence microscopy. The cells were washed with PBS, stained with Hoechst dye and observed under a fluorescence microscope (Vert.A1, ZEISS, Oberkochen, Germany).

4.3.9.4. *In vitro* cytotoxicity assay

The cytotoxicity of sgRNA/Cas9 RNP lipopolymeric nanoplexes was studied in HEK293T cells. Briefly, the cells were seeded in 96 well cell culture plates (5000 cells/well) and incubated at 37ºC/ 5% CO_2 overnight. After incubation, the cells were treated with the naked sgRNA/dCas9 RNPs and sgRNA/dCas9 RNP lipopolymeric nanoplexes equivalent to 200 nM/well of Cas9, followed by incubation for 48 h. The cells treated with blank nanoplexes and PBS were kept as controls. After 48 h, cell viability was determined by 3-(4,5-Dimethylthiazol-2-yl)-2,5-diphenyltetrazolium bromide (MTT) assay. Further, the RNPs lipopolymeric nanoplexes were evaluated for their *in vitro* toxicity in HEK293T cells in a dose and time-dependent manner. Wherein, the cells were treated with RNPs lipopolymeric nanoplexes with different doses (ranging from 2X to 50X of the working dose) and the cell viability was determined after 48 h and 96 h. Briefly, the cells were washed with PBS and 200 µL fresh DMEM (10% FBS) media containing 0.5 mg/mL MTT was added to each well, followed by incubation for 4 h at 37ºC/ 5% CO_2. After incubation, cells were washed with PBS, followed by dissolving formazan crystal, formed as a result of MTT metabolism by mitochondria, in 200 µL of DMSO. After that, samples were observed at 570 nm, and 630 nm under a microplate reader (BioTeK Epoch) and cell viability were calculated using the following equation [9, 22, 23].

$$\%\ \text{Cell viability} = \frac{\text{OD}\ (\ 570\ \text{nm} - \ 630\ \text{nm})\ for\ test\ sample}{\text{OD}\ (\ 570\ \text{nm} - \ 630\ \text{nm})\ for\ control\ sample} \text{X}\ 100$$

4.3.9.5. mGFP gene disruption assay

The mGFP gene disruption by Cas9 was assayed using microscopy-based fluorescent analysis as reported earlier [3]. The HEK293T cells with the mGFP gene (mGFP-HEK293T) integrated into the genome were seeded into 6-well cell culture plates (1×10^5 cells/well) and

allowed to adhere for 24 h. The cells were then treated with RNPs lipopolymeric nanoplexes targeting the mGFP gene for 6 h, the media was replaced with the fresh media and the cells were further cultured for 72 h. After 72 h, the cells were washed thrice with PBS and immediately observed with a fluorescent microscope (Vert.A1, ZEISS, Oberkochen, Germany) under a FITC channel with excitation and an emission wavelength of 488 nm and 525 nm, respectively. Herein, CRISPRMax was taken as the reference standard. The sgRNA sequence used in this assay is shown in Table 4.1.

4.3.9.6. T7 Endonuclease assay

HEK293T cells were transfected with sgBPR-Cas9 RNPs lipopolymeric nanoplexes at a concentration of 200 nM of Cas9 protein. After 6 hours, the media was replaced with fresh media, followed by incubation for 48 h at 37 ˚C and 5% CO2. Cells were washed, harvested using Trypsin/EDTA, centrifuged at 1200 rpm for 3 min and genomic DNA was isolated using Wizard® Genomic DNA purification kit (Promega, India). The purified genomic DNA was amplified for the target site using PCR and 2 µg of purified PCR product was treated with 1 µL (10U) of T7 Endo I and incubated at 37 ˚C for 15 min. The reaction was stopped by adding 2 µL of 0.25 M EDTA. The sample was loaded immediately on a 1.5% agarose gel for Indel (%) analysis. Herein, genomic DNA without T7 endo 1 was taken as a negative control [24] and CRISPRMax was taken as a standard transfecting agent. The primers used in this assay for sgRNA synthesis and PCR amplification are shown in Table 4.1. ImageJ software was used to process the gel image and the following formula was used to determine the Indel efficiency.[25]

$$\%\, Indel = 100\, X\, (1 - (1 - fraction\ cleaved)^{1/2})$$

4.3.9.7. Tracking of Indels by Decomposition (TIDE) Assay

The real-time quantitative assessment of the gene editing was evaluated as reported earlier.[26] Briefly, the HEK293T cells were transfected with RNPs lipopolymeric nanoplexes targeting the 5BPR gene, followed by incubation for 48 h. Next, the cells were harvested, the target gene site was amplified, followed by PCR purification, and Sanger's sequencing was performed. The sequenced PCR product was analyzed for indel efficiency using the TIDE Software (https://tide.nki.nl/).

4.3.10. *In vivo* transfection

To evaluate the *in vivo* stability of the developed lipopolymeric nanoplexes, *in vivo* transfection assay was performed in mice after the approval of protocol from IAEC (Protocol No-IAEC/RES/31/12) of BITS-Pilani, Pilani campus, Rajasthan (India). In brief, the mice were injected intra-muscularly with 50 µL of RNPs lipopolymeric nanoplexes containing 1 mg/kg of the eGFP-dCas9 protein and were kept under observation for 6 h. After that, the mice were sacrificed and the muscle tissue from the injection site was incised, frozen, and cryosectioned. The tissue was stained with DAPI and observed under a confocal microscope (CLSM, Carl Zeiss, Germany) to see the transfection.

4.3.11 Statistical analysis

The statistical analysis was carried out using a student *t*-test and analysis of variance (ANOVA) followed by Tukey's test to determine the statistical differences between two or more groups; the p-value of < 0.05 was considered as statistically significant.

4.4. Results

4.4.1. Synthesis of cationic amphiphilic copolymer

A full characterization of mPEG b-(CB-g-cationic chain; g-Chol; g-Morph) polymer can be accessed from Figure 2.2 and Table 2.1 of Chapter 2.

4.4.2. Preparation of ribonucleoprotein complexes (RNPs)

sgRNAs used in this study were synthesized *via* IVT reaction from dsDNA, obtained by annealing of forward and reverse primers, as shown in Table 4.1. Synthesized sgRNAs were characterized using agarose gel electrophoresis, confirming the size of ~110 bp (Figure 4.1a).

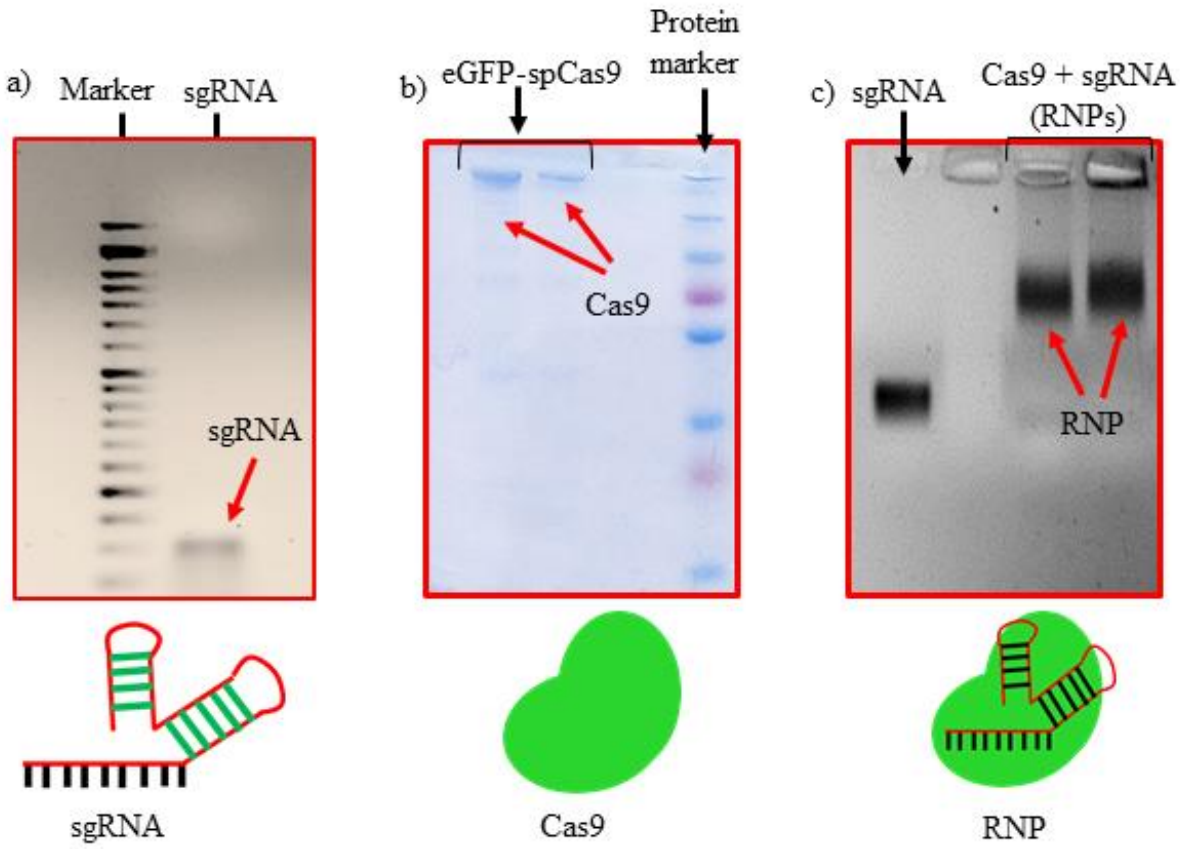

Figure 4.1. Characterization of RNPs formation. a) sgRNA from IVT, b) Purified Cas9 and c) sgRNA/Cas9 RNPs complex.

The purified spCas9 proteins were characterized using polyacrylamide gel electrophoresis (PAGE), where a dense band of approx. 200 kDa was observed (Figure 4.1b). After that, sgRNA and spCas9 were complexed in a 1:1 Mol ratio to obtain RNPs. The retardation in the mobility of sgRNA after being complexed with Cas9 protein (as shown in Figure 4.1c) indicates RNPs formation.

4.4.3. Preparation of lipopolymeric RNP nanoplexes

An emulsion-based method was used to prepare blank lipopolymeric nanoplexes from the synthesized cationic lipopolymer (mPEG-b-(CB-{g-cation chain; g-Chol; g- Morph})) in RNase-free HEPES buffer (10 mM, pH 6.7). Obtained blank lipopolymeric nanoplexes were incubated with sgRNA/Cas9 RNPs for 30 minutes at room temperature to obtain RNP lipopolymeric nanoplexes. Blank lipopolymeric nanoplexes and RNPs lipopolymeric nanoplexes showed a particle size of 73.75±6.2 (PDI-0.240) and 117.3±7.6 nm (PDI-0.399) nm, respectively, and zeta potential of 16.2±2.42 mV and 6.17±1.04 mV, respectively (Figure 4.2a and b). Furthermore, the encapsulation efficiency (%) of RNPs with the blank nanoplexes was determined at 5% theoretical loading (%) of the RNPs using bicinchoninic acid (BCA) assay. The encapsulation efficiency of > 90% was observed at 5% theoretical loading indicating efficient complexation of the sgRNA/cas9 RNPs with the lipopolymeric nanoplexes. The morphology of developed RNPs lipopolymeric nanoplexes was observed using transmission electron microscopy, indicating the spherical shape (Figure 4.2c).

4.4.4. Gel Retardation assay

A gel retardation assay was performed to determine the blank lipopolymeric nanoplexes to RNPs ratio (w/w) required to form the RNPs lipopolymeric nanoplexes. A fixed amount of

RNPs (in µg) was complexed with the different amounts (in µg) of blank nanoplexes in RNase-free water and kept for 30 minutes at room temperature. Gel electrophoresis results indicated a

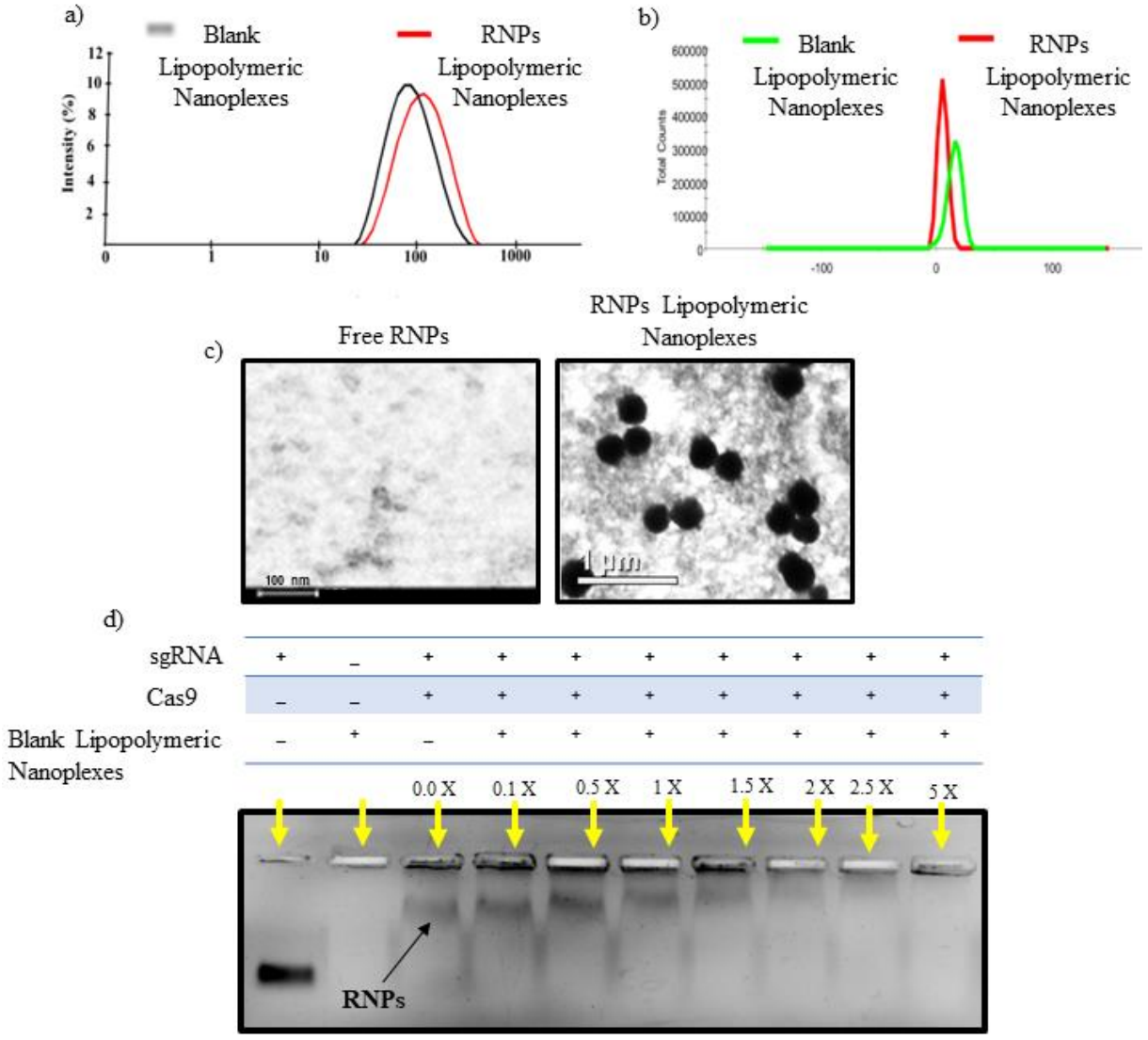

Figure 4.2. Characterization of developed RNPs lipopolymeric nanoplexes, a) particle size and b) zeta potential of blank lipopolymeric nanoplexes and RNPs lipopolymeric nanoplexes, c) transmission electron microscopy images of free RNPs and RNPs lipopolymeric nanoplexes, and d) complexation behavior of RNPs with lipopolymer evaluated via agarose gel electrophoresis. RNPs and lipopolymer were taken at different ratios (w/w, in µg) and run on a 0.8% agarose gel. X in the figure indicates the multiple lipopolymer w.r.t sgRNA/Cas9 RNPs.

decrease in the mobility of RNPs when the amount of blank lipopolymeric nanoplexes was increased (Figure 4.2d) with a complete complexation of the RNPs with 5X (w/w) of the blank lipopolymeric nanoplexes.

4.4.5. Heparin competition assay and endonuclease activity of the released RNPs

Heparin is a competitor anion that releases complexed DNA/RNAs from electrostatic complexes with cationic polymers and lipids [27]. We utilized a similar strategy to decomplex the RNPs lipopolymeric nanoplexes. It was observed that at 0.1 IU of heparin, RNPs got released from the lipopolymeric nanoplexes (Figure 4.3a). Further, the released RNPs were able to cleave the DNA substrate indicating the retention of their endonuclease activity after complexation and decomplexation with lipopolymeric nanoplexes (Figure 4.3b).

4.4.6. Stability of RNPs lipopolymeric nanoplexes in fetal bovine serum (FBS)

RNPs lipopolymeric nanoplexes were incubated with 20 % FBS for predetermined time points, followed by treatment with heparin (0.1 IU) and visualization on the agarose gel. Data indicated that the RNPs were stable in FBS for 12 h when complexed with the lipopolymeric nanoplexes as compared to the naked sgRNA/Cas9 RNPs, which were degraded in FBS within 2 h (Figure 4.3c).

4.4.7. Cyto-compatibility study

The toxicity profile of RNP lipopolymeric nanoplexes was determined in HEK293T cells using MTT assay, wherein cells were treated with naked RNPs (equivalent to 200 nM Cas9), blank lipopolymeric nanoplexes and RNPs lipopolymeric nanoplexes (equivalent to 200 nM Cas9) for 48 h. As per the observations. the lipopolymeric nanoplexes showed minimal toxicity at working concentration in HEK293T cells (Figure 4.4 a). Additionally, the lipopolymeric

nanoplexes showed non-significant toxicity up to the 20X dose of the working concentration after 48 h (Figure 4.4 a1).

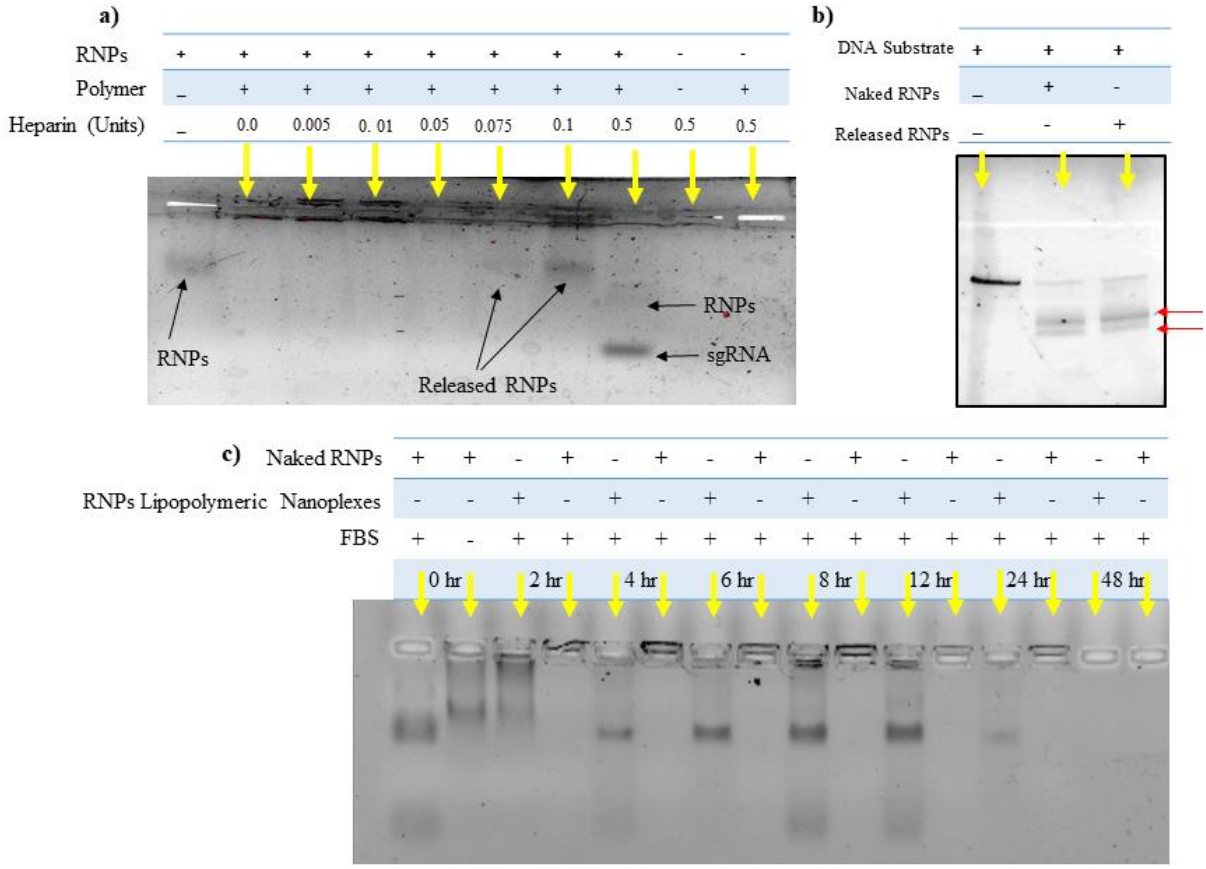

Figure 4.3. a) Release of RNPs from lipopolymeric nanoplexes using heparin competition assay, b) in vitro cleavage of a DNA substrate by RNPs released from lipopolymeric nanoplexes. The red arrow shows a cleaved DNA fragment. Herein, naked RNPs were taken as control, and c) stability of RNPs lipopolymeric nanoplexes in fetal bovine serum. Samples were treated with 20% fetal bovine serum for a predetermined period at 37º C, followed by release from lipopolymeric nanoplexes using heparin and visualization on 0.8% agarose gel electrophoresis. RNPs with and without treatment with fetal bovine serum (20%) were taken as a positive and negative control, respectively.

4.4.8. Hemocompatibility study

Lipopolymeric nanoplexes were screened for their compatibility with mice erythrocytes; therefore, naked RNPs (equivalent to 200 nM Cas9), blank nanoplexes, and RNPs lipopolymeric

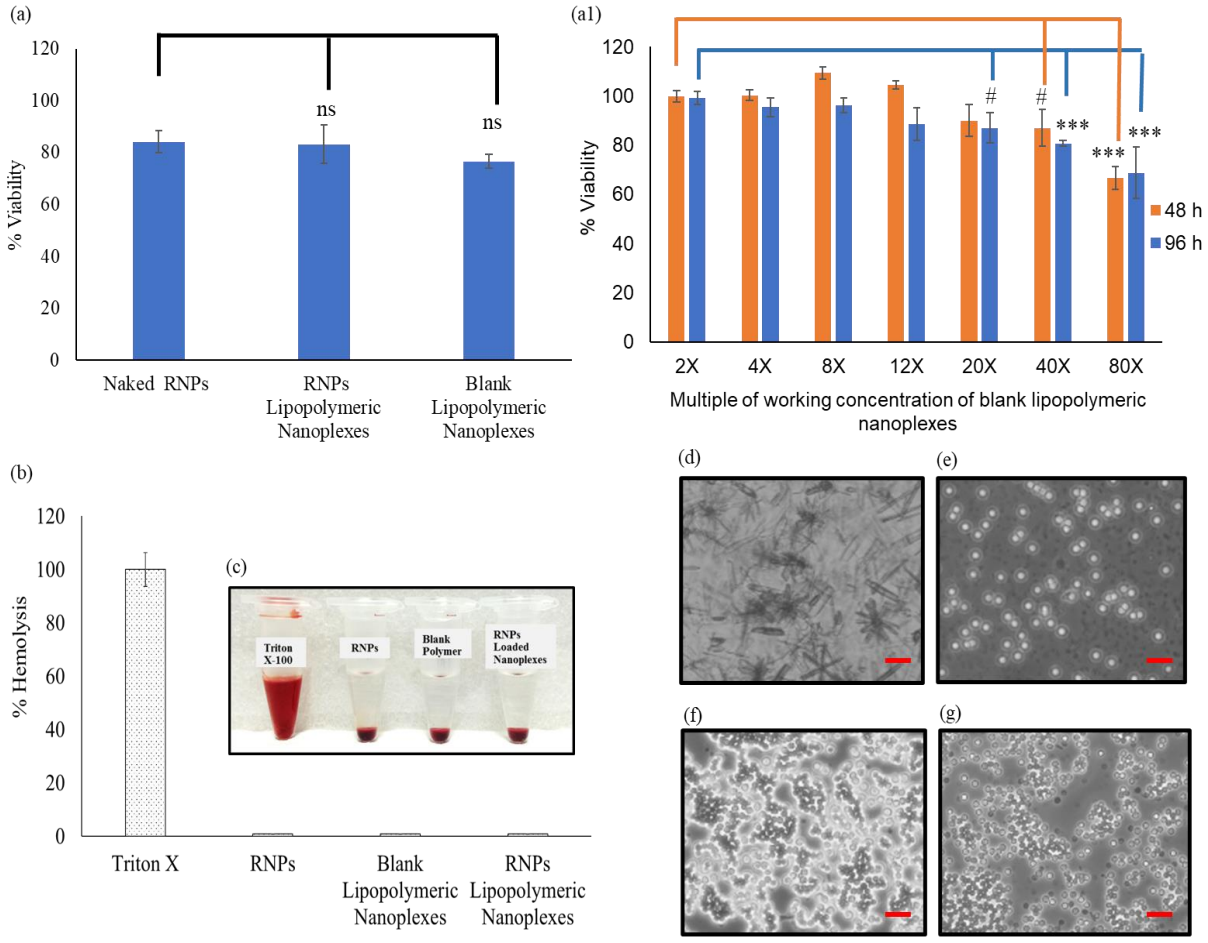

Figure 4.4**.** Cyto-compatibility of RNPs lipopolymeric nanoplexes at a) working concentration and a1) concentration and time dependent manner in HEK293T cells (data are presented as Mean±SD. ns, p≥0.05, #, p≤0.05 and ***, p≤0.01), b and c) % hemolysis and visual illustration of blood of *swiss albino* mice after incubation with RNPs lipopolymeric nanoplexes for 1 h, d-g) microscopic images of blood cells after treatment with Triton X-100, free RNPs, blank lipopolymeric nanoplexes and RNPs lipopolymeric nanoplexes, respectively.

nanoplexes (equivalent to 200 nM Cas9) were incubated with 1 mL of freshly collected mice erythrocytes for 1h. Triton X was taken as a positive control that causes 100 % hemolysis. Less than 1 % hemolysis was observed for naked RNPs, blank lipopolymeric nanoplexes, and RNPs lipopolymeric nanoplexes, indicating no significant hemolysis (Figure 4.4b&c) that was further corroborated with the visual and microscopic evaluation (Figure 4.4d-g).

4.4.9. Transfection efficiency

For evaluating the capability of lipopolymeric nanoplexes to transfect HEK293T cells, the cells were incubated with RNPs lipopolymeric nanoplexes containing eGFP-dCas9

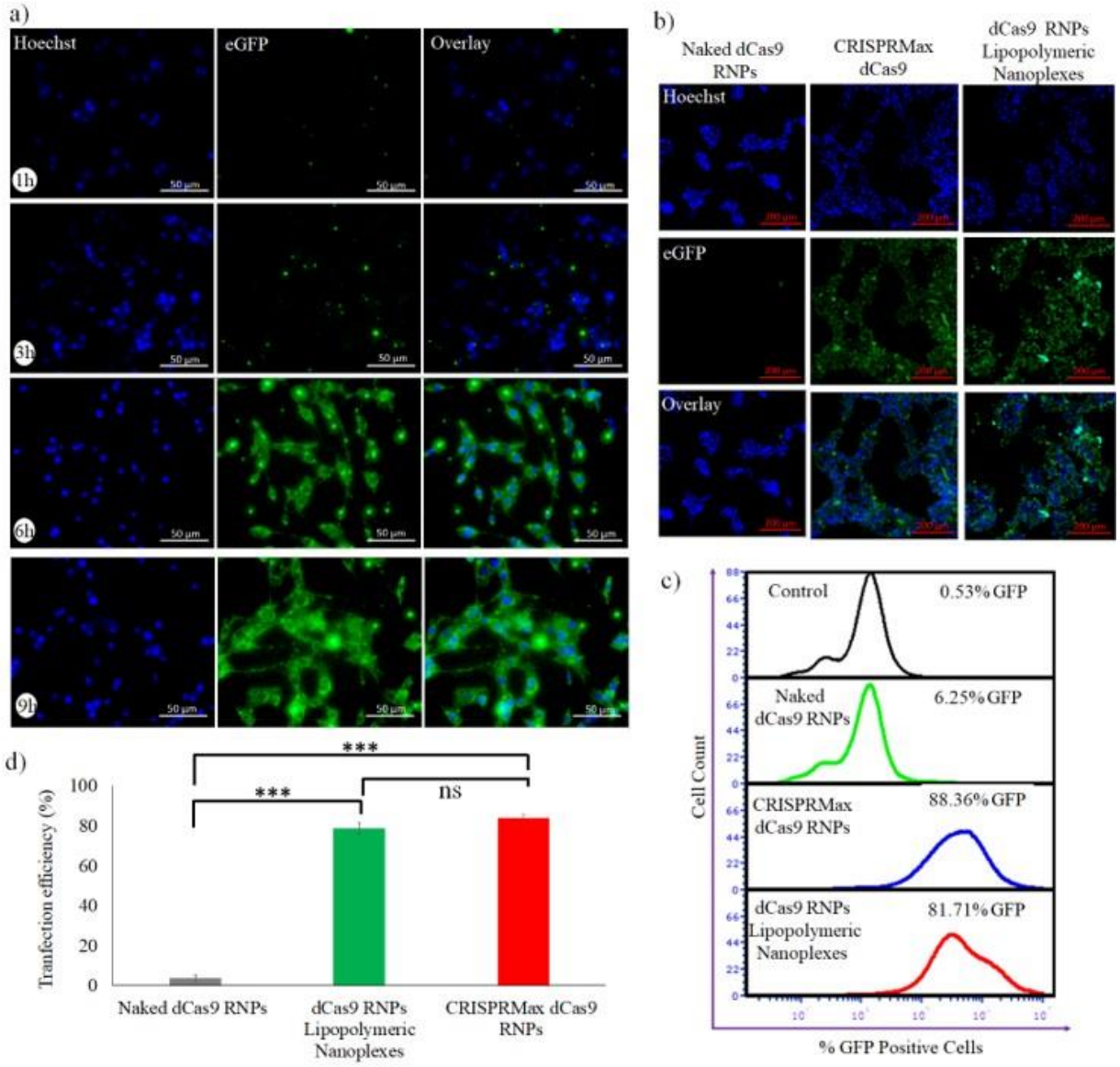

Figure 4.5. Evaluation of transfection efficiency of eGFP-dCas9 RNPs lipopolymeric nanoplexes in HEK293T cells, a) time-dependent transfection efficiency, b) evaluation of transfection with standard transfecting agent i.e CRISPRMax using fluorescence microscopy and c&d) flow cytometry. Data are presented as Mean±SD. ns, $p \geq 0.05$, and ***, $p \leq 0.01$).

(equivalent to 200 nM) for predetermined time points (1, 3, 6, and 9 h) followed by observation under fluorescence microscopy. The observations revealed that the RNPs, showing green fluorescence due to eGFP-dCas9, were delivered efficiently and time-dependent by the lipopolymeric nanoplexes in HEK293T cells (Figure 4.5a) and maximum transfection was seen after 6 h (Figure 4.5b). Herein, the blue color indicates the nucleus staining by the Hoechst dye and the green color is from eGFP-dCas9. Further, as per the flow cytometry data, the RNPs nanoplexes showed 81.71% of transfection with respect to the CRISPRMax, which showed 88.36% of transfection (Figure 4.5c&d).

4.4.10. CASFISH based nuclear localization

CRISPR/Cas9 RNPs should reach the nucleus with their intact endonuclease property, and the nanocarrier/vector delivering RNPs should not affect their native form. To evaluate this property of developed nanoplexes, we have performed a CASFISH experiment, wherein RNPs containing dead Cas9 (dCas9) and sgRNA (Telo-sgRNA) targeting telomere region (TTAGGA repeats) were used. The CLSM images showed a time-dependent nuclear localization of RNPs (Figure 4.6 a). After 6 h of the treatment, the RNPs were seen in the cytoplasm (green color), while after 48 h, the RNPs molecules were also observed in the nucleus. After 48 h RNPs could be observed majorly in the nucleus. The results clearly indicated that the lipopolymeric nanoplexes delivered the RNPs into the cellular environment in intact form and are localized to the nucleus and binding to the telomere region efficiently (Red arrow, Figure 4.6 a).

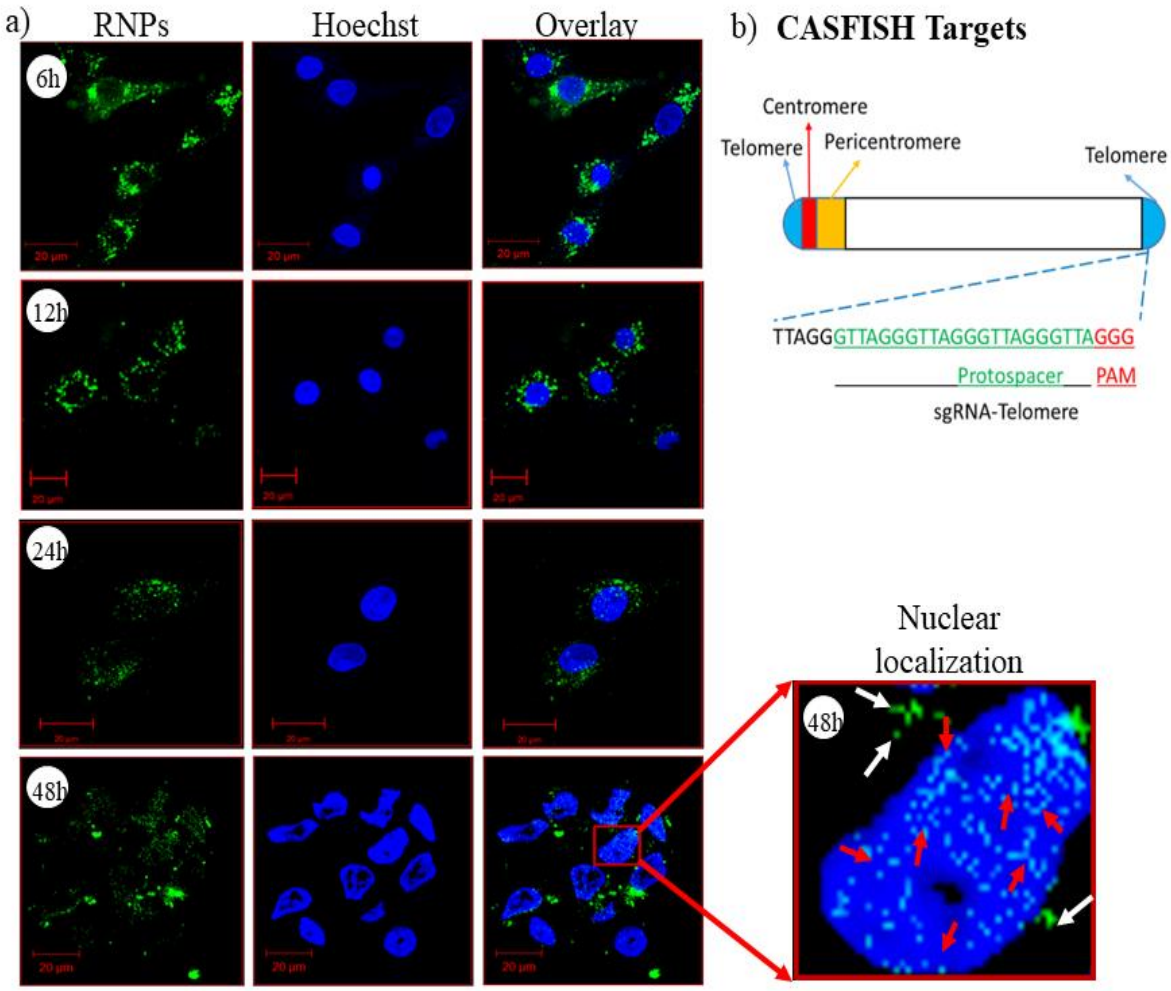

Figure 4.6. a) CLSM based time dependent nuclear localization of RNPs delivered *via* lipopolymeric nanoplexes and b) schematic representation of targeted telomere region and telo-sgRNA sequence used for CASFISH assay. Note: Herein, RNPs composed of the sgRNA targeting telomere (TTAGGG repeats) region along with eGFP-dCas9 protein were delivered using lipopolymeric nanoplexes. The white arrow indicates the cytoplasmic RNPs, while red arrow indicates the telomere specific binding of the RNPs.

4.4.11. Endocytic uptake pathway

To determine the uptake mechanism, HEK293T cells were treated with the endocytic uptake inhibitors i.e., nystatin (caveolae inhibitor), chlorpromazine (clathrin pathway inhibitor), methyl β-Cyclodextrin (lipid-mediated endocytic inhibitor) and amiloride (micropinocytic

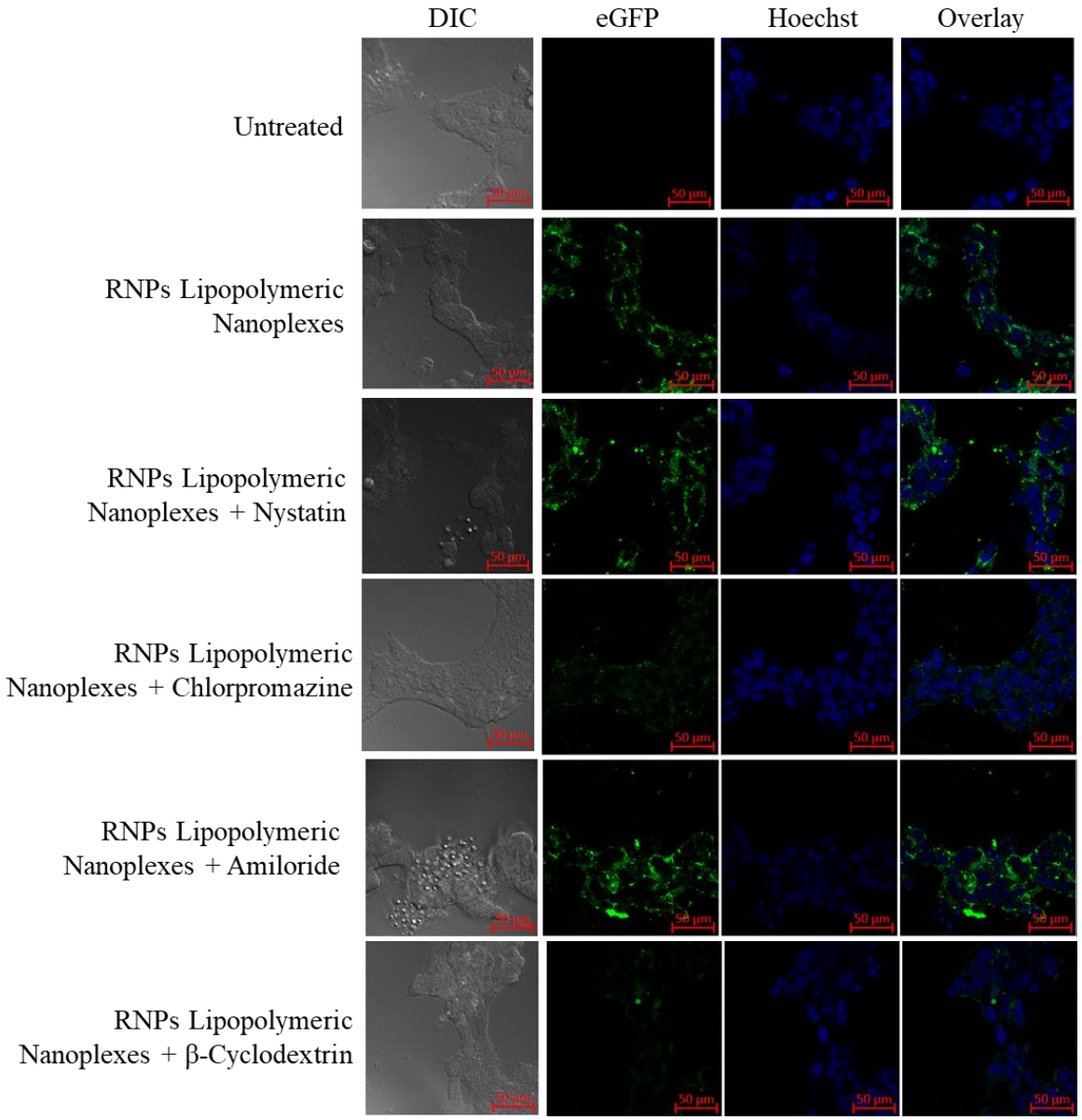

Figure 4.7. Uptake mechanism of RNPs lipopolymeric nanoplexes in presence of endocytic uptake inhibitors

inhibitor) followed by treatment with RNPs lipopolymeric nanoplexes (equivalent to 200 nM eGFP-dCas9). Data showed that the RNPs lipopolymeric nanoplexes followed a lipid-mediated as well as clathrin-based internalization since the uptake was inhibited majorly by the chlorpromazine (clathrin pathway inhibitor) and methyl β-Cyclodextrin (lipid-mediated endocytic inhibitor) (Figure 4.7).

4.4.12. *mGFP* gene disruption assay

A qualitative gene disruption assay was performed using fluorescent microscopy in mGFP-HEK293 cells. The cells were treated with mGFP-sgRNA/Cas9 RNPs lipopolymeric nanoplexes for 72 h followed by an examination of mGFP protein expression. Fluorescence microscopic data showed a decrease in mGFP intensity as compared to the control group indicating the disruption of mGFP gene inmGFP-HEK293 cells (Figure 4.8c). Overall, this data suggested the efficient delivery of Cas RNPs by lipopolymeric nanoplexes.

4.4.13. T7 Endonuclease assay

In vitro gene editing efficiency of Cas9 RNPs delivered via lipopolymeric nanoplexes was determined as previously described [24]. In this experiment, RNPs lipopolymeric nanoplexes targeting the BPR2 gene were delivered in HEK293T cells for 48 h. T7 endonuclease digestion indicated ~70 % of indel efficiency in the HEK293T cells treated with RNPs lipopolymeric nanoplexes and CRISPRMax RNPs (Figure 4.8d & e). Overall, this data suggested the efficient delivery of Cas9 RNPs by lipopolymeric nanoplexes.

4.4.14. Tracking of Indels by Decomposition (TIDE) Assay

The gene editing was further assessed using sequence trace decomposition or TIDE assay. Figure 4.8f showed the aberrant nucleotide sequence signal of the test sample (green) with

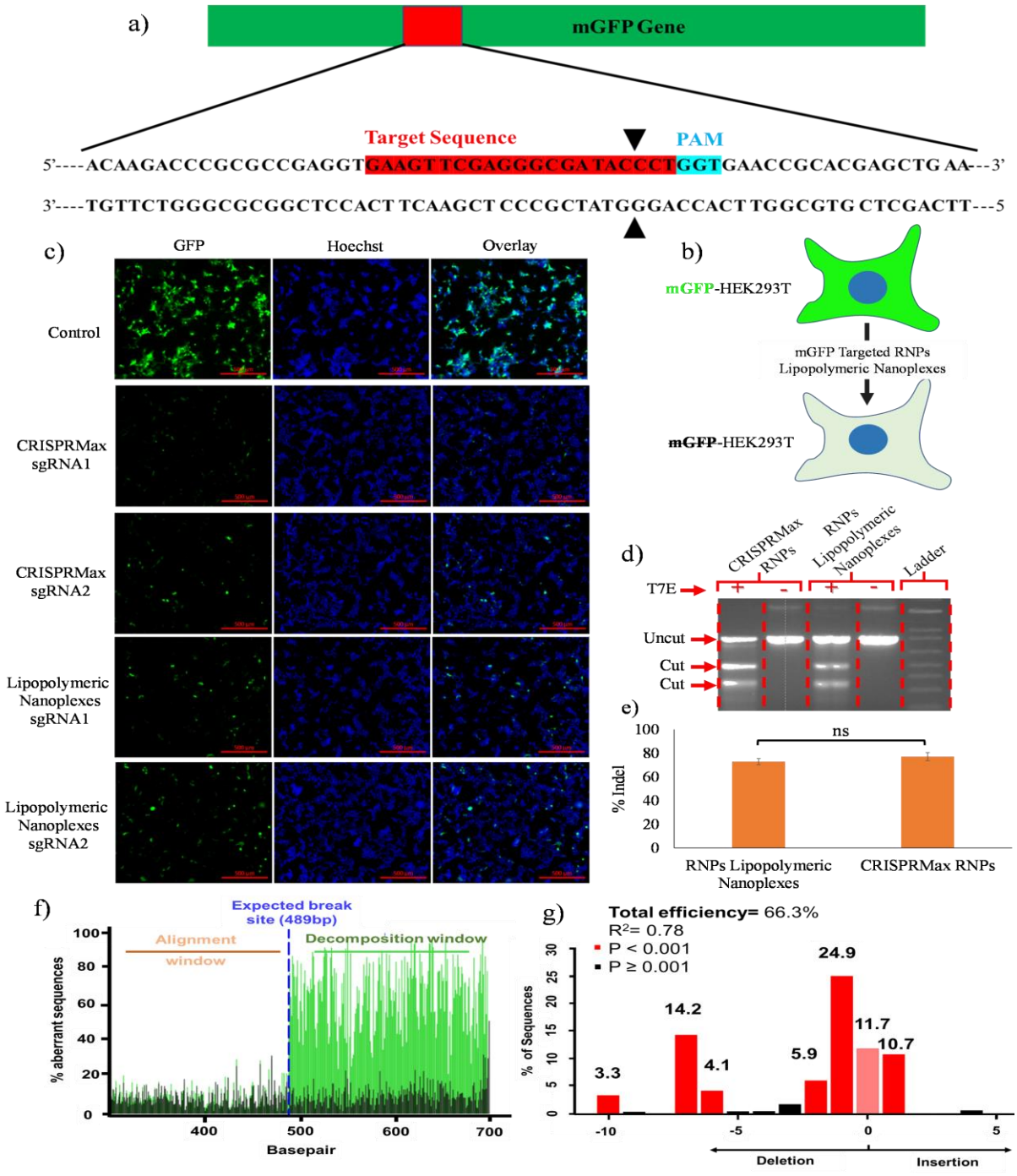

Figure 4.8. RNPs lipopolymeric nanoplexes mediated mGFP gene editing in mGFP-HEK293T cells. a) guide RNA sequence targeting mGFP gene, b) graphical illustration of the effect of mGFP gene editing on fluorescence of mGFP-HEK293T cells, and c) fluorescence microscopy-based evaluation of depletion of MGFP gene at protein level in terms of reduction in the fluorescence intensity, d & e) T7 Endonuclease assay data (Data are presented as Mean ± SD. ns, p≥0.05), and TIDE analysis data f) Aberrant nucleotide signal of the sample (green) compared to that of the control (black) and g) Indel spectrum determined by TIDE.

respect to that of the control sample (black), and Figure 4.8f&g showed the Indel spectrum and their frequencies determined by TIDE. Overall, the TIDE Software data showed 66.3% of Indel cells treated with RNPs lipopolymeric nanoplexes.

4.5. *In vivo* transfection

To evaluate the *in vivo* stability of the developed eGFP-dCas9 RNPs lipopolymeric nanoplexes, *in vivo* transfection was performed in mice after intra-muscular injection. As shown in Figure 4.9, the naked eGFP-dCas9 RNPs get vanished or get degraded from the muscle tissue.

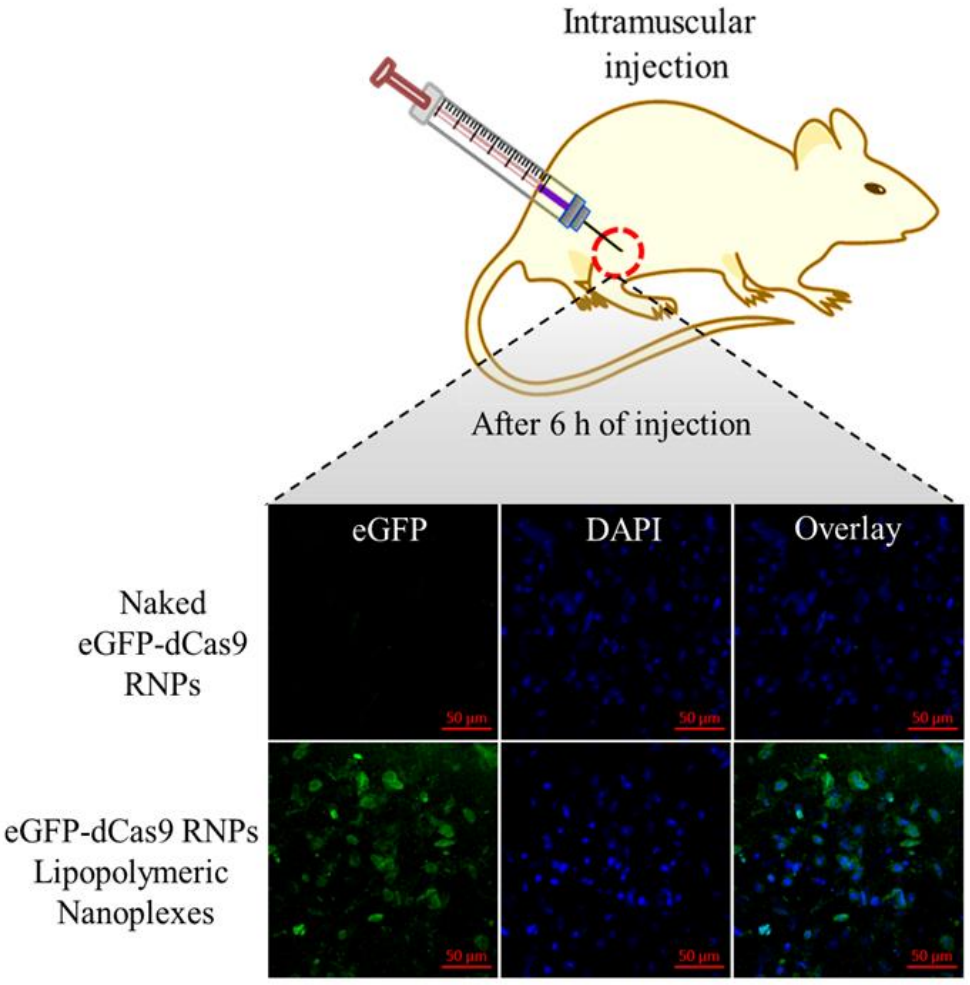

Figure 4.9. *In vivo* transfection of dCas9 RNPs lipopolymeric nanoplexes after intra-muscular injection in mice.

On the other hand, the eGFP-dCas9 RNPs lipopolymeric nanoplexes get transfected inside the muscle cells (Green color) after 6 h or the injection. These findings revealed the capability of developed lipopolymeric nanoplexes to work *in vivo* efficiently.

4.6. Discussion

By providing ample therapeutic potential *via* manipulating genetic material in prokaryotes and eukaryotes, the CRISPR/cas9 system (especially RNPs) is now a center of avidity. Delivery technologies for the CRISPR/Cas9 gene-editing system often require viral vectors that pose safety concerns for therapeutic genome editing. Ample interest has been generated in utilizing the *non-viral* vectors with established safety profiles to deliver the CRISPR/Cas9 tools. Several approaches have been taken for the intracellular delivery of the CRISPR/Cas9 system, such as plasmid (having Cas9 and sgRNA construct), Cas9-encoded mRNA, or direct Cas9 RNPs delivery. Cas9 RNPs offer advantages due to their low insertion mutagenesis, short persistence of Cas9 protein, low immunogenicity, and lesser off-target effect, thus making them attractive for gene editing applications *in vitro* and *in vivo* [28]. Besides, it has several limitations on delivery aspects because of its large molecular weight (~ 160 kD) and supra-electrostatic charge. Attempts have been made to design nanocarriers consisting of cationic polymers and lipids to deliver Cas9 RNPs intracellularly [1]. Recently, cationic polymers became a feasible approach to deliver Cas9 RNPs *via* electrostatic interaction since this approach was previously explored by delivering nucleotides. PEI polymers have also been used alone or in combination with liposomes for Cas9 protein delivery *in vivo* to help induce endosomal escape [29]. Sun et al. reported a polymeric core-shell nanoparticle with a PEI coating on a DNA nanoclew loaded with a Cas9-sgRNA complex [30]. Furthermore, Chen et al. synthesized glutathione cleavable polymeric nanocapsule using in situ polymerization. These nanocapsules

were found to have a 25 nm particle size with *in vitro* and *in vivo* gene editing efficiency without apparent toxicity [9]. Previously we have shown that the blank lipopolymeric nanoplexes prepared using cationic amphiphilic copolymer effectively complexed the negatively charged FAM-siRNA-34a and delivered it efficiently in MCF-7 and 4T1 cells with a transfection efficiency of 50.82% and 99.82%, respectively [15]. The outcomes of the work consolidated the role of cationic amphiphilic copolymers for the delivery of negatively charged nucleic acids. Despite cationic Cas9 protein, guide RNA is another major component of RNPs, which possess a net negative charge and could provide opportunities to deliver these RNPs using cationic polymer by electrostatic complexation.

An emulsion solvent evaporation method was used to prepare the blank lipopolymeric nanoplexes with a positive surface charge that could complex negatively charged sgRNA/Cas9 RNPs. The copolymer mPEG-b-(CB-{g-cation chain; g-Chol; g- Morph}) **(8)** was successfully synthesized as indicated by the ^{1}H NMR spectroscopy that showed the appearance of amidic, cholesterol and morpholine protons peaks (as discussed in Chapter 2). The lipopolymer has a polycarbonate backbone, which possesses biodegradability and biocompatibility, and several pendant groups that impart multifunctionality to the polymer. The cationic chain provides positive charge, which facilitates its complexation with negatively charged RNPs. Additionally, the morpholine group is known for its endosomal escape properties as reported earlier [15]. The blank lipopolymeric nanoplexes prepared using an emulsion-based method showed a zeta potential and particle size of +16.2±2.42 mV and 73.75±6.2 nm, respectively, which on complexation with the negatively charged RNPs showed an increase in nanoplexes size and a decrease in zeta potential [15, 20]. Similar observations have been reported previously as well, wherein, increase in particle size and a decrease in zeta potential was considered as the primary

indication of charge-based nano complex formation [9]. Further, gel retardation assay showed that 10 X of polymer (in mol) is sufficient to complex the RNPs (1X). The complexation of RNPs should be reversible and the same was confirmed by the heparin competition assay. Although there were no reports of Cas9 RNPs release from the cationic polymer or lipids using heparin, however, being a competitor anion, it is well reported to release the RNA/DNA/Plasmid complexes from cationic polymers or lipids [31]. In the present study, the heparin competition assay suggested that at a lower concentration of heparin, i.e., 0.005 to 0.075 IU, RNPs were observed to remain complex with the lipopolymeric nanoplexes, but as the concentration of heparin reaches 0.5 IU, RNPs were released from nanoplexes (Figure 4.3a). Such findings collectively consolidate the fact of the stability of RNPs lipopolymeric nanoplexes employing strong electrostatic interactions. Since RNPs being sensitive may lose their endonuclease activity on complexation [32], thus we confirmed the endonuclease activity of released RNPs [20] that showed endonuclease activity similar to that of the freshly prepared RNPs thereby indicating the potential of the developed lipopolymeric nanoplexes to deliver these RNPs in the intact form.

Cytotoxicity is one of the major concerns in using cationic carriers for gene delivery applications. We have previously reported the non-cytotoxic nature of the blank lipopolymeric nanoplexes in cancer cell lines. To further test the RNPs lipopolymeric nanoplexes, MTT assay was performed in HEK293 T cells wherein the developed RNPs lipopolymeric nanoplexes showed minimal toxicity up to a dose of 20X of the working concentration, and the probable reason for the reduced cytotoxicity could be the reduction in the net charge on the nanoplexes after complexation with the RNPs. The blank nanoplexes are cationic and possess a net positive charge of 16.2 ± 2.42 mV, while, upon complexation of RNPs with nanoplexes, the net charge gets reduced to 6.17 ±1.04 mV. On the other hand, at a higher dose, it was found toxic, and the

possible reason could be the excessive cationic charge of the polymers. Previously, it has been reported that the cationic polymers or lipids possess charge-dependent toxicities [33-35]. Further, the lipopolymeric nanoplexes were non-toxic towards erythrocytes as indicated by the hemocompatibility assays (Figure 4.4b-g). The Nanocarrier system could provide such transfection abilities owing due to their surface properties like potential, targeted ligand, which modulating their internalization through endocytic transporters on lipidic cellular membrane.[36] Huang et al. reported that the nanoformulation having high zeta potential possesses more transfection efficiency as compared to formulations having zeta potential near to neutral [37]. In the previous report, a cationic polymer with a zeta potential ∼ +39 mV successfully delivered miRNA-34a in MCF-7 and 4T1 cells with a transfection efficiency of approx. 99.82 % and 50.82 %, respectively. Similarly, in our current study, RNPs lipopolymeric nanoplexes were efficiently uptaken in HEK293T cells (Figure 4.5), which could be attributed to the nano-size, cationic surface charge, and presence of cholesterol group in the lipopolymer. We also examined the endocytic uptake pathway for RNPs lipopolymeric nanoplexes by fluorescence microscopy-based analysis in the presence of endocytic inhibitors (Figure 4.7). The receptor-mediated clathrin endocytosis is the most common cellular uptake pathway for plasma lipids and nutrients by covering almost 2% of the cellular surface. Since the uptake of nanoplexes was inhibited in the presence of a clathrin inhibitor (Chlorpromazine), indicating the uptake through clathrin vesicles could be attributed to the cholesterol group grafted in the hydrophobic chain of the polymer [38]. Also, the presence of methyl β-cyclodextrin inhibited the clathrin-mediated endocytosis by extracting cholesterol from the plasma membrane, negatively effects the uptake of RNPs lipopolymeric nanoplexes consolidating the mechanistic role of cholesterol in such findings [38]. Since, CRISPR/Cas9 system work by its targeted endonuclease activity on the

cellular genome, it needs to be delivered effectively and functionally inside the nucleus of the cell, bypassing many of the intracellular barrier *viz.*, cell membrane, endosomal-lysosomal acidic vesicle and nuclear membrane. Therefore, cytosolic transfection of RNPs alone cannot prove the downstream efficiency of RNPs nanoplexes. To understand the gene-editing functionality of RNPs after being delivered to the cytoplasm, we have performed a CASFISH assay, wherein a sgRNA (telo-sgRNA) targeting telomere TTAGGG repeats region (shown in Figure 4.6b) has been complexed with eGFP-dCas9 to form RNPs and delivered using polymeric nanoplexes. Since there are several repeats of TTAGGG in the internal loci on the long and short arms of chromosomes, many RNPs binding sites are available in the nucleus. Confocal microscopy images revealed the efficient binding of RNPs in the nucleus indicated by green punctuate fluorescence observed after 48 h of incubation with the RNPs lipopolymeric nanoplexes (Figure 4.6a, red arrow). While the green fluorescence at/before 12 h was observed in the cytoplasm that could be attributed to the time required for the endo-lysosomal escape of the RNPs lipopolymeric nanoplexes and the decomplexation of RNPs from nanoplexes. Since the CASFISH experiment is being explored previously to find out a specific gene location by Deng et al., 2015 [21]. These findings could prove the hypothesis that the polymeric nanoplexes functionally delivered the RNPs *in vitro* into the cellular environment. Further, these lipopolymeric nanoplexes could be used for gene editing applications by targeting various diseases. Previously, the loss of GFP expression after knockout of the GFP gene using CRISPR in GFP expressing cell line was used as *in vitro* model for visual evaluation and qualitative gene editing [3]. Utilizing this, we further evaluated the *in vitro* gene editing of the RNPs lipopolymeric nanoplexes by transfecting the mGFP-HEK293T cells with the RNPs targeting the mGFP gene using lipopolymeric nanoplexes. Loss of mGFP expression after 72 h of incubation indicated that the RNPs had successfully

edited the gene. Additionally, the T7 endonuclease assay showed a good gene editing efficiency (~70 % indel), which was further confirmed quantitatively using the TIDE assay [26] , where 66.3% of Indel was observed. This also indicates the functional delivery of RNPs to the cellular environment. After *in vitro* examination, we also evaluated the *in vivo* stability of the developed lipopolymeric nanoplexes via *in vivo* transfection assay. As per our observation, the RNPs lipopolymeric nanoplexes behaved similarly and were able to transfect the muscle cell after 6 h of intramuscular injection. The main advantage of the system is that even at low w/w ratio, the developed lipopolymeric nanoplexes were effective in delivering Cas9 RNPs with minimal cytotoxicity. Additionally, the lipopolymer nanoplexes could be further modified in terms of active targeting and could be used to enhance tissue specific RNP delivery in vivo. Collectively, the nanoplexes gave a good overall *in vitro* and *in vivo* outcomes and could be evaluated further in terms of their *in vivo* gene editing potential in diseases models.

4.7. Conclusions

The synthesized cationic amphiphilic copolymer has free -COOH moiety, which makes it feasible for grafting with pendant functional groups, namely cationic chain, morpholine, and cholesterol. The presence of these pendant groups makes this polymer an efficient delivery vehicle due to the predetermined role of these groups at various stages of the intracellular fate of the cargo. Rapid complex formation with RNPs, good payload capacity, and efficient transfection are the key advantages of this system. Since the complexation occurs on the surface, it could be a disadvantage at the same time. Although CASFISH data showed nuclear localization, nonetheless, further investigation will be required for gene editing efficiency *in vivo*. Although the lipopolymeric nanoplexes formed at an appropriate polymer/RNPs ratio but being a cationic polymer, the toxicity will be the challenge during *in vivo* application. Our initial

hemocompatibility data indicated the non-toxic nature of the complexes; however, a detailed *in vivo* toxicity assessment is warranted. Overall, cationic lipopolymer could be a suitable *non-viral* nanocarrier for CRISPR/Cas9 RNPs for gene editing applications.

References

[1] D.K. Sahel, A. Mittal, D. Chitkara, CRISPR/Cas system for genome editing: progress and prospects as a therapeutic tool, Journal of Pharmacology and Experimental Therapeutics, 370 (2019) 725-735.

[2] A. Lohia, D.K. Sahel, M. Salman, V. Singh, I. Mariappan, A. Mittal, D. Chitkara, Delivery Strategies for CRISPR/Cas Genome editing tool for Retinal Dystrophies: challenges and opportunities, Asian Journal of Pharmaceutical Sciences, (2022).

[3] M. Wang, J.A. Zuris, F. Meng, H. Rees, S. Sun, P. Deng, Y. Han, X. Gao, D. Pouli, Q. Wu, Efficient delivery of genome-editing proteins using bioreducible lipid nanoparticles, Proceedings of the National Academy of Sciences, 113 (2016) 2868-2873.

[4] J.A. Zuris, D.B. Thompson, Y. Shu, J.P. Guilinger, J.L. Bessen, J.H. Hu, M.L. Maeder, J.K. Joung, Z.-Y. Chen, D.R. Liu, Cationic lipid-mediated delivery of proteins enables efficient protein-based genome editing in vitro and in vivo, Nature biotechnology, 33 (2015) 73-80.

[5] S. Zhen, Y. Takahashi, S. Narita, Y.-C. Yang, X. Li, Targeted delivery of CRISPR/Cas9 to prostate cancer by modified gRNA using a flexible aptamer-cationic liposome, Oncotarget, 8 (2017) 9375.

[6] L. Zhang, P. Wang, Q. Feng, N. Wang, Z. Chen, Y. Huang, W. Zheng, X. Jiang, Lipid nanoparticle-mediated efficient delivery of CRISPR/Cas9 for tumor therapy, NPG Asia Materials, 9 (2017) e441-e441.

[7] E.Y. Cho, J.-Y. Ryu, H.A.R. Lee, S.H. Hong, H.S. Park, K.S. Hong, S.-G. Park, H.P. Kim, T.-J. Yoon, Lecithin nano-liposomal particle as a CRISPR/Cas9 complex delivery system for treating type 2 diabetes, Journal of nanobiotechnology, 17 (2019) 1-12.

[8] J.S. Ha, J. Byun, D.-R. Ahn, Overcoming doxorubicin resistance of cancer cells by Cas9-mediated gene disruption, Scientific reports, 6 (2016) 1-7.

[9] G. Chen, A.A. Abdeen, Y. Wang, P.K. Shahi, S. Robertson, R. Xie, M. Suzuki, B.R. Pattnaik, K. Saha, S. Gong, A biodegradable nanocapsule delivers a Cas9 ribonucleoprotein complex for in vivo genome editing, Nature nanotechnology, 14 (2019) 974-980.

[10] D. Lu, Y. An, S. Feng, X. Li, A. Fan, Z. Wang, Y. Zhao, Imidazole-bearing polymeric micelles for enhanced cellular uptake, rapid endosomal escape, and on-demand cargo release, Aaps Pharmscitech, 19 (2018) 2610-2619.

[11] H. Zhang, T.F. Bahamondez-Canas, Y. Zhang, J. Leal, H.D. Smyth, PEGylated chitosan for nonviral aerosol and mucosal delivery of the CRISPR/Cas9 system in vitro, Molecular pharmaceutics, 15 (2018) 4814-4826.

[12] Y. Liu, G. Zhao, C.-F. Xu, Y.-L. Luo, Z.-D. Lu, J. Wang, Systemic delivery of CRISPR/Cas9 with PEG-PLGA nanoparticles for chronic myeloid leukemia targeted therapy, Biomaterials science, 6 (2018) 1592-1603.

[13] L. Farbiak, Q. Cheng, T. Wei, E. Álvarez-Benedicto, L.T. Johnson, S. Lee, D.J. Siegwart, All-In-One Dendrimer-Based Lipid Nanoparticles Enable Precise HDR-Mediated Gene Editing In Vivo, Advanced Materials, 33 (2021) 2006619.

[14] A. Noureddine, A. Maestas-Olguin, E.A. Saada, A.E. LaBauve, J.O. Agola, K.E. Baty, T. Howard, J.K. Sabo, C.R.S. Espinoza, J.A. Doudna, Engineering of monosized lipid-coated mesoporous silica nanoparticles for CRISPR delivery, Acta Biomaterialia, 114 (2020) 358-368.

[15] S. Sharma, S. Mazumdar, K.S. Italiya, T. Date, R.I. Mahato, A. Mittal, D. Chitkara, Cholesterol and Morpholine grafted cationic Amphiphilic copolymers for miRNA-34a delivery, Molecular pharmaceutics, 15 (2018) 2391-2402.

[16] S. Sharma, S. Pukale, D.K. Sahel, P. Singh, A. Mittal, D. Chitkara, Folate targeted hybrid lipo-polymeric nanoplexes containing docetaxel and miRNA-34a for breast cancer treatment, Materials Science and Engineering: C, 128 (2021) 112305.

[17] S. Acharya, A. Mishra, D. Paul, A.H. Ansari, M. Azhar, M. Kumar, R. Rauthan, N. Sharma, M. Aich, D. Sinha, Francisella novicida Cas9 interrogates genomic DNA with very high specificity and can be used for mammalian genome editing, Proceedings of the National Academy of Sciences, 116 (2019) 20959-20968.

[18] B. Krieg, M. Hirsch, E. Scholz, L. Nuhn, I. Tabujew, H. Bauer, S. Decker, A. Khobta, M. Schmidt, W. Tremel, New techniques to assess in vitro release of siRNA from nanoscale polyplexes, Pharmaceutical Research, 32 (2015) 1957-1974.

[19] T. Dowler, D. Bergeron, A.-L. Tedeschi, L. Paquet, N. Ferrari, M.J. Damha, Improvements in siRNA properties mediated by 2′-deoxy-2′-fluoro-β-D-arabinonucleic acid (FANA), Nucleic acids research, 34 (2006) 1669-1675.

[20] K. Lee, M. Conboy, H. Park, F. Jiang, H. Kim, M. Dewitt, V. Mackley, K. Chang, A. Rao, C. Skinner, Nanoparticle Delivery of Cas9 Ribonucleoprotein and Donor DNA, in, Vivo.

[21] W. Deng, X. Shi, R. Tjian, T. Lionnet, R.H. Singer, CASFISH: CRISPR/Cas9-mediated in situ labeling of genomic loci in fixed cells, Proceedings of the National Academy of Sciences, 112 (2015) 11870-11875.

[22] Y. Li, J. Bolinger, Y. Yu, Z. Glass, N. Shi, L. Yang, M. Wang, Q. Xu, Intracellular delivery and biodistribution study of CRISPR/Cas9 ribonucleoprotein loaded bioreducible lipidoid nanoparticles, Biomaterials science, 7 (2019) 596-606.

[23] S. Sharma, S.S. Pukale, D.K. Sahel, D.S. Agarwal, M. Dalela, S. Mohanty, R. Sakhuja, A. Mittal, D. Chitkara, Folate-targeted cholesterol-grafted lipo-polymeric nanoparticles for chemotherapeutic agent delivery, Aaps Pharmscitech, 21 (2020) 1-21.

[24] Y. Rui, D.R. Wilson, J. Choi, M. Varanasi, K. Sanders, J. Karlsson, M. Lim, J.J. Green, Carboxylated branched poly (β-amino ester) nanoparticles enable robust cytosolic protein delivery and CRISPR-Cas9 gene editing, Science advances, 5 (2019) eaay3255.

[25] F. Ran, P.D. Hsu, J. Wright, V. Agarwala, D.A. Scott, F. Zhang, Genome engineering using the CRISPR-Cas9 system, Nature protocols, 8 (2013) 2281-2308.

[26] E.K. Brinkman, T. Chen, M. Amendola, B. Van Steensel, Easy quantitative assessment of genome editing by sequence trace decomposition, Nucleic acids research, 42 (2014) e168-e168.

[27] M. Bertschinger, G. Backliwal, A. Schertenleib, M. Jordan, D.L. Hacker, F.M. Wurm, Disassembly of polyethylenimine-DNA particles in vitro: implications for polyethylenimine-mediated DNA delivery, Journal of controlled release, 116 (2006) 96-104.

[28] D. Luther, Y. Lee, H. Nagaraj, F. Scaletti, V. Rotello, Delivery approaches for CRISPR/Cas9 therapeutics in vivo: advances and challenges, Expert opinion on drug delivery, 15 (2018) 905-913.

[29] X. Wang, D. Niu, C. Hu, P. Li, Polyethyleneimine-based nanocarriers for gene delivery, Current pharmaceutical design, 21 (2015) 6140-6156.

[30] R. Mout, M. Ray, G. Yesilbag Tonga, Y.-W. Lee, T. Tay, K. Sasaki, V.M. Rotello, Direct cytosolic delivery of CRISPR/Cas9-ribonucleoprotein for efficient gene editing, ACS nano, 11 (2017) 2452-2458.

[31] T. Okuda, T. Niidome, H. Aoyagi, Cytosolic soluble proteins induce DNA release from DNA–gene carrier complexes, Journal of controlled release, 98 (2004) 325-332.

[32] J. Qiao, W. Sun, S. Lin, R. Jin, L. Ma, Y. Liu, Cytosolic delivery of CRISPR/Cas9 ribonucleoproteins for genome editing using chitosan-coated red fluorescent protein, Chemical communications, 55 (2019) 4707-4710.

[33] H. Lv, S. Zhang, B. Wang, S. Cui, J. Yan, Toxicity of cationic lipids and cationic polymers in gene delivery, Journal of controlled release, 114 (2006) 100-109.

[34] S. Cui, Y. Wang, Y. Gong, X. Lin, Y. Zhao, D. Zhi, Q. Zhou, S. Zhang, Correlation of the cytotoxic effects of cationic lipids with their headgroups, Toxicology Research, 7 (2018) 473-479.

[35] X. Wei, B. Shao, Z. He, T. Ye, M. Luo, Y. Sang, X. Liang, W. Wang, S. Luo, S. Yang, Cationic nanocarriers induce cell necrosis through impairment of Na+/K+-ATPase and cause subsequent inflammatory response, Cell research, 25 (2015) 237-253.

[36] S. Mazumdar, D. Chitkara, A. Mittal, Exploration and insights into the cellular internalization and intracellular fate of amphiphilic polymeric nanocarriers, Acta Pharmaceutica Sinica B, 11 (2021) 903-924.

[37] X. Huang, W. Liao, G. Zhang, S. Kang, C.Y. Zhang, pH-sensitive micelles self-assembled from polymer brush (PAE-g-cholesterol)-b-PEG-b-(PAE-g-cholesterol) for anticancer drug delivery and controlled release, International journal of nanomedicine, 12 (2017) 2215.

[38] S. Behzadi, V. Serpooshan, W. Tao, M.A. Hamaly, M.Y. Alkawareek, E.C. Dreaden, D. Brown, A.M. Alkilany, O.C. Farokhzad, M. Mahmoudi, Cellular uptake of nanoparticles: journey inside the cell, Chemical Society Reviews, 46 (2017) 4218-4244.

Chapter 5

cRGD-modified hybrid lipopolymeric nanoplexes delivering CRISPR/Cas9 RNPs to the retina

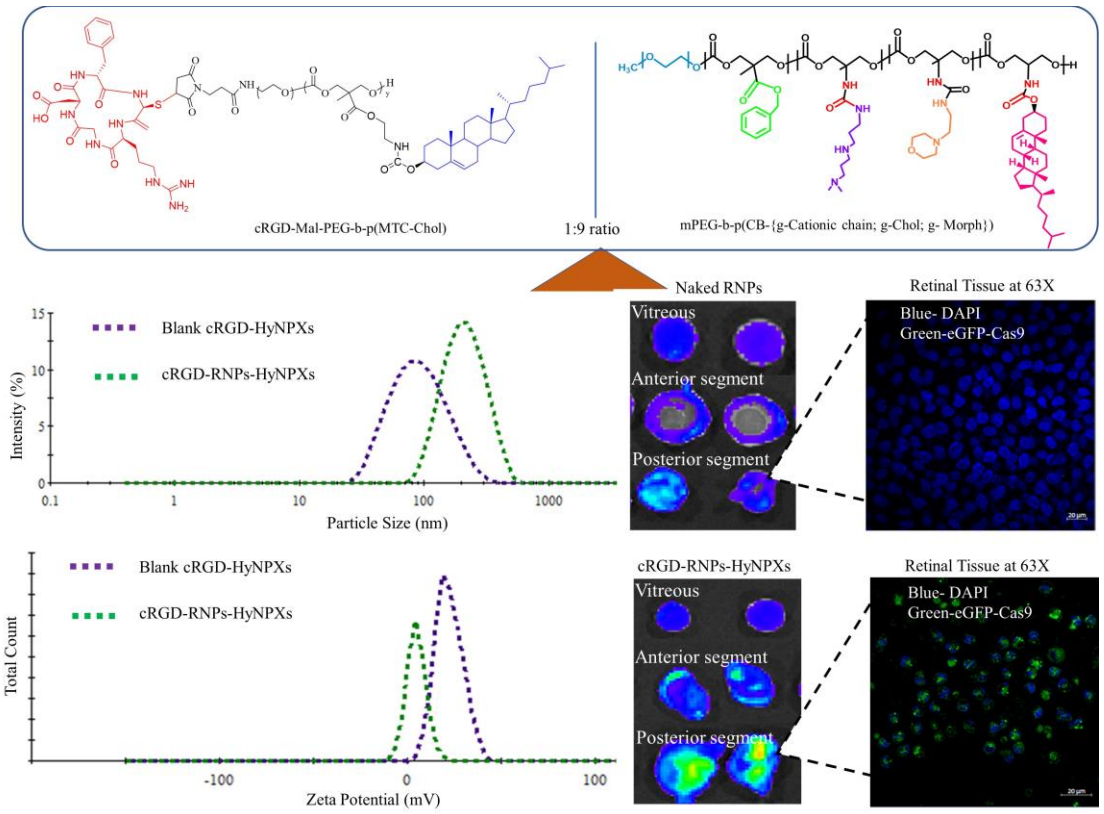

- Synthesis and characterization of cRGD-conjugated lipopolymer
- Development and characterization of RNPs loaded, cRGD-modified hybrid lipopolymeric nanoplexes
- *In vitro* evaluation in cell line model.
- *Ex vivo* vitreous diffusibility analysis
- *In vivo* retino vitreal distribution, VEGFA gene editing and retinal toxicity studies

5.1. Introduction

Retinal dystrophy (RD), such as wet Age-Related Macular Degeneration (wAMD), is a non-genetic disorder and is one of the leading causes of visual impairment, affecting 18.5% of people worldwide [1]. The wAMD is characterized by the growth of new blood vessels in the retina. The central pathophysiology of neovascular AMD is the aberrant blood vessel growth, which is clinically termed choroidal neovascularization (CNV) and requires alteration of the local balance between angiogenesis stimulators and inhibitors, such that the formation of new vessels is favored but in a controlled manner [2]. The anti-VEGF antibodies are the first-line treatment of wAMD. Still, they possess comprehensive limitations such as high cost, resistance, requiring medical professionals for intravitreal injections, increased risk of retinal damage due to frequent intravitreal dosing, etc., thus necessitating a novel treatment strategy [2, 3].

CRISPR/Cas9 is a versatile and precise genome editing tool, providing ample therapeutic opportunity in ailments with genetic and non-genetic causes. Till now, out of three available adaptive delivery forms of CRISPR (plasmid, mRNA, and direct Cas9 protein), protein delivery has lived up to the most effective genome editing due to advantages like lesser off-target effects, lower insertional mutagenesis, short persistent of Cas9 protein and more melancholy immunogenic responses. Recently CRISPR/Cas9 has emerged as a possible genome editing (specifically gene knockout) tool with high specificity and efficacy. Therefore, we hypothesized knocking out the VEGFA gene to downregulate angiogenesis for the treatment of wAMD so that it would be a one-time therapy that could overcome the limitations associated with existing therapies. However, despite precise and effective genome editing, the large molecular weight of Cas9 protein (~165 kD), hydrophilicity, supra-negative charge (~ -20 mV), and its sensitive and fragile nature hinder the delivery of RNPs *in vitro* as well as *in vivo* [4].

Previously, viral vectors were the only choice for delivering CRISPR/Cas9 tools which have a safety concern for therapeutic genome editing. Moreover, the viral vector has limitations related to immunogenicity, limited payload capacity, etc. [5, 6]. However, all three forms of CRISPR have their pros and cons, but CRISPR/Cas ribonucleoprotein (RNP) is the foremost form of CRISPR that provides highly specific, accurate, precise, and fast gene editing in both *in vitro* and *in vivo* [7]. Another major problem with *viral* vectors is their inability to deliver RNPs. However, the CRISPR/Cas9 ribonucleoproteins are very challenging to deliver since they get vanish in the cellular environment due to degradation by nucleases and proteases. Moreover, they showed almost negligible cellular uptake due to high molecular weight and supranegative charge. All these circumstances necessitated the development of a non-viral vehicle for the delivery of CRISPR/Cas9 RNPs.

Interestingly, Chen et al. prepared Cas9 RNP complexed polymeric biodegradable nanocapsule having a 25 nm hydrodynamic size with robust gene editing *in vivo* in murine retinal pigment epithelium (RPE) tissue and skeletal muscle after local administration [8]. Polymeric nanocarriers also offer the freedom of chemical modification in the structure according to the requirement [4]. For example, Lu et al. reported that micelles prepared using a polymer having an imidazole ring that escapes cargo from the endosome [9]. In another study, polyethylene glycol monomethyl ether (mPEG) conjugated chitosan has explored the delivery of the CRISPR/Cas system. PEGylated chitosan of low and medium molecular weight was complexed with the pSpCas9-2A-GFP plasmid, and it was observed that low molecular weight PEGylated chitosan showed optimal transfection at an N/P ratio of 20. In contrast, PEGylated medium molecular weight chitosan showed optimal transfection at N/P ratio 5 [10]. Liu et al. reported poly(ethylene glycol)-b-poly-(lactic acid-co-glycolic acid) (PEG-PLGA)-based cationic lipid-assisted polymeric

nanoparticles (CLANs) for delivering CRISPR/Cas9 plasmid (pCas9) that efficiently disrupted CML-related BCR-ABL fusion gene and increased the survival of a CML mouse model [11]. In the past few years, efforts have been made to develop several cationic lipids or polymer-based non-viral nanocarriers to make the CRISPR/Cas9 components (plasmid, mRNA, RNPs) deliverable. Interestingly, the non-viral nanocarriers showed considerable outcomes regarding payload capacity, transfection efficiency, *in vivo* stability, etc. For instance, in 2020, the Siegwart group developed a lipid nanocarrier comprising a novel cationic ionizable lipid (5A2-SC8), zwitterionic lipid (DOTAP), a PEGylated lipid (DMG-PEG), helper lipid (DOPE), and cholesterol. Further, a low and high % cationic lipid-containing nanocarrier system (5A2-SC8/DOPE/Chol/DMG- PEG/DOTAP = 15/15/30/3/7 (mol/mol)) was prepared by ethanol co-mixing method with particle size ranging from 10-150 nm. To evaluate the *in vivo* efficiency, the Cas9/sgTdTomato loaded LNPs were injected into the Ai9 (TdTomato model) mice *via* intramuscular injection at a dose of 1 mg kg−1 sgTOM. As per the observations, a higher Td-Tom fluorescence was detected in the muscle treated with 5A2-DOT-10 than in mice treated with RNAiMAX. Imaging of tissue sections confirmed gene editing producing brighter red fluorescence in the LNPs treatment group. Next, LNPs were injected into the brains *via* the intraventricular route of Td-Tom mice (0.15 mg kg^{-1} of sgTOM). Again, the bright red signal was observed near the injection site, confirming the editing of mouse brains. These were the observations of the local injection. Furthermore, the functionality of the LNPs was determined after the systemic intravenous injection. Therefore, LNPs with different molar percentages of DOTAP (5–60%) delivered RNPs to TdTomato mice i.v (1.5 mg kg^{-1} of sgTOM). Excitingly, the TdTomato fluorescence was observed exclusively in the liver 7 days following *i.v* injection. Increasing the incorporated DOTAP percentage from 5 to 60% resulted in gradual fluorescence

(CRISPR-guided gene editing) from the liver to the lungs. These results indicate that deep tissue editing can be achieved in a tissue-specific manner by adjusting the inner lipid component chemistry and molar ratios. Tissue-specific editing was further confirmed by confocal imaging of tissue sections and T7E assays, confirming the abovementioned hypothesis [12]. Trailing these outcomes, another study was recently published by the same research group wherein Selective ORgan Targeting (SORT) nanoparticles were prepared and utilized for the organ-specific delivery of CRISPR/Cas9 RNPs. Herein, the addition of the SORT lipid molecule changes the accumulation of RNPs containing LNPs in the extrahepatic organs. Conclusively, 50% DOTAP, 30% 18PA, and 20% DODAP in the final formulation act as the SORT for specificity for lungs, spleen, and liver, respectively, after intravenous injection. These findings conclusively consolidated the impact of formulation and its components in the organ-specific delivery of CRISPR/Cas9 components to the predetermined organ or tissues [13]. Other than lipids, polymers have also been employed for the *in vivo* delivery of CRISPR/Cas9 RNPs. In 2019, Chen et al. developed a customizable, biodegradable nanocapsule (~100 nm diameter) *via in situ* polymerization technique. The Nanocapsules were prepared strategically by employing a cationic monomer (provide positive charge), an anionic monomer (provide negative charge), an imidazole moiety (for endo/lysosomal escape), biodegradable thiol linker (degradation in the cytosolic GSH rich environment), an acrylate PEG (provide stealth effect) and a retinoic acid conjugated PEG (provide active targeting). By this strategy, the Nanocapsules with particle size and zeta potential of 25±6 nm and -4 ± 1 mV, respectively, could effectively deliver the Cas9 RNPs to the target organs. Moreover, the nanocapsules could perform *in vivo* gene editing with an efficiency of ~4% and 2.5%, respectively, in the eye and muscle tissue [8].

The *in vivo* performance of the nanocarriers could be improved using active targeting, and different targeted ligands have been used depending on the nature of the cells or tissue being targeted. The retinal cells express integrin receptors [14]; therefore, cyclic-RGD (a peptide that binds to the integrin receptor) has been reported as a potential targeted ligand.

In the current research, we have utilized a previously reported cationic lipopolymer (mPEG-b-(CB-g-cationic chain; g-Chol; g-Morph)) along with a cRGD-conjugated lipopolymer, i.e., cRGD-PEG-b-p-(MTC-Chol) to prepare a Cas9 RNPs loaded cRGD-conjugated hybrid lipopolymeric nanoplexes (cRGD-RNPs-HyNPXs). The cRGD-RNPs-HyNPXs were characterized for complexation efficiency, particle size, zeta potential, encapsulation efficiency, etc. Later, the cRGD-RNPs-HyNPXs were examined for qualitative and quantitative transfection efficiency in ARPE-19 and NIH3T3 retinal cells. Further, the nuclear localization and VEGF-A gene editing were investigated in cell lines. The cRGD-RNPs-HyNPXs were examined for their vitreous mobility using an *ex-vivo* chick eye model. Lastly, the cRGD-RNPs-HyNPXs were examined for their *in vivo* retino-ocular distribution, VEGFA gene editing, and retinal toxicities in the Wistar rats. Overall, the developed cRGD-RNPs-HyNPXs showed immense potential for delivering the Cas9 RNPs payload to the back of the eye treat wAMD by VEGFA knock out.

5.2. Materials

OptiMEM™ reduced serum media, Fetal Bovine Serum (FBS), Dulbecco's Modified Eagle Medium (DMEM), Snakeskin (3.5 kD), Micro BCA™ Protein Assay Kit, MEGAscript™ T7 Transcription Kit, Hoechst, CRISPRMax and DAPI (4',6-diamidino-2-phenylindole) were obtained from Thermo Fischer Scientific (Massachusetts, USA). T7 endonuclease I was purchased from Biolab (Delhi, India), while the Genomic DNA purification kit was purchased from Promega

(Delhi, India). 3-(4,5-Dimethylthiazol-2-yl)-2,5-diphenyltetrazolium bromide (MTT) was purchased from Merck (Jaipur, India). All the primers were purchased from Imperial Life Science (ILS, Delhi, India). N, N-dimethyldipropylenetriamine (DP), Benzyl bromide, tin(II) 2-ethyl hexanoate, cholesterol, methoxy poly(ethylene glycol) (mPEG, 5000 Da), hydroxybenzotriazole (HoBt), Bis(hydroxymethyl) propionic acid, 1-ethyl-3-(3-dimethyl aminopropyl) carbodiimide hydrochloride (EDC.HCl) and 4-(2-aminoethyl)morpholine, HEPES buffer from porcine intestinal mucosa were purchased from Sigma Aldrich (St. Louis, MO). All other chemicals and solvents are of analytical grade and purchased from local vendors.

5.3. Methodology

5.3.1. Synthesis and characterization of cationic amphiphilic lipopolymer

The synthesis and characterization of mPEG-b-(CB-g-cationic chain; g-Chol; g-Morph) polymer were identical to the protocol reported in Chapter 2, section 2.3.2.

5.3.2. Synthesis and characterization of cRGD-conjugated lipopolymer

The cyclic RGD-conjugated polymer was synthesized using the previously reported method with slight modification (Figure 5.1). Briefly, cholesterol-containing carbonate monomer, i.e., Cholester-3-yl)oxy)carbonyl)amino)ethyl 5-methyl-2-oxo-1,3-dioxane-5-carboxylate (MTC-Chol, **2**) was polymerized with maleimide-polyethylene glycol (Mal-PEG_{5000}, **(1)**) *via* ring-opening polymerization in the presence of $Sn(Oct)_2$ using mono wave (Monowave 400, Anton Parr) at 150° C for 1 h. The crude lipopolymer Mal-PEG-b-p(MTC-Chol) (**3)** was purified using the precipitation process, which involved dissolving it in chloroform and then precipitating it with an excess of cold diethyl ether. Purification was repeated twice, and the lipopolymer was vacuum dried and characterized by 1H NMR spectroscopy. Further, 10 mg of the purified lipopolymer

Mal-PEG-MTC-Chol (**3**) was dissolved in DMSO and added with 1 mg of Cyclic RGD (cRGD) peptide (**4**), followed by the addition of 20 µL of triethylamine and kept for stirring

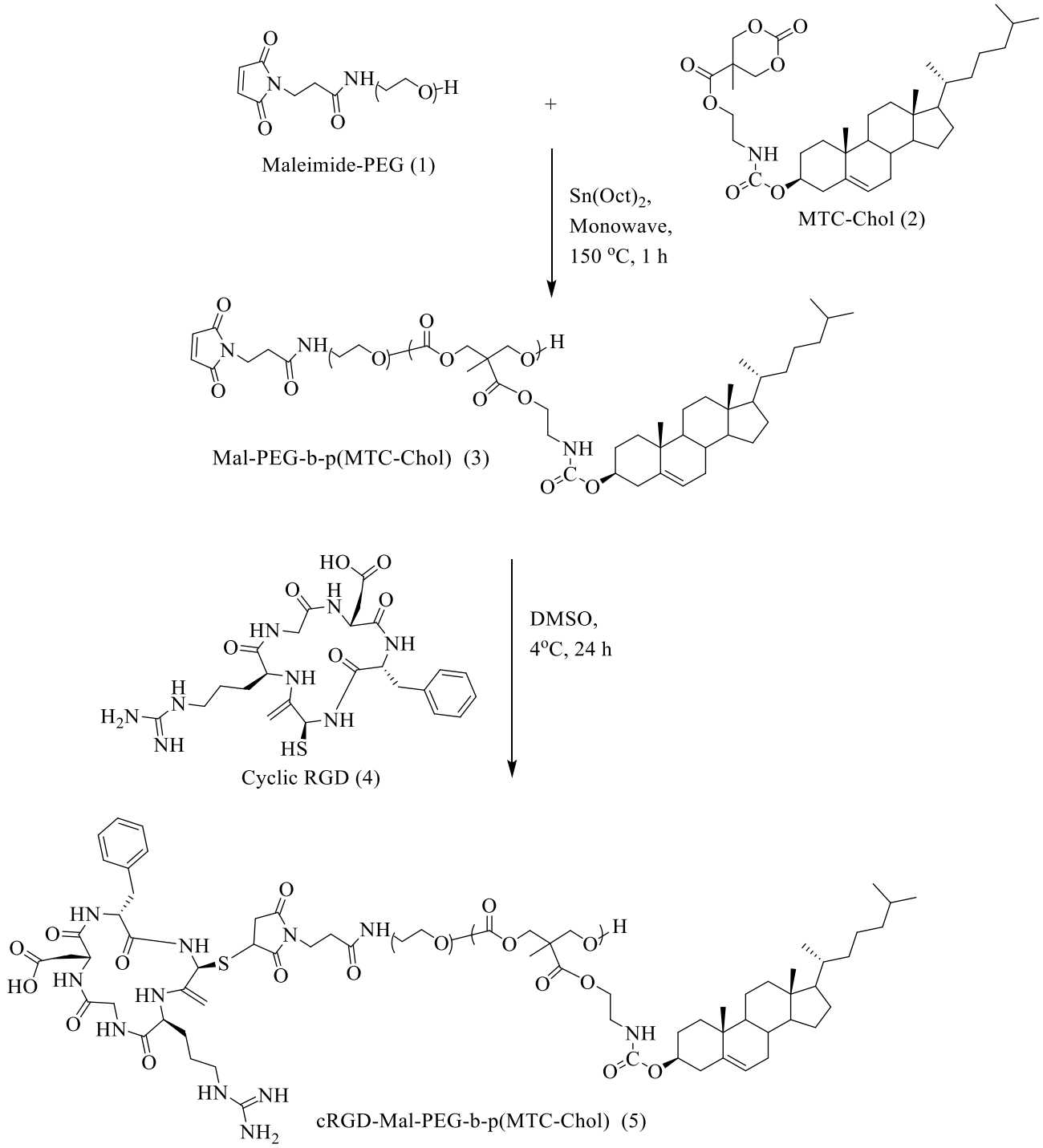

Figure 5.1. Scheme for the synthesis of cRGD-Mal-PEG-b-p(MTC-Chol) (**5**) lipopolymer

at 4º C temperature overnight. The reaction mixture was dialyzed using a dialysis membrane (M.W cut-off 3.5 KDa) against MilliQ water for 24 h and lyophilized to obtain purified cRGD-Mal-PEG-b-p-(MTC-Chol) (**5)** lipopolymer. The final polymer was characterized using ^{1}H NMR spectroscopy.

5.3.3. Preparation and characterization of Cas9 Ribonucleoprotein complex

The Cas9 ribonucleoprotein complexes were prepared and characterized as given in Chapter 4. The freshly prepared RNPs were utilized further for formulation development. The primer sequences used for sgRNA synthesis (targeting the VEGF-A gene) *via* IVT are shown in Table 5.1.

5.3.4. Preparation and optimization of blank cRGD-conjugated hybrid lipopolymeric nanoplexes (cRGD-HyNPXs)

The blank cRGD-HyNPXs were prepared per the previously reported method with slight modifications. The different ratios of cRGD-conjugated lipopolymer and cationic amphiphilic lipopolymer (1:9, 2:8, 3:7, and 5:5) were screened for blank cRGD-HyNPXs preparation. Briefly, a total of 10 mg of different ratios of cRGD-conjugated lipopolymer and cationic amphiphilic lipopolymer (1:9, 2:8, 3:7, and 5:5) were dissolved in 600 µL of dichloromethane (DCM,) followed by the addition of 100 µL of nuclease-free HEPES buffer (10 mM; pH 6.9). The mixture was sonicated at 20% amplitude for 30 seconds to obtain primary emulsion (W/O). The primary emulsion was added dropwise to 3 mL of HEPES buffer (10 mM; pH 6.7), followed by a probe

Table 5.1. Primers sequences

S. No.	Primer	Sequence
1	VEGFA_SgRNA_F.P_Human	5’GAAATTAATACGACTCACTATAGTGTGCCCCTGATGCGATG CGGTTTTAGAGCTAGAAATAGCAAG 3’
2	VEGFA_SgRNA_F.P_Mice/Rat	5’AAATTAATACGACTCACTATAGATTTACACGTCTGCGGATC TGTTTTAGAGCTAGAAATAGCAAG 3'
3	Universal R.P	5’AAAAGCACCGACTCGGTGCCACTTTTTCAAGTTGATAACGG ACTAGCCTTATTTTAACTTGCTATTTCTAGCTCTAAAAC 3’
4	VEGFA_T7E_F.P_Human	5' GTGGCATTACAGAGCTGGGT 3'
5	VEGFA_T7E_R.P_Human	5' CTTCCCAAAGATGCCCACCT 3'
6	VEGFA_T7E_F.P_Mice	5’ GCACTGTCCCTCATGGAAGC 3’
7	VEGFA_T7E_R.P_Mice	5’ GAAGGTAGCAGTCACCACGC 3’
8	VEGFA_T7E_F.P_Rat	5’ CTAGAGCGCTCGGATCTGTG 3’
9	VEGFA_T7E_R.P_Rat	5’ AATCACAGCAGCCTACCCAC 3’

sonication at 20% amplitude for 3.5 min on an ice bath to get secondary emulsion (W/O/W). The organic phase was removed under vacuum (Büchi® Rotavapor®) and centrifuged at 5000 rpm for 5 min to obtain the blank cRGD-HyNPXs in the supernatant. The blank cRGD-HyNPXs were evaluated for zeta potential (mV) and particle size. The selected formulation was used further to prepare cRGD-conjugated RNPs loaded hybrid lipopolymeric nanoplexes (cRGD-RNPs-HyNPXs). Herein, the non-targeted blank lipopolymeric nanoplexes (NT-NPXs) were prepared using cationic lipopolymer, as reported in Chapter 4.

5.3.5. Preparation and evaluation of cRGD-conjugated RNPs loaded hybrid lipopolymeric nanoplexes (cRGD-RNPs-HyNPXs)

Briefly, cRGD-RNPs-HyNPXs were prepared by mixing blank cRGD-HyNPXs with RNPs in the different ratios (w/w, RNPs: blank cRGD-HyNPXs, 1:0, 1:0.5, 1:1, 1:2.5, 1:5, 1:10, and 1:20) and incubated at room temperature for 30 min to allow electrostatic complexation followed by evaluation of zeta potential (Malvern Zeta Sizer, Nano ZS). Additionally, the same ratios of samples were mixed with 6X loading dye and subjected to agarose gel electrophoresis onto 0.8% agarose gel for 35 min at 90 V. The retardation in mobility resulting from electrostatic complexation was evaluated by visualizing the agarose gel under the Gel Doc system (Gel Doc™XR+ Gel Documentation system). From both assays, a best-fitted ratio was selected and further evaluated for particle size and zeta potential (Malvern Zeta Sizer, Nano ZS). The morphological evaluation of the cRGD-RNPs-HyNPXs was done using High Resolution-Transmission Electron Microscopy (HR-TEM; TECNAI 200 Kv TEM, FEI Electron Optics, Eindhoven, Netherlands). The complexation efficiency (%) of RNPs with the blank cRGD-HyNPXs was determined at 2 and 5% theoretical loading (%) of the RNPs using bicinchoninic acid (BCA) assay, as reported earlier. Briefly, RNP and blank cRGD-HyNPXs at 2 and 5% w/w

theoretical loadings were complexed at room temperature for 30 min to form cRGD-RNPs-HyNPXs followed by centrifugation at 18000 rpm for 45 min to pelletize nanoplexes, and the RNPs concentration in the supernatant was determined using the BCA kit as per manufacturers' protocol (Pierce™ BCA Protein Assay Kit, Thermo Scientific™). The stability of the cRGD-RNPs-HyNPXs was determined over time by incubating at room temperature in terms of change in particle size and zeta potential using Zeta Sizer (Malvern Zeta Sizer, Nano ZS).

The non-targeted RNPs lipopolymeric nanoplexes (NT-RNPs-NPXs) were prepared using NT-NPXs, as reported in Chapter 4.

5.3.6. *In vitro* assays

ARPE-19 cells were provided by Dr. Vivek Singh, Senior Scientist, L.V Prasad Eye Institute (LVPEI), Hyderabad, as a kind gift. The NIH3T3 cells were obtained from Dr. Indumathi Marriappan, Senior Scientist, L.V Prasad Eye Institute (LVPEI), Hyderabad. The cells were maintained in Dulbecco's Modified Eagle's Medium (DMEM) supplemented with 10% fetal bovine serum (FBS) and 1% antibiotics (100X penicillin/streptomycin) and kept at 37°C in a humidified atmosphere containing 5% CO_2.

5.3.6.1. Transfection assay

To evaluate the uptake of the RNPs in ARPE-19 and NIH3T3 cells, the eGFP-dCas9 RNPs were used. Briefly, ARPE-19 or NIH3T3 cells were seeded in 24-well cell culture plates (20,000 cells/well) in DMEM media (with 10 % FBS), followed by incubation at 37°C and 5% CO_2 overnight to allow the cells to adhere. The next day, cells were washed with PBS, and the media was replaced with OptiMEM media containing naked RNPs (200 nM eGFP-dCas9), NT-RNPs-NPXs (containing 200 nM eGFP-dCas9), and cRGD-RNPs-HyNPXs (containing 200 nM eGFP-

dCas9). In this study, CRISPRMax was used as a standard transfecting agent. After predetermined time points (i.e., 1, 3, 6 and 9 h), cells were washed with PBS and counterstained with Hoechst dye (100 µg/mL, for nucleus staining), followed by observation under a fluorescence microscope (Vert A1, Zeiss). For quantitative measurement of transfection efficiency, the cells were analyzed using Flow cytometry (Beckman Coulter, USA), and the data was processed using CytExpert software (version 2.3).

5.3.6.2. CASFISH assay

The essential requirement for the nanocarrier delivering CRISPR/Cas9 RNPs is related to its efficiency in delivering RNPs to the cytosol in its native form. Therefore, to evaluate such efficiency of developed lipopolymeric nanoplexes, a CASFISH experiment was performed. Briefly, RNPs (composed of sgRNA targeting telomere region and an eGFP-dCas9) were complexed with blank cRGD-HyNPXs to form cRGD-RNPs-HyNPXs, and transfection was done in ARPE-19 and NIH3T3 cells in the two-well plate (ibidi, Germany) followed by incubation for 48h. Further, the cells were washed thrice with PBS and counterstained with Hoechst for nucleus staining and analyzed using CLSM (Carl Zeiss, Germany). The sequence of sgRNA designed for the telomere region is similar to the CASFISH assay in Chapter 4 (Table 4.1).

5.3.6.3. T7E Assay

ARPE-19 and NIH3T3 cells were transfected with sgVEGFA-Cas9 RNPs containing cRGD-RNPs-HyNPXs at 200 nM of Cas9 protein. After 6 h, the media was replaced with fresh media, followed by incubation for 48 h at 37 ˚C and 5% CO2. Cells were washed, harvested using Trypsin/EDTA, centrifuged at 1200 rpm for 3 min, and genomic DNA was isolated using Wizard® Genomic DNA purification kit (Promega, India). The purified genomic DNA was amplified for

the target site using PCR (Step 1: 95ºC for 5 min, Step 2: 95º C (30 sec), 58º C (30 sec), 72º C (30 sec), 30 cycles, Step 3: 72ºC for 10 min, Step 4: 4º C for infinity) and 2 µg of purified PCR product was treated with 1 µL (10U) of T7 Endo I and incubated at 37 ˚C for 15 min. The reaction was stopped by adding 2 µL of 0.25 M EDTA. The sample was loaded immediately on a 1.5% agarose gel for Indel (%) analysis. Herein, genomic DNA without T7 endo I was taken as a negative control, and CRISPRMax was taken as a standard transfecting agent. The primers used in this assay for sgRNA synthesis and PCR amplification are shown in Table 5.1. ImageJ software was used to process the gel image, and the following formula was used to determine the Indel efficiency.

$$\% \text{ Indel} = 100 \text{ X } (1 - (1 - \text{fraction cleaved})^{1/2})$$

5.3.7. *Ex Vivo* vitreous mobility of cRGD-RNPs-HyNPXs

Vitreous fluid comprises hyaluronic acid (HA) that acts as a barrier for drug delivery to the posterior segment of the eye. HA provides a net negative charge, and therefore, the cationic cRGD-RNPs-HyNPXs could get retarded within the vitreous fluid through electrostatic interaction. Thus, the charge could be the rate-limiting factor in the vitreous mobility of the hybrid lipopolymeric nanoplexes. To explore the same, we have performed an *ex vivo* vitreous mobility assay in chick eyes as per the previously reported method [15]. Briefly, the chick eyes (n=03) were procured from the local slaughter-house and kept on the ice until use. To prepare the eyes, they were cleaned from muscles, nerves, and all other undesired tissues. Freshly prepared eyes were briefly dipped into 70% ethanol and then stored in PBS at 4 °C overnight. The eyes were sectioned circumferentially below the limbus to remove the anterior section, including the iris and lens, and a 100 µL of 0.25 mg/ml of cRGD-RNPs-HyNPXs with a net charge of +10.8 ± 4.3 mV and 1.5 ± 0.9 mV were injected into the vitreous fluid using Insulin syringe. Immediately, the cut surface was covered

with a microwell dish to avoid air bubbles between the vitreous and the glass window. The eye cup was then inverted to place the window surface facing down for imaging under a confocal microscope (Carl Zeiss, Germany). For observation, the video was recorded for 50 ms temporal resolution, and particles were tracked using a single particle tracking technique to monitor the mobility of the cRGD-RNPs-HyNPXs.

5.3.8. *In Vivo* evaluation of cRGD-RNPs-HyNPXs

All the experiments were performed as per the guidelines of the Committee for the Purpose of Control and Supervision of Experiments on Animals (CPCSEA) after the approval of protocol from the Institutional Animal Ethics Committee (IEAC), BITS-Pilani, Pilani, Rajasthan, India. The protocol approval numbers are IAEC/RES/27/06/Rev-2/32/24 and IAEC/RES/28/12.

5.3.8.1. Retino-ocular distribution

The primary aim of the research was to develop a nanocarrier that could deliver the CRISPR components to the posterior segment of the eye, i.e., the retina, by surpassing the vitreous barrier. Therefore, we have evaluated the efficiency of the eGFP-dCas9 RNPs loaded cRGD-RNPs-HyNPXs for its retino-ocular distribution. Briefly, the rats were randomly divided and anesthetized using ketamine and xylazine with a dose of 90 mg/kg and 8 mg/kg, respectively, *via* intraperitoneal injection. Further, 8 µg of eGFP-dCas9 protein containing cRGD-RNPs-HyNPXs in 5-7 µL were injected intravitreally in the right eye of the rat using Hamilton’s syringe. The left eye of the rat was injected with naked eGFP-dCas9 RNPs with the same dose. The rats were kept under observation for different time points, i.e., 6 h, 12 h, 24 h, and 48 h, followed by sacrifice and isolation of eyeballs. The eyeballs were fixed with Davidson's fixative and sectioned circumferentially, followed by observation under *In Vivo* Imaging System (IVIS) for fluorescence

detection qualitatively as well as quantitatively. Later, the posterior section of the eye was stained with DAPI and observed under a confocal microscope *via* stage scanning. Furthermore, the eyeballs were observed at higher magnification for the detection of uptake of eGFP-dCas9 cRGD-RNPs-HyNPXs in the retinal cells.

5.3.8.2. *In vivo* VEGFA knockout efficiency

Briefly, cRGD-RNPs-HyNPXs composed of Cas9 protein (8 µg) and sgRNA (4.5 µg) were mixed in 6 µL of injection volume. cRGD-RNPs-HyNPXs were injected into the vitreous fluid using a Hamilton syringe with a 28G needle. Animals with retinal hemorrhage were excluded from the study. RPEs were isolated using an established protocol with minor modifications. After enucleation, the anterior chamber, lens, and retina were removed, and the posterior eye cup was incubated with 0.05% trypsin-EDTA for 45 min at 37°C. After gently shaking the eye cup to isolate the RPEs, cell pellets were collected for genomic DNA extraction using DNeasy Blood & Tissue kit (Qiagen, 69504). Further, the T7E assay was performed as per the protocol given in section ***5.3.6.3***.

5.3.8.3. Retino-ocular toxicity assessment

Toxicity is one of the major concerns with the cationic polymeric or lipid nanocarrier; therefore, the toxicity of the cRGD-RNPs-HyNPXs was determined in the rat after intravitreal injection. Briefly, the rats were randomly divided and anesthetized using ketamine and xylazine with a dose of 90 mg/kg and 8 mg/kg, respectively, *via* intraperitoneal injection. The rats were randomly divided into four groups and intravitreally injected with 10 µL of cRGD-RNPs-HyNPXs with a dose of 25µg, 50 µg, 100 µg and 250 µg in the respective groups. The animals injected with 10 µL of sterile normal saline were taken as a negative control. After injection, the animals were

kept under observation for 7 days, and any physical toxicity in the eye, such as redness, eye bulging, or pigmentation, were monitored. After 7 days, the animals were sacrificed, and the eyeballs were inoculated, fixed with Davidson's fixative, followed by H&E staining. The H&E stained eye tissues were evaluated for cell damage or infiltration using a microscope (Vert A1, Zeiss) at 4X and 40X resolution.

5.3.9. Statistical analysis

The statistical analysis was carried out using a student *t*-test and analysis of variance (ANOVA) followed by Tukey's test to determine the statistical differences between two or more groups; the *p*-value of < 0.05 was considered statistically significant.

5.4. Results

5.4.1. Synthesis and characterization of cationic amphiphilic lipopolymer

The characterization of mPEG b-(CB-g-cationic chain; g-Chol; g-Morph) polymer was identical to data reported in Chapter 2 (Figure 2.2 and Table 2.1).

5.4.2. Synthesis and characterization of cRGD-conjugated lipopolymer

The intermediate lipopolymer Mal-PEG-b-p(MTC-Chol) **(3)** was synthesized *via* monowave (Monowave 400, Anton Parr) assisted ring-opening polymerization between MTC-Chol, **(2)** with Mal-$PEG_{5000,}$ **(1)** as chain initiator. The structure of Mal-PEG-b-p(MTC-Chol) **(3)** was determined using ^{1}H NMR (400 MHz, CDCl3) spectroscopy. Figure 5.2 showed ^{1}H NMR (400 MHz, CDCl3-d6) spectra of Mal-PEG-b-p(MTC-Chol) with characteristic peaks at δ6.9 (-CH=CH-) of maleimide, δ5.25 to 5.05 (-NH-) of cholesterol, δ4.05- δ4.25 ($-OCH_2-C-CH_2-$)

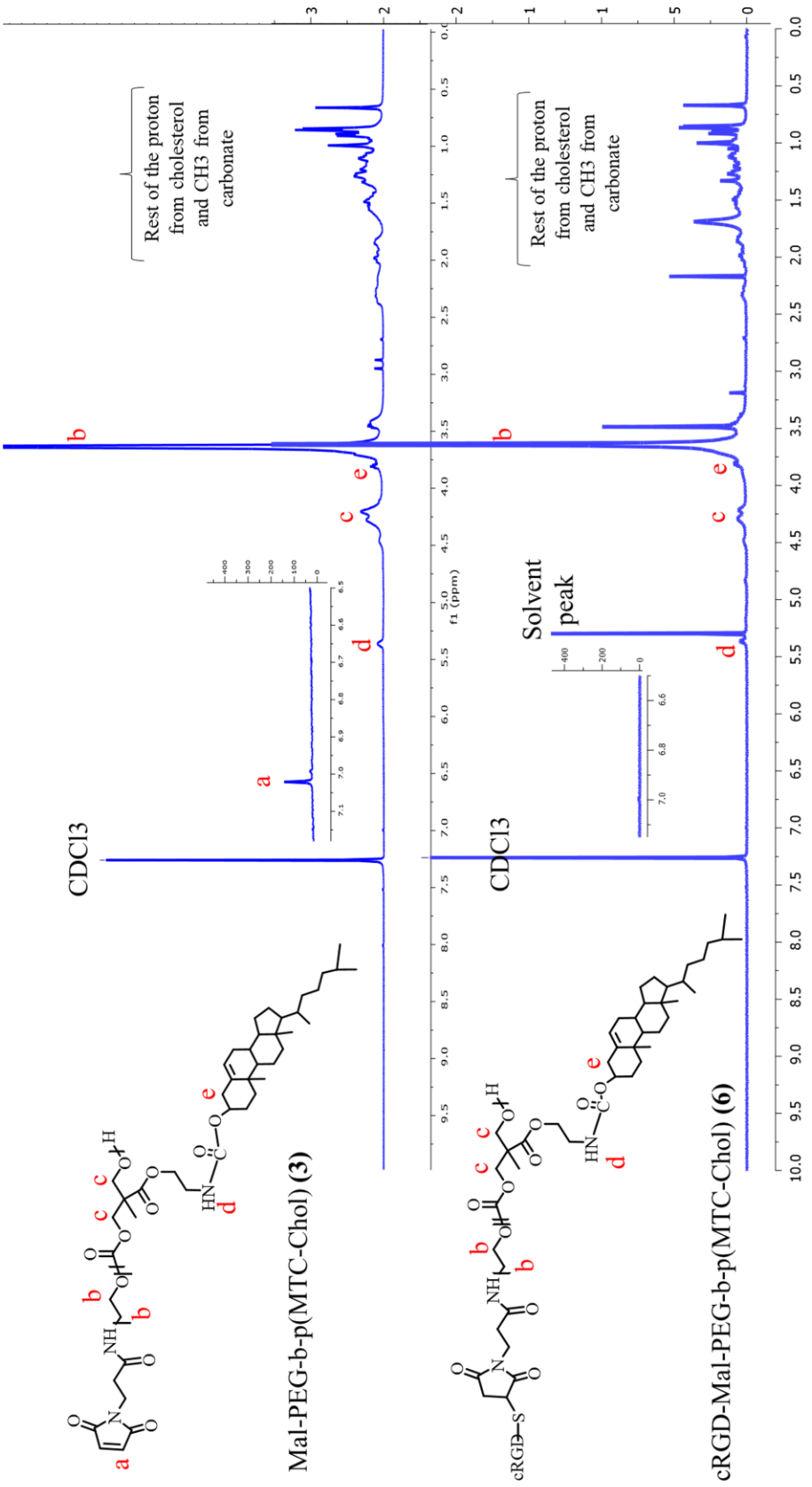

Figure 5.2. ^{1}H NMR spectra of a) Mal-PEG-b-p(MTC-Chol) polymer **(3)** and b) cRGD-Mal-PEG-b-p(MTC-Chol) **(5)** in CDCl3.

of MTC-Chol backbone, δ3.62–3.45 (-CH_2CH_2-O) of PEG, δ2.45–0.55 (protons from cholesterol and CH_3 in the MTC-Chol backbone). As per the peak integration, the number of MTC-Chol units in the Mal-PEG-b-p(MTC-Chol) lipopolymer were six. Figure 5.2 showed ^{1}H NMR (400 MHz, CDCl3) spectra of cRGD-Mal-PEG-b-p(MTC-Chol) with characteristic peaks at δ5.25 to 5.05 (-CH_2-C=CH-CH_2-) of cholesterol, δ4.05- δ4.25 (-OCH_2-C-CH_2-) of MTC-Chol backbone, δ3.62–3.45 (-CH_2CH_2-O) of PEG, δ2.45–0.55 (protons from cholesterol, CH_3 in the MTC-Chol backbone) and disappearance of peak at δ6.9 from maleimide (-CH=CH-) indicate the coupling between maleimide and cRGD peptide.

5.4.3. Preparation and optimization of cRGD targeted blank and RNPs loaded hybrid lipopolymeric nanoplexes

The different ratios of cRGD-conjugated lipopolymer and cationic amphiphilic lipopolymer (1:9, 2:8, 3:7, and 5:5) were used to prepare blank cRGD-HyNPXs and the zeta potential, particle size, and PDI of these formulations is shown in Table 5.2. As per the observations, a ratio 1:9 was selected for blank cRGD-HyNPXs for further experiments. The blank

Table 5.2. Characterization of blank cRGD-HyNPXs at different ratios of cRGD-targeted lipopolymer and cationic amphiphilic lipopolymer

cRGD-targeted lipopolymer (mg)	Cationic amphiphilic lipopolymer (mg)	Zeta potential (mV)	Particle size (nm)	PDI
1	9	18.6±1.2	85	0.353
2	8	14.6±1.6	98	0.421
3	7	12±1.0	119	0.482
5	5	9.6±0.8	154	0.532

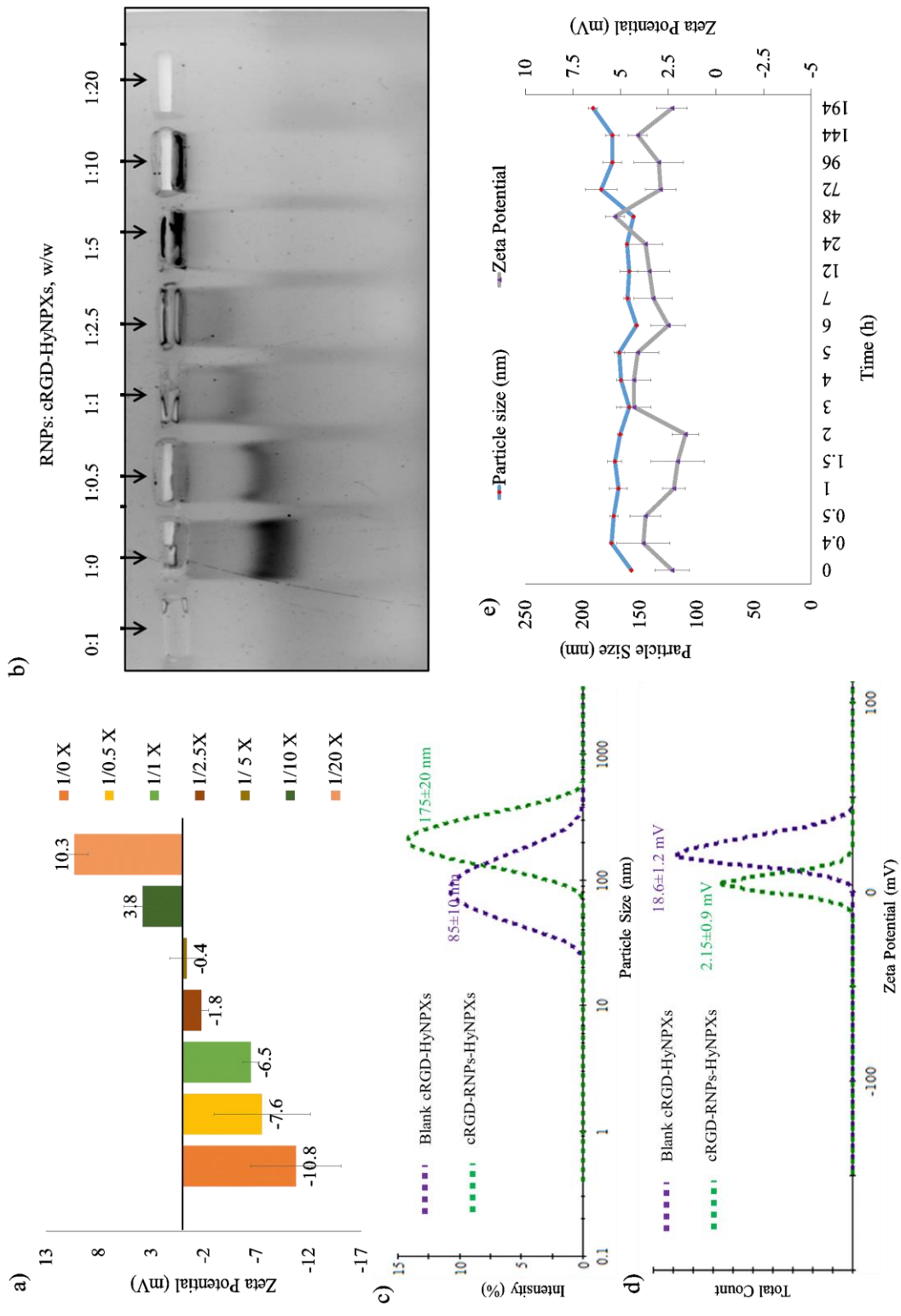

Figure 5.3. Characterization of blank cRGD-HyNPXs and cRGD-RNPs-HyNPXs. a) evaluation of complexation efficiency using zeta potential analysis and b) 0.8% agarose gel mobility shift assay, c) particle size, and d) zeta potential analysis of blank cRGD-HyNPXs and cRGD-RNPs-HyNPXs, and e) stability of cRGD-RNPs-HyNPXs in terms of particle size and zeta potential at RT.

cRGD-HyNPXs were incubated with RNPs in the different ratios (w/w, RNPs: blank cRGD-HyNPXs, 1:0, 1:0.5, 1:1, 1:2.5, 1:5, 1:10, and 1:20) to form cRGD-RNPs-HyNPXs and zeta potential was determined. Figure 5.3a showed the zeta potential of -10.8±4.3, -7.6±4.6, -6.5±0.8, -1.8±0.7, -0.4±1.6, 3.8±1.8, 10.3±1.3 for ccc at different ratio 1:0, 1:0.5, 1:1, 1:2.5, 1:5, 1:10, 1:20, respectively. To consolidate this data, a 0.8% agarose gel electrophoresis was performed for the cRGD-RNPs-HyNPXs at the same ratios. As per the data shown in Figure 5.3b, maximum retardation can be seen at the 1:20 ratio. However, cRGD-RNPs-HyNPXs prepared at a 1:10 ratio showed a particle size and zeta potential of 175±20 nm and 2.15±0.9 mV, respectively, with respect to the cRGD-HyNPXs which showed a particle and zeta potential of (Figure 5.3 c&d) 85±10 nm and 18.6±1.2 mV, respectively. When evaluated using the BCA kit, the encapsulation/complexation efficiency of the cRGD-RNPs-HyNPXs was ~90% at 10% theoretical loading. Furthermore, the cRGD-RNPs-HyNPXs were found to be stable in terms of particle size and zeta potential at room temperature for 194 h (Figure 5.3e).

5.4.4. Transfection assay

The transfection efficiency of the cRGD-RNPs-HyNPXs was evaluated in NIH3T3 and ARPE-19 cells. As per the qualitative fluorescence microscopy data shown in Figure 5.4a, a time-dependent transfection was observed in NIH3T3 cells, and a maximum fluorescence can be seen after 6 h. However, quantitatively, in NIH3T3 cells, the transfection was 71.80% in cRGD-RNPs-HyNPXs treated cells, while the NT-RNPs-NPXs and CRISPRMax RNPs, showed 63.50% and 75.05% transfection, respectively (Figure 5.4b). Similarly, in ARPE-19 cells, the cRGD-RNPs-HyNPXs showed a time-dependent transfection with maximum fluorescence after 6 h (Figure 5.5a). Further, quantitatively, in ARPE-19 cells, the transfection was 72.86% in cRGD-RNPs-

HyNPXs treated cells as compared to the NT-RNPs-NPXs and CRISPRMax RNPs that showed 54.56% and 76.06% transfection, respectively (Figure 5.5b).

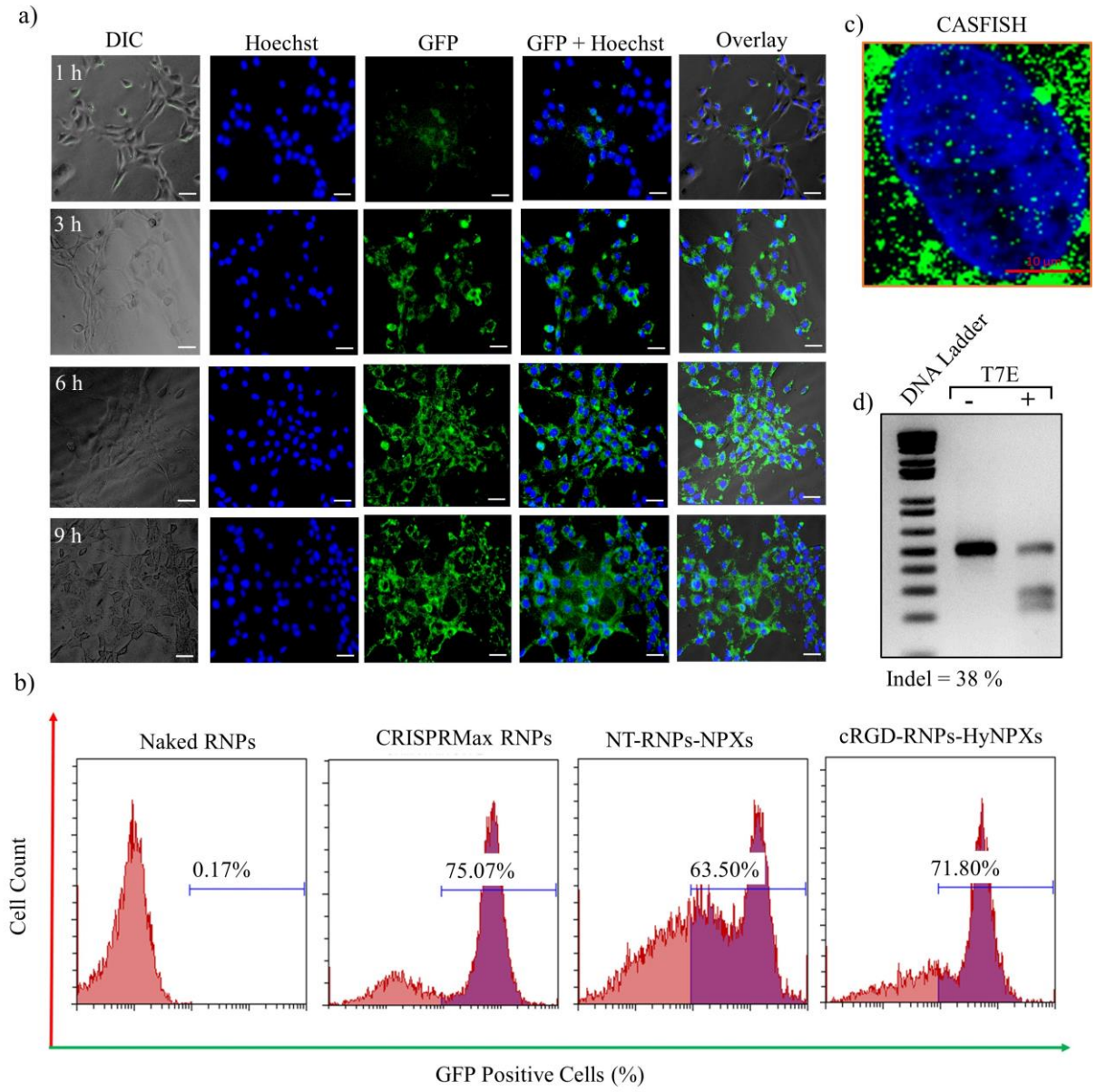

Figure 5.4. *In vitro* evaluation of cRGD-RNPs-HyNPXs in NIH3T3 cells. a) Fluorescence microscopy images after different time points, b) quantitative measurement of transfection (%) using flow cytometry, c) nuclear localization of eGFP-dCas9 RNPs after 48h and d) T7E-based evaluation of Indel (%) of VEGFA gene.

5.4.5. CASFISH assay

As shown in Figure 5.4c, the nuclear localization of eGFP-dCas9 RNPs can be seen after 48 h of incubation time in NIH3T3. Similarly, Figure 5.5c showed the nuclear localization of

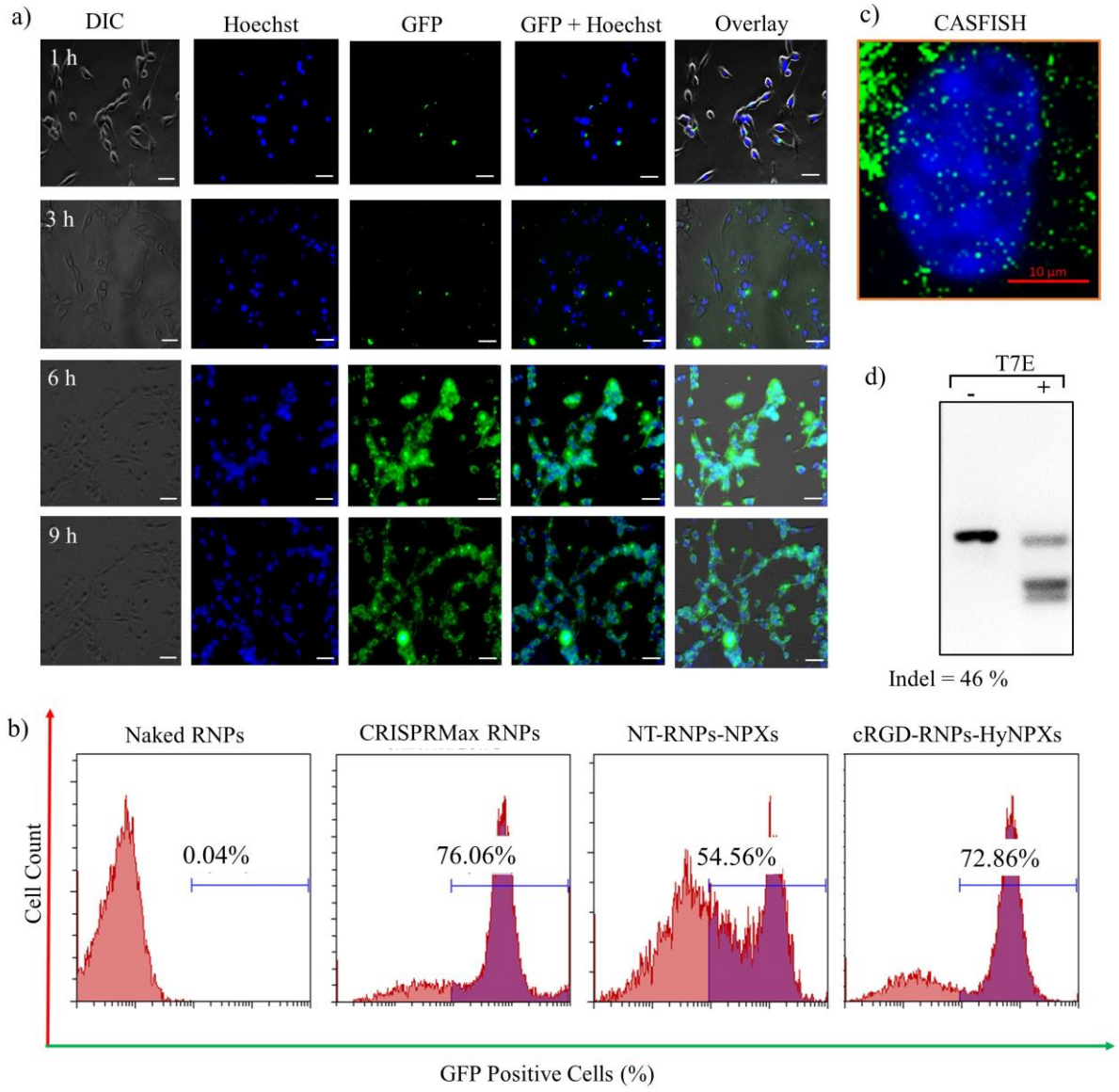

Figure 5.5. *In vitro* evaluation of cRGD-RNPs-HyNPXs in ARPE-19 cells. a) Fluorescence microscopy images after different time points, b) quantitative measurement of transfection (%) using flow cytometry, c) nuclear localization of eGFP-dCas9 RNPs after 48h and d) T7E based evaluation of Indel (%) of VEGFA gene.

eGFP-dCas9 RNPs in the ARPE-19 cells after 48 h. These findings suggest an incubation time of cRGD-RNPs-HyNPXs with cells to obtain gene editing.

5.4.6. Gene editing

As per the T7E assay data shown in Figure 5.4d, approximately 38 % of Indel frequency can be seen in the NIH3T3 cells. Similarly, in ARPE-19 cells, the Indel frequency was ~46 % (Figure 5.5d).

5.4.7. *Ex Vivo* vitreous mobility of cRGD-RNPs-HyNPXs

The mobility of cRGD-RNPs-HyNPXs was determined in the chick eye (Figure 5.6a), which is a crucial parameter for determining vitreous diffusibility of the cRGD-RNPs-HyNPXs

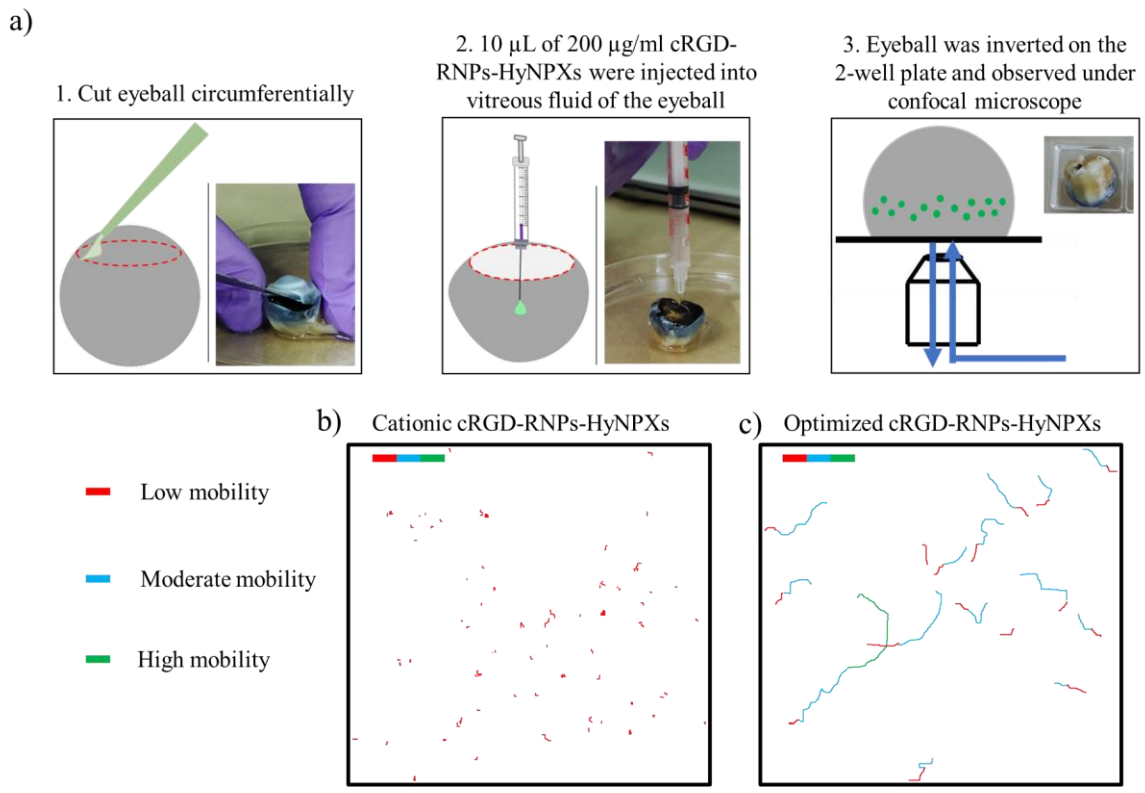

Figure 5.6. *Ex vivo* vitreal mobility of the cRGD-RNPs-HyNPXs in chick eye. a) protocol for the development of an *ex vivo* model in chick eye, b) trajectories of the cationic cRGD-RNPs-HyNPXs (zeta potential; +10.8 ± 4.3 mV), and c) optimized cRGD-RNPs-HyNPXs (zeta potential; 1.5 ± 0.9 mV).

during *in vivo* conditions. As per our observations, the cationic cRGD-RNPs-HyNPXs (Zeta potential, +10.8 ± 4.3 mV) showed lesser mobility in the vitreous fluid and were found to retard within the vitreous (Figure 5.6b). On the other hand, the optimized cRGD-RNPs-HyNPXs (Zeta potential, 1.5 ± 0.9 mV) showed good mobility with longer trajectories (Figure 5.6c).

5.4.8. *In vivo* assessment of cRGD-RNPs-HyNPXs

5.4.8.1. Retino-ocular distribution

The *in vivo* assessment of the cRGD-RNPs-HyNPXs was determined in terms of retino-ocular distribution after intravitreal injection in the rat. Figure 5.7 a&b shows the graphical illustration of intravitreal injection of naked RNPs and cRGD-RNPs-HyNPXs, respectively. Figure 5.7 a1&b1 shows the procedure to open the retinal cup circumferentially. Further, Figure 5.7 a2&b2 shows the IVIS images of the anterior segment, a vitreous and posterior segment of the eye, after the different time points of intravitreal injection in the rat. The naked RNPs clear immediately from the eye and cannot diffuse through the vitreous to reach the back of the eye (Figure 5.7 a2). On the other hand, the cRGD-RNPs-HyNPXs were able to diffuse through the vitreous and were accumulated within the posterior segment of the eye after 48 h (Figure 5.7 b2). Moreover, the stage scanning confocal images of the posterior segment of the eyes of cRGD-RNPs-HyNPXs injected rat showed green fluorescence (from RNPs) co-localized with the blue (DAPI) fluorescence (Figure 5.7 b3). On the other hand, the posterior segment of the eye of naked RNPs injected rats shows non-significant green fluorescence (from RNPs) (Figure 5.7 a3). The penetration of cRGD-RNPs-HyNPXs to the retinal cells was further confirmed using high-resolution confocal microscopy. As per Figure 5.7 a4&a5, the naked RNPs were not observed in the retinal cells. Interestingly, the cRGD-RNPs-HyNPXs were able to transfect the retinal cells (as shown in Figure 5.7 b4&b5). Overall, the cRGD-RNPs-HyNPXs showed good vitreous

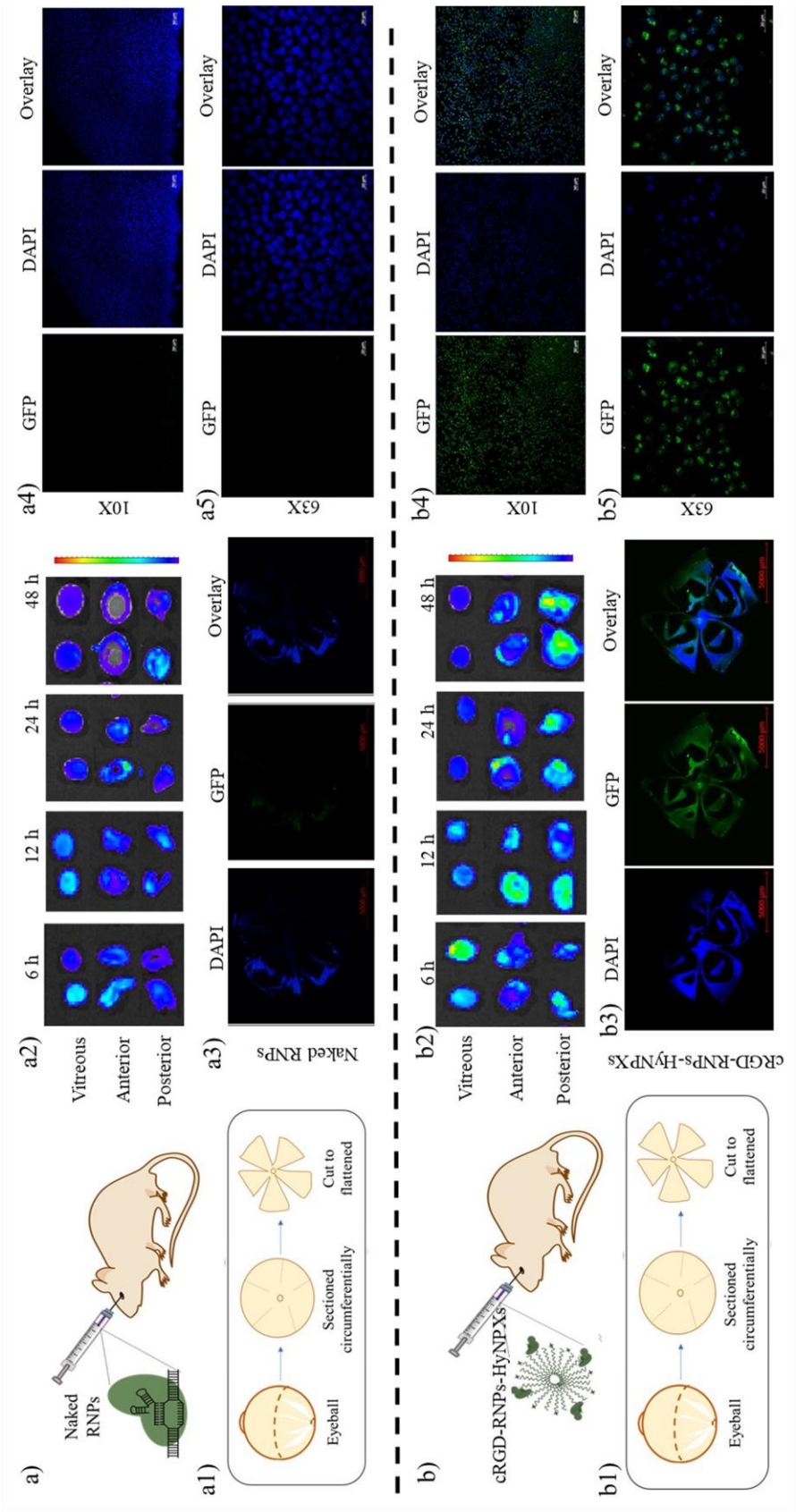

Figure 5.7. Retino-ocular distribution of cRGD-RNPs-HyNPXs after intravitreal injection in the rat. a)&b) Represents the schematic illustration of intravitreal injection of naked RNPs and cRGD-RNPs-HyNPXs, respectively. a1)&b1) Represent the graphical illustration of the isolation of the posterior segment of the eye by introducing a circumferential incision to the eyeball. a2)&b2) Represents are IVIS images of different sections of the eye (vitreous fluid, anterior section, and posterior section) after different time points i.e., 6 h, 12 h, 24 h, and 48 h. a3)&b3) Represent the stage scanning confocal images of the 48h time point posterior section of naked RNPs injected and cRGD-RNPs-HyNPXs injected rat eye, respectively. a4)&b4) Represent the 5X fluorescence images of posterior section of naked RNPs injected and cRGD-RNPs-HyNPXs injected rat eye, respectively. a5)&b5) Represent the 63X confocal images of posterior section of naked RNPs injected and cRGD-RNPs-HyNPXs injected rat eye, respectively. Herein, the green color represents the eGFP-DCas9 RNPs.

diffusibility and were able to transfect the retinal pigment epithelial cell after 48h of the intravitreal injection in rats.

5.4.8.2. *In vivo* gene editing

As per the T7E assay data shown in Figure 5.8, approximately 10 % of Indel frequency can be seen in the cells in the posterior segment of the rat eye. Figure 5.8e showed nucleotide signal of control sample (black) and test sample (green) and Figure 5.8f showed Indel spectrum determined by TIDE.

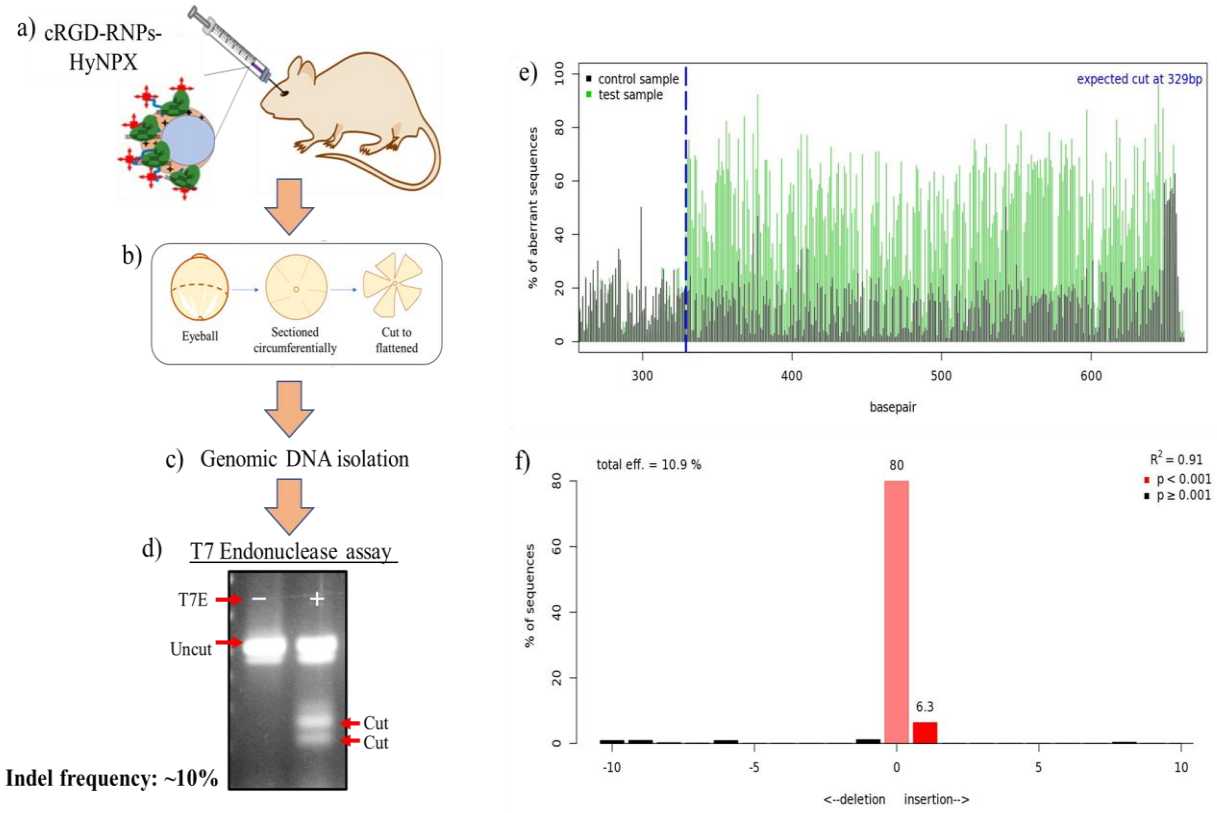

Figure 5.8. *In vivo* VEGFA gene editing in wistar rat a) Intravitreal injection, b) isolation of eyeball, c) genomic DNA isolation, d) gel image showing cleaved PCR amplified DNA after T7E treatment, e) nucleotide signal of control sample (black) and test sample (green) and f) Indel spectrum determined by TIDE.

5.4.8.3. Retino-ocular toxicity assessment

The retinal toxicity of cRGD-RNPs-HyNPXs with a dose of 25µg, 50 µg, 100 µg, and 250 µg was evaluated and compared with the negative control animals injected with 10 µL of sterile normal saline. As per visual observations, no physical toxicity in terms of redness in the eye, tearing, vitreous hemorrhage, restlessness, etc., was observed. Further, the eye tissues were stained with H&E staining, and as per Figure 5.9, no significant toxicity/abnormality was detected as compared to the negative control eyes.

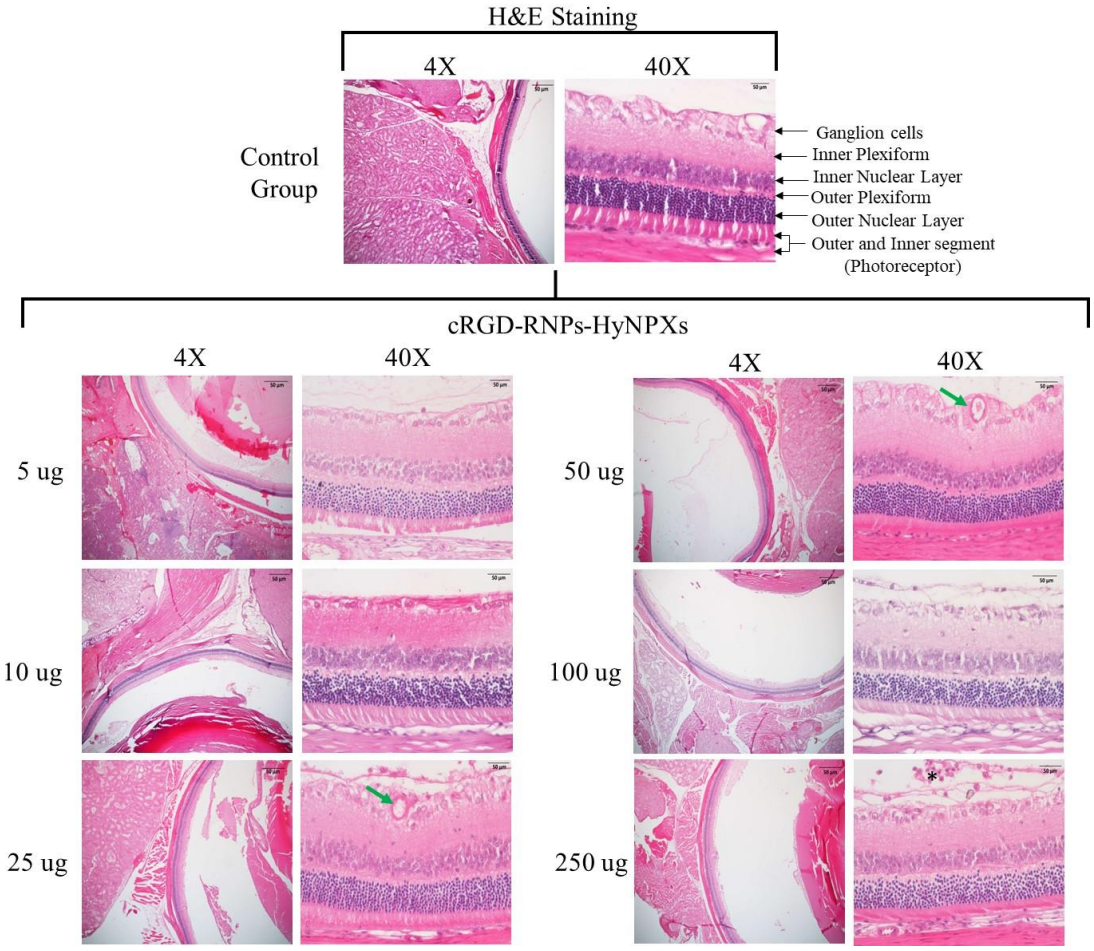

Figure 5.9. Hematoxylin and eosin staining of paraffin-embedded retinal cross sections of cRGD-RNPs-HyNPXs treated Wistar rats at different concentrations after 7 days. Green arrows suggest blood vessels on the surface of the retina, and star marks indicate minimal mononuclear cell infiltration in the eye; however, retinal pigment epithelium (RPE) shows a normal appearance

5.5. Discussion

Although gene therapy has been used with some success in inherited retinal diseases caused by a single gene defect, the concept of using gene therapy in complex, multifactorial diseases such as AMD has not been thoroughly investigated due to the complex interactions of various genetic factors and molecular pathways involved in the pathogenesis of these conditions [16]. However, CRISPR-Cas9 gene editing technology is particularly well-suited to address these situations because it allows for multiplexed targeting of diverse genes by producing a pool of gRNAs with the Cas9 endonuclease in a single dose [7]. In the context of different retinal ailments, other angiogenic, exudative, and inflammatory pathways, for example, can be addressed in addition to VEGF. Importantly, genomic alterations result in the irreversible disruption of the target gene/s. As a result, CRISPR-Cas9 gene editing offers significant benefits as a technique for human gene therapy [17]. Among three deliverable forms of CRISPR/Cas9, viz., plasmid DNA, mRNA, and RNPs, the foremost form, i.e., RNPs, offers immense advantages in terms of site specificity, gene editing efficiency, and time-consuming, etc.; however, the delivery of the RNPs is challenging due to high molecular weight, sensitive towards RNases and proteases, high charge, etc. Additionally, the viral vectors could not deliver the RNPs to conjugated retinal cells [18].

In the current research, we have employed a non-viral lipopolymeric nanocarrier system that could carry the CRISPR/Cas9 RNPs to the posterior segment of the eye. Since the RPE cells express integrin receptors, we conjugated the lipopolymer with cRGD peptide to improve *in vivo* efficiency in terms of transfection. The formulation (cRGD-RNPs-HyNPXs) was optimized at a 1:9 ratio of cRGD-conjugated lipopolymer and non-conjugated cationic lipopolymer, which showed a particle size and zeta potential of 175±20 nm and 2.15±0.9 mV, respectively. The cRGD-HyNPXs were able to complex the RNPs at a 1:20 (w/w) ratio. The *in vitro* transfection assay

showed good efficiency in both NIH3T3 and ARPE-19 cells. Also, the cRGD-RNPs-HyNPXs Showed significantly more transfection as compared to the non-conjugated RNPs-NPXs, and the reason could be the uptake of cRGD-RNPs-HyNPXs *via* receptor-mediated pathway [19]. Additionally, ~ 40% of gene editing was observed after 48h.

The vitreous fluid is one of the major barriers to the intravitreal trafficking of nanomedicines. Hyaluronic acid is the main component of the vitreous fluid, which possesses anionic nature due to the presence of the free COOH group [20]. Since the cRGD-RNPs-HyNPXs possess a cationic charge, it was assumed that the cationic cRGD-RNPs-HyNPXs get trapped within the vitreous humor and would not be able to diffuse and reach the posterior segment of the eye. However, interestingly, the charge of the cRGD-RNPs-HyNPXs was reduced by increasing the % loading of RNPs. To consolidate this hypothesis, the *ex vivo* assay was performed in the chick eye, and as per the particle trajectories, the optimized cRGD-RNPs-HyNPXs (zeta potential; +1.5 ± 0.9 mV) showed good vitreous mobility as compared to the cationic cRGD-RNPs-HyNPXs (zeta potential; +10.8 ± 4.3 mV). Similar kinds of observations were reported by various research groups [21, 22] wherein the author reported that the anionic particles could diffuse through vitreous at a better rate. They concluded that the electrostatic interactions between the polymer network of the vitreous humor and particles are mainly responsible for the observed suppression of particle diffusion; these interactions (and therefore the microscopic mobility of charged particles) should depend on the ion content of the vitreous [23]. Thus, the cRGD-RNPs-HyNPXs, when injected intravitreally, get accumulated within the posterior segment after 48h. Also, cRGD-RNPs-HyNPXs were found to transfect the retinal cells when observed under a high-resolution confocal microscope. This was further confirmed by the VEGFA gene editing i.e. ~10% in the cells in the posterior segment of the eyes. However, further studies are warranted to confirm the gene editing

in the particular cell types of the retinal tissue. The cRGD-RNPs-HyNPXs showed no visible toxicity to the retinal tissue, and the reason could be the biodegradability and biocompatibility of the polycarbonates [24]. However, we have previously reported a detailed toxicity profiling of polycarbonate lipopolymer after intravenous injection at different doses in *swiss* albino mice, and as per our observations, no significant toxicity in terms of narcosis or any visible tissue damage was detected [25]. Similar results were seen in the case of retinal toxicity studies also.

Collectively, the developed cRGD-RNPs-HyNPXs showed immense potential as a non-viral nanocarrier to deliver CRISPR/Cas9 RNPs to the back of the eye for the treatment of wAMD.

5.6. Conclusions

The developed cRGD-RNPs-HyNPXs possess ample advantages, such as rapid complex formation with RNPs, good complexation efficiency for RNPs, stability, efficient transfection, and gene editing. The active targeting with cRGD makes this nanocarrier system more efficient under *in vivo* conditions. The cRGD-RNPs-HyNPXs had good vitreous diffusibility and were able to transfect retinal cells *in vivo* in the rat after 48h of the intravitreal injection. The initial retinal toxicity data indicated the non-toxic nature of the cRGD-RNPs-HyNPXs. Overall, the developed lipopolymeric nanocarrier could be a suitable non-viral nanocarrier for delivering CRISPR/Cas9 RNPs for gene editing in the posterior segment of the eye to treat wAMD.

References

[1] L. Sobrin, J.M.J.P.i.r. Seddon, e. research, nature and nurture-genes and environment-predict onset and progression of macular degeneration, 40 (2014) 1-15.

[2] S.D. Hobbs, K. Pierce, Wet age-related macular degeneration (Wet AMD), StatPearls [Internet], StatPearls Publishing2022.

[3] J.L. Kovach, S.G. Schwartz, H.W. Flynn, I.U.J.J.o.o. Scott, Anti-VEGF treatment strategies for wet AMD, 2012 (2012).

[4] D.K. Sahel, M. Salman, M. Azhar, S.G. Goswami, V. Singh, M. Dalela, S. Mohanty, A. Mittal, S. Ramalingam, D.J.J.o.M.C.B. Chitkara, Cationic lipopolymeric nanoplexes containing the CRISPR/Cas9 ribonucleoprotein for genome surgery, (2022).

[5] I. Ansari, P. Singh, A. Mittal, R.I. Mahato, D. Chitkara, 2,2-Bis(hydroxymethyl) propionic acid based cyclic carbonate monomers and their (co)polymers as advanced materials for biomedical applications, 275 (2021).

[6] S. Sharma, S. Mazumdar, K.S. Italiya, T. Date, R.I. Mahato, A. Mittal, D. Chitkara, Cholesterol and Morpholine Grafted Cationic Amphiphilic Copolymers for miRNA-34a Delivery, 15 (2018).

[7] C.A. Lino, J.C. Harper, J.P. Carney, J.A.J.D.d. Timlin, Delivering CRISPR: a review of the challenges and approaches, 25 (2018) 1234-1257.

[8] G. Chen, A.A. Abdeen, Y. Wang, P.K. Shahi, S. Robertson, R. Xie, M. Suzuki, B.R. Pattnaik, K. Saha, S. Gong, A biodegradable nanocapsule delivers a Cas9 ribonucleoprotein complex for in vivo genome editing, 14 (2019).

[9] D. Lu, Y. An, S. Feng, X. Li, A. Fan, Z. Wang, Y.J.A.P. Zhao, Imidazole-bearing polymeric micelles for enhanced cellular uptake, rapid endosomal escape, and on-demand cargo release, 19 (2018) 2610-2619.

[10] H. Zhang, T.F. Bahamondez-Canas, Y. Zhang, J. Leal, H.D.J.M.p. Smyth, PEGylated chitosan for nonviral aerosol and mucosal delivery of the CRISPR/Cas9 system in vitro, 15 (2018) 4814-4826.

[11] Y. Liu, G. Zhao, C.-F. Xu, Y.-L. Luo, Z.-D. Lu, J.J.B.s. Wang, Systemic delivery of CRISPR/Cas9 with PEG-PLGA nanoparticles for chronic myeloid leukemia targeted therapy, 6 (2018) 1592-1603.

[12] T. Wei, Q. Cheng, Y.L. Min, E.N. Olson, D.J. Siegwart, Systemic nanoparticle delivery of CRISPR-Cas9 ribonucleoproteins for effective tissue specific genome editing, 11 (2020).

[13] Q. Cheng, T. Wei, L. Farbiak, L.T. Johnson, S.A. Dilliard, D.J. Siegwart, Selective organ targeting (SORT) nanoparticles for tissue-specific mRNA delivery and CRISPR–Cas gene editing, 15 (2020).

[14] A.D. Bhatwadekar, V. Kansara, Q. Luo, T.J.E.O.o.I.D. Ciulla, Anti-integrin therapy for retinovascular diseases, 29 (2020) 935-945.

[15] R. Ridolfo, S. Tavakoli, V. Junnuthula, D.S. Williams, A. Urtti, J.C.J.B. van Hest, Exploring the impact of morphology on the properties of biodegradable nanoparticles and their diffusion in complex biological medium, 22 (2020) 126-133.

[16] N.J.J.o.o. Samiy, v. research, Gene therapy for retinal diseases, 9 (2014) 506.

[17] G. Yiu, E. Tieu, A.T. Nguyen, B. Wong, Z.J.I.o. Smit-McBride, v. science, Genomic disruption of VEGF-A expression in human retinal pigment epithelial cells using CRISPR-Cas9 endonuclease, 57 (2016) 5490-5497.

[18] B.H. Yip, Recent advances in CRISPR/Cas9 delivery strategies, 10 (2020).

[19] I. Kemker, R.C. Feiner, K.M. Müller, N.J.C. Sewald, Size-Dependent Cellular Uptake of RGD Peptides, 21 (2020) 496-499.

[20] T. Meng, V. Kulkarni, R. Simmers, V. Brar, Q.J.D.d.t. Xu, Therapeutic implications of nanomedicine for ocular drug delivery, 24 (2019) 1524-1538.

[21] T. Sekiya, T. Iwabuchi, S.J.A.n. Okabe, Occurrence of vestibular and facial nerve injury following cerebellopontine angle operations, 102 (1990) 108-113.

[22] B.T. Käsdorf, F. Arends, O.J.B.j. Lieleg, Diffusion regulation in the vitreous humor, 109 (2015) 2171-2181.

[23] T.F. Martens, D. Vercauteren, K. Forier, H. Deschout, K. Remaut, R. Paesen, M. Ameloot, J.F. Engbersen, J. Demeester, S.C.J.N. De Smedt, Measuring the intravitreal mobility of nanomedicines with single-particle tracking microscopy, 8 (2013) 1955-1968.

[24] I. Seah, C. Ong, Z. Liu, X.J.F.i.M. Su, Polymeric biomaterials in the treatment of posterior segment diseases, (2022) 2425.

[25] S. Sharma, S. Pukale, D.K. Sahel, P. Singh, A. Mittal, D. Chitkara, Folate targeted hybrid lipo-polymeric nanoplexes containing docetaxel and miRNA-34a for breast cancer treatment, 128 (2021) 112305.

Chapter 6

Conclusions and future prospects

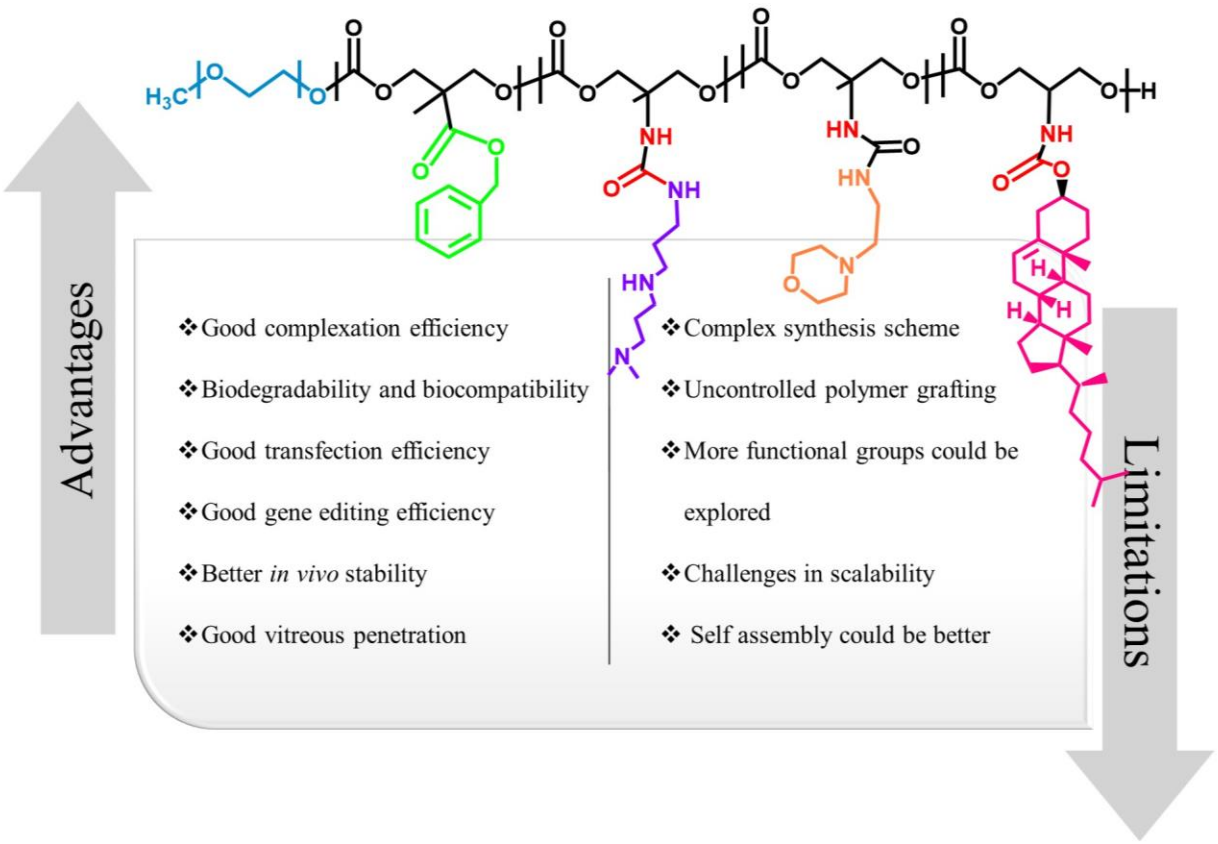

6.1. Conclusions

CRISPR/Cas9 is a gene-editing tool that could provide site-specific, precise gene editing in prokaryotes as well as in eukaryotes. The heart of the technology lies within a Cas9 protein that possesses endonuclease properties directed by a single guide RNA. The technology has evolved very fast and has now been adopted as a mainstream gene editing technique. There are three deliverable forms of the CRISPR/Cas9, including plasmid DNA, mRNA, and a functional Cas9 ribonucleoprotein complex. Despite its potential gene editing efficiency, the delivery of CRISPR/Cas9 components to cells/tissue is challenging due to its unique physicochemical and biopharmaceutical properties, viz., large molecular weight, supranegative charge, degradation in the presence of nucleases, poor cellular uptake, etc. CRISPR/Cas9 delivery was first done using *viral vectors* that possess ample limitations related to immunogenicity, limited payload capacity, mutagenesis, etc. Even the viral vector cannot deliver the foremost form of the CRISPR/Cas9 i.e., ribonucleoprotein. The overall aim of this thesis is the development and evaluation of a *non-viral* nanocarrier system that could deliver the CRISPR/Cas9 components, specifically the foremost form of CRISPR/Cas9, i.e., ribonucleoproteins to the posterior segment of the eye. **Chapter 1** introduces the CRISPR/Cas system and limitations associated with the *viral* vectors, followed by the need, potential, and challenges in *non-viral* nanocarriers for delivering CRISPR/Cas9 components. Gene therapeutics, either alone or when combined with gene editing strategies, can enable the delivery of regular gene copies, *in situ* mutation editing for normal protein and RNA expression, and targeted disruption of dominant mutant alleles or their transcripts for the reversal of retinal disease phenotypes. However, CRISPR/Cas9 has inherent limitations related to the off-target effects. Ample artificial intelligence-based software could help design a CRISPR/Cas9 system with minimal off-target effects. The specificity of the CRISPR/Cas9 could be seen by the

fact that by the end of 2022, more than 50 clinical trials been approved by Food and Drug Administration (FDA), and interestingly, some of these are trials are reported with positive outcomes in the primary phases.

Chapter 2 comprises the rational design of a cationic, amphiphilic lipopolymer (mPEG-b-(CB-{g-cationic chain; g-Chol; g-Morph}). In brief, we have utilized the polycarbonate backbone, since it has been reported for its biocompatibility and biodegradability, with mPEG (5000 Da) to provide a stealth effect to the final polymeric nanoparticles. Nucleic acids possess a negative charge due to phosphate groups; therefore, ionizable lipids or monomers are used to condense them into the nanocarrier. Herein, we have used a cationic chain, i.e., N, N-dimethyldipropylenetriamine. As per reports, the nanocarriers have better cellular uptake through endocytic pathways, but the major hurdle *via.*, these pathways is the endo/lysosomal degradation of the nucleic acid payload. Therefore, a tertiary amine group containing moieties is incorporated into the nanocarrier to escape from lysosomal degradation. We have used a 4-(2-aminoethyl) morpholine pendant group on the polymer backbone, which is reported for its endo/lysosomal escape property *via.*, the proton sponge effect. Further, to improve the stability and cellular uptake, we have also incorporated the cholesterol moiety into the polymer. The final cationic lipopolymer was synthesized using ring-opening polymerization and characterized using ^{1}H NMR spectroscopy that was found to have a molecular weight of 24,553 Da with 18 cationic chains units, 22 cholesterol units and 25 morpholine units. The elemental analysis showed a 7.07 %, 6.72 % and 44.19 % of nitrogen, hydrogen and carbon content, respectively, in mPEG-b-(CB-{g-cation chain; g-Chol; g- Morph}) amphiphilic copolymer. The lipopolymer was used to prepare blank nanoplexes with a particle size of ~93 ± 12 nm with a cationic charge (+15.8 ± 0.7). To evaluate the nucleic acid delivery potential of the developed nanocarrier system, we utilized CRISPR/Cas9

plasmid (pCas9-TURBO-GFP). As per our observations, the plasmid-carrying lipopolymeric nanoplexes were found efficient in terms of complexation efficiency(>95%), transfection efficiency (~70%), gene editing (~22%), and *in vivo* stability. From the research outcomes in Chapter 2, we could conclude that cationic lipopolymer-based ionic complexation could be used for the CRISPR/Cas9 plasmid delivery.

In **Chapter 3,** we transformed and expressed pTCas9 plasmid in E.Coli cells, followed by protein induction and purification using an HPLC system assisted with the HisTrap column. The purified Cas9 proteins were found ~90% pure, and also showed ribonucleoprotein (RNPs) complex formation with guide RNA. The purified Cas9 also exhibited green fluorescence and functional endonuclease property. The final yield of the Cas9 protein from 1 liter of the growth medium was ~ 4 to 5 mg.

In **Chapter 4**, we utilized the lipopolymeric nanoplexes to load the anionic CRISPR/Cas9 RNPs to form RNPs lipopolymeric nanoplexes. The formation of RNPs lipopolymeric nanoplexes was confirmed using particle size, zeta potential, mobility shift assay, etc. As per our observation, the RNPs lipopolymeric nanoplexes were formed at a 10X w/w ratio of the polymeric nanoplexes. The nanoplexes could transfect the HEK293T cells in a time-dependent manner and transfect ~ 75% of the cells. As per the CASFISH experiment, the RNPs were found localized within the cell's nucleus after 48h of incubation time. Further, the gene editing assays, i.e., T7E and TIDE, showed >50% Indel efficiency for the 5BPR-2 gene. Additionally, the *in vivo* stability of the RNPs lipopolymeric nanoplexes was determined using *in vivo* transfection assay in *swiss albino* mice after intramuscular injection. As per our observations, the RNPs lipopolymeric nanoplexes were able to transfect the muscle cell after 6 h of the intramuscular injection.

The eye is a separate sac within the body with the feasibility of local injection, immune compromise nature, and diseases conditions that seek gene editing, therefore could be an ideal target organ for evaluating gene editing approaches. The above-proposed *non-viral* vector-based delivery strategy could be employed for CRISPR/Cas9 RNPs delivery to the posterior segment, *i.e., the* retina of the eye. However, the vitreous fluid could be the primary barrier to the intravitreal delivery of nanocarrier. The hyaluronic acid is the major component of the vitreous fluid which possesses a net negative charge due to the COO^- groups and, therefore, could hamper the movement/diffusion of cationic lipopolymeric nanocarrier towards the posterior segment of the eye. Thus, the cationic charge of the lipopolymeric nanocarrier would have been required to be minimized. Interestingly, the increase in the % payload (anionic RNPs) could decrease the overall charge of the RNPs lipopolymeric nanocarrier. But the positive charge is also reported to improve the nanoparticle's cellular uptake, and a decrease in charge could also compromise the cellular uptake *in vivo*. As per the documented evidence, the retinal layer epithelium (RPE) cells express integrin receptors; therefore, we aimed to actively target the lipopolymeric nanocarrier with cell-penetrating peptide, i.e., cyclic RGD to improve cellular uptake *in vivo*.

In **Chapter 5**, we explored a cRGD-targeted lipopolymeric hybrid nanocarrier containing RNPs to transfect retinal cells *in vitro* and *in vivo*. The RNPs loaded, cRGD-targeted nanoformulation (cRGD-RNPs-HyNPXs) was prepared using 1:9 ratio of cRGD-targeted lipopolymer and cationic amphiphilic lipopolymer by w/o/w double emulsion solvent evaporation method, exhibited a particle size and zeta potential of 175±20 nm and 2.15±0.9 mV, respectively. The cRGD-RNPs-HyNPXs possess ample advantages, such as rapid complex formation with RNPs, good complexation efficiency for RNPs, stability up to 194 h, efficient transfection (~70%), and VEGF-A gene editing (~40%). The active targeting with cRGD makes this nanocarrier system

more efficient under *in vivo* conditions. The cRGD-RNPs-HyNPXs had good vitreous diffusibility and were able to transfect retinal cells *in vivo* in the rat after 48h of the intravitreal injection. The initial retinal toxicity data indicated the non-toxic nature of the cRGD-RNPs-HyNPXs up to a dose of 250 ug/animal. Overall, the developed lipopolymeric nanocarrier could be a suitable non-viral nanocarrier for delivering CRISPR/Cas9 RNPs for gene editing in the posterior segment of the eye to treat wAMD.

The research work conducted in this thesis resulted in the development and characterization of an actively targeted *non-viral* lipopolymeric nanocarrier for *in vitro* and *in vivo* delivery of the CRISPR/Cas9 payload.

6.2. Future prospects

Despite best efforts, no research can yield satisfactory results; there will always be opportunities or scope for improvement. Our study also bears some limitations related to the complex, time-consuming non-uniformity in the chemical reactions for lipopolymer synthesis. However, lipopolymer synthesis was done to the best of our predetermined rationale. Still, a better approach could be adopted to improve the control over the number of units of different pendant groups such as cholesterol, morpholine, and cationic chain. Further, different cationic chains and lipids could be screened for structure-activity relationship (SAR) to get a more versatile delivery nanocarrier.

In the current research work, we proposed to knock out the VEGFA gene using CRISPR/Cas9 RNPs loaded, cRGD-targeted lipopolymeric nanoplexes for the treatment of wAMD; however, the knock out is not always a good/universal strategy since one gene could be involved in different biological functions and knocking out could lead to unpredictable loss of

cellular processes. Interestingly, new variants of Cas9, such as Cas13a, which has mRNA editing efficiency, could be delivered to the retinal cells to get better control over the VEGFA gene by surpassing knockout.

The following could be the future directions of the current research:

- The developed lipopolymeric nanoplexes could be explored for their transfection efficiency in hard-to-transfect cell lines such as iPSCs.
- The developed lipopolymeric nanocarrier could be explored for different routes/injection sites (e.g., subretinal injection) in rodent model of wAMD.
- The developed lipopolymeric nanocarrier could be explored for delivering other forms of the CRISPR (e.g., mRNA).
- Different targeting ligands could be explored for better *in vivo* efficiency.
- There are different variants of CRISPR/Cas system such as Cas13a, which could provide mRNA editing and could be explored to control VEGFA expression at the pre-translational level.
- Different pendant groups, such as cationic lipids, could be explored for their efficiency to make the nanocarrier system efficient in terms of *in vivo* efficiency.

Annexures

ANNEXURE-I

List of Patents

S. No	Patent
01	Deepak Chitkara, **Deepak K. Sahel**, Kishan S. Italiya, Saurabh Sharma, Shruti Shah, Anupama Mittal, Reena Jatyan, Title: *A Self-Assembling Drug Conjugate and method of preparation thereof.* Indian Patent Application no. 201911018304, Filed on May 06, 2020, Applicant: Birla Institute of Technology and Science (BITS), Pilani (Granted, Patent Number: 393113).
02	Deepak Chitkara, **Deepak K. Sahel**, Imran Ansari, Anupama Mittal, Title: *A lipopolymeric RNPs nanoplexes and preparation thereof.* Indian Patent Application no. 202011052036, Filed on Nov 30, 2020, Applicant: Birla Institute of Technology and Science (BITS), Pilani (Complete Specification).

ANNEXURE-II

List of Publications

Thesis Publications

S. No	Title
1	**Deepak Kumar Sahel**, Sangam Giri Goswami, Reena Jatyan, Mohd Salman, Vivek Singh, Sivaprakash Ramalingam, Anupama Mittal, Deepak Chitkara. A cRGD targeted CRISPR/Cas9 nanomedicine for VEGF-A knock-out to regress neovascularization in treating wAMD. ***(Communicated)***
2	**Deepak Kumar Sahel**, Sangam Giri Goswami, Reena Jatyan, Sivaprakash Ramalingam, Anupama Mittal, Deepak Chitkara. A lipopolymeric nanocarrier enables effective delivery of CRISPR/Cas9 plasmid. ***Macromolecular Rapid Communications.*** 2300101. **(IF: 5.0)**
3	**Deepak Kumar Sahel,** Anupama Mittal, Deepak Chitkara. CRISPR/Cas system for genome editing: progress and prospects as a therapeutic tool. ***Journal of Pharmacology and Experimental Therapeutics***. 2019 Sep 1;370(3):725-35. **(IF: 4.4)**
4	**Deepak Kumar Sahel**, Mohd Salman, Mohd Azhar, Sangam Goswami, Vivek Singh, Manu Dalela, Sujata Mohanty, Anupama Mittal, Sivaprakash Ramalingam, Deepak Chitkara. Cationic Lipopolymeric Nanoplexes Containing CRISPR/Cas9 Ribonucleoprotein for Genome Surgery. ***Journal of Materials Chemistry B.*** 2022. 10 (37), 7634-7649. **(IF: 7.57)**
5	Aayushi Lohia***, Deepak Kumar Sahel***, Mohammad Salman, Vivek Singh, Indumathi Mariappan, Anupama Mittal, Deepak Chitkara., Delivery Strategies for CRISPR/Cas Genome editing tool for Retinal Dystrophies: challenges and opportunities. ***Asian Journal of Pharmaceutical Sciences***. 2022. (*Equal First Author, Published). **(IF: 9.27)**

Other Publications

S.No	Title
1	Reena Jatyan, Prabhjeet Singh, **Deepak Kumar Sahel**, Karthik YG, Anupama Mittal, Deepak Chitkara. Polymeric and small molecule-conjugates of temozolomide as improved therapeutic agents for glioblastoma multiforme. *Journal of controlled release*. 2022. 350, 494-513. **(IF:11.47)**
2	Tushar Date, Kaushik Kuche, Dasharath Chaudhari, Rohan Ghadi, **Deepak Kumar Sahel,** Deepak Chitkara, Sanyog Jain. Hitting multiple cellular targets in triple-negative breast cancer using dual-action cisplatin (IV) prodrugs for safer synergistic chemotherapy. ***ACS Biomaterials Science & Engineering***. 2022. (Published). **(IF: 5.39)**
3	Sudeep Pukale, **Deepak Kumar Sahel**, Anupama Mittal, Deepak Chitkara. Coenzyme Q10 loaded lipid-polymer hybrid nanoparticles in gel for the treatment of psoriatic-like skin condition. ***Journal of Drug Delivery Science and Technology.*** 2022. 76, 103672. **(IF: 5.25)**
4	Mohammad Salman, Anshuman Verma, Vijay Kumar Singh, Jilu Jaffet, **Deepak Kumar Sahel**, Sunita Chaurasia, Deepak Chitkara, Muralidhar Ramappa, Vivek Singh. New Frontier in the Management of Corneal Dystrophies: Basics, Development, and Challenges in Corneal Gene Therapy and Gene Editing. ***Asia-Pacific Journal of Ophthalmology***. 2021. 11 (4), 346-359. **(IF: 2.87)**
5	Saurabh Sharma, Sudeep Pukale, **Deepak Kumar Sahel**, Anupama Mittal, Deepak Chitkara. Folate-targeted hybrid lipo-polymeric nanoplexes containing docetaxel and miRNA-34a for breast cancer treatment**.** ***Materials Science and Engineering: C***. 2021 Sep 1;128:112305. **(IF: 7.328)**
6	Saurabh Sharma, Sudeep Sudesh Pukale, **Deepak Kumar Sahel**, Devesh S. Agarwal, Manu Dalela, Sujata Mohanty, Rajeev Sakhuja, Anupama Mittal, Deepak Chitkara. Folate-Targeted Cholesterol-Grafted Lipo-Polymeric Nanoparticles for Chemotherapeutic Agent Delivery. ***AAPS PharmSciTech***. 2020 Oct;21(7):1-21. **(IF: 4.0)**
7	Kishan S. Italiya, Moumita Basak, Samrat Mazumdar, **Deepak K. Sahel**, Richa Shrivastava, Deepak Chitkara, and Anupama Mittal. Scalable self-assembling micellar system for enhanced oral bioavailability and efficacy of lisofylline for treatment of type-I diabetes. ***Molecular pharmaceutics***. 2019 Oct 24;16(12):4954-67. **(IF: 5.36)**

ANNEXURE-III

List of Awards and conferences

S. No	Award
01	**Sun Pharma Foundation Science Scholar Award-2022**
02	**ICMR-Senior Research Scholarship (SRF)-2019**
03	Awarded with **best poster** presentation prize **(AUS$100)** for work presented at **Drug Delivery Australia (DDA)** Annual Meeting, 2021, in collaboration with **Controlled release Society (CRS) Australian Local Chapter** on the theme of Advanced Materials in Drug Delivery held on 18-19 November in Australia.
04	Awarded **1st prize (INR 15000/-)** in an oral presentation for the research work presented at the **Controlled release Society (CRS) Indian Local Chapter** at Nirma University on 28th Oct 2021.
05	Awarded **1st prize (INR-5000/-)** in an oral presentation for the research work presented at the **2nd Student research congress** held on 28-30 September 2021 at Dr. Bhanuben Nanavati College of Pharmacy, co-hosted by the University of Mumbai.
06	Awarded **1st Prize (INR-3000/-)** for the oral presentation category at **Prof. Ambikanandan Misra International Conference** on "Recent Advances & TRENDS in Novel Drug Delivery Systems" held on 23rd to 25th Sept 2021.
07	**Deepak Kumar Sahel**, Sangam Giri Goswami, Reena Jatyan, Siva Prakash Ramalingam, Anupama Mittal, Deepak Chitkara. Poster presentation on "Cationic lipopolymeric nanocarrier delivering CRISPR/Cas9 plasmid for gene editing" in NIPERCon-2022.

ANNEXURE-IV

Biography of Supervisor

Dr. Deepak Chitkara is an Associate Professor at the Department of Pharmacy, Birla Institute of Technology and Science (BITS)-Pilani, Vidya Vihar Campus, India. He obtained his B. Pharmacy degree from UIPS, Panjab University, Chandigarh in 2004, following which he did M.S. (Pharm.) in Pharmaceutics from the National Institute of Pharmaceutical Education and Research (NIPER), SAS Nagar. Further, he obtained his Ph.D. in Pharmaceutical Sciences from NIPER, SAS Nagar. He was an exchange research scholar at the University of Tennessee Health Science Center, Memphis, TN, for one year. After that, he did his post-doctoral training at the University of Nebraska Medical Center, Omaha, NE, in the area of miRNA therapeutics for pancreatic cancer in Prof. Mahato's lab. His research interests include nano-based delivery systems for small molecules, nucleic acids (miRNAs, mRNA and CRISPR/Cas genome editing tools), wherein his lab is involved in designing biodegradable lipo-polymers grafted with varying pendant groups to impart multifunctionality. These lipo-polymers are being investigated as carriers for gene and protein-based therapeutics. His lab is well-funded from various government agencies, including DBT, DST, and ICMR and Pharmaceutical Industries. He has published over 60 peer-reviewed publications, edited one book, and currently, he is editing two special issues, one for Journal of Controlled Release on Brain Targeting and the other on protein and peptide therapeutics for Journal of Pharmacology and Experimental Therapeutics. Further he has filed 6 Indian patents and one international PCT patent application out of which 4 Indian patent applications has been granted. He is also the founding director of a faculty-led nanotechnology-based start-up (Nanobrid Innovations Private Limited) incubated at Pilani Innovations and Entrepreneurship Development Society at BITS-Pilani and BITS-BioCyTIH Foundation to further take-up the commercialization activities.

Biography of Co-Supervisor

Prof. Anupama Mittal, currently working as an Associate Professor in the Department of Pharmacy, BITS, Pilani, Pilani campus, is an established researcher and scientist in the field of Nanomedicine. She has been the recipient of prestigious Young scientist award-2015 (SERB-DST) and Ranbaxy Science Scholar award-2011 (Ranbaxy Science Foundation) in Pharmaceutical Sciences. She has been involved actively in teaching (on campus as well as industry professionals from various pharmaceutical industries) and independent research since nearly last 8 years. Her research interests and expertise primarily focusses upon generating nanotechnology-based solutions for diseases like cancer and diabetes. Her lab has been engaged in research activities in the areas of nanoparticles and polymeric micelles for site-specific drug delivery, polymer/fatty acid drug conjugates for effective treatment of cancer and diabetes, stem cells and exosomes as biogenic carriers of miRNA and proteins in cancer, and growth factor and peptide-based therapeutics for wound healing and diabetes. She has published 42 research and review articles in peer reviewed international journals, edited 01 book (CRC press), authored 03 book chapters and filed 07 Indian/PCT patent applications among which 04 have been successfully granted. She has also received several awards for best papers presented at National/International conferences. Her lab is generously funded by several extramural research grants from SERB-DST, DST-Rajasthan, DST-Nanomission, ICMR and DBT. She has guided several M. Pharm and B. Pharm students and is currently supervising 07 Ph.D. students. She also serves as the co-director of a start-up company, Nanobrid Innovations Pvt. Ltd. aimed towards the translation of nanotechnology-based products.

ANNEXURE-V

Biography of Research Scholar

Mr. Deepak Sahel is a Ph.D. scholar working with Dr. Deepak Chitkara since early 2018. He obtained his Master's in Pharmacology from Maharshi Dayanand University, Rohtak, Haryana, in 2017 and was awarded a "*Gold Medal Certificate"* for securing the *first rank*. He joined BITS Pilani as Junior Research Fellow (JRF) and was later awarded Senior Research fellow (SRF) by the Indian Council of Medical Research (ICMR), Government of India. During his Ph.D. tenure, he has >10 research papers published in international peer-reviewed journals and 02 patents (01 granted, 02 filed) credited to his profile. Moreover, he has been awarded four 1st prizes for presenting his research work at national and international conferences (01 international and 03 national). He has been awarded as Sun Pharma Foundation Research Scholar Award-2022 and credited a cash prize of INR 50,000/- along with a citation, trophy, certificate, and a travel grant of INR 50,000/-. His area of research focuses on developing *non-viral* nanocarrier systems (lipidic, polymeric, and lipid-polymer hybrid) for the gene (miRNA/siRNA/mRNA/CRISPR/Cas9 RNPs) delivery applications for the treatment of a wide range of debilitating diseases.